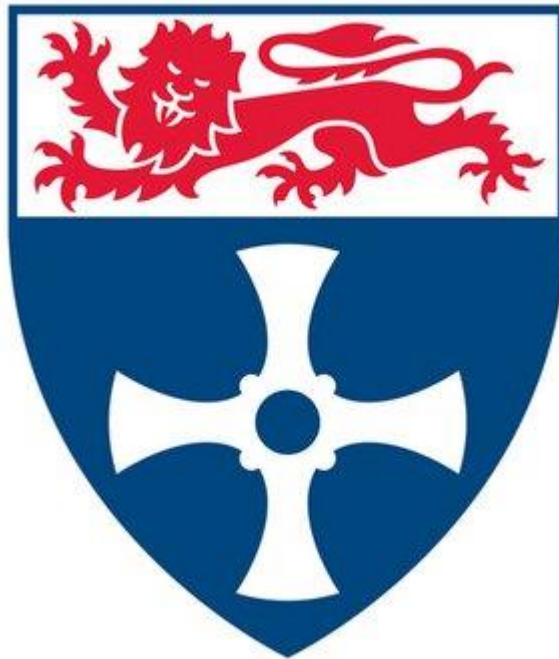


Regional statistical modelling of hourly extreme precipitation in the United Kingdom



Motasem Darwish

School of Engineering

Newcastle University

A thesis presented for the degree of Doctor of Philosophy

February 2019

This page intentionally left blank

For Dad and Mum

This page intentionally left blank

Abstract

1
2 In the UK, various studies have investigated daily extreme precipitation; however,
3 increases in recent flash flood events indicate the need for improved understanding
4 and methods associated with sub-daily extremes. This thesis attempts to fill this gap
5 by examining quality-controlled hourly precipitation data from 1992-2014 at 197
6 gauges across the UK, and using climatological predictors to develop a regional
7 statistical model which quantifies the frequency and intensity of hourly extreme
8 precipitation.

9 Regional annual exceedance probabilities for sub-daily extreme precipitation were first
10 estimated using the daily UK extreme regions. Results suggested these regions did
11 not adequately reflect the spatial variation of sub-daily extreme precipitation. The sub-
12 daily extremes showed clear seasonality with short-duration extremes (1h and 3h)
13 predominantly in summer, and longer duration extremes (12h and 24h) distributed
14 throughout late autumn and winter. Moreover, the diurnal cycle of short-duration
15 extremes centres on the afternoon, with a peak typically between 1400 and 1700,
16 especially in southern and eastern regions.

17 Hourly gauges were clustered using a statistical approach, employing the annual
18 maxima, peak over threshold indices and weather types to develop five new regions,
19 which reflect the impacts of orography, seasonality, and atmospheric. Regional
20 frequency analysis with L-Moments was then used to estimate growth curves for the
21 new homogeneous hourly extreme precipitation regions.

22 Time-dependent Poisson-GP regional statistical models were developed to simulate
23 hourly extreme precipitation, using atmospheric circulation, temperature, and moisture
24 content as predictive covariates. The model indicated a noticeable peak in the
25 occurrence of hourly extremes in summer, especially in southern regions. A simple
26 pseudo global warming scenario of 2°C was used to demonstrate the model potential.
27 It projected an increase in the frequency and intensity of hourly extremes of up to 17%,
28 which is higher than suggested by Clausius-Clapeyron, highlighting a need to review
29 design guidelines for future extreme precipitation in the UK.

30

31

32

This page intentionally left blank

33
34
35
36
37
38
39
40
41
42
43
44
45
46
47
48
49
50
51
52
53
54
55
56
57
58
59
60
61
62

Acknowledgement

63

64 First, I would thank my supervisors Prof. Hayley Fowler, Dr. Stephen Blenkinsop, and
65 Dr. Mari Tye for their unlimited and unconditional support throughout this journey.
66 During this PhD, they offered an outstanding guidance, advice, and feedback. Their
67 support, guidance, and contribution is greatly appreciated, and beyond description.
68 Moreover, their encouragement to pursue numerous opportunities by attending
69 workshops, conferences, and visiting various research centres is invaluable. I have
70 been extremely lucky to have them as my supervisors for the last four years, and hope
71 to continue collaborating with them in my future research.

72 I am grateful also to my parents. During this journey, their continuous encouragement,
73 support, and enthusiasm were enough to provide me with faith to keep going. In many
74 times, there was no single reason to believe that this journey would finish successfully
75 except their words and voices. I owe them an apology for all the stressful times I put
76 them in when I felt down. I feel so little for what they offered throughout this journey.

77 With a special thanks to my three sisters, Meray, Tamara, and Rima who experienced
78 all of the ups and downs of my research. They were always available from the dawn
79 of my personal stories to the inevitable dusk

80 A very special gratitude goes to Andreas Prein and Rachel Hauser from the national
81 center of atmospheric research (NCAR) in Colorado/USA. During my research visit,
82 they offered all the possible support and help to enhance my experience, and they
83 were ready to offer every help when I know they were already so busy. I am also so
84 grateful for Andreas contribution and Ideas in Chapter 4, which improved the work
85 remarkably.

86 Thanks are due to Middle East University- Jordan (MEU) for funding this research
87 through their program of academic excellence sponsorship.

88 And finally, last but by no means least, a considerable thank to all my friends and
89 colleagues Nurten, Francesco, Carmela, Xiaodong, Hana, Mustafa, and Reza for all
90 the support during this journey. It was pleasure to work with you for the last few years.

91

92

93

Table of Contents

Abstract.....	i
Acknowledgement.....	iii
Table of Contents	iv
List of publications	vii
List of figures.....	viii
List of tables	xiv
Abbreviations	xvi
Chapter 1. Introduction	1
1.1. UK daily Precipitation.....	2
1.2. UK Sub-daily extreme precipitation.....	4
1.3. Statistical downscaling.....	5
1.4. Research aims and objectives	7
1.5. Thesis structure.....	7
Chapter 2. Literature Review	9
2.1. Precipitation overview	9
2.2. Sub-daily extremes in Europe.....	11
2.3. Historical and future precipitation in the UK	12
2.3.1. UK Mean precipitation.....	13
2.3.2. UK daily extreme precipitation	17
2.3.3. UK sub-daily precipitation	20
2.3.4. Future Projections.....	22
2.4. Extreme precipitation related climatic variables	23
2.4.1. Atmospheric Circulation	23
2.4.2. Oceanic circulation.....	25
2.4.3. Temperature.....	26
2.4.4. Atmospheric moisture	28
2.5. Summary.....	29
Chapter 3. regional frequency analysis of UK hourly and multi-hourly extreme precipitation	31
3.1. Introduction.....	31
3.2. Data	35
3.3. Methodology	37

3.3.1.	<i>Exploratory data analysis</i>	37
3.3.2.	<i>Extreme value theory (EVT)</i>	39
3.3.3.	<i>Regional Frequency Analysis (RFA)</i>	41
3.4.	Results	43
3.4.1.	<i>Diurnal cycle and seasonality of AMAX events</i>	43
3.4.2.	<i>Regional frequency analysis</i>	51
3.5.	Discussion	58
3.6.	Conclusion	62
Chapter 4. New hourly extreme precipitation regions and regional annual probability estimates for the UK		65
4.1.	Introduction	65
4.2.	Data	68
4.3.	Methodology	71
4.3.1.	<i>Variable Selection</i>	71
4.3.2.	<i>Clustering Analysis</i>	74
4.3.3.	<i>Regional Frequency Analysis (RFA)</i>	75
4.3.4.	<i>Data independence</i>	76
4.3.5.	<i>Goodness of fit measure (Zdist)</i>	77
4.4.	Results	77
4.4.1.	<i>Principal Components Analysis</i>	77
4.4.2.	<i>Regional Clustering Analysis</i>	80
4.4.3.	<i>Regional homogeneity</i>	86
4.4.4.	<i>Regional Frequency Analysis and AEP Estimates</i>	89
4.5.	Discussion and conclusions	93
Chapter 5. Statistical modelling of UK extreme hourly precipitation and future climate change responses		96
5.1.	Introduction	96
5.2.	Data	100
5.2.1.	<i>Precipitation data</i>	100
5.2.2.	<i>Predictors</i>	100
5.3.	Methodology	109
5.3.1.	<i>Generalized linear model (GLM)</i>	110
5.3.2.	<i>Extreme Value Theory (EVT)</i>	111
5.3.3.	<i>Poisson-GPD Distribution relation</i>	114
5.3.4.	<i>Data independence</i>	114
5.3.5.	<i>Regional Data Pooling</i>	115

5.3.6.	<i>Parameter Estimation</i>	115
5.3.7.	<i>Model selection</i>	116
5.3.8.	<i>Model predictions</i>	117
5.4.	Results	117
5.4.1.	<i>Climatic predictor initial selection</i>	118
5.4.2.	<i>Poisson model</i>	120
5.4.3.	<i>Pseudo Global Warming Method</i>	125
5.5.	Discussion and Conclusion	128
Chapter 6. Conclusion		133
6.1	Summary of results	133
6.2	Results in the context of the existing literature	138
6.3	Future work	141
6.3.1	<i>Data collection</i>	141
6.3.2	<i>Seasonal assessment</i>	141
6.3.3	<i>Statistical model transferability</i>	142
6.3.4	<i>Comparison with existing approaches</i>	142
6.3.5	<i>Urbanised area adaptation plans</i>	142
References		144
Appendices		160
Appendix A: Supporting figures		160
Appendix B: Supporting tables		170

List of publications

The following journal article is product of this thesis and referenced at the beginning of the relevant chapters. I took the lead role in the article and was responsible for code development, figure drawing and writing. The co-authors contributed to research ideas and manuscript editing:

Darwish, M., Fowler, H.J., Blenkinsop, S. and Tye, M.R. (2018) 'A regional frequency analysis of UK sub-daily extreme precipitation and assessment of their seasonality', International Journal of Climatology, 38(13), pp. 4758–4776. doi.org/10.1002/joc.5694

List of figures

- Figure 1: Distribution of 197 hourly rain gauges (blue dots) and UK extreme precipitation regions as defined by Jones et al (2014). Boundary and text in red denote merged regions (MW and SW were merged to form MSW due to limited gauge data in MW). Numbers in brackets denote the total number of gauges in each region.36
- Figure 2: Regional hourly frequency density plots and diurnal profiles of 1h and 3h AMAX for selected regions. The smoothed diurnal profiles were fitted using kernel density estimations. The 3h AMAX is calculated as the accumulation of the hourly record for hour n , $n-1$, and $n-2$, and plotted at hour n . For example, an accumulation at 15:00 is the total of precipitation at 13:00, 14:00, and 15:00. N denotes the number of gauges in each region. Frequency density of event (y-axis), and hours of the day (x-axis).44
- Figure 3: Regional monthly frequency densities of 1-, 3-, 6-, 12- and 24h AMAX in the UK. Red (italicised) values denote the frequency density scale.46
- Figure 4: Regional circular statistics representing seasonality of occurrence of hourly and multi-hourly AMAX. Figure (A), mean AMAX occurrence day (Julian day, θ); Figure (B), degree of dispersion (r) indicating the degree to which AMAX are seasonally concentrated, ranging from 0 to 1, with higher values indicating greater concentration around θ . Refer to Figure 1 for region abbreviations.48
- Figure 5: Monthly 1h AMAX regional frequency density (black), and hourly AMAX standardised by the regional median (red) for selected regions. The regional median (mm) is stated for each region, and radial lines denote 1st day of each month.50
- Figure 6: Return level plots of fitted regional GEV distributions for 1h AMAX (red) and 95% confidence interval (grey shaded), 24h AMAX (black), and daily AMAX (from Jones et al. 2014) (green). Return level estimates in mm (y-axis), return periods in years (upper x-axis) and Gumbel reduced variate (lower x-axis). The 1h AMAX GEV distribution parameters μ , σ and ξ are also shown.54
- Figure 7: Q-Q plots for the AMAX fitted GEV distributions. Sample (observed) growth curve quantiles (y-axis) and theoretical growth curve quantiles (x-axis). The growth curve represents the multiple increase of a given return level over an index value, in this case the 2-year return level.55

Figure 8: Return level estimates (mm h⁻¹) for UK 1h AMAX precipitation at each gauge for return periods of 5-, 10-, 25- and 50 years (20%, 10%, 4%, 2% annual exceedance probabilities (AEPs)). Estimates for each gauge are calculated from the fitted regional GEV growth curve multiplied by the site scaling factor (gauge RMed).57

Figure 9: Potential rationalisation of precipitation regions based on subjective assessment of the 1h AMAX fitted GEV distributions. H denotes the heterogeneity measure for each region using Hosking and Wallis (1998).62

Figure 10: Scree plot of the principle component analysis (PCA) for the various climatological variables in Table 4. Eigenvalue of each component (left Y-axis) (Blue line), cumulative explained variance (right Y-axis) (Red line), and component number (X-axis).....80

Figure 11: PCA clustering results for UK hourly precipitation using Wards clustering approach for (a) 4 regions; (b) 5 regions; and (c) 6 regions. Kernel-smoothed PCA scores for all components PC1 to 3 (left column) and individually (i.e. PC1, PC2, and PC3) (right three columns) are illustrated. Yellow line are the existing daily extreme regions by Jones et al, (2014), and presented here for reference only.82

Figure 12: Proportion of days exceeding Q99 hourly precipitation for each gauge across the 8 weather types identified by Neal et al. (2016) over the period 1992-2014. Numbers in brackets represent the percentage of all days on which each weather type occurs. Circle diameter indicates the proportion of Q99 events within each weather type for each gauge.....84

Figure 13: Comparison between (a) the PCA clustering results for UK hourly precipitation using Wards clustering approach for 5 regions; and (b) the proportion of days exceeding Q99 hourly precipitation for each gauge across weather types 1 to 4 identified by Neal et al. (2016) over the period 1992-2014. Yellow line (Figure 13a) are the existing daily extreme regions by Jones et al, (2014), and presented here for reference only. Numbers in brackets represent the percentage of all days on which each weather type occurs. Circle diameter indicates the proportion of Q99 events within each weather type for each gauge.85

Figure 14: Final delineation of UK extreme hourly precipitation regions. Regions are: South East (SE), South West, Mid-East (ME), North West (NW), and North West (NW). The value in parentheses denotes the number of hourly gauges in each region.....87

Figure 15: Fitted regional GEV and GP growth curves for 1h standardized AMAX (blue) and Q99 (red) respectively, and confidence intervals for the fitted GEV distribution (blue shading) and GP distribution (red shading). Growth factor (y-axis), Annual Exceedance Probability (AEP) in % (upper x-axis), and Gumbel reduced variate (lower x-axis). The growth curve represents the multiple increase of a given AEP over an index value, here the 50% AEP.90

Figure 16: Estimates for the UK 1h extreme precipitation in mm for 20%, 4%, 2% annual exceedance probabilities (AEPs)) using the GEV distribution (a) and GP distribution (b). Estimates for each gauge are calculated from the fitted regional growth curve multiplied by the site scaling factor (gauge RMed).91

Figure 17: Median of hourly Q99 precipitation 1992–2014 for each region (SE, SE, ME, NW, and NE) and for each of the 8 weather patterns (Neal et al., 2016) (X-Axis), expressed as the median of each region and weather type relative to the region mean (Y-axis). The weather types are ordered left to right from the lowest UK relative median precipitation to the highest. Y-axis (after Richardson et al., 2018 Figure 5).93

Figure 18: The $0.75^\circ \times 0.75^\circ$ grid, where the daily average of all potential climatic variables (except the NAO) over the UK are extracted from European Center for Medium-Range Weather Forecasts (ECMWF) Interim reanalysis dataset between 1990-2015 (Dee et al., 2011). For each variable, a daily area average of each grid cell was calculated (red dots), thereafter, the value was assigned to the gauges within the grid cell..... 103

Figure 19: The domains located in the north west (42°N – 52°N , 52°W – 40°W) (Domain 1) and south east (35°N – 42°N , 35°W – 20°W) (Domain 2) of the North Atlantic, where the sea surface temperature (SST) between 1990-2015 was extracted, to investigate its relation with hourly extremes in the UK. Longitude (x-axis) and latitude (y-axis)..... 108

Figure 20: The Spearman correlation between hourly extreme intensities above the Q99 and potential climatological predictors. The assessed predictors are:

convective available potential energy (CAPE), convective inhibition (CIN), dew point temperature (DPT), sea level pressure (SLP), pressure level height 700-, 850hPa (Z700-, Z850), and North Atlantic oscillation (NAO). The positive and negative significantly correlated gauges are indicated by red and blue colour respectively. Moreover, positive and negative non-significantly correlated gauges are indicated by black upward and downward arrows respectively..... 119

Figure 21: As for Figure 20 but assessed predictors are: sea surface temperature average over NW (42°N–52°N, 52°W–40°W), and SE (35°N–42°N, 35° W–20°W) domains of the North Atlantic on Q99 days (SST-Avg), 4-month lagged sea surface temperature average (SST-Avg-lag), sea surface temperature difference between NW and SE domains on Q99 days (SST index), 4-month lagged sea surface temperature difference between NW and SE domains (SST-index-lag), near-surface air temperature (T-2m), and total column water vapour (TCWV). The positive and negative significantly correlated gauges are indicated by red and blue colour respectively. Moreover, positive and negative non-significantly correlated gauges are indicated by black upward and downward arrows respectively..... 120

Figure 22: Q-Q plots for Q99 hourly extreme frequency predicted by the Poisson GLM for the years 1992-2011 in each region. Q99 hourly extreme occurrence by Julian day for observed quantiles (x-axis), and Poisson predicted quantiles using NAO, Z-700, DPT, and sine/cosine Julian day as predictors (y-axis). Confidence bands are developed from 500 bootstrapped samples. The continuous solid line is the prediction regression line, while the dotted line is the 1-1 reference line. 122

Figure 23: Validation Q-Q plots for the Q99 hourly extremes frequency predicted by the Poisson model for years 2012-2014 in each region. Q99 hourly extremes occurrence by Julian day for observed quantiles (x-axis), and Poisson predicted quantiles (y-axis). Details as for Figure 22..... 123

Figure 25: Q-Q plots for Q99 hourly extremes predicted intensity by the GPD for the years 1992-2011 in each region. Q99 hourly extreme intensity for observed quantiles in mm/hr (x-axis), and GPD predicted extreme intensity quantiles in mm/hr (y-axis). The continuous solid line is the prediction regression line, while the dotted line is the 1-1 reference line..... 124

Figure 26: Validation Q-Q plots for the Q99 hourly predicted intensities by the GPD for the years 2011-2014 in each region. Q99 hourly extreme intensity for observed quantiles in mm/hr (x-axis), and GPD predicted extreme intensity quantiles in mm/hr (y-axis). The continuous solid line is the prediction regression line, while the dotted line is the 1-1 reference line. 125

Figure 27: Comparison of daily probability of Q99 occurrence under current climate (solid line) and predicted global temperature increase of 2C (dotted line) in a) NW and b) SE. Julian days of occurrence (X-axis), and the probability of occurrence (Y-axis). 127

Figure 28: Comparison of extreme precipitation intensity under current climate (solid line) and predicted global temperature increase of 2C (dotted line) according to Paris agreement in a) NW and b) SE. Julian days of occurrence (X-axis), and the intensity in mm/hr (Y-axis). 128

Figure A 1: Regional monthly frequency densities of 24h AMAX rolling window accumulation (dark blue) and 24h AMAX fixed window accumulation at 09:00 (cyan) in the UK. Values in red denote the frequency density scale. 160

Figure A 2: Monthly 3h AMAX frequency density (blue), and 3h AMAX standardised by the regional median (red). The regional median (mm) is stated for each region, and radial lines denote 1st day of each month. Selected regions shown as in main paper..... 161

Figure A 3: Monthly 12h AMAX frequency density (blue), and 12h AMAX standardised by the regional median (red). The regional median (mm) is stated for each region, and radial lines denote 1st day of each month. Selected regions shown as in main paper..... 162

Figure A 4: Return level plots of fitted regional GEV distributions for daily AMAX (from Jones et al. 2014) (green), 24h AMAX fixed window accumulation at 09:00 (dashed black), 24h AMAX rolling window accumulation (red), and 1h AMAX (cyan). Return level estimates in mm (left y-axis), return periods in years (upper x-axis) and Gumbel reduced variate (lower x-axis). The 1h AMAX GEV distribution parameters μ , σ , and ξ are also shown..... 163

- Figure A 5: Fitted growth curves for 24h standardized AMAX accumulation (black), and daily AMAX (from Jones et al. 2014) (green), and confidence interval for each distribution (dashed lines). Growth factor (y-axis), return periods in years (upper x-axis) and Gumbel reduced variate (lower x-axis). The growth curve represents the multiple increase of a given return level over an index value, here the 2-year return level. 164
- Figure A 6: Fitted growth curves for standardized 1h AMAX (red), 24h AMAX (black), and daily AMAX (from Jones et al. 2014) (green). Growth factor (left y-axis), return periods in years (upper x-axis) and Gumbel reduced variate (lower x-axis). The 1h AMAX GEV distribution parameters μ , σ , and ξ are also shown. The growth curve represents the multiple increase of a given return level over an index value, here the 2-year return level. 165
- Figure A 7: Return level estimates (mm h⁻¹) for UK 3h AMAX precipitation at each gauge for return periods of 5-, 10-, 25- and 50 years (20%, 10%, 4%, 2% annual exceedance probabilities (AEPs)). Estimates for each gauge are calculated from the fitted regional GEV growth curve multiplied by the site scaling factor (gauge RMed). 166
- Figure A 8: Return level estimates (mm h⁻¹) for UK 12h AMAX precipitation at each gauge for return periods of 5-, 10-, 25- and 50 years (20%, 10%, 4%, 2% annual exceedance probabilities (AEPs)). Estimates for each gauge are calculated from the fitted regional GEV growth curve multiplied by the site scaling factor (gauge RMed). 167
- Figure A 9: Occurrence proportion of days exceeding the Q99 hourly precipitation for each gauge across the 8 weather types identified by Neal et al. (2016) in the winter half year (Oct-March, N-WQ99) over the period 1992-2014. Circle diameter indicates the proportion of events within each weather type for each gauge. . 168
- Figure A 10: Occurrence proportion of days exceeding the Q99 hourly precipitation for each gauge across the 8 weather types identified by Neal et al. (2016) in the summer half year (Apr-Sept, N-SQ99) over the period 1992-2014. Circle diameter indicates the proportion of events within each weather type for each gauge. . 169

List of tables

Table 1: Extreme precipitation regional homogeneity assessment for 1h AMAX and the gauge discordancy assessment (Hosking and Wallis, 2005). Region is homogenous if $H < 1$, possibly heterogeneous if $1 \leq H < 2$, and definitely heterogeneous if $H \geq 2$, and the gauges are not discordant if the maximum gauge discordancy test value $< D_{critical}$	51
Table 2: <i>Descriptions of the eight weather patterns from the European and North Atlantic Daily to Multi-decadal Climate Variability (EMULATE) MSLP (EMSLP) data (1850–2003) as derived in Neal et al, 2016. Weather type names and descriptions are relevant to the UK. MSLP and NAO denote mean sea level pressure and North Atlantic Oscillation respectively.</i>	71
Table 3: Variables used to identify homogeneous regions for hourly extreme precipitation using principal components analysis. Each variable’s contribution to the PCA results were assessed, and the most representative variables (shaded) were retained.	73
Table 4: Loadings of each variable in the first three principal components and proportional contribution to the explained variance. Values in bold are the 2 most significant contributing variables for each principal component. Loadings smaller than ± 0.1 are not reported for clarity.	79
Table 5: Gauge discordancy (D), region homogeneity (H) and goodness of fit (Z) assessment for the UK hourly extreme precipitation regions (SE, SW, ME, NW, and NE) shown in Figure 14. The table shows the number of gauges in each region and the maximum recommended gauge discordant value (D_{crit}) for each region.	88
Table 6: Proportion of Weather types (WT) 1 to 8 (Neal et al, 2016) across all the proposed UK 5 regions annually, in winter, and in summer (underlined).	92
Table 7: Potential predictors used to develop a statistical model of the frequency and intensity of hourly precipitation extremes.	102
Table B 1: Regional circular statistics representing seasonality of occurrence of hourly and multi-hourly AMAX events. Statistic θ denotes mean occurrence day (Julian	

day); r indicates the degree to which events are seasonally concentrated, ranging from 0 to 1, with higher values indicating greater concentration around θ 170

Abbreviations

AEP: Annual exceedance probability
AIC: Akaike Information Criterion
AMAX: Annual maximum
AMO: Atlantic Meridional Oscillation
AMOC: Atlantic Meridional Overturning Circulation
CA: Cluster analysis
CAPE: Convective available potential energy
CC: Clausius–Clapeyron
CDF: Cumulative distribution function
CPM: Convective permitting models
DDF: Depth-Duration-Frequency
DEFRA: Department for Environment, Food & Rural Affairs
DEM: Digital elevation model
DPT: Dew point temperature
EA: East Anglia
Elev: Elevation
ENSO: El Nino Southern Oscillation
ES: East Scotland
EVT: Extreme value theory
FEH: Flood estimation handbook
FOR: Forth
FSR: Flood studies report
GCM: General circulation models
GEV: General extreme value
GLM: Generalized linear modelling
GP: General Pareto
GPD: General Pareto distribution
HadUKP: Hadley Centre UK Precipitation
HUM: Humber
i.i.d: independent and identically distributed

INTENSE: INTElligent use of climate models for adaptatioN to non-Stationary hydrological Extremes
IPCC: Intergovernmental panel on climate change
Lat: Latitude
Lon: Longitude
ME: Mid East
MIDAS: Met office integrated data archive system
MSLP: Mean sea level pressure
MSW: Mid South West
MW: Mid Wales
NAO: North Atlantic oscillation
NE: North East
NHI: North Highlands and Islands
NI: North Ireland
N-SQ99: Number of summer (April-September) events exceeding SQ99
NW: North West
N-WQ99: Number of winter (October-March) events exceeding WQ99
PC: Principal component
PCA: Principal component analysis
PGW: Pseudo global warming
POT: Peaks over threshold
Q99: Precipitation 0.99 quantile
RCM: Regional climate models
RFA: Regional frequency analysis
RMed: Median of annual maximum precipitation
SE: South East
SEPA: Scottish Environmental Protection Agency
SLP: Sea level pressure
SOL: Solway
SQ99: Summer (April-September) precipitation 0.99 quantile
SS: South Scotland
SST: Sea surface temperature

SW: South West
TCWV: total column water vapour
Tmax: Median of maximum temperature on Q99 days
Tmin: Median of minimum temperature on Q99 days
UKCP: UK climate projections
WQ99: Winter (October-March) precipitation 0.99 quantile
WT: Weather types

Chapter 1. Introduction

1
2
3
4
5
6
7
8
9
10
11
12
13
14
15
16
17
18
19
20
21
22
23
24
25
26
27
28
29
30
31
32
33

Daily and sub-daily extreme precipitation events are major cause of flooding, soil erosion, pollution and landslides, which have potentially high impacts on urbanised areas, transportation, human society, and infrastructure (IPCC, 2012). Various studies of daily observations have indicated an increase in the frequency and intensity of extreme precipitation across the globe in the last few decades (Alexander *et al.*, 2006; Westra *et al.*, 2013; Donat *et al.*, 2017). The changing behaviour of the extremes has attracted researchers from different fields to characterise their patterns, estimate associated risks, and evaluate their relationship to climate change and related, potentially driving, climatic variables (e.g. temperature, moisture content).

In the last few decades, significant flood events arising as a consequence of extreme precipitation have occurred in the UK. Examples include the Boscastle 2004 flood which was caused by intense convective precipitation (50mm/hr) (Golding *et al.*, 2005) and the UK 2007 floods which were caused by frontal precipitation associated with slow moving depressions across the British Isles (Blackburn *et al.*, 2008). The latter resulted in high insurance claims and a significant hit for infrastructure and critical services (Chatterton *et al.*, 2010). In 2012, Newcastle experienced a flood caused by intense precipitation where ~50mm precipitation occurred in 2 hours and affected more than 1200 properties (Archer and Fowler, 2018). Stern (2006) reported that floods are among the most costly extreme events in the UK, while the UK environment agency warned that flood related damages could increase up to 60% more by 2035, unless prompt actions and adaptation policies are implemented (Chatterton *et al.*, 2010).

However, the response of extremes to ongoing climate change is considered a challenge for scientists and decision makers due to the numerous, complex physical and thermodynamic contributions governing extreme events (Herring *et al.*, 2014). Climate change studies which have investigated daily extremes frequency and return estimates using physical theory (e.g. O'Gorman and Schneider, 2009), observations (e.g. Fischer and Knutti, 2016), and model simulations (e.g. Kharin *et al.*, 2007) have agreed that extremes have intensified and predicted to continue to increase in response to warming climate especially in wet regions, however, the response to future climate change is noticeably uncertain with high sensitivity, especially for convective conditions. Extreme precipitation are generated from various processes, and might be associated with a range of conditions depending on location and seasonality such as

34 the large atmospheric circulation, multitude and tropical cyclones, atmospheric rivers,
35 and local convective complexes, which makes understanding and predicting changes
36 difficult (Schumacher and Johnson, 2005; Gosling et al., 2011). Furthermore, the IPCC
37 (2012) reported strong spatial and temporal variation in extreme precipitation, which
38 adds more challenges to extremes simulating.

39 Recently, Donat et al. (2017) reported that existing storm management infrastructure
40 is inadequate to control the increasing precipitation extremes and totals in different
41 regions. Policy makers and designers have highlighted the need for adaptation
42 planning strategies and reliable risk estimates (Stocker et al., 2013). Arnbjerg-Nielsen
43 et al. (2013), who reviewed current methods for assessing future precipitation changes
44 and their impacts on urban drainage systems, reported that in spite of the improved
45 understanding and characterisation of precipitation under climate change, the
46 estimation of risks remains challenging due to the needed high spatio-temporal
47 resolution, besides the difficulty in monitoring and quantifying the extremes. Therefore,
48 investigating the temporal and spatial characteristics of precipitation extremes, in
49 addition to their related climatological variables is crucial to quantify extremes intensity
50 and frequency, evaluate the potential risks, and implement adaptation plans.

51 Theoretically, the physical processes generating precipitation are well established,
52 especially for mean (climatological) precipitation, however, simulating and describing
53 the exact interaction between the various processes is not practically possible due to
54 its complexity and associated uncertainties (Demirdjian et al., 2018). Furthermore, the
55 relationship between mean and extreme precipitation is not straightforward, particularly
56 for increasingly extreme precipitation events (Zhou and Lau, 2017), which adds more
57 ambiguity in understanding extremes, while using general circulation models (GCMs)
58 and regional climate models (RCMs) to simulate extremes frequency and intensity at
59 small spatial scales is computationally expensive (Chan et al., 2013). Extremes are
60 rare by nature, and quantifying their occurrence frequency and intensity is challenging.
61 Consequently, statistical analysis and modelling have been adopted due to its potential
62 in characterising extremes patterns without prior knowledge of all complex atmospheric
63 processes (Rohrbeck et al., 2018).

64 **1.1. UK daily Precipitation**

65 Similar to the trend of globally increasing extremes, various studies have reported
66 increasing daily and multi-daily precipitation intensity and frequency in the UK (Osborn

67 *et al.*, 2000; Fowler and Kilsby, 2003a; Fowler and Kilsby, 2003b; Simpson and Jones,
68 2014). These increasing trends have been reported for different periods, and durations,
69 which indicates the consistency of the reported increasing trends.

70 Daily mean and extreme precipitation have been investigated thoroughly in the UK
71 taking the advantage of a rich data archive and dense gauge network. The UK
72 precipitation record goes back to 1766, where the daily, monthly, seasonal, and annual
73 precipitation data is produced by the Hadley Centre for climate prediction and research
74 (HadUKP). Originally, the monthly data series was constructed by Wigley *et al.* (1984),
75 and was updated by Wigley and Jones (1987), Gregory *et al.* (1991), Jones and
76 Conway (1997), and Alexander and Jones (2000). The data series are updated in real
77 time for all regions and used in various hydrological applications (e.g. calculating
78 regional totals, estimated return levels). However, Simpson and Jones (2012) indicated
79 that uncertainties and potential inhomogeneities associated with the HadUKP
80 datasets, are higher for regions with sparse gauges than dense gauged regions.

81 Therefore, Wigley *et al.* (1984) identified 5 regions in England and Wales using mean
82 daily precipitation, which were subsequently extended to 9 regions for the UK and
83 Northern Ireland by Gregory *et al.* (1991). Identifying precipitation regions provides the
84 ability to pool data from different locations across each region, which provides data for
85 ungauged locations, and reduce the uncertainties in sparsely gauged regions (Hosking
86 and Wallis, 2005). The regions have been used to estimate return levels and evaluate
87 the changes in trends and patterns of mean precipitation (e.g. Jones and Conway,
88 1997; Simpson and Jones, 2014), extreme precipitation (e.g. Fowler and Kilsby,
89 2003b; Jones *et al.*, 2013), and future projections of extremes (e.g. Fowler and Wilby,
90 2010). However, Jones *et al.* (2014) reported that the HadUKP regions do not
91 represent the variability of the frequency, magnitude, and seasonality of daily extremes
92 within each region efficiently.

93 Thus, a new 14 region classification has been developed using daily extremes between
94 1961-2009 to provide reliable estimates of return levels, and describing spatial and
95 temporal characteristics of extremes (Jones *et al.*, 2014). The regions were developed
96 using regional frequency analysis (RFA) and extreme value theory (EVT) suggested
97 by Hosking and Wallis (2005), with a focus on different extremes characteristics such
98 as seasonal timing and magnitude of extremes. The 14 regions showed an improved
99 performance in estimating return levels compared to the HadUKP regions, especially

100 for daily extremes, and indicated clearer upward trends in annual maxima for the
101 investigated period between 1961-2009 (Jones et al., 2014).

102 On the other hand, hydrological designs in the UK adopted the Flood Estimation
103 Handbook (FEH) (Faulkner, 1999) approach as standard practice to estimate return
104 levels and produce growth curves for anticipated locations. The FEH approach
105 propose having data that equals to five times the desired event return frequency. For
106 example, 20-years event requires having data for 100 years. The FEH provides UK-
107 wide growth curves for hourly and daily durations (1h up to 8days), therefore, different
108 bodies have adopted this approach primarily for flood mapping studies, flood risk
109 assessments, and the design of flood mitigation (Kjeldsen *et al.*, 2008). However, using
110 the method to estimate sub-daily events is challenged by the limited and scarce data
111 availability. Furthermore, the FEH approach recommends using similar catchments to
112 assess ungauged locations (Faulkner, 1999), which might provide misleading results
113 for the estimated precipitation levels, especially convective and extreme precipitation,
114 due to noticeable spatial variation in extreme precipitation (Brunsdon et al., 2001;
115 Arnbjerg-Nielsen et al., 2013).

116 Nevertheless, neither the regional estimation approaches (e.g. HadUKP regions), nor
117 the point of interest estimation approaches (e.g. FEH) consider the climatological
118 variable in the UK when estimating return levels, even though significant relationships
119 have been reported between climatological variables (e.g. temperature, atmospheric
120 rivers, atmospheric pressure) and precipitation in the UK (e.g. Wilby et al., 1997; Kilsby
121 et al., 1998; Frei et al., 2006; Lavers et al., 2013; Blenkinsop et al., 2015). Furthermore,
122 the HadUKP regions (Gregory et al., 1991) were defined using precipitation data only
123 and without incorporating the other related climatological variables.

124 **1.2. UK Sub-daily extreme precipitation**

125 In contrast with longer timescales, few studies have investigated sub-daily extreme
126 precipitation in the UK due to the scarcity of quality-controlled, long, and homogeneous
127 observations (Westra et al., 2014; Blenkinsop et al., 2017), despite their relation to
128 pluvial floods and impact on urbanised areas (Dale et al., 2017; Archer and Fowler,
129 2018). Recently, Blenkinsop et al. (2017) investigated the UK observed climatology of
130 sub-daily extreme precipitation and reported noticeable seasonality. Furthermore,
131 investigating the scaling relationship between observed sub-daily extremes and
132 temperature in the UK indicated a potential increase in precipitation intensities events

133 under warmer climate (Blenkinsop et al., 2015). Climatological studies, using climate
134 models, projected an increase in sub-daily precipitation, especially in summer (Chan
135 et al., 2014a; Kendon et al., 2018), while a significant relation with large scale
136 atmospheric circulation (e.g. mean sea level pressure (MSLP), convective available
137 potential energy (CAPE)) has been reported (Chan et al., 2017). Moreover, Kendon *et*
138 *al.* (2018) reported a noticeable difference between hourly and daily extremes
139 predictions in the UK, where the model indicates that hourly extremes would intensify
140 5-10 years and decades earlier than daily extremes in winter and summer seasons
141 respectively. Lately, Lewis et al. (2018) produced 1 km resolution gridded hourly
142 precipitation dataset for the UK, developed using more than 1900 quality controlled
143 gauges.

144 Despite the importance of having a regional assessment of sub-daily extremes in the
145 UK and their potential impacts, none of the studies to date have performed regional
146 frequency analysis using observational data. Studies which have evaluated extreme
147 precipitation events in terms of their impacts and potential adaptations have reported
148 that the lack of thorough choice of statistical distributions and models for extreme
149 events increases the uncertainty, especially when used for generating design
150 guidelines (Hailegeorgis et al., 2013; Simpson and Jones, 2014). Existing studies of
151 sub-daily extremes have focused on individual sites, which is usually challenged by
152 the limited data record, gauging network density, instrumental and human errors
153 (Paixao et al., 2011). Regional assessment would benefit stakeholders to evaluate any
154 location (gauged or ungauged) without limitations related to administrative and
155 regulatory boundaries, and reduce the impact of data scarcity (Durrans and Kirby,
156 2004; Dittrich et al., 2016). Therefore, this research attempts to quantify hourly and
157 multi-hourly extreme precipitation regionally, assess the usage of existing precipitation
158 regions, define the statistical relationship between hourly extremes and related
159 (potentially driving) climatological variables.

160 **1.3. Statistical downscaling**

161 Typically, GCMs and RCMs are used to simulate atmospheric circulation and predict
162 future events. However, the spatial resolution of these is too coarse, and they are
163 usually used to simulate large scale atmospheric circulation. Moreover, Prudhomme *et*
164 *al.* (2002) reported that GCM/RCM simulations and predictions for short time scale
165 events (i.e. less than monthly) has a lower confidence compared to longer durations.

166 Various studies (e.g. Xu, 1999; Maraun *et al.*, 2010b) have reported that using
167 GCMs/RCMs for hydrological assessment might not be suitable due to:

- 168 1- The decreasing accuracy of GCMs/RCMs when applied to hydrological
169 applications of interest, which have fine spatial and temporal scales.
- 170 2- The decreasing accuracy of simulated hydrological variables of interest (e.g.
171 precipitation, potential evapotranspiration) compared to other climatic variables
172 (e.g. temperature, sea level pressure).

173 Therefore, convective permitting models (CPMs) are usually used to simulate
174 atmospheric circulation and climatological events (e.g. precipitation) for small scale
175 and short duration hydrological applications (i.e. high spatial and temporal resolution).
176 However, using CPMs is challenged by the need for high computational resources and
177 long run times (Prein *et al.*, 2015).

178 Consequently, statistical downscaling approaches have been applied to GCM/RCM
179 outputs, especially over urbanised areas, where dynamical simulations are
180 computationally expensive (Maraun *et al.*, 2010b). Statistical downscaling employs the
181 empirical relation between observed weather variables (e.g. precipitation,
182 temperature), and the related climatological variables (e.g. sea level pressure (SLP),
183 surface temperature, dew point temperature (DPT), geopotential height, sea surface
184 temperature (SST), and North Atlantic oscillation (NAO)) to simulate future
185 precipitation patterns at a finer resolution (Benestad, 2010; Arnbjerg-Nielsen *et al.*,
186 2013). Large scale predictors are better represented in models than the variables being
187 predicted (Maraun *et al.*, 2010b), thus statistical downscaling provides the flexibility of
188 modelling extremes and ability to determine regression relations using well established
189 frameworks such as generalized linear modelling (GLM) (e.g. Hertig *et al.*, 2014) and
190 artificial neural network modelling (e.g. Paulin *et al.*, 2005). However, it should be noted
191 that statistical downscaling results and performance depends on the reliability of the
192 defined relationship between the precipitation and climatological predictor variables,
193 which indicates the importance of having accurate climate model outputs (Maraun *et al.*
194 *et al.*, 2010b).

195 Therefore, this research attempts to quantify the statistical relationship between hourly
196 extremes and related (potentially driving) climatological variables, and to use this
197 relationship to develop a reliable statistical model and simulate extreme hourly
198 precipitation in the UK. This statistical model would provide an alternative to the
199 computationally expensive RCMs and/or CPMs, employing the statistical downscaling

200 approach to estimate extreme precipitation frequency and intensity, and quantify the
201 characteristics of extremes (i.e. frequency and intensity) under various climatic
202 scenarios.

203 **1.4. Research aims and objectives**

204 The overall aim of this research is to develop a statistical model employing recently
205 available quality controlled hourly precipitation data and related climatological
206 variables to simulate hourly extreme precipitation intensity and frequency. The
207 outcome of this research would be a methodology to estimate regional return
208 estimates, quantify extremes frequency and intensity, and evaluate potential behaviour
209 under future climate change

210 Therefore, this research will address the following research objectives:

- 211 1- To perform an exploratory analysis of hourly and multi-hourly extremes
212 precipitation, seasonality, diurnal cycle, and return estimates using annual
213 maximum (AMAX) precipitation data.
- 214 2- To assess the efficacy of using existing extreme precipitation regions in the UK
215 to characterise the sub-daily extremes.
- 216 3- To define potentially new UK extreme precipitation regions based on hourly
217 data and other climatological variables.
- 218 4- To estimate hourly precipitation regional return levels by fitting regional
219 statistical distributions using extreme value theory (EVT).
- 220 5- To investigate the statistical relationships between hourly extremes and
221 potential climatological drivers such as the North Atlantic Oscillation (NAO), sea
222 surface temperature (SST), and air temperature.
- 223 6- To build a statistical model to simulate extreme hourly precipitation in the UK
224 using the climatological variables identified in Objective 5.
- 225 7- To apply the statistical model developed to meet Objective 6 to evaluate the
226 frequency and intensity of hourly extreme precipitation under potential climate
227 changes.

228 **1.5. Thesis structure**

229 Chapter 2 reviews literature relating to daily and sub-daily extreme precipitation in the
230 UK. The chapter examines trends in the historical mean and extreme daily precipitation
231 in the UK, and the commonly used methods to analyse precipitation. Furthermore, the
232 chapter outlines the advancement in UK sub-daily extreme precipitation analysis,

233 including a quality controlled hourly precipitation dataset that is used throughout the
234 thesis. Moreover, the chapter highlights future projections of sub-daily precipitation for
235 the UK and associated challenges.

236 Chapter 3 provides an exploratory analysis of hourly and multi-hourly extreme
237 precipitation in the UK. The diurnal cycle, seasonality, and frequency of extremes
238 across the UK are investigated regionally. Furthermore, regional estimation of the
239 return estimates across the UK, and the efficacy of using the existing daily extreme
240 precipitation regions are introduced in this chapter. The work presented in this chapter
241 has been published in Darwish *et al.* (2018), and indicates the need for sub-daily
242 extreme precipitation regions.

243 Chapter 4 presents the development of new UK hourly extreme precipitation regions,
244 which were defined using the quality controlled precipitation dataset, additional
245 climatological variables, and the novel use of European weather patterns.
246 Furthermore, the assessment of the new regions' homogeneity, and their efficacy to
247 analyse hourly extreme precipitation in the UK and estimate return levels, indicates an
248 improved performance compared to the existing UK daily extreme precipitation
249 regions.

250 Chapter 5 employed the new defined regions to develop a statistical model that is
251 simple and efficient to quantify hourly extreme precipitation intensity and frequency in
252 the UK. The model was developed using the extreme value theory and the generalized
253 linear modelling approach. Furthermore, the model included various climatological
254 variables to account for the varying nature of extreme precipitation in the UK.

255 Finally, the main conclusions, summary of results, and the potential future work to
256 enhance and extend this research are presented in Chapter 6.

257

258

259

260

261

262

263

Chapter 2. Literature Review

264

265 This chapter begins with a review of the literature on precipitation trends with a broad,
266 global context and then a focus on the United Kingdom. It is divided into four main
267 sections: firstly, it presents an overview of precipitation formation processes, reviewing
268 global and regional studies (Section 2.1). Second, studies of the climatology and trends
269 in European sub-daily extreme precipitation are reviewed (Section 2.2). Next, trends
270 in UK daily and sub-daily precipitation are reviewed (Section 2.3), then, variables which
271 have an effect on UK precipitation such as atmospheric circulation, oceanic circulation
272 and temperature, are discussed (Section 2.4). Finally, a summary and identified gaps
273 in the existing literature are presented (Section 2.5).

274 **2.1. Precipitation overview**

275 Precipitation usually occurs when moist air rises to higher altitudes where it cools and
276 condenses due to the lower temperature in high atmospheric layers. The rise of the
277 moist air forms clouds full of water drops, which in turn grow larger either due to
278 additional condensation or due to further collision with other droplets. As they grow
279 larger, the droplets' own weight eventually overcome the uplifting air forces and fall
280 due to gravity as precipitation.

281 The geographical location of the UK is responsible for its rapidly changing and unstable
282 weather conditions. To illustrate, seven major air masses from both warm (tropical)
283 regions and cold (polar) regions, each of which has distinctive temperature and
284 humidity characteristics, may affect the United Kingdom causing different precipitation
285 and extreme events to occur (Mayes and Wheeler, 2013). Consequently, precipitation
286 amounts vary significantly across the United Kingdom. The UK Met Office average
287 annual precipitation maps between 1981-2010, show that generally the further west
288 and the higher the altitude, the greater the annual precipitation (Met-Office, 2016).
289 Moreover, the maps show that the mountains of Wales, Scotland, Northern England
290 and South West England are the wettest parts of the country, compared to the south
291 and the southeast geographical. This may be attributed to the different precipitation
292 generating mechanisms in the UK, the varied configuration of the coastline, and the
293 rain shadow effect, where mountainous parts of the South West and Wales force the
294 ascent of air to higher altitudes, leading to precipitation occurrence before moving
295 further towards the southern and southeast regions (Mayes, 2013).

296 Each precipitation type is generated in different temporal and spatial circumstances as
297 follows:

298 1- Relief precipitation occurs when warm, moist air is forced to rise over high areas,
299 cools, and condensation occurs to form precipitation.

300 2- Frontal precipitation, which is common in the UK (Holt *et al.*, 2001), forms as a
301 result of warm and cold air masses meeting. As the air masses have different
302 characteristics, they will not mix and a front will be formed. The warmer air mass,
303 which is less dense than the cold air mass, is forced to rise and accordingly cool
304 with condensation leading to precipitation occurrence.

305 3- Convective precipitation, which is very common in the southern part of the UK
306 during summer (Holt *et al.*, 2001; Holley *et al.*, 2014; Blenkinsop *et al.*, 2015), is
307 a result of heating of an air mass over a warm land surface. This process will
308 cause the air to become warmer and lighter, and be lifted higher, with cooling
309 and subsequently condensation causing precipitation.

310 In the UK, relief and frontal precipitation events are due to synoptic scale systems while
311 convective precipitation is due to local scale events (Mayes, 2000).

312 In recent decades, daily precipitation has shown increasing frequency/intensity trends
313 across different areas around the globe (Westra *et al.*, 2013). Extreme precipitation
314 and climate change with its consequences of increasing, floods, and other
315 environmental, economic and societal impacts have particularly attracted researchers
316 from different fields and disciplines to study and understand their occurrence,
317 frequency, and magnitudes. IPCC (2012) claimed that the impacts of the increasing
318 frequency and intensity of daily extreme precipitation over vast areas of the globe have
319 increased, indicating that it is therefore essential to analyse and predict such events.

320 Recent studies have confirmed that precipitation intensity has increased considerably
321 over recent decades, for both daily (Westra *et al.*, 2013; Alexander, 2016) and sub-
322 daily precipitation (Westra *et al.*, 2014), while 65% of the studied areas around the
323 world experienced increasing annual maximum daily intensity and/or frequency (Min
324 *et al.*, 2011) , which indicates increasing potential for flooding. Lenderink and Van
325 Meijgaard (2008) reported that sub-daily extremes are more sensitive to climate
326 change and potential temperature increase, leading to a greater intensification
327 compared to daily extremes. In the UK, investigating the scaling relationship between
328 the observed hourly extremes and temperature, suggested that precipitation will
329 intensify with temperature according to the Clausius–Clapeyron (CC) relationship

330 (Blenkinsop et al., 2015; Blenkinsop et al., 2018). The CC relationship explains the
331 increased capacity of warmer air to hold moisture under constant relative humidity; a
332 ~6–7% increase in precipitation per 1°C increase in temperature. A general agreement
333 between the studies is that increasing atmospheric temperature could increase
334 precipitation intensities for daily and sub-daily precipitation events.

335 The assessment of a range of data in relation to the impacts of climate change
336 indicates that floods arising as a result of intense precipitation are among the most
337 costly and critical hazards arising as a consequence of climate change (Stern, 2006).
338 These may lead to casualties, infrastructure damage, disruption of transportation links
339 as well as damages to natural ecosystems (Stern, 2006; Gosling *et al.*, 2011; IPCC,
340 2012; Hallegatte *et al.*, 2013). The UK has one of the most vulnerable economies to
341 damages from flooding (Ramsbottom et al., 2012). DEFRA (2012) highlights that
342 insurance claims would increase dramatically in the next decades, which indicates the
343 importance of characterising and understanding intense precipitation. Moreover,
344 Chatterton et al. (2010) predict an increase in the UK flooding costs and damages
345 unless strategic actions and solutions are planted, which makes predicting and
346 simulating extreme events crucial elements in national and international plans in this
347 respect. However, sub-daily extremes have not been studied extensively due to the
348 shortage of the robust data and records that cover long period of time.

349 **2.2. Sub-daily extremes in Europe**

350 Investigating various studies of changes in sub-daily precipitation regionally suggested
351 that most focused on individual sites, while fewer considered regional scale
352 assessment (Westra *et al.*, 2014; Blenkinsop *et al.*, 2018). In Europe, Leahy and Kiely
353 (2011), studied short extreme precipitation in Ireland using thirteen hourly precipitation
354 stations extending from 1957 to 2008. They used the general Pareto distribution (GPD)
355 to fit peaks over threshold (POT) observations for each station, reporting that
356 significant changes were observed in short duration extreme precipitation, where a 30
357 year return period storm shifted to be a 10 year return period, though noticeable spatial
358 variability was observed in the results. The variability and the local variation, which
359 might occur due to the differences in exposure or orography of the stations (Leahy and
360 Kiely, 2011), shows the complexity of the short duration extreme precipitation events
361 and the need for more investigation rather than using traditional statistical methods.

362 Furthermore, Arnone et al. (2013) studied hourly and sub-daily annual maxima for
363 extreme precipitation events (1-, 3-, 6-, 12- and 24 hours) in Sicily using 60 rain gauges
364 for the period 1956 to 2005. They quantified changes in extreme precipitation,
365 observing an increasing trend in sub-daily extremes intensity and a significant increase
366 in their occurrence especially at 1-hour duration, while longer durations (i.e. 12-, and
367 24 hour) extreme precipitation events showed a negative trend. Moreover, an
368 increasing trend in the relative contribution and occurrence of heavy precipitation
369 events occurred, however the total annual precipitation showed a decrease.

370 Hanel et al. (2016) analysed sub-daily heavy summer precipitation events for the
371 Czech Republic, using 17 gauges between 1961–2011. They reported that most of the
372 investigated gauges showed significantly positive intensity trends, and more frequent
373 occurrence of extreme events. Furthermore, more than 50% of the gauges
374 experienced an increasing contribution from extreme precipitation to the total summer
375 precipitation.

376 Recently, Forestieri et al. (2018) used regional frequency analysis approach to analyse
377 the hourly and multi-hourly extremes in Sicily, which helped to identify extremes
378 homogeneous regions, derive regional growth curves, and provide updated return
379 estimates. The results showed that, for low return periods, different distribution
380 performed similarly and accurately, yet for long duration results varied spatially
381 (Forestieri et al., 2018). This indicates the need of having longer hourly extremes
382 record, to assure more accurate results.

383 In concise terms, quantifying sub-daily precipitation is necessary for the management
384 of urban drainage (Arnbjerg-Nielsen et al., 2013) especially under a changing climate,
385 while the lack of long hourly precipitation records and spatial variation of extreme
386 precipitation, makes adaptation to the risk of flash flooding problematic. In particular,
387 this high spatial variability suggests using regional approaches and other related
388 climate variables to understand the sub-daily extremes (Leahy and Kiely, 2011; Arnone
389 et al., 2013; Westra et al., 2014).

390 **2.3. Historical and future precipitation in the UK**

391 In recent decades the UK has experienced significant extreme precipitation derived
392 floods such as the 2004 Boscastle floods (Burt, 2005; Golding et al., 2005) and 2007
393 UK summer floods (Blackburn et al., 2008). UK flood magnitudes and frequency have
394 increased significantly in recent decades (Pattison and Lane, 2012), and are expected

395 to increase in the future (IPCC, 2012), which shed light on the importance of
396 understanding extreme precipitation patterns in the UK, especially that adapting to
397 extreme is a national priority as advised by the UK climate change risk assessment
398 (CCRA, 2017) .

399 UK daily precipitation has been studied using the rich archive of data to analyse and
400 describe trends in extremes and their drivers. These have used both instrumental
401 observations (Alexander and Jones, 2000; Fowler and Kilsby, 2003b; Maraun et al.,
402 2008; Jones et al., 2014; Simpson and Jones, 2014), and climate models (Dale, 2005;
403 Fowler and Wilby, 2010) across different spatial and temporal scales. These studies
404 could be used in risk assessment and management to produce the required
405 recommendations and design guidelines to achieve both adaptation and mitigation of
406 extreme events impacts (Dale *et al.*, 2017). The evidence showed that it is profoundly
407 complicated to simulate and understand the behaviour of extreme precipitation events
408 due to the complex and disproportionate relation between climatological events and
409 their potential drivers (Dale, 2005; IPCC, 2012; Hulme, 2014).

410 Relatively few of studies have investigated sub-daily precipitation events either globally
411 or in in the UK (Westra et al., 2014; Blenkinsop et al., 2018; Darwish et al., 2018), due
412 to sparse observations (Blenkinsop et al., 2017). Besides, the difficulty and the
413 computationally demanding simulation of these events using climate models induce
414 additional challenges to the analysis process (Chan et al., 2014b). Overall, these
415 studies agreed that UK sub-daily extreme precipitation events show a noticeable
416 seasonal behaviour, and further investigation is required to quantify sub-daily extremes
417 frequency, intensity, and future projections (Chan et al., 2014a; Blenkinsop et al., 2015;
418 Tye et al., 2016; Blenkinsop et al., 2017).

419 Hence, this chapter will 1) review major studies that have analysed mean and extreme
420 precipitation including: sub-daily, daily, and multi-daily precipitation, patterns and
421 behaviour of events during different seasons in the UK; 2) review climate model future
422 projections; 3) review the relationship between extreme precipitation and related
423 climatic variables.

424 **2.3.1. UK Mean precipitation**

425 A great deal of literature has investigated precipitation events and their patterns in the
426 mid-latitude and northern hemisphere regions. These indicate a significant increase in

427 the intensity and frequency of precipitation events during the last century (Osborn et
428 al., 2000; Meehl et al., 2007; Pattison and Lane, 2012; Burt et al., 2014).

429 One of the benefits of having a long precipitation data archive in the UK is that it has
430 enabled the study of UK precipitation trends using different methods and techniques
431 for different periods. These studies showed no significant trend in annual UK
432 precipitation (Perry, 2006; de Leeuw *et al.*, 2016). Nevertheless, significant long-term
433 trends and noticeable spatial variations were observed in seasonal precipitation in
434 particular, during winter and summer (Alexander and Jones, 2000; Osborn *et al.*, 2000;
435 Mills, 2005; Leeuw *et al.*, 2015). Trends in UK daily precipitation for each season will
436 be reviewed in this section.

437 • **Winter (Dec-Jan-Feb)**

438 Jones and Conway (1997), who updated the study of Wigley and Jones (1987), studied
439 UK precipitation using nine spatially coherent precipitation regions, where an
440 unweighted regional average approach was adopted for each region during the period
441 between 1767 and 1995. The study found a significant long-term precipitation trend
442 increase of 67 mm and 139 mm over the whole period in England and Wales, and
443 Scotland respectively.

444 Further, Osborn *et al.* (2000) studied trends in the daily intensity of UK precipitation
445 using 110 reasonably evenly distributed gauges recording daily observations for the
446 period between 1961 and 1995. The study categorized total precipitation into ten
447 categories based on their seasonal contributions. The results showed an upward trend
448 in mean winter precipitation, where an increasing number and greater intensity of wet
449 days (day with at least 0.3 mm of precipitation) confirmed this rise. This increase was
450 linked to an upward trend of the North Atlantic Oscillation (NAO) index during the same
451 period. Additionally, Alexander and Jones (2000) used the 9 HadUKP spatially
452 coherent precipitation regions, and average monthly precipitation data for the period
453 1961 to 2000 to find a significant increase in monthly precipitation over the UK with a
454 noticeable increase in the western part of Scotland were in line with previous studies.
455 Extending this study, Mills (2005) tried to model precipitation in the UK using different
456 trends modelling techniques between the year 1766 and 2002 based on monthly
457 series. The results showed that the winter precipitation trend increased 12% between
458 1766 and 2002. Simpson and Jones (2014) also reported an increase in the trend of
459 the 50th, 90th, 95th, and 99th percentile precipitation between 1931 and 2011, although

460 this was not significant in all regions; most of the significant precipitation intensity
461 increase occurred in northern regions and Scotland. Extending the analysis back up to
462 1766 showed significant mean increasing trends over the longer term, especially in
463 England and Wales.

464 Recently, Leeuw et al. (2015) studied the variability and trends of mean precipitation
465 in the UK. The study used the daily average of the spatially distributed rain gauges in
466 the 9 UK precipitation regions which were used by Alexander and Jones (2000) for the
467 period 1931 to 2014. The results agreed with previous research, detecting a positive
468 winter precipitation trend. Moreover, a decrease in the contribution of lighter
469 precipitation events and an increase in the contribution of extreme precipitation events
470 to the total seasonal precipitation are observed.

471 • **Spring (Mar-April-May)**

472 Generally speaking, spring has shown no significant long term trends (Alexander and
473 Jones, 2000; Osborn *et al.*, 2000; Mills, 2005; Jones *et al.*, 2013; Leeuw *et al.*, 2015;
474 de Leeuw *et al.*, 2016). Osborn *et al.* (2000) reported a weak increase in mean
475 precipitation in Northern Ireland and Scotland due to an increasing number of wet days,
476 while England has experienced a decline in the number of wet days resulting in a slight
477 decrease in mean precipitation.

478 Using spatially averaged monthly series, Alexander and Jones (2000) found that an
479 increasing trend is observed in March while a decreasing trend was observed in April
480 for the period between 1766 and 2000 over England and Wales. On the other hand,
481 Mills (2005) supported the results of (Osborn *et al.*, 2000), and showed that spring
482 experienced a fluctuating trend for the period from 1766 to 2002, with a weak
483 increasing trend. The study showed that a positive trend was observed in March and
484 April, while May showed a negative trend. More recently, de Leeuw *et al.* (2016) who
485 studied the spring precipitation trend for the period 1931 to 2014 and three sub periods
486 1961-2006, 1961-2014, and 1979-2014, reported that large interannual variability were
487 observed in spring, and no significant trend can be determined.

488 • **Summer (June-July-August)**

489 A great deal of literature has reported that long term mean summer precipitation has
490 shown a negative trend (Wigley and Jones, 1987; Jones and Conway, 1997; Alexander
491 and Jones, 2000; Osborn *et al.*, 2000; Mills, 2005; Simpson and Jones, 2014);
492 nevertheless, some recent research has shown that recent decades experienced a

493 positive trend in summer precipitation in the UK (Simpson and Jones, 2014; de Leeuw
494 et al., 2016). Osborn et al. (2000), using daily observations between 1961 and 1995
495 from 110 gauges, reported a weak decline in seasonal summer precipitation totals at
496 most UK gauges, with a reduction in the contribution of heavy precipitation categories.
497 Additionally, the study found that the number of wet days decreased in 90% of the
498 gauges during the same period, which in turn results in a decline in mean seasonal
499 precipitation levels. These results were confirmed by Alexander and Jones (2000) who
500 reported a significant decrease in the total precipitation amount in every region during
501 July and August between 1873 and 2000 across England and Wales. Alexander and
502 Jones (2000) explained that the precipitation decrease could be due to an increase in
503 anticyclonic conditions which might be the reason for the negative trend . Mills (2005)
504 used monthly data extended back to 1766, reporting consistent results with the
505 previous research and confirmed a negative trend in summer precipitation, specifically,
506 during June and July.

507 Later, Simpson and Jones (2014) reported a similar pattern for daily precipitation over
508 the period 1931 to 2011 with mostly negative intensity trends in the 9 regions except
509 in North East England, though the researchers argued that this negative trend is within
510 the range of natural variability. Most recently, de Leeuw *et al.* (2016) analysed daily
511 precipitaton over a similar period and reported that the seasonal precipitation trend
512 showed a decrease up to the end of the last century, changing to become positive
513 between 2007 and 2012. The study attributed this change to the fact that these years
514 had greater total precipitation than the long term average (1931 to 2014), and both
515 2007 and 2012 were the wettest summer season in the record.

516 • ***Autumn (Sep-Oct-Nov)***

517 Mean autumn precipitation in the UK has generally shown no significant long-term
518 trend. Osborn *et al.* (2000) reported a weak decrease in the number of wet days (days
519 with at least 0.3 mm of precipitation) in England, although the mean wet days
520 precipitation total increased in 91 out of 110 gauges. This increased the seasonal mean
521 precipitation especially in North Scotland and Southwest England, though no
522 significant trend was observed. Nevertheless, Alexander and Jones (2000) found an
523 increase in the precipitation amount in Scotland and North Ireland during October and
524 November between 1931 and 2000, though not enough evidence for a significant long-
525 term trend in autumn mean precipitation.

526 Mills (2005) supported the preceding argument and pointed out that observing a
527 significant and a clear trend for autumn precipitation in the UK is relatively difficult to
528 identify due to annual and seasonal variability. Mills (2005) reported that different
529 trends were found throughout the record (1766-2002), and no significant trend can be
530 determined. This result was validated by Simpson and Jones (2014), who extended
531 the precipitation data record period to 2011, reporting that the monthly mean record
532 revealed a significant increasing trend only in Scotland, and a decreasing trend in
533 England and Wales, though both are within the bounds of natural variability.

534 **2.3.2. UK daily extreme precipitation**

535 Different studies have attempted to identify, describe and characterise extreme
536 precipitation events in the UK using various methods and techniques (e.g. Fowler and
537 Kilsby, 2003b; Maraun *et al.*, 2008; Fowler and Wilby, 2010; Burt and Ferranti, 2012;
538 Simpson and Jones, 2014). The studies agree on significant seasonal behaviour in the
539 trends of extreme precipitation events in recent decades, with a noticeable spatial
540 variation (Fowler and Kilsby, 2003a; Jones *et al.*, 2014; Simpson and Jones, 2014).
541 The UKCP18 reported an increase about 17% in the total precipitation from extremely
542 wet days in the last decade compared to the 1961-1990 period, especially in northern
543 regions (i.e. Scotland), while a non-significant increase occurred in southern regions
544 (Lowe *et al.*, 2018). The increases in extremes is likely to result in increased flooding
545 (Fowler and Wilby, 2010; Westra *et al.*, 2014). Trends in UK daily extreme precipitation
546 in each season will be discussed and presented in this section.

547 • **Winter (Dec-Jan-Feb)**

548 Generally speaking, the analysis of winter daily extremes has used different indices to
549 characterise trends in precipitation such as the annual maxima precipitation
550 accumulation, multi-daily precipitation extremes, 90th-, 95th-, and 99th- percentile,
551 indicated a significant increase in winter precipitation intensity trends.

552 Simpson and Jones (2014), extracted daily precipitation data from the Met Office
553 Hadley Centre 5km gridded dataset extending from 1931 to 2011. Using the HadUKP
554 regions (Alexander and Jones, 2000), they adopted different indices for each season
555 such as, the 50th, 90th, 99th percentiles, maximum 5-day precipitation total and the
556 consecutive dry day index (longest number of consecutive days with less than 1 mm
557 precipitation) to evaluate extreme precipitations trends. The results showed an

558 increase in trends in daily extremes in all UK regions and for all indices, especially, in
559 the Scottish and northern regions.

560 Similarly, Jones *et al.* (2013), who extended the Fowler and Kilsby (2003b) extreme
561 precipitation analysis, and used 223 gauges covering the UK, reported a significant
562 increase in the intensity of the 1-day extremes in all regions with an inter-decadal
563 behaviour. Furthermore, long duration events (5- and 10 days) showed an increasing
564 trend in northern parts of the UK. In addition, Fowler and Kilsby (2003b) who studied
565 204 rain gauges using the regionalization method and HadUKP regions, reported that
566 most regions showed a significant increase in the daily and multi-daily (2-, 5-, 10 day)
567 extreme precipitation intensity, especially in Scotland, though some regions in England
568 only showed a slight increase.

569 Burt and Ferranti (2012), who used precipitation data between 1961 and 2006, adopted
570 the analysis method used by Osborn *et al.* (2000) and Maraun *et al.* (2008), studying
571 percentiles of extreme precipitation events across regions using different indices, and
572 focusing on the top category of each gauge, contributing 10% of the total precipitation.
573 They also analysed the daily total that is equalled or exceeded on 0.25% of all days (1
574 in 400 years), the results agreeing with the earlier results of Osborn *et al.* (2000) and
575 Maraun *et al.* (2008), indicating extreme precipitation intensity has increased
576 significantly, especially in northern and western parts of the UK.

577 Finally, Brown *et al.* (2008) analysing daily precipitation data for 1958 to 2004 reported
578 that return level estimates for 1-day extremes show wetter winters with higher intensity,
579 yet less frequent extreme events, especially in the west of the UK.

580 • **Spring (March-April-May)**

581 Extreme spring precipitation has shown fluctuating results. Simpson and Jones (2014),
582 used a range of indices to identify upward trends, especially in Scotland, though few
583 of these were statistically significant. Jones *et al.* (2013) reported similar results, with
584 the regional median seasonal maxima for the spring between 1961 and 2009 showing
585 an increase across most UK regions, though the results are significant in northern
586 regions only. They attributed the increasing trend in these regions to the exceptionally
587 heavy long duration events which dominated the 1991-2000 decade. Furthermore,
588 eastern regions in the UK had a “marginal increase” in the 1-day precipitation 10 year
589 return period totals, while varying trends were observed at longer return periods (25

590 and 50 years). In addition, the most significant return estimate increases were
591 observed for long duration accumulations (5- and 10-days).

592 Maraun *et al.* (2008) reported positive trends and a higher contribution from extreme
593 precipitation events to the total precipitation in Scotland, North Ireland, and Southwest
594 England, while, other regions displayed either little or marginal negative trends. These
595 results agree with Osborn *et al.* (2000), who observed high spatial variability in the
596 results with an increasing contribution of heavy precipitation events to total spring
597 precipitation in Scotland and central and eastern England, while the opposite was
598 observed in Wales, North and Southwest England.

599 Finally, Fowler and Kilsby (2003a) found that the greatest changes and the most
600 regionally varying trends in HadUKP regions (Alexander and Jones, 2000) occurred in
601 spring and autumn, in agreement with Osborn *et al.* (2000), who reported an increasing
602 contribution of heavy precipitation to total precipitation in Scotland and central and
603 eastern England, while the opposite occurred in Wales, North and Southwestern
604 England.

605 • **Summer (June-July-August)**

606 Studies that considered summer precipitation trends have consistently identified
607 decreasing trends in most UK regions, especially the southern part of the UK. Simpson
608 and Jones (2014) observed that extreme summer precipitation intensity trends
609 declined (not statistically significant) across most UK regions for daily extremes, except
610 in eastern England.

611 The findings of Jones *et al.* (2013), using precipitation data between 1961 and 2009,
612 were in line with those of Fowler and Kilsby (2003b) and reported significant decrease
613 in estimated summer extreme precipitation return levels and median seasonal
614 maximum event, especially for 1-day events in southern regions. In addition, Jones *et al.*
615 (2013) and Burt and Ferranti (2012) agreed that the percentage contribution of the
616 heaviest precipitation to total summer amount has decreased.

617 Maraun *et al.* (2008) and Osborn *et al.* (2000) reported that UK summer precipitation
618 intensity time series shows an inter-annual behaviour, which was evidenced by a
619 distinct maximum in the late 1960s followed by a downward and varying behaviour.

620 • ***Autumn (September-October-November)***

621 Spatially and temporally varying trends have been identified in autumn extreme
622 precipitation. Recently, Tye et al. (2016) simulated the spatial and temporal patterns of
623 extreme daily precipitation occurrence using a generalized additive model, and
624 reported that autumn extreme daily precipitation has a higher likelihood across the UK
625 than in the previous century. Moreover, autumn extreme daily precipitation events are
626 mostly associated with a higher probability of occurrence during either early autumn in
627 the north and west, or later in the season in the south and east(Tye *et al.*, 2016).

628 Simpson and Jones (2014) observed that trends in autumn 1-day extreme precipitation
629 over the past century were weak and showed mixed signals. On the other hand, the
630 authors agreed with previous results in which a positive trend was observed in the
631 intensity during autumn multi-day (5- and 10-days) extreme precipitation in several
632 regions, especially Scotland (Fowler and Kilsby, 2003a; Maraun et al., 2008; Jones et
633 al., 2013; Jones et al., 2014). These trends were though statistically insignificant in
634 most regions, with no clear evidence to discern the trends from naturally short-term
635 variability.

636 Furthermore, Maraun et al. (2008) confirmed earlier results by Osborn et al. (2000),
637 and reported spatially varying results, where a significant rise in the contribution of
638 autumn heavy precipitation events to total precipitation across the UK was identified,
639 with the exception of Northern Ireland and Northwest England, which showed
640 insignificant decreasing contribution trends.

641 Allan et al. (2009) also found that autumn trends were within the limits of natural and
642 decadal variability and thus, in the absence of definitive evidence contrary to that
643 reviewed from the literature, it may be assumed that no long-term trend can be
644 identified during autumn.

645 ***2.3.3. UK sub-daily precipitation***

646 As discussed earlier, long-term sub-daily data observations are scarce in both: globally
647 and in the UK. Therefore, climatological analysis of sub-daily (including hourly) UK
648 extremes are limited in the literature (Westra et al., 2014; Blenkinsop et al., 2018;
649 Kendon et al., 2018). Extreme short precipitation is the major source for pluvial
650 flooding, which is expected to increase under different climate change scenarios, and
651 add more challenges to adaptation plans (Murray and Ebi, 2012). Hand et al. (2004)
652 analysing 50 UK precipitation events identified as extreme by the Flood Studies Report

653 (NERC, 1975) showed that among the investigated events, all those of less than 5 hr
654 duration were convective, which indicates the importance of characterising short
655 intense precipitation.

656 The Flood Estimation Handbook (FEH) provides UK-wide estimates of annual
657 maximum median (RMed) precipitation for hourly and daily durations (1h up to 8 days),
658 and is used to produce design precipitation estimates (Faulkner, 1999). However, the
659 AMAX gauges data average record length is less than 23 years (22.7 years), while
660 some gauges have a record length of 2 years only, and further data is needed to assure
661 reliable estimates (Kjeldsen *et al.*, 2008). Furthermore, Dale *et al.* (2017), using a
662 climate analogue approach and a very high-resolution (1.5 km) climate model, reported
663 that new hourly precipitation projections are higher than existing UK climate change
664 allowances for intense precipitation, while flood volume and pollution events are
665 expected to increase in the future. Therefore, characterising hourly extremes in the UK
666 is essential to update the precipitation estimates, design guidelines, and to implement
667 adaptation plans.

668 Blenkinsop *et al.* (2017) reported that when investigating hourly precipitation totals in
669 the UK, 1-, 3-, and 6 hour totals show a similar spatial intensity behaviour, where
670 precipitation is more intense to the west of the UK. Moreover, these short duration
671 totals are mainly a function of local scale events, while events of periods longer than
672 12 hours are usually mediated by synoptic scale features. Blenkinsop and Fowler
673 (2013) also drew attention to the importance of assessing hourly precipitation events
674 using different approaches such as seasonal maxima and POT seasonal data to
675 ensure having reliable results.

676 Thus, Blenkinsop *et al.* (2017) produced precipitation dataset, which were collated from
677 precipitation gauges spanning across the UK between 1949 and 2011, and subjected
678 to a series of strict quality-control (QC) procedures to identify potentially suspect
679 values, and assure having a reliable dataset. Moreover, Lewis *et al.* (2018) extended
680 the work up to 2014 and developed a sub-daily gridded dataset.

681 Blenkinsop *et al.* (2017) investigated hourly precipitation extremes in the UK using the
682 annual maxima, and reported that during summer, southern parts experience the
683 greatest intensity and frequency of hourly precipitation, while the diurnal cycle peaks
684 in late afternoon to early evening. This is indicative of the generating mechanism of
685 extremes during summer, where sub-daily events are generated with a significant

686 contribution of convection occurring due to the relatively high temperatures, in contrast
687 with extremes occurring at other times of the year through other mechanisms (e.g.
688 frontal or orographic precipitation).

689 Recently, Xiao et al. (2018), who analysed mean hourly precipitation intensities
690 collected from 90 stations in the UK for the period 1998 to 2015 to characterise UK
691 hourly precipitation, reported that UK precipitation frequency and intensity peaks in the
692 early morning and the late afternoon respectively. A noticeable relationship between
693 the peak time and both the location and the duration of the precipitation event was
694 observed, with most of the long duration events (i.e. lasting > 6h) occurring in the early
695 morning and along the western coast, and short precipitation events (i.e. lasting < 6
696 hr) occurring in the late afternoon. They also reported noticeable spatial variation in
697 frequency especially during summer and spring, which is consistent with Blenkinsop et
698 al. (2017) who used hourly extremes, though a larger dataset was used.

699 **2.3.4. Future Projections**

700 Climate model projections show an increase in precipitation frequency and intensity
701 over the northern regions of the hemisphere and northern Europe, which highlights the
702 potential related hazards such as increasing flooding and the need of reliable future
703 estimates (Hartmann et al., 2013).

704 In the UK, daily and multi-daily extremes have been studied and simulated using
705 climate models, where projections have shown that the frequency of extreme
706 precipitation events are projected to increase during winter, whereas, in summer less
707 intense extreme precipitation is likely to occur (Fowler and Ekström, 2009; Murphy et
708 al., 2009; Fowler and Wilby, 2010). The recently released UKCP18 (Lowe *et al.*, 2018)
709 projections indicate reductions in summer precipitation intensity trends, especially over
710 England and Wales, while a gradual increase is projected in winter. Climate model
711 projections show broad agreement with observational studies (Osborn *et al.*, 2000;
712 Burt and Ferranti, 2012; Simpson and Jones, 2014), though daily and multi-daily
713 extremes are well simulated by regional climate models in all seasons except in
714 summer (Lean et al., 2008; Hanel et al., 2009; Chan et al., 2013).

715 However, to date few studies have examined projections of changes in sub-daily
716 precipitation extremes because of the inability of coarse-resolution dynamical models
717 to reliably simulate sub-daily precipitation and in particular extremes (Chan *et al.*,
718 2018b; Kendon *et al.*, 2018).

719 Kendon *et al.* (2014) investigated hourly extreme precipitation with climate change in
720 the UK using a high resolution model, and reported that the model simulations indicate
721 an increase in hourly extremes intensity in winter, while a significantly intensification
722 and increasing number of extreme events in summer leading to flash floodings.
723 Recently, Kendon *et al.* (2018), using the 1.5 km climate model to assess southern UK
724 region, confirmed the projected intensification, and projected hourly extremes would
725 intensify 5-10 years and decades earlier than daily extremes in winter and summer
726 seasons respectively. Therefore, reliable observational and statistical studies are
727 required to improve future simulations and enhance our return estimates and
728 hydrological design guidelines.

729 **2.4. Extreme precipitation related climatic variables**

730 Hydrological and climatological studies have constantly indicated a strong relation
731 between the extreme precipitation and various climatic variables. The studies
732 emphasised on the climate variability and extreme precipitation caused by the oceanic-
733 atmospheric across the UK. Thus, this section will present the associated climatic
734 circulation with extreme precipitation in the UK.

735 **2.4.1. Atmospheric Circulation**

736 European climate is highly variable and affected by wide range of large-scale
737 circulations, which are produced by atmospheric and oceanic conditions. The impact
738 of these large circulations is obvious in Europe due to its location in mid and high-
739 latitudes, bounded by the North Atlantic and Arctic Oceans (Jones and Conway, 1997;
740 Hurrell and Deser, 2010; Woollings, 2010). These large-scale circulations affect winds,
741 precipitation and temperature in Europe.

742 The uneven solar heating of the planet causes differences of atmospheric pressure
743 which controls the movement of airflow (Woollings, 2010). In Europe, the irregular
744 fluctuation of atmospheric pressure over the North Atlantic Ocean has a strong effect
745 on the atmospheric circulation pattern especially over Western Europe and it is
746 considered as the dominant mode of northern hemisphere atmospheric variability
747 (Scaife *et al.*, 2008; Hurrell and Deser, 2010; Woollings, 2010). This fluctuation of
748 atmospheric pressure called the North Atlantic Oscillation (NAO), is characterised by
749 the pressure difference between high pressure centred over the Azores islands and
750 low pressure centred over Iceland (Hurrell and Deser, 2010). The NAO has two phases
751 representing the pressure gradient between the Azores and Iceland, where the positive

752 phase denotes strong and higher than usual pressure difference, and the negative
753 phase denotes weak and lower than usual pressure difference (Osborn et al., 1999).

754 This atmospheric pressure gradient between the two locations (i.e. Azores islands and
755 Iceland) controls the westerly winds, which flow from North America towards Europe,
756 particularly, during winter (Jones and Conway, 1997; Trenberth et al., 2007). The
757 westerly winds control the transport of heat and moisture, which in turn have impacts
758 on both temperature and precipitation over western Europe (Uvo, 2003).

759 During the positive NAO mode, the westerly winds become stronger and convey more
760 moist air over northern Europe. This contributes to a rise in temperature and
761 precipitation over northern parts of Europe and the opposite over southern parts
762 (Guerreiro et al., 2014). Conversely, the negative NAO mode creates weaker westerly
763 winds, consequently, the temperature decreases along with precipitation over northern
764 Europe; with the opposite over southern Europe.

765 In the UK, precipitation tends to be inversely correlated with atmospheric pressure, and
766 highly influenced by the NAO phase, therefore the NAO index has been used to study
767 UK weather (Murphy and Washington, 2001). Osborn et al. (2000) reported that during
768 UK winter, the positive NAO phase generates strong westerly winds, leading to more
769 intense and frequent precipitation events, especially in west and north parts of the UK.
770 Furthermore, observed increases in the total amount of precipitation and the number
771 of wet days are associated with a positive NAO (Osborn et al., 2000).

772 In the previous century, the NAO showed significant variability. During the first four
773 decades (1900-1940), the NAO showed a strong positive and increasing trend, which
774 was followed by a downward trend for the period between 1940 and 1970, and an
775 increasing trend from 1970 until the end of the century. This increasing trend in recent
776 decades might explain the observed increasing precipitation and intensity in northern
777 and western parts of the UK (Gillett, 2005; Simpson and Jones, 2014). This variability
778 in the NAO has been attributed to different variables and processes. Osborn (2004)
779 claimed that this upward trend is associated with a stratospheric cooling and deeper
780 polar vortex. However, the IPCC (2007) suggested that NAO decadal variability might
781 be due to extratropical ocean influences, land surface forcing and other external
782 factors. Yet, no solid scientific agreement or explanation for NAO variability during the
783 last century has been established (Woollings, 2010).

784 Recently, Brown (2018) reported that positive NAO would reduce the extreme
785 precipitation during spring and autumn, however, increasing the likelihood during
786 winter. Positive NAO phase during winter would increase both: intensity and frequency
787 of extremes, which is similar to the NAO driven changes in extra-tropical cyclones

788 Alternatively, other studies have found that in the UK, airflow strength, direction and
789 vorticity may be used as covariates to represent atmospheric circulation (Jenkinson
790 and Collison, 1977; Jones et al., 1993; Maraun et al., 2010a). Airflow strength
791 represents the air mass speed over a specific area and it is highly likely to be related
792 to the NAO, while airflow direction signifies its source (Marshall et al., 2001). Moreover,
793 the airflow vorticity indicates whether a cyclonic or an anticyclonic airflow is dominant.
794 Maraun et al. (2010a) reported that for the western coast of the UK, especially in
795 Scotland, using the airflow strength only as a covariate would provide a better
796 prediction for the 90% quantile precipitation compared to the base model. These
797 results are consistent with the previous results (Osborn et al., 2000) in which a
798 significant relation between the NAO phase and precipitation in the western part of the
799 UK was found.

800 Maraun et al. (2010a) reported that airflow direction is a crucial covariate in predicting
801 precipitation in the UK except in Scotland and the western coast, while airflow vorticity
802 is a better predictor in Scotland and the northern parts of the UK. Conway et al. (1996),
803 using the airflow indices (i.e. strength, direction and vorticity) in GCMs, found that
804 vorticity has a strong influence on the probability of precipitation and the mean wet day
805 amount in all regions of the UK, especially in winter. On the other hand, the influence
806 of flow strength and the direction indices is weaker than the vorticity, and is regionally
807 dependent. These results were confirmed by Osborn et al. (1999) who found that
808 vorticity has a higher correlation with the precipitation amount compared to other
809 indices. However, the studies agreed that airflow indices predict the wet day probability
810 more precisely than the mean wet day amount (Conway et al., 1996; Osborn et al.,
811 1999).

812 **2.4.2. Oceanic circulation**

813 Oceanic circulation has a significant impact on our climate and weather globally. It has
814 a key role in transferring heat, water mass movement, cycling and storage of chemical
815 species, and nutrient content of the oceans (Kuhlbrodt et al., 2007). The oceanic
816 circulation is a result of the combined oceanic current that moves the seawater in the

817 oceans, forming a global conveyor belt which moves due to winds, heat and density
818 difference (Trenberth and Caron, 2001). In the mid to high-latitude, the Atlantic
819 Meridional Overturning Circulation (AMOC) is the dominant current which affects the
820 Atlantic Ocean and the climate of the northern and western countries in Europe.

821 The Atlantic Meridional Overturning Circulation (AMOC) conveys the salty and warm
822 water in its upper layer toward the northern parts of the Atlantic ocean while colder
823 water is transferred to the southern parts of the Atlantic by deep water layers (U.S.
824 Geological Survey, 2012). This movement of warm water toward the northern parts of
825 the Atlantic Ocean brings heat (up to 10^{15} W) from the tropics and southern hemisphere
826 toward the North Atlantic, which maintains the mild climate in northwestern Europe
827 (Trenberth and Caron, 2001; Kuhlbrodt et al., 2007).

828 In recent decades, there has been a concern about the AMOC response to climate
829 change and its impacts. This concern is raised due to the melting of the Greenland ice
830 sheet and the increasing precipitation events at high-latitudes which cause a
831 weakening of the AMOC (Allen and Ingram, 2002). A reduction of the AMOC could
832 affect the El Nino Southern Oscillation (ENSO), the position of the intertropical
833 convergence zone, Atlantic Ocean fauna and flora, Atlantic ocean sea surface
834 temperature, and sea level, resulting in more severe winters in north and western
835 Europe (Trenberth and Caron, 2001; Vellinga and Wood, 2002; Levermann *et al.*,
836 2005; Schmittner, 2005; Timmermann *et al.*, 2005). In contrast, other researchers
837 reported that a weakening of the AMOC could counterbalance the effect of the globally
838 increasing temperature (Meehl et al., 2007).

839 However, studies agree that despite uncertainties in the AMOC behaviour, it is unlikely
840 for the AMOC to have unforeseen significant weakening or a complete shutdown, and
841 an abrupt change or shutdown of the AMOC would need a long duration to take place,
842 while the expected maximum reduction is 30% (Meehl *et al.*, 2007; Clark *et al.*, 2008).
843 The occurrence of such an event would have a significantly severe effect on north
844 western Europe winter, temperature levels and precipitation events, and it is highly
845 unlikely to happen in the 21st century (Meehl *et al.*, 2007; Clark *et al.*, 2008).

846 **2.4.3. Temperature**

847 The global mean temperature has increased significantly in the last century mostly due
848 to anthropogenic activities which increased the concentration of greenhouse gases in
849 the atmosphere (IPCC, 2013). Based on different climate models, using different

850 emission scenarios, this increase is projected to escalate during the current century to
851 between 2°C to 4°C (IPCC, 2012). The increase in mean global temperature would be
852 accompanied by changes in atmospheric and oceanic circulation, which in turn would
853 impact on precipitation globally, while substantial changes in the mid and high-latitude
854 precipitation will be observed (Collins et al., 2013; IPCC, 2013).

855 The Clausius-Clapeyron (C-C) equation describes the thermodynamic response of the
856 atmosphere to a change in temperature, indicating that under constant relative
857 humidity an increase of the moisture holding capacity of the atmosphere at a rate of 6-
858 7% per 1°C increase in temperature would occur, leading to a corresponding increase
859 in precipitation (Trenberth et al., 2003). However, increases in precipitation in different
860 places globally might not follow the C-C equation due to two main reasons: the
861 nonlinearity in the C-C equation, and the dependency of precipitation on other factors
862 such as the relative humidity, the atmospheric circulation, and the ability of the
863 troposphere to radiate away latent heat released by precipitation (Allen and Ingram,
864 2002).

865 Furthermore, different models have suggested that a latitudinal dependence is
866 expected in the increasing precipitation, with a higher increase expected closer to the
867 higher-latitudes (Trenberth, 2011; Utsumi *et al.*, 2011; O’Gorman, 2015). Further, the
868 mid-latitudes precipitation increases would be the most consistent with the C-C
869 equation, while low-latitudes and high-latitudes are suggested to have an increase of
870 3-4%/°C and 7%/°C consecutively (Allen and Ingram, 2002; Huntington, 2006; Pall *et*
871 *al.*, 2007). Recently, Westra et al. (2014) have shown that an increase at a rate
872 between 5.9%-7.7%/°C in the median intensity of the annual global maximum has been
873 observed.

874 Observational studies, which have investigated daily precipitation events, indicated an
875 increase following the C-C relation. Liu and Allan (2012) using global satellite
876 observations reported a precipitation increase of 6%/°C. Haerter *et al.* (2010),
877 investigated daily extreme precipitation in Germany and its relation to other variables
878 using the C-C equation, and reported that there is an increasing trend, though less
879 than expected according to the C-C relation.

880 On the other hand, sub-daily extreme precipitation events have shown markedly
881 varying results. Berg and Haerter (2013) reported that hourly precipitation intensity in
882 Germany has increased at a rate higher than the C-C relation for convective

883 precipitation events only, which emphasize the impact of seasonal dependence as
884 convective precipitation primarily occurs in summer. In the Netherlands, western
885 Europe and Hong Kong, the precipitation relationship with temperature was double the
886 C-C rate for the temperature range between 12°C to 20°C (Lenderink and Van
887 Meijgaard, 2008; Lenderink *et al.*, 2011). Hardwick Jones *et al.* (2010) found that the
888 rise on the hourly precipitation intensity rate exceeds the C-C relation in Australia for
889 the for temperatures between 20°C to 26°C. Contrary, hourly extreme precipitation
890 intensity in the UK, showed an increase following the C-C scaling rate, with marginal
891 seasonal differences (Blenkinsop *et al.*, 2015; Chan *et al.*, 2016).

892 **2.4.4. Atmospheric moisture**

893 Atmospheric moisture availability, which has a significant relation with temperature and
894 evapotranspiration levels, plays a crucial role in determining precipitation occurrence
895 and intensity (Barry and Chorley, 2009). The moisture cycle begins with oceans, in
896 which the water vapour enters the atmosphere by evaporation from the oceans and
897 returns to the surface as a precipitation through the condensation process (Barry and
898 Chorley, 2009). This moisture is responsible for 60% of global terrestrial precipitation
899 (Trenberth *et al.*, 2007; Gimeno *et al.*, 2012). Recent decades showed an increase in
900 the oceanic evaporation due to climate change, which lead to the occurrence of
901 extreme events including, heavy precipitation, floods, and droughts (Galarneau *et al.*,
902 2010; Knippertz and Wernli, 2010; Chang *et al.*, 2012; Xu *et al.*, 2015).

903 The literature suggests that the change in the atmospheric moisture capacity might
904 affect the nature of precipitation events, causing increased occurrence of heavy
905 precipitation, with no change or even a decrease in mean precipitation (Allen and
906 Ingram, 2002; Trenberth *et al.*, 2003; Frei *et al.*, 2006). In recent decades, over the
907 northern hemisphere regions, human anthropogenic activities were the main reason
908 for the increasing atmospheric moisture capacity (Gabriele *et al.*, 2015), where an
909 increase at a rate consistent with the C-C relation has been observed (Santer *et al.*,
910 2007; Durre *et al.*, 2009; Trenberth, 2011). This is consistent with observations of
911 change over the ocean (e.g. Trenberth and Shea, 2005; Chung *et al.*, 2014), land (e.g.
912 Willett *et al.*, 2010), and future projections (e.g. Allen and Ingram, 2002). Furthermore,
913 studies have linked the change in the atmospheric moisture capacity over oceans to
914 the C-C relationship, while the increases are somewhat less over land, especially
915 where water availability is limited (Allen and Ingram, 2002; Trenberth *et al.*, 2003).

916 Trenberth *et al.* (2007) reported that an increase in cloud cover and atmospheric
917 moisture over oceanic areas since 1970 has been observed, which lead to an
918 increasing frequency of intense precipitation events. These results are consistent with
919 (Labat *et al.*, 2004), who used reanalyses of the world continental runoff from major
920 rivers between 1920 and 1995, where it was found that a more intense hydrological
921 cycle of evapotranspiration and intense precipitation globally has occurred. This
922 increase in the moisture capacity could affect both the greenhouse effect and the
923 hydrological cycle by providing positive feedback to the climate change and more
924 atmospheric moisture which would be condensed and turned into heavy precipitation
925 (Huntington, 2006; Trenberth, 2011; Gabriele *et al.*, 2015).

926 **2.5. Summary**

927 Intense precipitation has increased noticeably in the last few decades both globally
928 and in the UK, leading to economic, infrastructure, urbanisation, and health challenges.
929 Different plans and design guidelines are required to adapt to extreme precipitation,
930 yet, further analysis is required to characterise and simulate these extremes. In the
931 UK, studies have analysed extremes on different time scales (i.e. multi-daily, daily, and
932 sub-daily) using both observational and modelling analyses.

933 Daily and multi-daily extreme precipitation have been studied thoroughly in the UK
934 using the advantage of having a rich archive of rain gauge data. Observational studies,
935 using different metrics and indices, have agreed that precipitation trends show wetter
936 winters and drier summers. These are accompanied by trends indicating a higher
937 contribution of extremes to the total seasonal precipitation, which indicates the
938 importance of characterising extremes in the UK (Jones and Conway, 1997; Alexander
939 and Jones, 2000; Fowler and Kilsby, 2003b; Maraun *et al.*, 2008; Jones *et al.*, 2013).
940 Furthermore, autumn and spring showed a spatial and temporal varying trend through
941 the last few decades, though no significant trends were observed in these seasons
942 (Alexander and Jones, 2000; Simpson and Jones, 2014). These results are consistent
943 with projected future changes, and indicate that general circulation models (GCM) and
944 regional climate models (RCM) can simulate daily and multi-daily precipitation reliably
945 (Fowler and Wilby, 2010; Maraun *et al.*, 2010b).

946 Relatively few studies have characterised sub-daily extremes in the UK due to the
947 limited data availability, though they have a strong association with flash flooding,
948 especially in urbanised areas and fast responding catchments (Dale *et al.*, 2017; Prein

949 *et al.*, 2017). Observations of UK hourly extremes show spatial and seasonal variation,
950 with a higher frequency in summer, especially in southern regions (Blenkinsop *et al.*,
951 2017). On the other hand, modelling studies agreed that using RCMs to simulate hourly
952 extremes is computationally expensive, while return estimates don't agree with
953 observational studies, especially in summer (Chan *et al.*, 2018a; Kendon *et al.*, 2018).
954 Thus, convective permitting models (CPMs) are used to simulate sub-daily extremes
955 with high resolution, due to its potential of providing dynamical representation of
956 convective conditions. Studies indicated that CPM simulates the sub-daily extremes
957 better than standard climate models, and might be used to provide improved
958 precipitation projections (Prein *et al.*, 2017; Blenkinsop *et al.*, 2018; Chan *et al.*, 2018a;
959 Kendon *et al.*, 2018). Therefore, further observational studies are of importance to
960 validate and calibrate modelling performance (Blenkinsop *et al.*, 2018).

961 Observational and modelling studies in the UK agree that hourly extremes are mostly
962 generated by convective mechanisms, while daily extremes might be caused by
963 different precipitation generating mechanisms (Blenkinsop *et al.*, 2017; Chan *et al.*,
964 2017). However, a noticeable relation with large-scale circulation systems such as
965 atmospheric and oceanic circulations including the NAO, and with temperature, have
966 been observed for both hourly and daily extremes (Jones *et al.*, 1997; Blenkinsop *et al.*,
967 2015; Hofstätter *et al.*, 2018), therefore, quantifying their relationship would
968 enhance our future projections and simulation.

969 Currently, the flood estimation handbook (FEH) (Faulkner, 1999), provides design
970 growth curves to estimate hourly precipitation, yet, the data used has short record
971 length. Therefore, statistical regional analysis for hourly extremes, where extreme
972 regions are delineated based on climatological characteristics is required to enhance
973 estimations of sub-daily precipitation, especially for ungauged locations. Regional
974 analysis pools climatologically similar data, increases data availability, and produces
975 statistically homogeneous and reliable estimates. Furthermore, most existing studies,
976 which investigated return estimates, growth curves, and precipitation changes for
977 extremes have used on-site analysis rather than regional analysis approach.

978

979

980

Chapter 3. regional frequency analysis of UK hourly and multi-hourly extreme precipitation

- *The material in this chapter has been published in the following journal article:*

Darwish, M., Fowler, H.J., Blenkinsop, S. and Tye, M.R. (2018) 'A regional frequency analysis of UK sub-daily extreme precipitation and assessment of their seasonality', International Journal of Climatology, 38(13), pp. 4758–4776. doi.org/10.1002/joc.5694

Floods related to extreme precipitation events, especially intense, short duration precipitation, may cause significant damage in urbanised areas, including transport infrastructure, electricity networks, and property. These events are expected to increase in frequency with climate change but their characteristics, at either hourly or multi-hourly timescales, have been little studied compared with daily timescales due to short and poor quality data records. A central objective of this research is to quantify hourly and multi-hourly extreme precipitation, its seasonality, and diurnal cycle using annual maximum (AMAX) precipitation data.

In this chapter, AMAX hourly and multi-hourly (3-, 6-, 12-, and 24h) precipitation accumulations in the UK are investigated using a recently available, quality controlled hourly precipitation dataset for the period 1992-2014. This includes the seasonality and diurnal cycle, and the use of the regional frequency analysis (RFA) approach with L-moments to produce at-site return level estimates. Existing extreme precipitation regions are used to provide regional-scale return levels. The chapter concludes with a new, subjectively defined regionalisation for hourly extremes based on the results presented.

Moreover, the research also shows that the existing UK extreme precipitation regions may not appropriately reflect regional differences in sub-daily extreme precipitation behaviour

3.1. Introduction

An increased understanding of extreme weather events is essential given that climate change will likely lead to an increase in the occurrence and magnitude of some types of events. The IPCC Special Report on Extremes IPCC (2012) stated that the frequency and intensity of extreme weather events have increased over large parts of

1013 the globe and extreme precipitation events on daily timescales are observed to have
1014 increased in frequency and intensity in some parts of the world (Alexander *et al.*, 2006;
1015 Alexander, 2016; Donat *et al.*, 2017). This is consistent with research by Min *et al.*
1016 (2011) who reported increasing trends in the annual maxima of daily precipitation for
1017 65% of the data-covered land area over the period 1951-1999. Moreover, Arnell and
1018 Gosling (2016) reported that the frequency of floods with a 1% annual exceedance
1019 probability (100 year return period) will be doubled across 40% of the globe by 2050.
1020 According to Tye (2015) and Arnell and Gosling (2016), such increases will affect man-
1021 made infrastructure mostly through increases in surface water runoff, leading to
1022 flooding and other destructive events.

1023 In the UK, several studies have reported significant increasing trends in daily and multi-
1024 day extreme precipitation events (Osborn *et al.*, 2000; Fowler and Kilsby, 2003a;
1025 Maraun *et al.*, 2008; Simpson and Jones, 2014). Osborn *et al.* (2000) reported an
1026 increased contribution of heavy precipitation events to total precipitation, especially in
1027 winter. Moreover, Fowler and Kilsby (2003b) reported increasing intensity of heavy
1028 multi-day (5 and 10 day) precipitation events in northern and western parts of the UK,
1029 particularly in autumn and winter. Maraun *et al.* (2008) confirmed an increasing
1030 contribution of daily heavy precipitation events in the UK and identified an increasing
1031 trend in the intensity of winter daily events in northern and western parts of the UK,
1032 and a negative trend in summer intensities in most UK regions. Recently, Jones *et al.*
1033 (2013) confirmed an increasing frequency of extreme daily precipitation events in the
1034 UK during spring, autumn, and winter, contrary to a recognised decrease in summer.
1035 Moreover, Tye (2015) reported a statistically significant increase in the probability of
1036 multi-day extreme precipitation events during the late summer and autumn, when most
1037 UK daily precipitation extremes occur. Simpson and Jones (2014) analysed extreme
1038 precipitation events and found a similar, statistically significant, pattern of wetter
1039 winters, and drier summers in the UK, though they reported a recent succession of wet
1040 summers and dry winters.

1041 Although daily and multi-day extreme precipitation events have been studied
1042 extensively, relatively little research has analysed sub-daily precipitation due to the
1043 scarcity of quality-controlled, long, and homogeneous observations (Westra *et al.*,
1044 2014; Blenkinsop *et al.*, 2017). However, such events are important because they
1045 produce pluvial floods which especially affect urban areas and small steep catchments,
1046 and can be very flashy in nature (Archer *et al.*, 2017; Archer and Fowler, 2018). The

1047 Stern Review (Stern, 2006) suggested that, globally and in the UK, intense
1048 precipitation derived floods are among the costliest and most critical of climate change
1049 impacts, leading to the loss of human life, infrastructure damage, water resource and
1050 transportation disruption, as well as considerable damage to ecosystems.

1051 The relationship between intense precipitation and pluvial floods suggests that both
1052 the intensity and frequency of pluvial floods in urbanised areas will be significantly
1053 affected by any change in extreme sub-daily precipitation events (Westra *et al.*, 2014).
1054 Their significance was demonstrated by the UK summer floods of 2007, where two-
1055 thirds of affected properties were inundated by pluvial flooding (Pitt, 2008), and it is
1056 currently estimated that ~3 million properties are at risk from surface water flooding in
1057 England (Environment Agency, 2014). There is therefore a clear need for a better
1058 understanding of likely future changes in extreme sub-daily precipitation event
1059 intensities to enhance adaptation potential capabilities (Westra *et al.*, 2014).

1060 Relatively few studies have investigated changes in observed sub-daily extreme
1061 precipitation events around the world, but those undertaken to date have generally
1062 indicated increasing intensities (Westra *et al.*, 2014) albeit generally at local to regional
1063 scales. Madsen *et al.* (2009) reported an intensification in Denmark extreme sub-daily
1064 precipitation events, consistent with results from Sicily (Arnone *et al.*, 2013), Canada
1065 and the United States (Burn *et al.*, 2011; Kunkel *et al.*, 2013; Muschinski and Katz,
1066 2013; Barbero *et al.*, 2017) and South Africa (Roy and Rouault, 2013). Kendon *et al.*
1067 (2018) provide evidence of an increase in the intensity of UK summer hourly extremes
1068 over the last 30 years but suggest that this (and recent variability in winter trends) may
1069 be strongly influenced by large-scale modes of variability such as the Atlantic
1070 Meridional Oscillation (AMO) and North Atlantic Oscillation (NAO). The most extensive
1071 analyses of sub-daily precipitation have focussed on the relationship between extreme
1072 precipitation intensity and temperature (Lenderink and Van Meijgaard, 2008; Hardwick
1073 Jones *et al.*, 2010; Utsumi *et al.*, 2011; Berg and Haerter, 2013), including for the UK
1074 (Blenkinsop *et al.*, 2015), known as Clausius-Clapeyron (CC) scaling. The CC
1075 relationship explains the increased capacity of warmer air to hold moisture under
1076 constant relative humidity; a ~6-7% increase in precipitation per 1°C increase in
1077 temperature. A general agreement between the studies is that increasing atmospheric
1078 temperature could increase precipitation intensities for daily and sub-daily precipitation
1079 events, with enhanced scaling (super-CC) for the latter (Westra *et al.*, 2014) though
1080 this is not the case in UK observations (Blenkinsop *et al.*, 2015).

1081 Recently, Blenkinsop *et al.* (2017) summarised the climatology of UK hourly extremes,
1082 noting that the highest frequency and intensity of hourly extreme precipitation events
1083 occur in summer, with most events (excluding winter) during late afternoon as might
1084 be expected from convective precipitation. Hand *et al.* (2004) analysed 50 UK
1085 precipitation events identified as extreme by the Flood Studies Report (NERC, 1975)
1086 and reported that among the investigated events, all extreme events of less than 5
1087 hours duration were convective; while events of up to 12 hours had at least a
1088 convective component. In addition, Hand *et al.* (2004) reported that extreme
1089 precipitation events are unlikely to occur in February, March and April, while convective
1090 events are most likely in June, July, and August. A key point to note however is that
1091 short duration, intense precipitation is poorly simulated by regional climate models,
1092 typically at resolutions of 12-25km (Chan *et al.*, 2014b; Westra *et al.*, 2014) due to the
1093 use of convection parameterisation schemes. Very high-resolution, convection-
1094 permitting models offer improved simulation of these events (Chan *et al.*, 2014b;
1095 Kendon *et al.*, 2014; Prein *et al.*, 2015), but are computationally demanding and have
1096 so far been run for only limited regions (Kendon *et al.*, 2017). This emphasises the
1097 importance of observational-based research to enhance understanding of sub-daily
1098 precipitation event characteristics, drivers and processes, in addition to providing the
1099 means for climate model validation.

1100 Most studies of sub-daily extreme precipitation so far have focused on individual sites
1101 (Westra *et al.*, 2014). However, in this research, we investigate the spatial and
1102 temporal distribution of UK hourly and multi-hourly (3-, 6-, 12-, and 24h) extreme
1103 precipitation using regions identified for daily extreme precipitation by Jones *et al.*
1104 (2014). Annual maxima (AMAX) are used to examine the seasonal and diurnal cycles
1105 of sub-daily extremes and to estimate the at-site and regional intensities of low
1106 probability events using a regional frequency analysis (RFA) approach with L-Moments
1107 estimation. RFA has been applied in hydrological and climatological studies in different
1108 countries across the world (Fowler and Kilsby, 2003b; Lee and Maeng, 2003; Trefry *et*
1109 *al.*, 2005; Norbiato *et al.*, 2007; Wallis *et al.*, 2007) and provides advantages over at-
1110 site estimation, including the assessment of ungauged areas, reduced impact of
1111 instrumental or human error, and therefore enhanced capacity for planning, designing,
1112 and managing infrastructure in a changing climate (Paixao *et al.*, 2011).

1113 This research is the first to examine both hourly and multi-hourly AMAX precipitation
1114 events and assess the appropriateness of the existing UK extreme precipitation

1115 regions (Jones *et al.*, 2014) for sub-daily extremes. We also describe the first
1116 application of RFA to the UK hourly precipitation dataset. The chapter is presented as
1117 follows. In Section 3.2 we describe the datasets used in the research, then, in Section
1118 3.3, we present the methods and statistical tools used to explore and analyse the data.
1119 Next, the spatial and temporal distribution of UK hourly and multi-hourly AMAX are
1120 described and return level estimates of AMAX are presented in Section 3.4.
1121 Subsequently, the results and their implications for urban drainage design are
1122 discussed in Section 3.5. Finally, we present our conclusions and recommendations in
1123 Section 3.6.

1124 **3.2. Data**

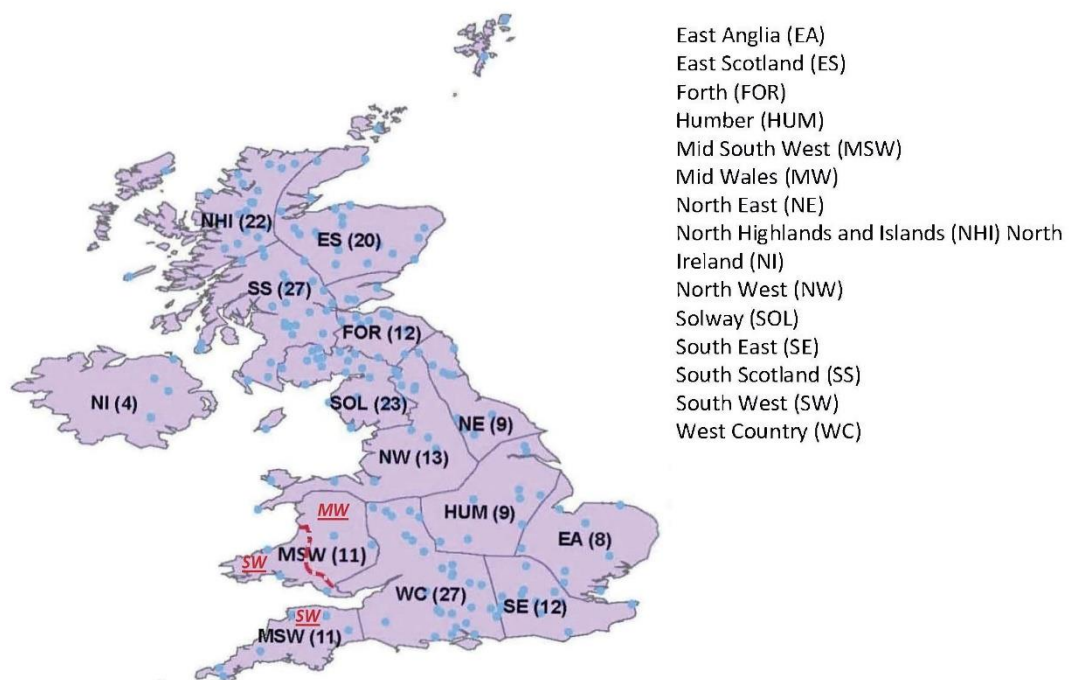
1125 This research uses an hourly precipitation dataset for the UK derived from rain gauges
1126 spanning different periods between 1949 and 2014 (Blenkinsop *et al.*, 2017; Lewis *et*
1127 *al.*, 2018). The dataset (up to 2011) was collected by Blenkinsop *et al.* (2017) from
1128 three sources: the UK Met Office Integrated Data Archive System (MIDAS), the
1129 Scottish Environmental Protection Agency (SEPA), and the UK Environment Agency
1130 (EA). Blenkinsop *et al.* (2017) performed a series of site-specific quality control (QC)
1131 procedures on the data to detect accumulated totals, malfunctioning gauges and
1132 unfeasible extreme precipitation totals including a comparison with a gridded daily
1133 precipitation dataset. This was subsequently extended to 2014 and subjected to
1134 additional quality control checks against neighbouring gauges (Lewis *et al.*, 2018).

1135 Blenkinsop *et al.* (2017) reported that the rain gauges' coverage increase noticeably
1136 from the mid- 1980s, while most of the gauges started functioning in the early- to mid-
1137 1990s. Furthermore, implementing the QC procedure on the gauges reduces data
1138 availability and capacity for a meaningful analysis (Blenkinsop *et al.*, 2017; Lewis *et*
1139 *al.*, 2018). Previous analyses considered a gauge to be suitable for climatological
1140 analysis and have a "complete" record if no more than 15% of hourly data are missing
1141 in a given year/ season, and selected the data between 1992-2014 for the analysis as
1142 a trade-off between having a long records and data availability (Blenkinsop *et al.*, 2017;
1143 Lewis *et al.*, 2018).

1144 Hence, to facilitate the comparison with other researchers, and to ensure the use of a
1145 reliable dataset that reflect the climatology of extremes well, the same gauge selection
1146 criteria were adopted in this research. Consequently, gauges which have more than
1147 85% of their record complete (i.e. non-missing and data not flagged by the QC process)

1148 for each year in the period 1992-2014 are used in this research. In total, 197 gauges
1149 fulfilled these criteria (Figure 1) and have been selected for further analysis.

1150 Finally, the 14 UK daily extreme precipitation regions (Figure 1), created by Jones *et*
1151 *al.* (2014), are used to assess the temporal and spatial characteristics of extreme
1152 hourly and multi-hourly precipitation. Although these regions are defined from extreme
1153 daily precipitation for the period 1961-2009, it is the only UK regional precipitation
1154 classification based on extremes and is a reasonable first basis by which to assess
1155 sub-daily extremes. However, we modify this slightly as the “Mid Wales” region
1156 contained only two gauges, merging this with the “South West” to create a modified
1157 “Mid Wales and South West” region (MSW). Both regions are located on the west coast
1158 of the UK and are highly influenced by north-westerly frontal systems (Lapworth and
1159 McGregor, 2008). Figure 1 shows the regions pre- and post-modification, with
1160 subsequent analyses presented using the 13 ‘post-modification’ UK extreme
1161 precipitation regions.



1162

1163 Figure 1: Distribution of 197 hourly rain gauges (blue dots) and UK extreme
1164 precipitation regions as defined by Jones *et al* (2014). Boundary and text in red denote
1165 merged regions (MW and SW were merged to form MSW due to limited gauge data in
1166 MW). Numbers in brackets denote the total number of gauges in each region.

1167

1168 3.3. Methodology

1169 3.3.1. Exploratory data analysis

1170 Multi-hour accumulations for 3-, 6-, 12-, and 24h periods were calculated for each
1171 gauge meeting the record completeness criterion presented in the data section. The
1172 3-, 6-, and 12h accumulations were calculated using a rolling window, while the 24h
1173 accumulation was calculated using both a 24h rolling window and a fixed window
1174 starting at 09:00 to be comparable with existing analyses using daily records (e.g.
1175 Maraun *et al.*, 2008; Jones *et al.*, 2014; Simpson and Jones, 2014) Analysis showed
1176 similar results for accumulations derived using both approaches (Figure A1, Appendix
1177 A) and so only a 24h fixed window is presented here to facilitate the comparison with
1178 other studies. An individual 3-, 6-, 12-, and 24h accumulation was treated as missing
1179 if at least 1, 2, 3, or 4 values respectively were absent in each accumulation window.
1180 For multi-hourly precipitation, the n hour accumulation is obtained as the sum of the
1181 accumulation at a given hour and the preceding n-1 hours, for example, a 3h
1182 accumulation at 15:00 is derived from the 1h accumulated total at 13:00, 14:00, and
1183 15:00. Annual maxima (AMAX) were then extracted for each gauge. Subsequently, the
1184 AMAX for all gauges in each region were pooled, and regional frequency density plots
1185 (for 1h and 3h AMAX) were constructed to show the diurnal cycle of extreme
1186 occurrence. The 3h AMAX diurnal cycle was constructed by counting each 3h AMAX
1187 at the end of the measuring window hour n, and fitting a smoothed diurnal profile using
1188 a kernel density estimation. The resulting diurnal profile of AMAX in each region was
1189 assessed for 1h and 3h accumulations only as most of the convective and intense
1190 precipitation events in the UK have a short duration (Hand *et al.*, 2004),
1191 notwithstanding the trivial value of deriving the diurnal cycle for 6h and 12h
1192 accumulations.

1193 Multi-hour accumulations for 3-, 6-, 12-, and 24h periods were calculated for each
1194 gauge meeting the record completeness criterion presented in the data section. The
1195 3-, 6-, and 12h accumulations were calculated using a rolling window, while the 24h
1196 accumulation was calculated using both a 24h rolling window and a fixed window
1197 starting at 09:00 to be comparable with existing analyses using daily records (e.g.
1198 Maraun *et al.*, 2008; Jones *et al.*, 2014; Simpson and Jones, 2014) Analysis showed
1199 similar results for accumulations derived using both approaches (Figure A1, Appendix
1200 A) and so only a 24h fixed window is presented here to facilitate the comparison with

1201 other studies. An individual 3-, 6-, 12-, and 24h accumulation was treated as missing
 1202 if at least 1, 2, 3, or 4 values respectively were absent in each accumulation window.
 1203 For multi-hourly precipitation, the n hour accumulation is obtained as the sum of the
 1204 accumulation at a given hour and the preceding n-1 hours, for example, a 3h
 1205 accumulation at 15:00 is derived from the 1h accumulated total at 13:00, 14:00, and
 1206 15:00. Annual maxima (AMAX) were then extracted for each gauge. Subsequently, the
 1207 AMAX for all gauges in each region were pooled, and regional frequency density plots
 1208 (for 1h and 3h AMAX) were constructed to show the diurnal cycle of extreme
 1209 occurrence. The 3h AMAX diurnal cycle was constructed by counting each 3h AMAX
 1210 at the end of the measuring window hour n, and fitting a smoothed diurnal profile using
 1211 a kernel density estimation. The resulting diurnal profile of AMAX in each region was
 1212 assessed for 1h and 3h accumulations only as most of the convective and intense
 1213 precipitation events in the UK have a short duration (Hand *et al.*, 2004),
 1214 notwithstanding the trivial value of deriving the diurnal cycle for 6h and 12h
 1215 accumulations.

1216 In contrast, the seasonality was examined for all accumulation periods, for both the
 1217 frequency and magnitude of AMAX. The AMAX seasonality for each accumulation
 1218 period was investigated using circular statistics (Reed and Robson, 1999). Circular
 1219 statistics convert the angular position of the calendar day at noon, θ , (also called Julian
 1220 day in this research, which is the number of elapsed days since the beginning of a
 1221 particular calendar year) in radians, to a vector based quantity of mean direction, \bar{r} ,
 1222 and centroid of action, $\bar{\theta}$. Thus, for n events at i stations, the mean day of the year for
 1223 events, $\bar{\theta}$, and the concentration of the seasonal distribution, \bar{r} . are calculated with
 1224 event dates represented by the angle θ on a circle of unit radius, and are calculated
 1225 from the number of days since the start of the calendar year:

$$1226 \quad \theta = (\text{day no.}) \frac{2\pi}{\text{no. of days in year}} \quad (1)$$

1227 Then the centroid of the events is determined by the coordinates:

$$1228 \quad \bar{x} = \frac{1}{n} \sum_{i=1}^n \cos(\theta_i) \text{ and } \bar{y} = \frac{1}{n} \sum_{i=1}^n \sin(\theta_i) \quad (2)$$

1229 while the values of the mean day of the year for event occurrence, $\bar{\theta}$, and the overall
 1230 dispersion of events (\bar{r}) around the mean day are calculated by:

1231

$$1232 \quad \bar{\theta} = \begin{cases} \tan^{-1} \frac{\bar{y}}{\bar{x}}, & \text{when } \bar{x} \geq 0, \bar{y} \geq 0 \\ \tan^{-1} \frac{\bar{y}}{\bar{x}} + \pi, & \text{when } \bar{x} < 0 \\ \tan^{-1} \frac{\bar{y}}{\bar{x}} + 2\pi, & \text{when } \bar{x} \geq 0, \bar{y} \leq 0 \end{cases} \quad (3)$$

$$1233 \quad \bar{r} = \sqrt{\bar{x}^2 + \bar{y}^2} \quad (4)$$

1234 Values of \bar{r} closer to 1 indicate a higher concentration of occurrence around $\bar{\theta}$, and
 1235 therefore a stronger seasonal signal. Conversely, values of \bar{r} closer to 0 indicate large
 1236 dispersion and a less clear seasonal signal.

1237 **3.3.2. Extreme value theory (EVT)**

1238 The extreme value theory (EVT) statistical approach has been adopted widely in
 1239 hydrological applications to analyse and model extremes where precipitation data are
 1240 assumed to represent a random draw from an underlying probability distribution, and
 1241 characterising extreme values corresponds to defining the upper tail of the distribution
 1242 (Coles et al., 2001; Katz et al., 2002). The EVT approach fits a probability distribution
 1243 to the data, estimates the distribution parameters, and estimates the hydrological event
 1244 return levels (Davison and Huser, 2015). EVT, unlike the standard statistical
 1245 approaches which are concerned with mean data behaviour, are designed to reflect
 1246 the behaviour of rare extreme events (Coles et al., 2001).

1247 EVT results thus provide the recurrence average of each event, which may be
 1248 expressed as annual exceedance probability (AEP), and are used in practical
 1249 applications such as drainage system design. For instance, an event with a specific
 1250 magnitude that occurs on average once every 25 years, has an annual exceedance
 1251 probability (probability of annual recurrence for a similar or greater event magnitude)
 1252 of 4% (i.e. 1/25), while the corresponding intensity of the event is referred to as the 25-
 1253 year return level. However, it should be noted that the AEP is the probability of a similar
 1254 event occurrence in each year, while the occurrence of an event in any year does not
 1255 affect the occurrence probability in any subsequent year. Therefore, for the
 1256 aforementioned example (i.e. an event of magnitude X and AEP of 4%) the probability
 1257 of having an event of magnitude X or greater in each year is 4%, regardless of the
 1258 occurrence of such an event in any other year.

1259 To determine the behaviour of extremes using EVT, general extreme value (GEV) and
 1260 general Pareto (GP) distributions have been used often for hydrological and

1261 climatological data. The GEV distribution usually employs the high (or low) values of a
 1262 dataset, where the datasets are defined as block maxima, while the GP distribution
 1263 employs the data over a predefined threshold (Coles et al., 2001). Generally speaking,
 1264 GEV is commonly used for large datasets, whereas, GP is used when data availability
 1265 is limited (Katz et al., 2002). For instance, You et al. (2011) employed EVT to evaluate
 1266 changes in precipitation and temperature extremes across China and their relation to
 1267 large scale circulation, while Fowler and Kilsby (2003a) investigated the implications
 1268 of changes in seasonal and annual extreme precipitation in the UK. Furthermore,
 1269 Durrans and Kirby (2004) employed EVT to analyse extreme frequencies either on-site
 1270 or regionally, while Jones et al. (2014) adopted the EVT approach to define new daily
 1271 extreme precipitation regions in the UK. Schindler et al. (2012) also used it to validate
 1272 RCM simulations over the UK.

1273 The cumulative distribution function (CDF) for the GEV distribution F , is expressed as
 1274 follows:

$$1275 \quad F(x; \theta) = \exp \left\{ - \left[1 + \xi \left(\frac{x-\mu}{\sigma} \right) \right]^{-1/\xi} \right\} \quad (5)$$

1276 where x is the event maxima value of interest and θ is the parameter set (μ, σ, ξ) used
 1277 to specify the distribution, while the centre is given by the location (μ) , the spread by
 1278 the scale (σ) and the behaviour of the upper tail by the shape (ξ) . Based on the shape
 1279 parameter, the GEV can take one of three forms: Gumbel, or light tailed, when ξ is
 1280 zero; Fréchet, or heavy tailed, if ξ is positive; and Weibull, or bounded, when ξ is
 1281 negative.

1282 On the other hand, the cumulative distribution function (CDF) for the GP distribution F ,
 1283 is expressed as follows:

$$1284 \quad F(x; \theta) = 1 - \left[1 + \xi \left(\frac{x}{\sigma} \right) \right]^{-1/\xi} \quad (6)$$

1285 where x is the event maxima value of interest and θ is the parameter set (σ, ξ) used to
 1286 specify the distribution, while the spread is given by the scale (σ) and the behaviour of
 1287 the upper tail by the shape (ξ) . The two distributions are directly related through the
 1288 shape parameter (Coles *et al.*, 2001; Katz, 2010)

1289

1290 In this chapter, the traditional stationary extreme precipitation frequency analysis
1291 approach, where the observations are assumed to be independent and identically
1292 distributed (i.i.d.), is adopted. Recently, Serinaldi and Kilsby (2015) reported that the
1293 common used length of AMAX data is usually insufficient to provide reliable return
1294 estimates for both stationarity and nonstationary cases, while using a nonstationary
1295 model would add unavoidable uncertainties due to the unknown evolution of the
1296 process dynamics. Serinaldi and Kilsby (2015) suggested that additional information
1297 will be needed to reduce the nonstationary model uncertainties including hydroclimatic,
1298 socio-economic, and historical data. Moreover, they concluded that due to the multiple
1299 interacting factors in hydrometeorological data sets, inferring non-stationarity of data
1300 might not be easy, and stationarity should remain the default assumption. It has been
1301 suggested that using non-stationarity should be accompanied by socio-economic,
1302 technical, and legislation considerations (Serinaldi and Kilsby, 2015). Therefore, model
1303 parameters (μ , σ , ξ) derived from the observed precipitation record in this chapter are
1304 assumed to remain constant across the period of record and into the future.

1305 **3.3.3. Regional Frequency Analysis (RFA)**

1306 A regional frequency analysis (RFA) using L-Moments estimation (Hosking and Wallis,
1307 2005) was adopted to represent and characterise hourly extreme precipitation.
1308 According to Sarhadi and Heydarizadeh (2014), the main benefits of RFA compared
1309 to at-site estimation are improved estimates of the distribution tails, and the ability to
1310 estimate events in ungauged locations. Furthermore, L-moments parameter estimation
1311 is more robust to outliers compared with conventional moments or Maximum
1312 Likelihood Estimation (Hosking and Wallis, 2005). Following Hosking and Wallis
1313 (2005), we applied RFA using L-Moments by first assessing region homogeneity using
1314 the heterogeneity measure (H), screening each region's data using the discordancy
1315 measure (D), then fitting a regional distribution and constructing growth curves,
1316 enabling the estimation of regional and at-site return levels.

1317 Hosking and Wallis (2005) derived D and H by calculating different L-moment ratios
1318 relations and combinations. The value D assesses the similarity between each
1319 station's L-moment ratios and the average L-moment ratios of the other stations in the
1320 region. Accordingly, D is calculated as:

1321

1322
$$D_i = \frac{1}{3} [(u_i - \underline{u})^T (u_i - \underline{u}) S^{-1}] \quad (7)$$

1323 where u_i is a vector containing three L-moment ratios (i.e., L-variation, L-skewness and
 1324 L-kurtosis) for site i , \underline{u} is the vector containing the simple average L-moment ratios,
 1325 S is the sample covariance matrix of L-moments of all sites, and T denotes
 1326 transposition of a vector or matrix. The site is considered non discordant if the D_i value
 1327 does not exceed the $D_{critical}$ value. Hosking and Wallis (2005) have provided guidelines
 1328 to determine $D_{critical}$ value in each region based on the number of gauges used.

1329 The heterogeneity measure (H), compares the between-site variability of L-moments
 1330 with what would be expected for a homogeneous region. The between site-variability
 1331 is compared with repeated Monte-Carlo simulations of a homogeneous region with the
 1332 same site's record length. Accordingly, H is calculated as:

1333
$$H = \frac{(V - \mu_v)}{\sigma_v} \quad (8)$$

1334 where μ_v and σ_v are the mean and standard deviation of N_{sim} values of V (N_{sim} is the
 1335 number of simulation data). V is calculated from the regional data as follows:

1336
$$V = \left\{ \frac{\sum_{i=1}^N n_i [t^i - t^R]^2}{\sum_{i=1}^N n_i} \right\}^{\frac{1}{2}} \quad (9)$$

1337 Where n stands for record length of site i , t^i is L-moment ratios (i.e., L-variation, L-
 1338 skewness and L-kurtosis) for site i , and t^R is the regional average of L-moment ratios;
 1339 Hosking and Wallis (2005) consider the region as "acceptably homogeneous" if $H < 1$,
 1340 "possibly heterogeneous" if $1 \leq H < 2$, and "definitely heterogeneous" if $H \geq 2$.

1341 To minimise the impact of localised extreme precipitation events and variations
 1342 between gauge locations, we take the standard RFA approach and first standardise
 1343 AMAX data for each gauge by dividing by the gauge's median AMAX (RMed). Then, a
 1344 regional mean RMed weighted by each gauge record length was calculated for each
 1345 region. This regional RMed was used to estimate regional return levels, while individual
 1346 gauge RMed were used to estimate the return levels at each location. Regional return
 1347 level estimates were derived from generalized extreme value (GEV) distributions fitted
 1348 to the regionally pooled AMAX. Further details on this approach can be found in Jones
 1349 *et al.* (2013). The fitted distributions were used to estimate the individual gauge and
 1350 regional precipitation intensities corresponding to defined annual exceedance
 1351 probabilities (20%, 10%, 4%, 2%) or return periods (5-, 10-, 25-, and 50 years) by

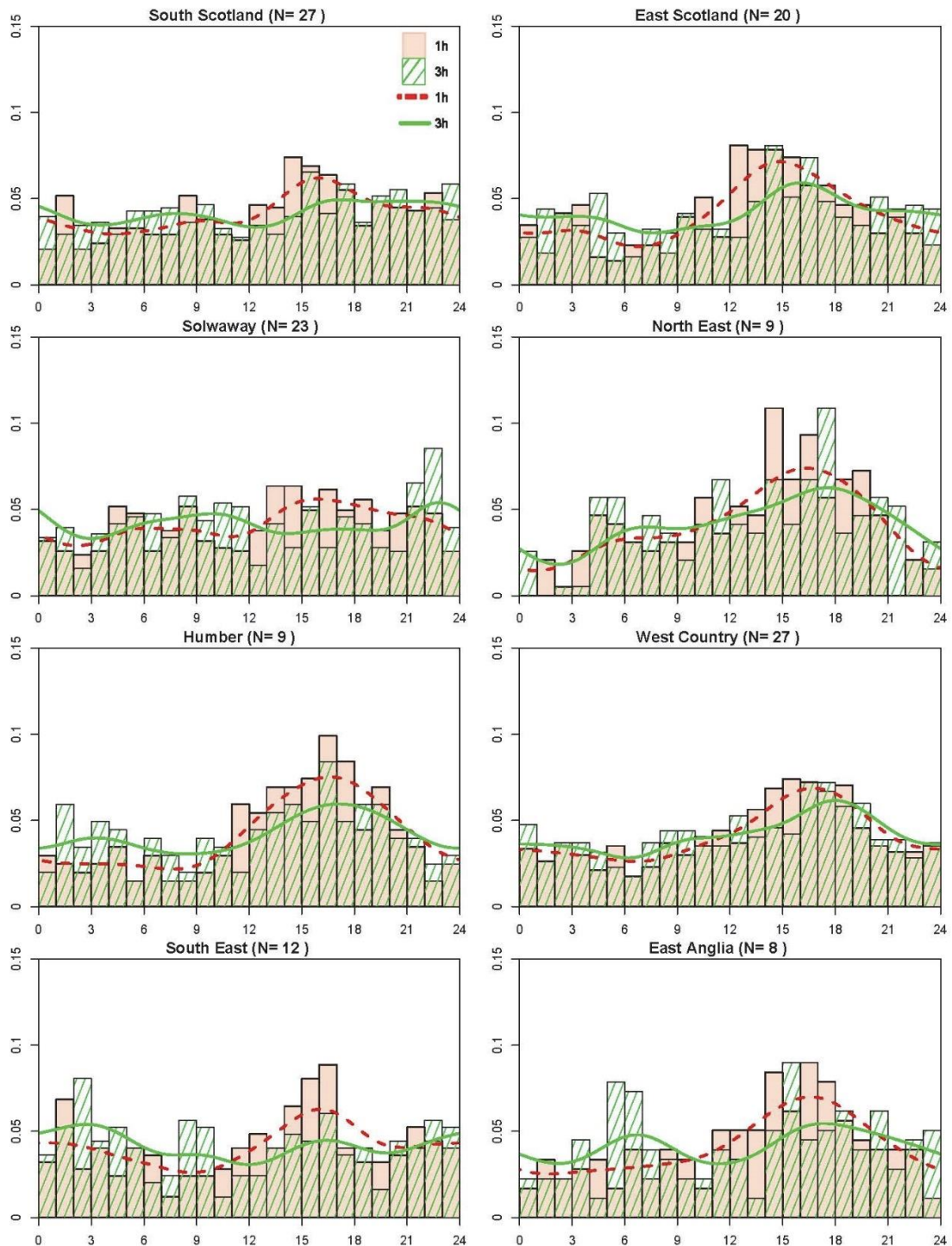
1352 multiplying the standardised return level estimates by the gauge RMed or weighted
1353 regional RMed for the gauge and regional estimates respectively.

1354 Finally, independence and stationarity are important underlying assumptions for
1355 regional frequency analysis. In this research, using AMAX at each gauge assures the
1356 use of independent events, with only one event selected per calendar year. On the
1357 other hand, it has been noted that the typically used length of AMAX data is insufficient
1358 to detect trends, and therefore using a nonstationary model would add unavoidable
1359 uncertainties (Serinaldi and Kilsby, 2015). Moreover, Madsen *et al.* (2013) reviewed
1360 European design guidelines and reported that all existing design guidelines are based
1361 on stationary data analysis and it has been suggested that stationarity should remain
1362 the default assumption in the absence of longer observation records (Madsen *et al.*,
1363 2013; Serinaldi and Kilsby, 2015), which is presumed in this research.

1364 **3.4. Results**

1365 **3.4.1. Diurnal cycle and seasonality of AMAX events**

1366 The diurnal profiles in Figure 2 show that most 1h AMAX occur during the afternoon
1367 between 12:00 and 18:00, with a peak typically between 14:00 and 17:00, especially
1368 in south-eastern and eastern regions such as the North East, Humber, East Anglia,
1369 and South East. However, the profile in northern regions (e.g. South Scotland) is
1370 relatively flat, indicating a weaker diurnal cycle. Blenkinsop *et al.* (2017) also describe
1371 the diurnal cycle for summer mean wet hour intensities with over half of the regions
1372 possessing a clear diurnal cycle, also peaking in the mid- to late afternoon though with
1373 lower amplitude cycles in the west. This spatial variation is likely associated with
1374 different mechanisms generating extreme 1h precipitation, as convective processes
1375 become less dominant to the north and west of the UK where AMAX are also more
1376 likely to occur outside summer. The diurnal profile for 3h AMAX shows that in most UK
1377 regions the frequency density also peaks during the afternoon but over a longer period
1378 compared to the 1h AMAX and with a smaller amplitude. It is possible that this
1379 difference could arise as the 3h AMAX accumulation reduces the influence of very
1380 short, heavy events by including other more moderate events occurring across three
1381 successive hours, but is also likely to arise partially as an artefact of the rolling window
1382 approach to calculate 3h accumulations.

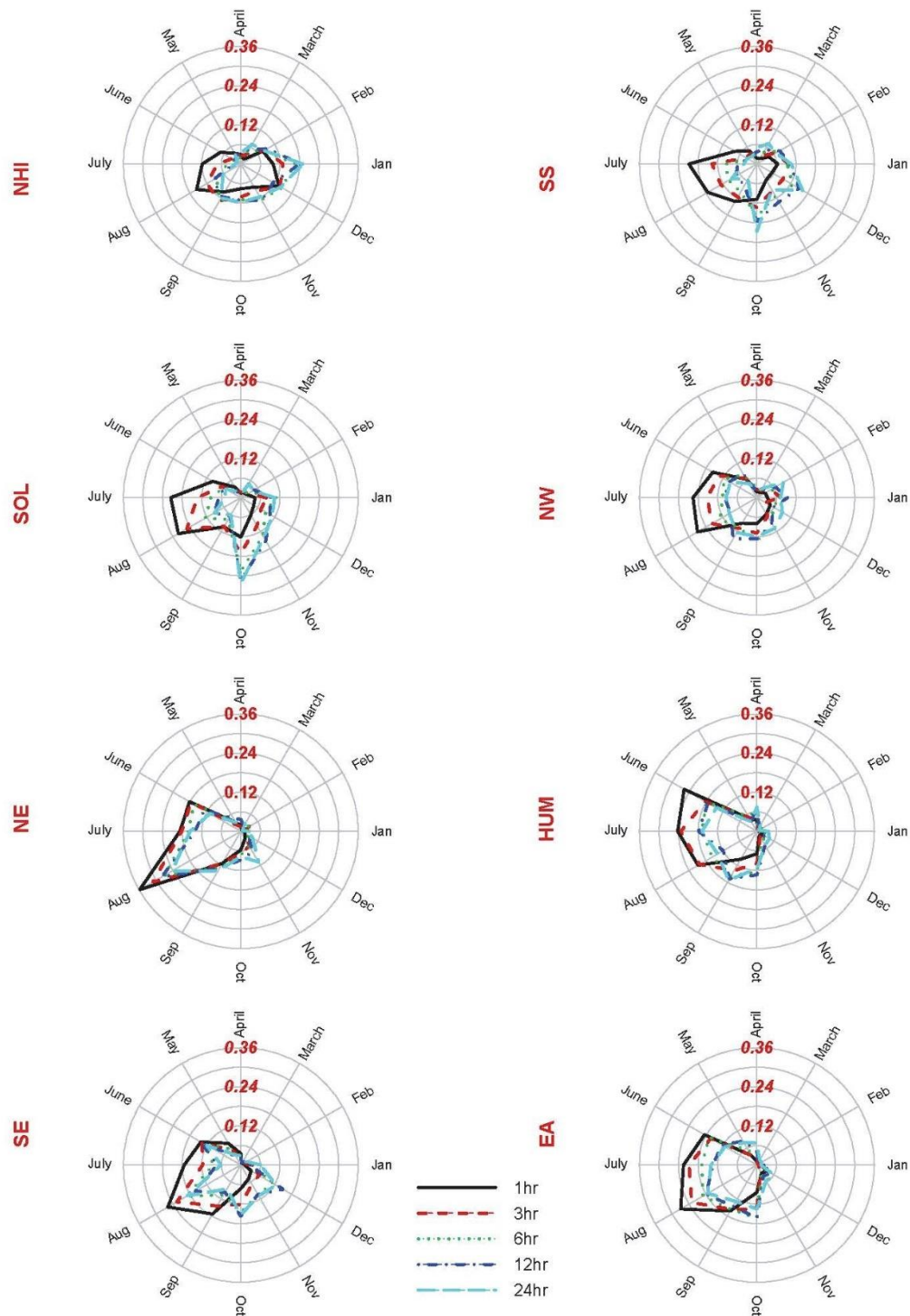


1383

1384 Figure 2: Regional hourly frequency density plots and diurnal profiles of 1h and 3h
 1385 AMAX for selected regions. The smoothed diurnal profiles were fitted using kernel
 1386 density estimations. The 3h AMAX is calculated as the accumulation of the hourly
 1387 record for hour n, n-1, and n-2, and plotted at hour n. For example, an accumulation at
 1388 15:00 is the total of precipitation at 13:00, 14:00, and 15:00. N denotes the number of
 1389 gauges in each region. Frequency density of event (y-axis), and hours of the day (x-
 1390 axis).

1391 The annual distribution of AMAX for all durations is summarised in Figure 3 for eight
 1392 regions (NHI, SS, SOL, NW, NE, HUM, SE, and EA). All demonstrate distinct

1393 seasonality in hourly and multi-hourly AMAX – notably 1h AMAX occurrence is highly
1394 concentrated in summer (JJA) in most regions. In the most northerly regions (NHI, SS,
1395 SOL) 1h AMAX are concentrated mostly from late summer (July, August) through to
1396 mid-autumn (and for NHI, to winter) whilst in other regions these occur most frequently
1397 during the period from June to September, with a strong August peak. Comparing the
1398 distributions of multi-hourly AMAX indicates for northerly regions (NHI, SS, SOL, NW)
1399 a gradual shift in the peak frequency from the summer months to later in the year as
1400 the accumulation period increases (Figure 3). However, in southern and eastern
1401 regions (NE, HUM, EA, SE) there is less difference between accumulation periods
1402 which may suggest that in these areas AMAX are predominantly produced by the same
1403 mechanism regardless of accumulation period. In these regions the timing of 1h and
1404 3h AMAX (short duration) peak frequencies are similar whilst the timing of 12h and 24h
1405 AMAX (longer duration) are very similar across all regions. For 6h AMAX, the timing is
1406 similar to longer durations in some regions but in others the monthly distributions are
1407 intermediate between those of short and longer durations. Finally, we note that the
1408 seasonality of 24h AMAX derived using a rolling window accumulation is similar to that
1409 derived using a fixed window at 09:00 (Figure A1, Appendix A), thus we focus on
1410 results using the latter to allow comparison with previous studies of daily precipitation.

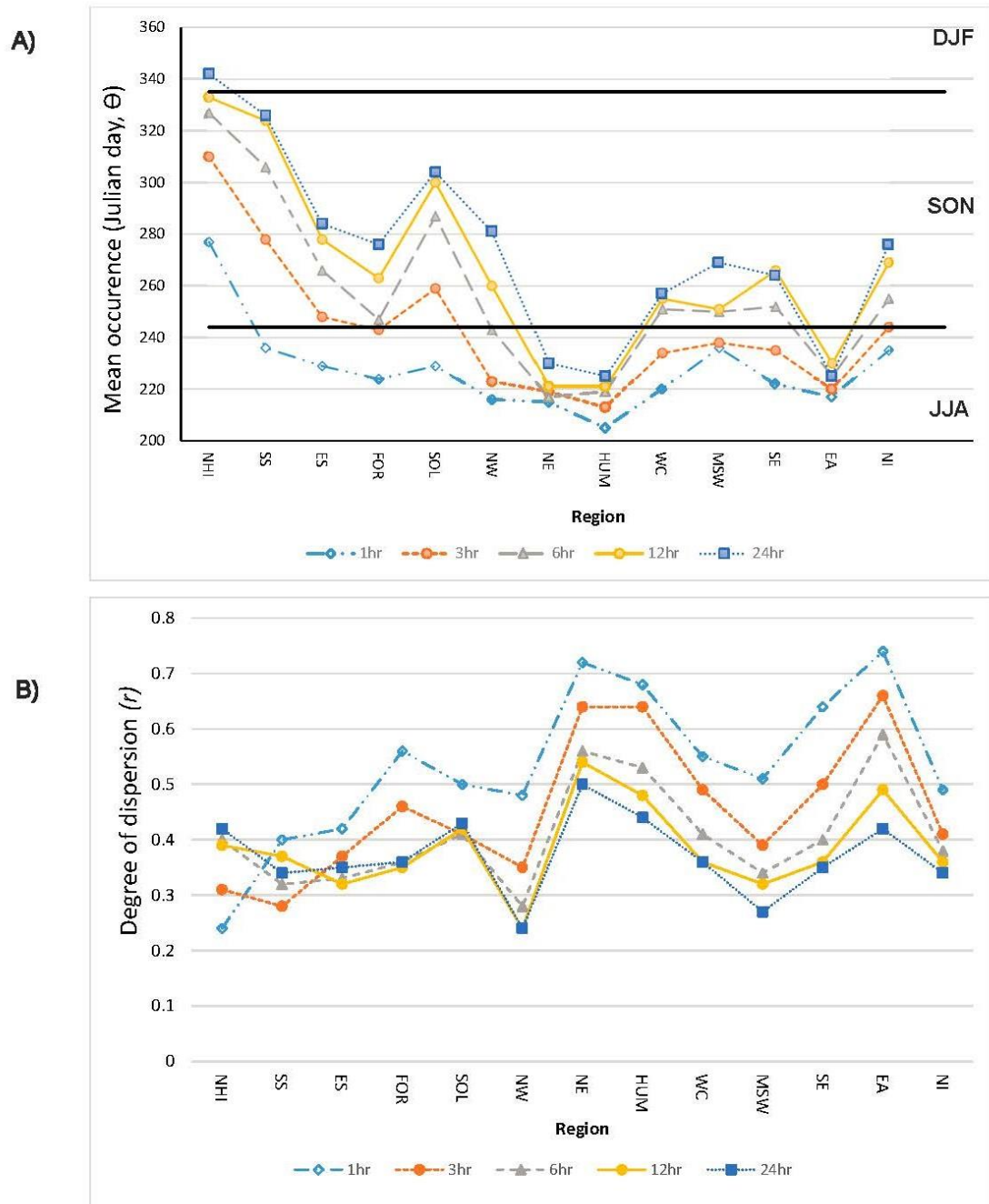


1411

1412 Figure 3: Regional monthly frequency densities of 1-, 3-, 6-, 12- and 24h AMAX in the
 1413 UK. Red (italicised) values denote the frequency density scale.

1414 The seasonality of hourly/multi-hourly AMAX was further quantified using circular
 1415 statistics (Reed and Robson, 1999). Blenkinsop *et al.* (2017) assessed the n-largest
 1416 1h accumulations in the UK during 1992-2011, but hourly and multi-hourly AMAX have
 1417 not yet been assessed. Figure 4 (quantified in Table B1, Appendix B) shows that the
 1418 mean occurrence of 1h AMAX is in summer (Julian day 200 to 244) for most regions,

1419 with a mean occurrence day (θ) in August for 11 of the 13 regions, and in July and
1420 October for HUM and NHI respectively. Moreover, r values are higher in eastern and
1421 southern regions compared to western and northern regions, increasing from 0.24
1422 (NHI) to 0.74 (EA). High r values indicate that AMAX occurrence is more strongly
1423 clustered around θ , confirming a summer dominance for 1h AMAX in the southern and
1424 eastern UK. The weaker seasonality in northern regions could be attributable to either
1425 within gauge or between gauge variability in the occurrence of AMAX and indicates
1426 that gauges across individual regions could be characterised by significantly variable
1427 seasonality. Figure 4 also indicates increasing θ values (i.e. mean occurrence later in
1428 the year) and decreasing r values (i.e. greater dispersion) for multi-hourly AMAX
1429 compared to hourly. For example, for SE, θ shifts from early-August (1h) to late-
1430 September (24h) whilst the dispersion increases, as r decreases from 0.64 to 0.35.
1431 This is consistent with Figure 3, which shows that longer duration AMAX (12h and 24h)
1432 occur later in the year and display weaker seasonality compared with 1h AMAX. These
1433 results are also consistent with those obtained by Blenkinsop *et al.* (2017) using the
1434 same dataset but using an n-largest approach, finding greater 1h dispersion in northern
1435 regions (i.e. NHI, ES, SS) compared to southern and eastern regions (i.e. NE, HUM,
1436 EA, SE). They also showed that the seasonality of the largest events broadly reflects
1437 that of mean wet hour intensities and that spatial patterns in seasonal 99th quantile
1438 intensities were consistent with those for mean intensities across the UK. Similarly,
1439 Jones *et al.* (2013) showed a summer seasonality for 1d (24h) AMAX in eastern
1440 regions, especially late summer, while other regions tended to experience 24h AMAX
1441 in late autumn. Figure 4 therefore suggests a stronger seasonality at all accumulation
1442 periods in eastern regions (NE, HUM and EA) compared with other parts of the country
1443 though this becomes much weaker as the period increases.

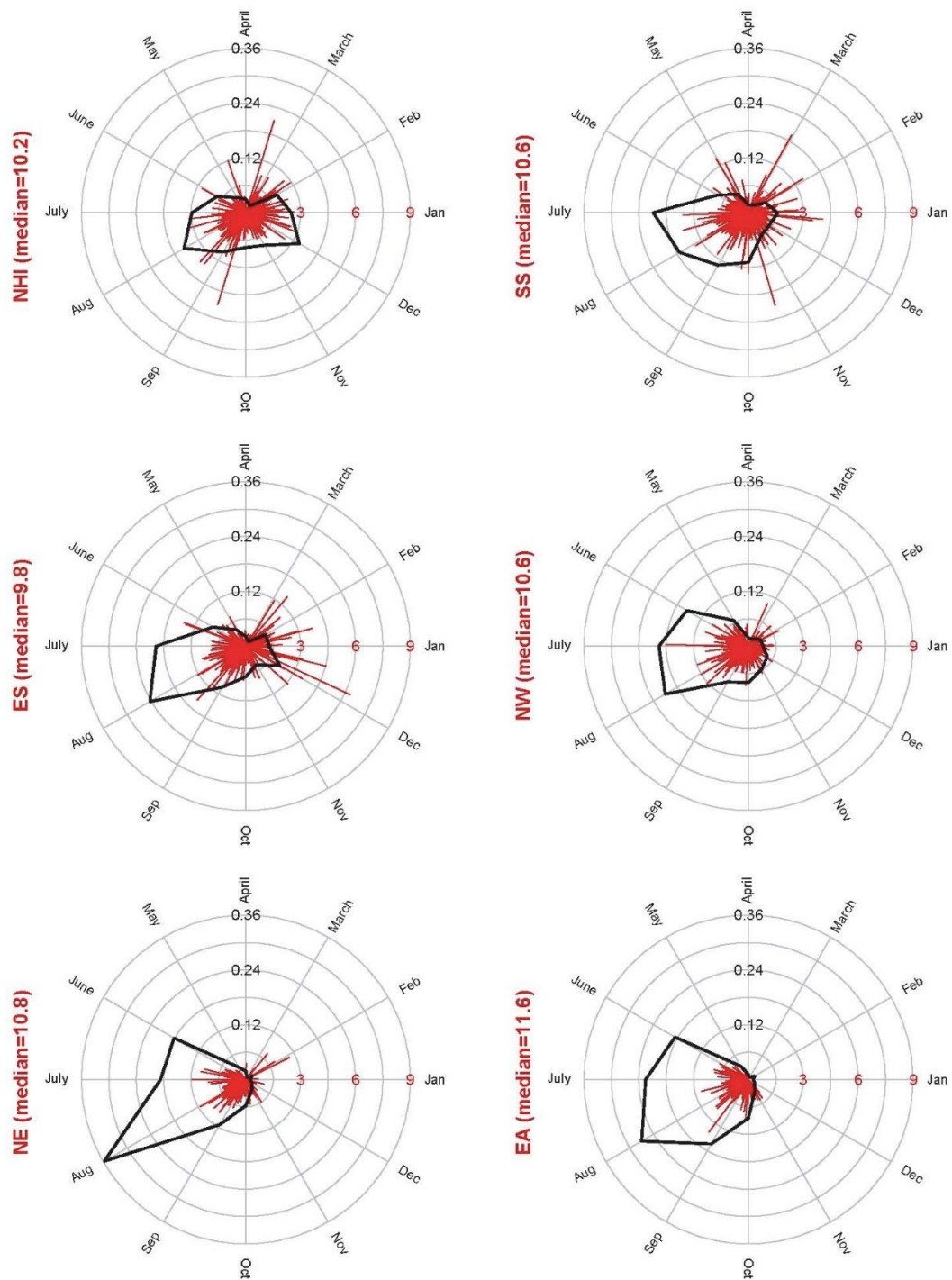


1444

1445 Figure 4: Regional circular statistics representing seasonality of occurrence of hourly
 1446 and multi-hourly AMAX. Figure (A), mean AMAX occurrence day (Julian day, θ); Figure
 1447 (B), degree of dispersion (r) indicating the degree to which AMAX are seasonally
 1448 concentrated, ranging from 0 to 1, with higher values indicating greater concentration
 1449 around θ . Refer to Figure 1 for region abbreviations.

1450 Figure 5 shows the frequency density of 1h AMAX per month (black), and the
 1451 magnitude of the standardised AMAX (red). This reveals that in Scotland (e.g. NHI,
 1452 ES, and SS), the peak magnitude of maxima does not necessarily coincide with the

1453 peak frequency. Many of the most intense 1h AMAX occur in winter through to early
1454 spring (Dec - Mar). In contrast, the most intense 1h AMAX in southern or eastern
1455 regions (e.g. NE and EA) generally occur during summer, consistent with the period of
1456 peak frequency. The coincidence of peak AMAX occurrence and frequency in these
1457 regions may be attributable to the dominance of one precipitation mechanism
1458 producing most of the AMAX. As these occur mostly in summer, precipitation in
1459 southern and eastern regions are likely to be generated primarily by convection. In
1460 contrast, in regions where peak AMAX frequency and intensity do not coincide,
1461 different mechanisms are likely to be responsible for AMAX occurring at different times
1462 of the year. Results for 3h and 12h AMAX are presented in Figures A2 and A3
1463 respectively for comparison given their representativeness of other durations noted
1464 above.



1465

1466 Figure 5: Monthly 1h AMAX regional frequency density (black), and hourly AMAX
 1467 standardised by the regional median (red) for selected regions. The regional median
 1468 (mm) is stated for each region, and radial lines denote 1st day of each month.

1469

3.4.2. Regional frequency analysis

1470 Regional frequency analysis (Hosking and Wallis, 2005) was used to estimate return
 1471 levels for different durations. The homogeneity assessment (Table 1) shows that most
 1472 of the existing extreme precipitation regions are homogeneous ($H < 1$) whilst the West
 1473 Country marginally exceeds the homogeneity test ($H=1.01$), North West (NW) is
 1474 classified as possibly heterogeneous ($H=1.62$), and Solway (SOL) is definitely
 1475 heterogeneous ($H=2.71$). The discordancy measure, D , for the gauges in each region
 1476 showed that none of the gauges is discordant. A region is homogenous if $H < 1$,
 1477 including negative H values, possibly heterogeneous if $1 \leq H < 2$, and definitely
 1478 heterogeneous if $H \geq 2$, and the gauges are not discordant if the maximum gauge
 1479 discordancy value is less than $D_{critical}$ ($D_{max} < D_{critical}$). Hosking and Wallis (2005) provide
 1480 guidelines to determine $D_{critical}$ based on the number of gauges used.

Region name	Homogeneity (H)	No. of gauges	Max. gauge discordancy value/ max. allowed value ($D_{critical}$)
East Anglia	0.02	8	1.78 / (2.14)
East Scotland	0.99	20	2.21 / (3.00)
Forth	0.27	12	2.24 / (2.63)
Humber	-0.40	9	1.77 / (2.33)
Mid South West	0.13	11	1.68 / (2.63)
North East	0.82	9	1.89 / (2.33)
North Highland and Islands	0.39	22	2.97 / (3.00)
North Ireland	0.94	4	1.00 / (1.00)
North West	1.62	13	2.31 / (2.87)
Solway	2.71	23	2.56 / (3.00)
South East	0.73	12	1.76 / (2.76)
South Scotland	-0.63	27	2.70 / (3.00)
West Country	1.01	27	2.25 / (3.00)

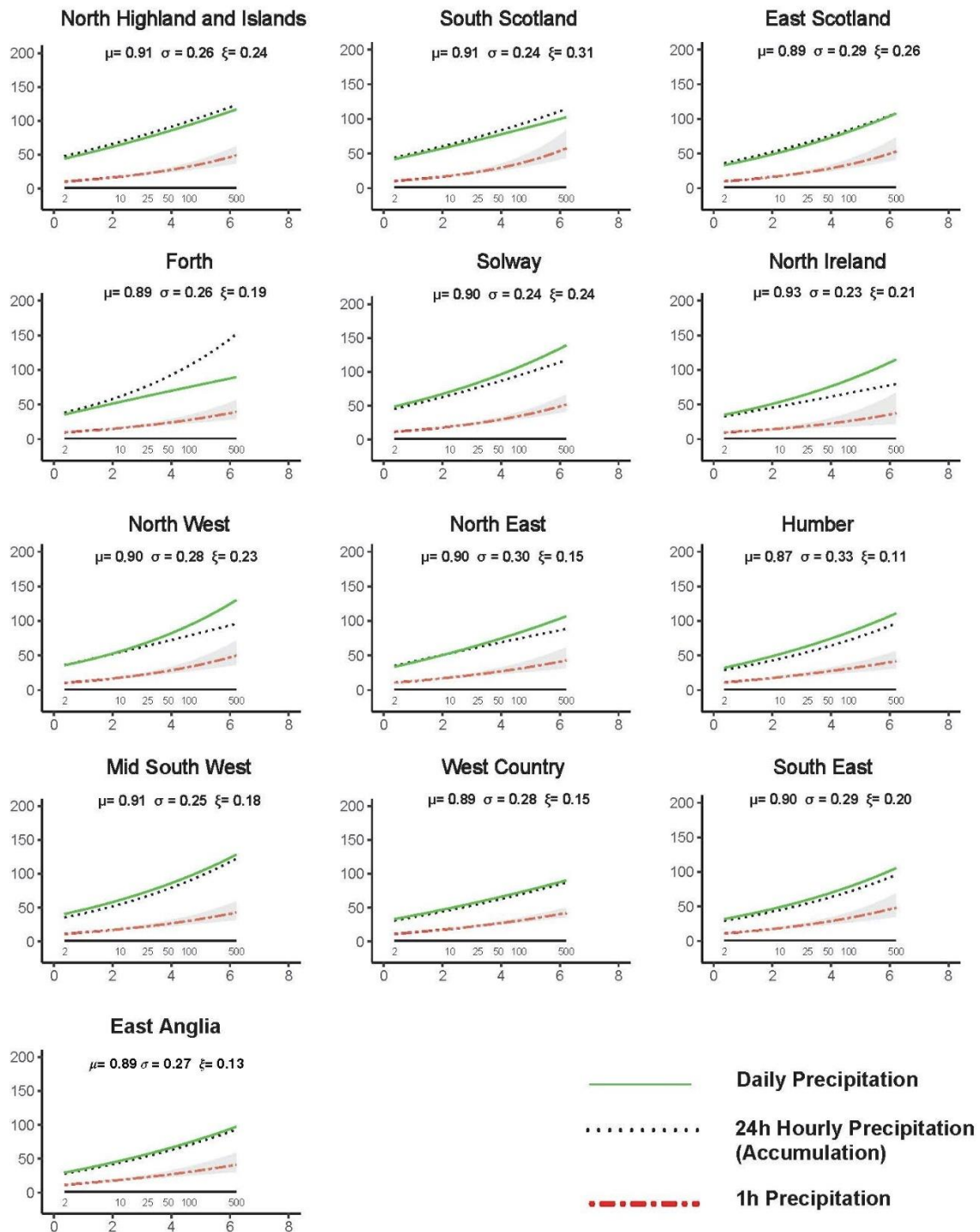
1481 Table 1: Extreme precipitation regional homogeneity assessment for 1h AMAX and the
 1482 gauge discordancy assessment (Hosking and Wallis, 2005). Region is homogenous if
 1483 $H < 1$, possibly heterogeneous if $1 \leq H < 2$, and definitely heterogeneous if $H \geq 2$, and the
 1484 gauges are not discordant if the maximum gauge discordancy test value $< D_{critical}$.

1485 The two non-homogeneous regions (NW and SOL) were also reported as such for
 1486 daily extreme precipitation by Jones *et al.* (2014). Further investigation of AMAX data

1487 for these regions showed that in NW just two gauges provide four of the five highest
1488 recorded AMAX, with both located on the region borders. However, since these gauges
1489 were non-discordant they were retained within the NW region analysis. For SOL, one
1490 gauge recorded a 1h AMAX of 82mm h⁻¹ which is 20mm greater than the next ranked
1491 AMAX and more than double the 3rd ranked value in the region. This gauge has the
1492 highest D value, but is not discordant. This gauge is also located on the region borders
1493 and is one of only two gauges located at an elevation exceeding 350m (all other 21
1494 gauges in the region are located at elevations < 250m). Since the AMAX have been
1495 verified against neighbouring gauges, this gauge was retained for analysis within the
1496 SOL region. We therefore retained the 13 extreme precipitation regions to estimate
1497 regional hourly and multi-hour return levels. This also facilitates comparison with the
1498 1d AMAX return levels estimated by Jones *et al.* (2014) using daily gauge data.

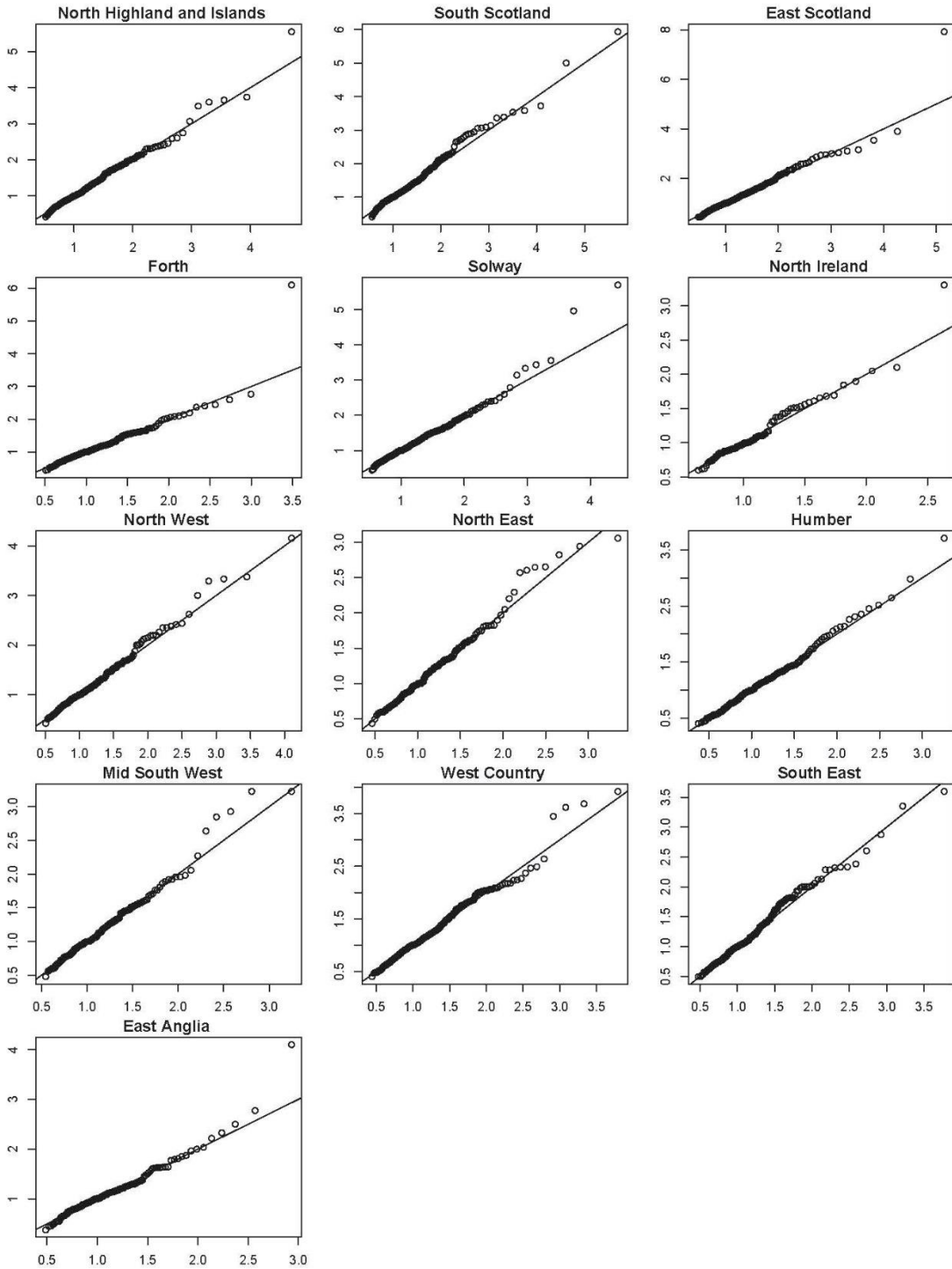
1499 The regional return level estimates for 1h, 24h, and daily AMAX (Jones *et al.*, 2014)
1500 are presented in Figure 6. We also compared the results for 24h AMAX using the fixed
1501 09:00 accumulation period with those using rolling 24h windows to test for
1502 underestimation of AMAX due to aggregation at constant time intervals (e.g. Morbidelli
1503 *et al.*, 2017) but this produced comparable results (see Figure A4 Appendix A). The 1h
1504 AMAX (Figure 6, red line) return levels have a similar distributional shape across the
1505 UK, with heavy tails since the shape parameter, ξ , is greater than 0 ($\xi > 0$). A Q-Q plot
1506 (Figure 7) assesses the method and assumptions, showing that the fitted model and
1507 the observed data are a good match, and the assumptions of independence and
1508 stationarity do not affect the quality the fitted distributions. On the other hand, the 24h
1509 AMAX (Figure 6, black line) and daily AMAX return level estimates by Jones *et al.*
1510 (2014) (green line), are generally slightly flatter indicating that ξ is closer to 0. The
1511 results for 24h and daily AMAX are similar for all regions except NI, FOR and NW. The
1512 differences in North Ireland (NI) are likely due to differences in the number of gauges
1513 used in both studies: daily gauges (25) and sub-daily gauges (4). In Forth (FOR) the
1514 difference is due to the occurrence of 24h AMAX exceeding 150mm and 200mm in
1515 May 2006 and August 2007 respectively, while daily AMAX in Jones *et al.* (2014) did
1516 not exceed 85mm. This is because the hourly data used here is derived from a different
1517 set of rain gauges to those of Jones *et al.* (2014) which only provided precipitation
1518 accumulations at 09:00 and at different locations over a different period (1961-2009).
1519 For the North West (NW), it is uncertain what is causing the difference, but is again
1520 likely due to the different gauges and periods used. For most regions the fitted

1521 distributions for both 24h AMAX accumulations and daily AMAX are similar despite
1522 these differences. Figure 6 (and growth curves in Figure A5) show that the fitted GEV
1523 of the daily precipitation return level estimates by Jones *et al.* (2014) and the 24h
1524 accumulation used in this research are similar in most regions, especially for return
1525 periods of up to 100 years (i.e. annual exceedance probability $\geq 1\%$), providing
1526 confidence in the data used in this study. We note though that as the daily precipitation
1527 records used in Jones *et al.* (2014) have a longer duration (1960-2009) and a larger
1528 sample size compared to the 24h accumulation record length used in this research
1529 (1992-2014), the confidence intervals for the daily return estimates are narrower than
1530 those for the 24h accumulations. Moreover, the results in Figure 6 show that the 1hr
1531 AMAX return levels and confidence intervals show some similarity across regions with
1532 no significant difference, which suggests the need for new and potentially fewer
1533 representative regions to reflect the spatial differences between gauges. This similarity
1534 across regions is confirmed by the fitted growth curves in Figure A6.



1535

1536 Figure 6: Return level plots of fitted regional GEV distributions for 1h AMAX (red) and
 1537 95% confidence interval (grey shaded), 24h AMAX (black), and daily AMAX (from
 1538 Jones et al. 2014) (green). Return level estimates in mm (y-axis), return periods in
 1539 years (upper x-axis) and Gumbel reduced variate (lower x-axis). The 1h AMAX GEV
 1540 distribution parameters μ , σ and ξ are also shown.



1541

1542 Figure 7: Q-Q plots for the AMAX fitted GEV distributions. Sample (observed) growth
 1543 curve quantiles (y-axis) and theoretical growth curve quantiles (x-axis). The growth
 1544 curve represents the multiple increase of a given return level over an index value, in
 1545 this case the 2-year return level.

1546 The hourly return level estimates for each gauge in Figure 8 are derived from the
1547 regional fitted GEV distributions multiplied by the site-scaling factor (the gauge RMed).
1548 The return level estimates indicate higher values for central and southern UK regions
1549 compared to northern regions for all return periods (5-, 10-, 25-, and 50-years) but
1550 especially for shorter return periods. For example, the 5- and 25-year return level
1551 estimates are less than 13mm and 19mm respectively for many gauges in northern
1552 regions, while for the same return periods, only one gauge in central and southern UK
1553 has a similar return estimate, with all other gauges exceeding these values. This is
1554 consistent with results from Figure 5, and confirms that 1h AMAX typically tend to be
1555 lowest in the most northern regions although the largest absolute magnitudes do not
1556 follow this pattern. Further results for multi-hourly (3h and 12h) return level estimates
1557 are presented in Figures A7 and A8 in Appendix A.



1558

1559 Figure 8: Return level estimates (mm h⁻¹) for UK 1h AMAX precipitation at each gauge
 1560 for return periods of 5-, 10-, 25- and 50 years (20%, 10%, 4%, 2% annual exceedance
 1561 probabilities (AEPs)). Estimates for each gauge are calculated from the fitted regional
 1562 GEV growth curve multiplied by the site scaling factor (gauge RMed).

1563 3.5. Discussion

1564 Growing evidence of intensifying extreme precipitation and its associated impacts has
1565 created a need to better characterise sub-daily precipitation events. Such events are
1566 associated with flash flooding and adversely affect urban areas and fast responding
1567 catchments. In this research, we have examined the temporal and spatial patterns of
1568 hourly and multi-hourly extreme precipitation events in the UK.

1569 Our results in Figures 3-5 show that 1h AMAX are most likely to occur in summer
1570 compared to other, longer durations, typically extending from early summer through to
1571 early autumn (June-September) with a peak in August for most regions, extending later
1572 in the year in northern and western regions. We observe that 1h and 3h AMAX have
1573 similar seasonality in southern and eastern regions in terms of mean and most frequent
1574 occurrence although 3h AMAX are slightly more widely distributed throughout the year.
1575 We also show that 12h and 24h AMAX are less likely to occur in summer than other
1576 seasons, apart from in southeast and eastern regions of England (e.g. NE, HUM, SE,
1577 EA). 6h AMAX were found to have a seasonal occurrence and intensity pattern broadly
1578 transitional between short and longer accumulation periods. These differences in the
1579 characteristics and seasonality of precipitation at different accumulations demonstrate
1580 that using a scaling factor or regression relationship to estimate 1h extremes from
1581 those on daily timescales will likely produce misleading results, as they occur at
1582 different times of the year in some regions and are therefore likely to be caused by
1583 different processes. Consequently, many of our current tools for climate adaptation,
1584 such as uplifts used for drainage system design or sustainable drainage systems
1585 (National Suds Working Group, 2004; Dale *et al.*, 2017) may need to be revised using
1586 new 1h AMAX information.

1587 Seasonal patterns in 24h and 1h AMAX occurrence are similar to previously published
1588 results for daily and hourly extreme precipitation (Jones *et al.*, 2013; Blenkinsop *et al.*,
1589 2017). Jones *et al.* (2013) found that UK 1d to 10d AMAX in HadUKP northern regions
1590 (e.g. South Scotland, North Scotland, East Scotland, which are analogous but not
1591 identical to NHI, ES, SS, and parts of FOR and SOL in this research) mostly occur in
1592 late autumn and winter, which is similar to results presented here for 24h AMAX in
1593 northern regions (e.g. NHI, SS, SOL, and NW). In contrast, results showing that for
1594 most regions (e.g. SS, NW, SE, HUM, EA, NE) 1h AMAX mainly occur between
1595 summer and early autumn are consistent with the seasonal distributions of n-largest

1596 events identified by Blenkinsop *et al.* (2017). Results presented here also demonstrate
1597 that the mean occurrence day, calculated from circular statistics, tends towards
1598 autumn and winter as event duration increases from 1h to 24h (most noticeably in
1599 northern regions) which is consistent with the seasonality presented by Jones *et al.*
1600 (2013) for daily precipitation accumulations.

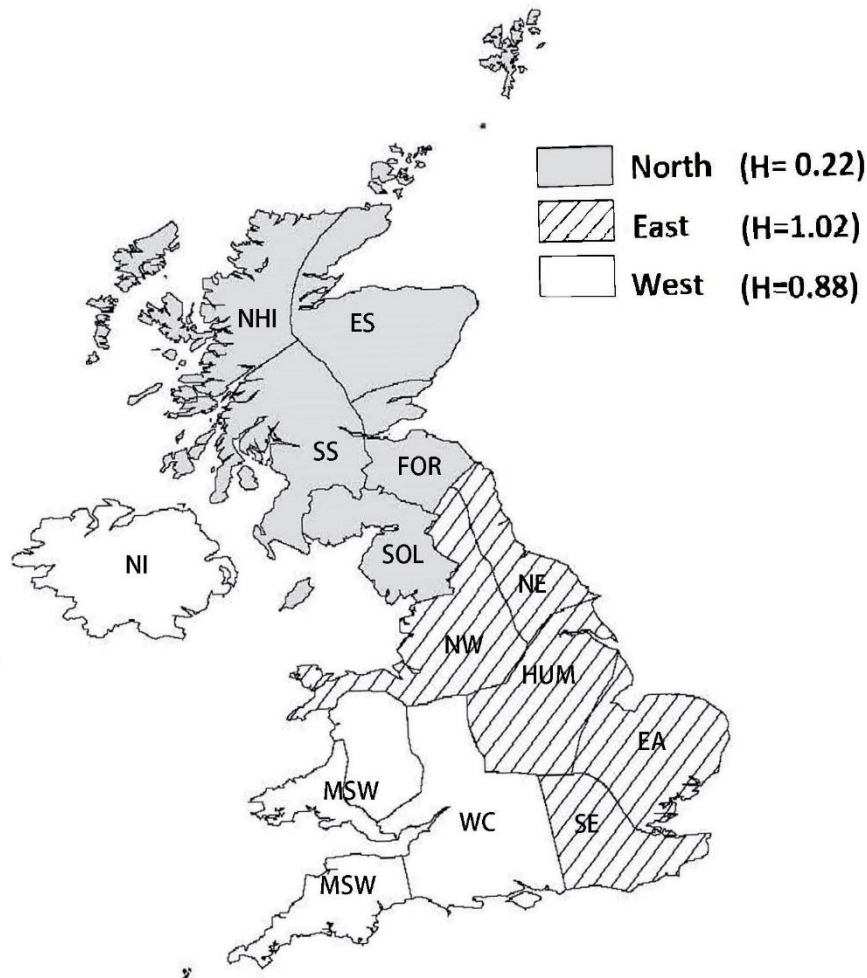
1601 These results also indicate some similarity between the 1h and 3h (short duration)
1602 AMAX, and between the 12h and 24h (longer duration) AMAX. For short duration
1603 AMAX, mean occurrence day (θ) mostly occurs in summer (Figure 4A) between mid-
1604 July and September (Julian day 200 to 273). In contrast, for longer duration AMAX θ
1605 is generally between September and December (Julian day 244 to 365). In particular,
1606 12h and 24h AMAX behave similarly to each other in terms of their mean day of
1607 occurrence and dispersion throughout the year regardless of region. For 1h and 3h
1608 AMAX though the similarity is confined to mean (summer) occurrence in southern and
1609 eastern regions whilst for northern and western regions there are greater differences
1610 between these two accumulation periods. For example, the difference in 1h and 3h θ
1611 is less than 2 weeks for central and southern regions, reaching up to 6 weeks for
1612 northern regions (e.g. NHI), whilst for longer durations the difference in θ between 12h
1613 and 24h AMAX is less than 3 weeks across all regions. The consistency at longer
1614 durations might be expected as both 12h and 24h extremes are less sensitive to short,
1615 very intense events and are both likely to be more strongly influenced by large-scale
1616 weather systems that affect large areas of the UK and produce less intense but more
1617 persistent precipitation throughout the year and particularly in autumn and winter which
1618 may also contribute to the greater dispersion (lower r) observed as duration increases.
1619 This is particularly the case in northern and western regions, which are less influenced
1620 by convective precipitation and where larger differences between 1h and 3h AMAX
1621 occurrence could be due to the reduced influence of short, heavy events in 3h AMAX
1622 and the greater contribution of moderate precipitation sustained over 3 hours with
1623 orographic enhancement of precipitation from weather systems across upland areas.
1624 The similarity of the mean occurrence of 1h and 3h AMAX in central and southern
1625 regions meanwhile could conversely be in part related to the dominance of
1626 convectively driven short, intense events which will produce a 1h AMAX and contribute
1627 significantly to the 3h accumulation, leading to a 3h AMAX in the same day. The future
1628 availability of a sub-hourly dataset for the UK could enable the role of short, convective
1629 events to be explored in more detail.

1630 Collectively therefore the circular statistics and seasonality plots reflect the principal
1631 precipitation generation mechanisms throughout the year. That is, short duration
1632 extremes, shown to mainly occur from summer through to early autumn, predominantly
1633 arise from convective processes (Hand *et al.*, 2004), particularly in the south and east
1634 of the UK (e.g. van Delden, 2001) where there is least variability in the timing of AMAX
1635 (generally higher r values). This is consistent with the high convective available
1636 potential energy (CAPE) in this region (Holley *et al.*, 2014) and with thunderstorm
1637 climatologies for the UK (Holt *et al.*, 2001). The relationship between UK hourly and
1638 daily extremes and temperature has also been shown to be stronger in summer
1639 (approximate CC scaling) compared with winter (Blenkinsop *et al.*, 2015; Chan *et al.*,
1640 2016) which also points to local thermodynamics as a significant driver of these
1641 extremes. In contrast, longer duration AMAX are more likely to occur either in autumn
1642 or winter in some regions and with a noticeably lower frequency in summer compared
1643 to short duration extremes in all regions. This suggests that longer duration extremes
1644 are less strongly influenced by convective processes and, as discussed above, are
1645 more likely caused by mid-latitude cyclonic systems which dominate throughout
1646 autumn and winter. Synoptic scale circulation systems have been shown to play a
1647 strong role in daily precipitation intensity across the UK with strong, cyclonic flow
1648 producing higher intensities throughout the year and westerly flow producing higher
1649 intensities in the north west of the UK (Osborn *et al.*, 1999; Tye *et al.*, 2016). This is
1650 partly associated with the North Atlantic Oscillation which has particularly strong
1651 correlations with precipitation over this region in winter (Murphy and Washington,
1652 2001). Recent research suggests that atmospheric rivers also have a role in the
1653 development of winter floods over the UK but have little influence over summer
1654 extreme precipitation (Lavers *et al.*, 2011; Champion *et al.*, 2015). Local factors may
1655 also modify large-scale behaviour; Svensson and Jakob (2002) identified the
1656 importance of orographic enhancement and land-sea contrasts in producing a morning
1657 peak in the occurrence of heavy precipitation at a site in southern Scotland. A greater
1658 understanding however is needed of the various drivers of sub-daily precipitation and
1659 the interactions between them. The investigation of drivers of sub-daily extremes is
1660 part of ongoing work in the INTENSE (INTElligent use of climate models for adaptatiON
1661 to non-Stationary hydrological Extremes) project (Blenkinsop *et al.*, 2018).

1662 Applying the homogeneity assessment approach by Hosking and Wallis (2005), we
1663 demonstrated that most of the existing extreme daily precipitation regions (Jones *et*

1664 *al.*, 2014) are homogeneous for 1h AMAX. Fitted GEV distributions for the 24h AMAX
1665 between 1992-2014 show close results to the fitted distributions for daily AMAX
1666 precipitation between 1961-2009 by Jones *et al.* (2014). The similarity of these results
1667 indicates that the data used in this research has an adequate record length, when
1668 pooled regionally, to analyse UK precipitation extremes. Moreover, this provides
1669 evidence that the quality control approach adopted by Blenkinsop *et al.* (2017) and
1670 Lewis *et al.* (2018), has produced a reliable precipitation dataset. The 1h AMAX return
1671 level estimates derived here showed a similar pattern and magnitude in neighbouring
1672 regions which indicates the potential for reshaping or merging the existing regions into
1673 fewer regions for future 1h extreme precipitation analysis.

1674 In an attempt to rationalise these regions into fewer, more representative regions for
1675 hourly precipitation, an initial examination is presented here as a precursor to a more
1676 extensive new regionalisation for hourly precipitation. Combining the existing regions
1677 into new regions is a simple approach that offers the potential to enhance statistical
1678 estimates through providing more gauges per region, thus improving results for
1679 ungauged areas. To illustrate the potential for redefining regions for sub-daily
1680 precipitation, the whole UK as a single region was examined and the heterogeneity
1681 test results showed a high value ($H= 2.61$), indicating a definitely heterogeneous
1682 region. Since some of the return level plots in Figure 6 (and growth curves in Figure
1683 A6) were so similar, the existing regions were then subjectively merged into 3 regions
1684 (Figure 9), defined as North, West, and East. These were created using the simple
1685 approach of subjectively grouping the existing regions based on the return levels of the
1686 individual gauges for the 1h AMAX return periods shown in Figure 8 (5-, 10-, 25-, and
1687 50 years). Different combinations of regions were examined using the same approach,
1688 yet this grouping resulted in the best homogeneity results. Indeed, the homogeneity
1689 measure (H) (Hosking and Wallis, 2005) for each region suggests that the proposed
1690 regions are homogeneous. Further improvements may be achieved by using statistical
1691 analyses of hourly precipitation variables and associated metrics in a more formal
1692 methodology such as that of Jones *et al.* (2014). This will be undertaken in the
1693 subsequent chapter.



1694

1695 Figure 9: Potential rationalisation of precipitation regions based on subjective
 1696 assessment of the 1h AMAX fitted GEV distributions. H denotes the heterogeneity
 1697 measure for each region using Hosking and Wallis (1998).

1698 **3.6. Conclusion**

1699 The results presented in this paper have implications for a number of aspects of
 1700 research into sub-daily extreme precipitation. Significantly, they demonstrate the
 1701 reliability of the hourly data used in this research, which could be used to provide better
 1702 guidance for practitioners in the UK water sector by updating and improving the Flood
 1703 Estimation Handbook (FEH) (Faulkner, 1999) design precipitation depths generated
 1704 by the Depth-Duration-Frequency (DDF) model. The FEH approach uses historical
 1705 data, hence, having updated, robust, and quality controlled hourly datasets up to 2014
 1706 (Blenkinsop *et al.*, 2017; Lewis *et al.*, 2018) would enhance the FEH estimations.

1707 The analysis of hourly and multi-hourly AMAX has demonstrated that 1h AMAX in the
 1708 UK show a different seasonality to that of daily AMAX and that the relationship between

1709 the two durations varies spatially. This suggests that using existing approaches to
1710 design and assess drainage systems which use a weather generator (e.g. UKCP09)
1711 to simulate hourly resolution data might produce misleading results. The climate model
1712 output, precipitation estimates, and other variables in the UKCP09 weather generator
1713 are primarily estimated at the daily level, with simple disaggregation methods to
1714 generate hourly resolution data (Jones *et al.*, 2009; Kellagher *et al.*, 2009; CIWEM,
1715 2016). Our research suggests that disaggregation methodologies that use this spatially
1716 extensive dataset and better reflect the differences between daily and sub-daily
1717 extremes (and their spatial variability) could be used to produce more reliable
1718 estimates of sub-daily extremes.

1719 Our research also shows that the existing UK extreme precipitation regions may not
1720 appropriately reflect regional differences in sub-daily extreme precipitation behaviour,
1721 as return level estimates show similarity across neighbouring regions. The
1722 development of new regions is recommended, based on the characteristics of hourly
1723 extreme precipitation events and allowing for the limited availability of data. It is likely,
1724 however, that the number of regions needed to describe variability in sub-daily extreme
1725 precipitation across the UK is significantly smaller than that needed for daily extremes.

1726 One of the major challenges in implementing plans and guidelines to manage pluvial
1727 flooding in the UK is the ability to predict potential changes in short, intense
1728 precipitation events. These challenges have impacts on urban drainage design
1729 guidelines, precipitation event risk assessments, and infrastructure management.
1730 However, as regional climate models (RCMs) use convection parameterisation
1731 schemes, they are generally unable to reproduce the small-scale convective systems
1732 that produce short duration events (Fowler and Ekström, 2009) such as the 1h and 3h
1733 AMAX examined here and which dominate summer UK extremes. Although, very high
1734 resolution convection-permitting models are able to better simulate convective
1735 precipitation events (e.g. Chan *et al.*, 2014b; Chan *et al.*, 2018a; Kendon *et al.*, 2018)
1736 they are computationally intensive and have, so far, only been run over small domains
1737 (see Prein *et al.* (2015) and Kendon *et al.* (2017) for review). Recent advances have
1738 been made in connecting hourly extreme precipitation simulated by convection-
1739 permitting models to synoptic-scale predictors in coarser resolution RCMs, and
1740 producing simple downscaling relationships (Chan *et al.*, 2018b). Further, statistical
1741 analysis of observed sub-daily extreme precipitation and its relation with climatological
1742 variables (e.g. temperature, sea level pressure, vertical velocity, humidity) will allow us

1743 to build observation-based statistical models for hourly and multi-hourly precipitation
1744 events. Such models could improve our understanding of short duration precipitation
1745 extremes and their potential future behaviour by validating the outputs of climate
1746 models and potentially providing a statistical downscaling short-cut (e.g. Fowler and
1747 Kilsby, 2007; Chan *et al.*, 2018b) to convection-permitting modelling. This research
1748 also has further implications for how such analyses of model projections are
1749 undertaken. Although the most frequent occurrence of short duration precipitation
1750 extremes is during summer, many hourly and multi-hourly AMAX occur between May
1751 and October depending on the region. The traditional seasonal division (summer: JJA)
1752 may therefore not be appropriate for the analysis of changes in such events if warming
1753 extends the 'convective season'.

1754 Finally, the difference in seasonality between sub-daily and daily extreme precipitation
1755 in the UK highlights the challenges in simulating and understanding extreme events
1756 using current statistical scaling and modelling approaches, particularly across
1757 durations. Better understanding of the characteristics of extreme precipitation and its
1758 drivers (Pfahl *et al.*, 2017), including at sub-daily timescales would help in exploiting
1759 and delivering the synergies between observational and modelling studies to reduce
1760 the uncertainties in our future predictions, guidelines and adaptation plans.

1761

1762

1763

1764

1765

1766

1767

1768

1769

1770 **Chapter 4. New hourly extreme precipitation regions and regional**
1771 **annual probability estimates for the UK**

1772 Existing UK extreme precipitation regions and urban drainage design guidelines are
1773 based on daily datasets, while various studies predict noticeable differences in the
1774 response of daily and sub-daily extremes in the UK to potential climate change. Recent
1775 flooding related to extreme precipitation in the UK has highlighted the importance of
1776 characterising these events, therefore, defining new hourly extreme precipitation
1777 regions would enhance our understanding of extremes, and provide a more
1778 appropriate tool to analyse sub-daily extremes.

1779 In this chapter, the quality controlled hourly precipitation dataset from 1992-2014,
1780 geographical and topographical characteristics (e.g. latitude, elevation), and other
1781 climatological variables (e.g. temperature) are used to characterise the hourly extreme
1782 precipitation climatology in the UK, and to define five new, homogeneous hourly
1783 extreme regions. Furthermore, this chapter demonstrates the novel use of a European
1784 weather patterns classification to reflect the role of the large scale circulation, and
1785 provide a dynamical basis for the hourly extreme regions.

1786 In meeting a central objective of this research by defining UK extreme precipitation
1787 regions based on hourly data and related climatological variables, this chapter
1788 concludes by employing these regions to quantify return estimates of hourly extreme
1789 precipitation across the UK.

1790 **4.1. Introduction**

1791 Recent decades have seen increases in the frequency and intensity of extreme
1792 precipitation in different regions which lead to increases in pluvial and fluvial flooding
1793 (Alexander *et al.*, 2006; Min *et al.*, 2011; IPCC, 2012; Westra *et al.*, 2014). Such
1794 increases impose challenges for wastewater and flood risk management, including the
1795 planning and designing of hydraulic structures, storm water drainage systems, and
1796 flood control structures, where accurate and reliable precipitation estimates are
1797 paramount (Durrans and Kirby, 2004; Madsen *et al.*, 2009). Furthermore, potential
1798 hazards of intense precipitation and associated flash floods in the UK can have
1799 significant effects on infrastructure, transportation, society and urbanized areas (Stern,
1800 2006). However, most observational based studies to date have examined historic
1801 changes in precipitation only at daily and multi-day timescales due, in part, to the

1802 limited availability of high-resolution precipitation observations and the statistical
1803 challenges of accurately determining sub-daily precipitation probability. These
1804 challenges are due to the lack of high quality long hourly precipitation records and to
1805 sparsely distributed gauge networks (Westra *et al.*, 2014). The latter is particularly
1806 important due to the highly variable nature of hourly extreme precipitation reflecting the
1807 localised nature of intense storms and their relationship to location and climatological
1808 factors (e.g. latitude, temperature gradient) (Alexander and Arblaster, 2009; Mishra *et*
1809 *al.*, 2012; Westra *et al.*, 2014; Forestieri *et al.*, 2018).

1810 Globally, most analyses of sub-daily precipitation extremes have reported increasing
1811 intensities (Westra *et al.*, 2014). In Europe, Madsen *et al.* (2009) reported an
1812 intensification in Denmark, lending support to results from the Netherlands (Lenderink
1813 *et al.*, 2011), Italy (Arnone *et al.*, 2013; Vallebona *et al.*, 2015), and the Czech Republic
1814 (Hanel *et al.*, 2016). Researchers on the other side of the Atlantic have reported similar
1815 increasing intensities in Canada and the USA (Burn *et al.*, 2011; Kunkel *et al.*, 2013;
1816 Muschinski and Katz, 2013; Barbero *et al.*, 2017). Recently, similar increases have
1817 also been reported in Australia (Zheng *et al.*, 2015; Hajani *et al.*, 2017; Guerreiro *et al.*,
1818 2018). Such increases in intensity have been linked to the enhanced moisture holding
1819 capacity of the atmosphere as described by the Clausius-Clapeyron relationship.
1820 Whether the increases are more closely related to air temperature or dew point
1821 temperature has been the subject of debate (e.g. Lenderink and Van Meijgaard, 2010;
1822 Ali and Mishra, 2017), with more recent research favouring the latter as less dependent
1823 on a constant relative humidity assumption (Ali *et al.*, 2018). The relationship between
1824 temperature and sub-daily extremes has been investigated in numerous observational
1825 analyses (Hardwick Jones *et al.*, 2010; Lenderink *et al.*, 2011; Mishra *et al.*, 2012;
1826 Blenkinsop *et al.*, 2015; Barbero *et al.*, 2017).

1827 While historical precipitation events are often used to estimate structural design
1828 capacity (Smithers and Schulze, 2001), extreme precipitation analysis based on
1829 observational data is strongly influenced by data quality, record length, and the spatial
1830 and temporal distribution of data (Westra *et al.*, 2014). Thus, regional frequency
1831 analysis (RFA), or region of influence approaches (ROI), are often used to supplement
1832 and improve extreme hydrological analyses where there is limited temporal or spatial
1833 data availability (Hosking and Wallis, 2005; Sarhadi and Heydarizadeh, 2014). The
1834 RFA methodology has also been used successfully in different locations to estimate
1835 the annual exceedance probability (AEP) of extremes (Fowler and Kilsby, 2003a;

1836 Fowler and Kilsby, 2003b; Lee and Maeng, 2003; Trefry *et al.*, 2005; Norbiato *et al.*,
1837 2007; Jones *et al.*, 2014). AEPs are more commonly referred to as “return periods” or
1838 “recurrence intervals”. In keeping with recent research on the communication of risks
1839 (e.g. Grounds *et al.*, 2018) and for clarity, we use the term AEP throughout this chapter.

1840 A requirement of the RFA approach, employed widely to examine UK precipitation
1841 data, is the pooling of data within homogeneous regions. Previously, Wigley *et al.*
1842 (1984) identified 5 regions in England and Wales using mean daily precipitation, which
1843 were subsequently extended to 9 regions for the UK and Northern Ireland by Gregory
1844 *et al.* (1991). Alexander and Jones (2000) used these regions to develop the Hadley
1845 UK precipitation (HadUKP) regional daily observation series which is updated in near
1846 real-time. These regions have been widely used, including for the analysis of UK
1847 precipitation trends (Osborn *et al.*, 2000; Simpson and Jones, 2014) and to perform
1848 RFA (Fowler and Kilsby, 2003a; Fowler and Kilsby, 2003b; Jones *et al.*, 2013; Jones
1849 *et al.*, 2014).

1850 Jones *et al.* (2014) reported that the HadUKP regions do not reflect regional variations
1851 in the frequency, magnitude and seasonality of UK daily extreme precipitation and
1852 therefore derived 14 regions that are more appropriate to analyse daily extremes.
1853 However, Darwish *et al.* (2018) presented a similar argument that neither the HadUKP
1854 regions nor those of Jones *et al.* (2014) are suitable for analysing sub-daily
1855 precipitation extremes, motivating the current research.

1856 In this chapter, we use an objective clustering of rain gauges and a regional frequency
1857 analysis of extreme precipitation as in Jones *et al.* (2014) to identify new, statistically
1858 homogeneous regions for UK hourly precipitation extremes, which reflect spatial
1859 variation and improve AEP estimates for hourly precipitation extremes. These new
1860 regions are identified from different climatological and site characteristics, including
1861 extreme precipitation intensity and frequency, seasonality measures, and prevailing
1862 weather types.

1863 The chapter is organised into four further sections; Section 4.2 describes the datasets
1864 used in the research whilst Section 4.3 presents the methods and statistical tools used
1865 to explore and analyse the data and to identify the new homogeneous regions. Section
1866 4.4 presents the new UK hourly extreme precipitation regions and the estimated annual
1867 exceedance probabilities derived from the RFA. Section 4.5 discusses the practical
1868 implications of the new regions as well as the research conclusions.

1869 4.2. Data

1870 This chapter uses a range of variables describing at-site characteristics (precipitation,
1871 temperature), site characteristics (location, elevation), as well as large-scale conditions
1872 (atmospheric circulation patterns) across the UK to identify homogeneous regions and
1873 characterise hourly extreme precipitation.

1874 The primary at-site characteristics were derived from the UK hourly precipitation
1875 dataset, comprising rain gauges from three sources: the UK Met Office Integrated Data
1876 Archive System (MIDAS), the Scottish Environmental Protection Agency (SEPA), and
1877 the UK Environment Agency (EA). The dataset (up to 2011) was collected by
1878 Blenkinsop *et al.* (2017) who performed a series of site-specific quality control (QC)
1879 procedures on the data, with additional QC checks against neighbouring gauges
1880 undertaken by Lewis *et al.* (2018) while extending the dataset to 2014. To ensure a
1881 reliable dataset of sufficient record length, and to facilitate comparison with other
1882 research, only gauges with more than 85% of their record complete (i.e. non-missing
1883 and data not flagged by the QC process) for each year is used here. These criteria
1884 were selected as a trade-off between having long records and data completeness.
1885 Further details on the adoption of these criteria can be found in Section 3.2.

1886 Moreover, site characteristics including the longitude and latitude of each rain gauge
1887 were derived from rain gauge metadata. However, not all gauges were accompanied
1888 by elevation data; absent data were derived from a global digital elevation model
1889 (DEM) with a horizontal grid spacing of approximately 250 metres (Jarvis *et al.*, 2008).

1890 For each rain gauge, corresponding series of daily maximum, minimum and mean
1891 temperature between 1992 and 2014 were obtained from the UKCP09 gridded dataset
1892 at a resolution of 5x5 km, and based on surface observations from 1960 to 2014
1893 covering the whole of the UK (Hollis and McCarthy, 2017). Consequently, a total of 197
1894 rain gauges distributed across the UK covering the period 1992-2014 were used in this
1895 study alongside the gridded daily temperature series.

1896 Atmospheric circulation over the North Atlantic ocean has a strong effect on Western
1897 European weather, affecting air flow, moisture content, and other characteristics which
1898 in turn control precipitation patterns (Scaife *et al.*, 2008; Hurrell and Deser, 2010;
1899 Woollings, 2010). WTs developed from climatic variables (i.e. mean sea level pressure
1900 (MSLP), wind speed, and wind direction) have long been used both in Europe (e.g.
1901 Lamb, 1991; Bissolli and Dittmann, 2001) for different purposes including: assessing

1902 UK precipitation and global meteorological relationships (Knight *et al.*, 2017),
1903 investigating future European precipitation (Fereday *et al.*, 2018), forecasting coastal
1904 floods around the UK (Neal *et al.*, 2018), and in the construction of a precipitation and
1905 drought climatology for the UK (Richardson *et al.*, 2018). Thus, the final dataset used
1906 here is that of Neal *et al.* (2016) who classified large-scale atmospheric circulation
1907 conditions over Europe into 30 Weather Types (WTs), deriving a smaller set of 8 WTs
1908 (Table 2), using K-means clustering, for the purposes of evaluating forecasts.

1909 Here, the subset of 8 WTs between 1992-2014 are used to provide additional
1910 understanding of the physical processes of UK hourly extreme precipitation,
1911 underpinning the new precipitation regions and associated AEP estimates. The final
1912 investigated hourly extremes dataset is relatively limited, therefore, using the 8 WTs
1913 provides a balance to reflect the relationship between WTs and hourly extremes,
1914 providing a reasonable sample of events across the types. Using the classification of
1915 30 WTs would split the extremes across too large a number of WTs which is impractical
1916 for further analysis, and makes the relationship indistinguishable. Thus, the 8 WTs
1917 were selected for the analysis in this research.

1918

Weather type (WT)	Description
1. NAO-	All sub-types going into this type in general have positive MSLP anomalies to the north of the UK and negative MSLP anomalies to the south of the UK, resulting in a negative NAO pattern.
2. NAO+	All sub-types going into this type in general have negative MSLP anomalies to the north of the UK and positive MSLP anomalies to the south of the UK, resulting in a zonal (positive NAO) type.
3. Northwesterly	All sub-types going into this type in general have negative MSLP anomalies to the northeast of the UK and positive MSLP anomalies to the southwest of the UK, resulting in a northwesterly flow. Sub-patterns going into this type vary between being cyclonic and anticyclonic, but the direction of flow is the same.
4. Southwesterly	All sub-types going into this type in general have negative MSLP anomalies to the northwest of the UK and positive MSLP anomalies to the southeast of the UK, resulting in a southwesterly flow. Sub-types going into this type vary between being cyclonic and anticyclonic but the direction of flow is the same.
5. Scandinavian high	All sub-patterns going into this type in general have negative MSLP anomalies to the west of the UK and positive MSLP anomalies to the east of the UK, resulting in a south to southeasterly flow. Most sub-patterns in this type are anticyclonic.
6. High pressure center over UK	Both sub-types going into this type have positive MSLP anomalies over the UK and to the south of the UK, with weak negative MSLP anomalies to the north of the UK. This results in an anticyclonic westerly or southwesterly flow.
7. Low close to UK	Both sub-types going into this type extend a trough over the UK. Negative MSLP anomalies are centred just to the west of the UK resulting in a cyclonic southwesterly flow.

8. Azores high	Only one of the 30 types goes into this type which shows an anticyclonic westerly flow over the UK, with an Azores high extension.
----------------	--

1920 Table 2: *Descriptions of the eight weather patterns from the European and North*
1921 *Atlantic Daily to Multi-decadal Climate Variability (EMULATE) MSLP (EMSLP) data*
1922 *(1850–2003) as derived in Neal et al, 2016. Weather type names and descriptions are*
1923 *relevant to the UK. MSLP and NAO denote mean sea level pressure and North Atlantic*
1924 *Oscillation respectively.*

1925 **4.3. Methodology**

1926 We apply a statistical approach to cluster gauges with similar characteristics together
1927 and create homogeneous regions for assessing the spatial pattern of hydrological
1928 processes. This method has been used widely in the literature (Wigley *et al.*, 1984;
1929 Dales and Reed, 1989; Jones *et al.*, 2014; Sarhadi and Heydarizadeh, 2014; Forestieri
1930 *et al.*, 2018). In addition, the frequency of occurrence of UK weather types is
1931 incorporated into the analysis, and used to delineate the new regions, to ensure that
1932 the new regions reflect both the statistical and physical behaviour of hourly extreme
1933 precipitation.

1934 The following sections describe the process of selecting appropriate variables (Section
1935 4.3.1), identification of new homogeneous regions (Section 4.3.2), an estimation of
1936 regional AEP for UK hourly extreme precipitation (Section 4.3.3), data independence
1937 (Section 4.3.4), and goodness of fit (Section 4.3.5).

1938 **4.3.1. Variable Selection**

1939 The UK is located downstream of the Atlantic storm track, which produces a strong
1940 temporal variation in precipitation (de Leeuw *et al.*, 2016). Furthermore, extreme hourly
1941 UK precipitation displays geographical and seasonal variability, with most hourly
1942 extremes occurring in summer, especially in the southern and eastern UK (Blenkinsop
1943 *et al.*, 2017; Darwish *et al.*, 2018). This seasonality is associated with different daily
1944 and sub-daily extreme precipitation generating mechanisms. North-western areas are
1945 more strongly influenced by extreme precipitation arising from large scale circulation
1946 and frontal systems occurring in autumn and winter than in the south and southeastern
1947 parts of the UK where extremes tend to be dominated by short duration, convective
1948 precipitation occurring in summer (Jones *et al.*, 2014; Darwish *et al.*, 2018). Previous
1949 studies at daily timescales have selected variables which reflect these topographical

1950 and climatological variations (Wigley *et al.*, 1984; Dales and Reed, 1989; Reed and
1951 Robson, 1999; Maraun *et al.*, 2008; Jones *et al.*, 2014).

1952 In this research, statistics for different climatological variables are investigated and the
1953 extent to which they reflect variability in hourly extreme precipitation frequency and
1954 intensity patterns in the UK were assessed before selecting the most relevant variables
1955 for further analysis. Data availability, possible correlation between variables, the
1956 relevance to hourly precipitation extremes and their generating processes were
1957 considered prior to further analysis.

1958 Firstly, the geographical and topographical characteristics, latitude (Lat), longitude
1959 (Lon) and elevation (Elev), were allocated for each gauge as detailed in Section 4.2
1960 (see also Table 3). Previous examination of UK hourly and daily extremes used annual
1961 maxima (AMAX), the 0.99 wet day/hour quantiles (Q99) (Alexander and Jones, 2000;
1962 Jones *et al.*, 2014; Simpson and Jones, 2014; Darwish *et al.*, 2018), or N maximum
1963 events per year to define extremes (Blenkinsop *et al.*, 2017). Here, the median AMAX
1964 (RMed) and the 0.99 wet hour quantile for annual (Q99), summer half year (April-
1965 September) (SQ99), and winter half year (October-March) (WQ99) hourly precipitation
1966 were calculated for each gauge to capture the variability in regional annual and
1967 seasonal precipitation intensity. As an approximation to the regional and seasonal
1968 differences in extreme frequency, the number of hours exceeding SQ99 in summer
1969 and WQ99 in winter were derived (denoted as N-SQ99, and N-WQ99 respectively). In
1970 reality, this value will be skewed by the number of complete record years as well as
1971 the wet hour frequency; however, this offers a characterisation of the spatial
1972 differences in the number of wet hours. We calculated these statistics using hourly
1973 declustered precipitation (the highest hourly value per day) for each gauge to ensure
1974 independent precipitation values.

1975 Precipitation seasonality was then quantified using circular statistics (Reed and
1976 Robson, 1999) to represent the mean occurrence day of hourly precipitation extremes
1977 ($\bar{\theta}$), and the overall dispersion (\bar{r}) of the events around $\bar{\theta}$. The circular statistics were
1978 calculated for each gauge using hourly precipitation greater than Q99, using the
1979 method stated in Section 3.3.1. Values of r closer to 1 (0) indicate a higher (lower)
1980 concentration of events around θ , and therefore a stronger (weaker) seasonal signal.

1981 Furthermore, the median of maximum and minimum recorded temperature values
1982 (Tmax, Tmin) on the Q99 precipitation days was extracted for each gauge. The relation

1983 between UK extreme hourly precipitation and temperature has been investigated by
 1984 Blenkinsop *et al.* (2015) who showed that UK hourly extremes scale with temperature
 1985 according to the thermodynamic Clausius-Clapeyron (CC) relation, which states a 6-
 1986 7% increase in atmospheric moisture holding capacity per 1°C increase in
 1987 temperature, under constant relative humidity. Table 3 provides a summary of the
 1988 selected variables and their description.

Variable	Description
Lat	Latitude of rain gauge
Lon	Longitude of rain gauge
Elev	Elevation of rain gauge
Q99	Precipitation 0.99 quantile (wet hours)
SQ99	Summer (April-September) precipitation 0.99 quantile (wet hours)
WQ99	Winter (October-March) precipitation 0.99 quantile (wet hours)
RMed	Median of AMAX precipitation 1992-2014
$\bar{\theta}$	Average day of occurrence of events exceeding Q99 (rotated seasonal statistics)
\bar{r}	Dispersion of events exceeding Q99 around $\bar{\theta}$ (rotated seasonal statistics)
N-SQ99	Number of summer (April-September) events exceeding SQ99
N-WQ99	Number of winter (October-March) events exceeding WQ99
Tmax	Median of maximum temperature on Q99 days
Tmin	Median of minimum temperature on Q99 days

1989 Table 3: Variables used to identify homogeneous regions for hourly extreme
 1990 precipitation using principal components analysis. Each variable's contribution to the
 1991 PCA results were assessed, and the most representative variables (shaded) were
 1992 retained.

1993 To reduce the number of variables used for each gauge, and to identify the most
 1994 meaningful variables from those chosen for the analysis, principal component analysis
 1995 (PCA) was performed. PCA reduces large multivariate statistical datasets to smaller
 1996 and equally descriptive datasets that capture their similarities by creating linear
 1997 combinations of the original data (Wilks, 2011). Each combination describes a
 1998 proportion of the original data, called a principal component (PC). Hosking and Wallis
 1999 (2005) reported the sensitivity of clustering algorithms to the Euclidean distance or
 2000 scale of the variables used, and suggested rescaling the input variables before

2001 performing the clustering, to avoid the dominance of variables with large absolute
2002 values (e.g. altitude). Hence, all the variables in Table 3 were rescaled by dividing each
2003 variable value by its corresponding median before analysing the PCs.

2004 Finally, different combinations of the variables in Table 3 were investigated using the
2005 variable loadings and variance, to determine the most representative combination of
2006 variables. The loadings, shown in Table 4, indicate the association between the original
2007 variables and the new linear combinations, while the proportion of variance explained
2008 by each PC indicates the importance of the PC. Combinations which achieved the
2009 highest explained variance, and variables showing high loadings were chosen for
2010 further analysis.

2011 **4.3.2. Clustering Analysis**

2012 To identify homogeneous regions for UK hourly extreme precipitation, a cluster
2013 analysis was undertaken on the final PC scores for each gauge. Cluster analysis (CA)
2014 using PC scores has been widely adopted in the literature (e.g. Gottschalk, 1985;
2015 Jones *et al.*, 2014; Sarhadi and Heydarizadeh, 2014; Forestieri *et al.*, 2018). Sarhadi
2016 and Heydarizadeh (2014) reported that CA is the most practical method to assess and
2017 pool similar hydrological and climatological data in homogeneous regions using their
2018 geographical, physical and statistical characteristics. It is assumed that all stations
2019 within the homogeneous regions identified by the CA will have similar distributions and
2020 characteristics, facilitating reliable probability estimates at data scarce or ungauged
2021 sites (Hosking and Wallis, 2005).

2022 Generally, cluster analysis (CA) methods for hydrological studies adopt either a
2023 hierarchical clustering approach such as average and complete linkage (Jackson and
2024 Weinand, 1995; Ramos, 2001), and Wards method (Jackson and Weinand, 1995;
2025 Ramos, 2001; Sarhadi and Heydarizadeh, 2014), or a non- hierarchical clustering
2026 approach such as K-means method (Jones *et al.*, 2014).

2027 The hierarchical approach clusters the two most similar objects together and continue
2028 to combine until all objects are in the same cluster. This approach has the advantage
2029 of visualising the clusters using a tree structure (i.e. dendrogram), and providing
2030 different groups based on the level of resolution being examined, without the need of
2031 determining the targeted number of clusters as an input (Tan, 2018). On the other
2032 hand, the non-hierarchical approach (e.g. K-means) clusters the data in independent
2033 groups, where the objects within each group are similar to each other and dissimilar to

2034 other groups (Tan, 2018). Furthermore, the K-means approach is sensitive to
2035 erroneous values, and requires the identification of the targeted number of clusters as
2036 an input, which requires a priori knowledge to avoid clustering the objects inaccurately
2037 (Ferro and Segers, 2003).

2038 Therefore, Wards method was used in this study, which employs dendrograms to
2039 assess and visualise the correlation between input and output dissimilarities between
2040 different clusters. In addition, Wards method achieved the highest “Cophenetic
2041 correlation” coefficient values compared to both: K-mean and average and complete
2042 linkage, which measure how faithfully a dendrogram preserves the pairwise distances
2043 between the original unmodelled data points (Rao and Srinivas, 2006; Isik and Singh,
2044 2008). The spatial and topographical contiguity of the regions were also reviewed to
2045 ensure coherency and relevancy to UK geographical and climatological conditions.

2046 Rather than rely solely on a statistical estimation of hourly extreme precipitation
2047 regions, a dynamical approach was also employed by using the 8 European weather
2048 types (WTs) defined by Neal *et al.* (2016). The WTs indicate the prevalent circulation
2049 patterns over Europe and the UK each day. By assigning the appropriate WT to each
2050 gauge record of Q99, WQ99 or SQ99, it was possible to analyse the proportion of time
2051 each WT generated an extreme hourly precipitation. Mapping these proportions for
2052 each station, hence, provided insight into the atmospheric circulation patterns and
2053 physical processes associated with short-duration extreme precipitation and enabled
2054 dynamical confirmation of the statistically-derived regional clusters.

2055 **4.3.3. Regional Frequency Analysis (RFA)**

2056 The new regions’ homogeneity and the gauges’ discordancy within each region were
2057 assessed with respect to RFA guidelines as in Section 3.3.3 (see also Darwish *et al.*
2058 (2018)). Furthermore, the precipitation data in each gauge were standardised by
2059 dividing on the corresponding median to reduce the impact of potential spatial variation
2060 caused by imprecise recorded values. Then regional Generalised Extreme Value
2061 (GEV) and Generalised Pareto (GP) distributions were fitted to standardised annual
2062 maxima (AMAX) and wet hours exceeding the 0.99 quantile (Q99), respectively, to
2063 estimate AEPs for different durations as in Section 3.3.3 (see also Darwish *et al.*
2064 (2018)).

2065

4.3.4. Data independence

2066 Independence and stationarity are important underlying assumptions for regional
2067 frequency analysis. Therefore, the AMAX at each gauge was used to ensure having
2068 independent extremes for the fitted GEV distribution. Additionally, further steps were
2069 performed to ensure independent data for the GP distribution, where multiple
2070 observations might occur at the same time within each region.

2071 Initially, the 0.99 quantile (Q99) for each gauge was calculated, then observations
2072 above Q99 were declustered and retained for further analysis. Subsequently, the Q99
2073 observation from all the gauges within each region were grouped, and only the highest
2074 hourly precipitation value per day in each region was selected.

2075 In this chapter, the “runs declustering” approach by Leadbetter *et al.* (1989), has been
2076 adopted to ensure Q99 data independence. The approach considers exceedances to
2077 belong to the same cluster if they are separated by less than a fixed number of
2078 occurrences r called “run length” (T_c). However, choosing the “run length” is arbitrary,
2079 and depends on investigated datasets (Acero *et al.*, 2011). Therefore, the improved
2080 and automated “run length” technique by Ferro and Segers (2003) was employed in
2081 the analysis which uses an extremal index variable ($E\Theta$) to measure the degree of
2082 clustering of extremes instead of the arbitrary choice of the “run length”. This technique
2083 allows the assessment of the independence of each gauge data, using a different “run
2084 length”, that is determined automatically as a function of the degree of clustering of
2085 extremes instead of using the same “run length” across the whole region.

2086 Therefore, to find the suitable (T_c) for each gauge, an automated approach is used
2087 that only depends on the extremal index ($E\Theta$), which is calculated from the N
2088 exceedances of the threshold considering the interexceedance times T_i expressed as
2089 following (Ferro and Segers, 2003):

$$E\theta(u) = \frac{2[\sum_{i=1}^{N-1}(T_i - 1)]^2}{(N - 1) \sum_{i=1}^{N-1}(T_i - 1)(T_i - 2)} \quad (10)$$

2090 where N is the exceedances of the threshold (u) considering the interexceedance times
2091 T .

2092 The extremal index ($E\Theta$) takes a value in the interval $[0, 1]$, where independent data,
2093 $E\Theta = 1$, while $E\Theta = 0$ indicates full data dependence (clustering). The analysed gauges
2094 in this research have values higher than 0.7, indicating generally independent values.

2095

4.3.5. Goodness of fit measure (Z_{dist})

2096 Hosking and Wallis (2005) suggested using the Z_{dist} measure to assess the goodness
2097 of fit for a potential fitted distribution. Z_{dist} assesses the goodness-of-fit by comparing
2098 the difference between the L- kurtosis of the potential distribution and the regional
2099 average L- kurtosis of the region of interest, weighted proportionally to the sites' record
2100 lengths. The L- kurtosis of the potential distribution is estimated by simulating a large
2101 number of regions having the potential distribution, with L-moments ratios (i.e. L-
2102 variation, L-skewness, and L- Kurtosis) equal to the average regional L-moments ratios
2103 of the region of interest, besides having the same number of sites and record lengths.
2104 Therefore, Hosking and Wallis (2005) suggested that for each distribution, the
2105 goodness-of-fit measure is calculated as:

$$2106 \quad Z_{dist} = (\tau_4^{DIST} - \tau_4^R + B^4) / \sigma^4 \quad (11)$$

2107 Where τ_4^{DIST} is the L-kurtosis of the fitted distribution, and DIST can be any distribution
2108 (e.g. GEV, GPD), τ_4^R is the regional average L-kurtosis , B^4 is the bias of τ_4^R , and σ^4 is
2109 the standard deviation of L- Kurtosis values from simulation. The bias (B^4) is calculated
2110 as:

$$2111 \quad B^4 = \frac{1}{N_{sim}} \sum_{m=1}^{N_{sim}} \tau_4^m - \tau_4^R \quad (12)$$

2112 while the standard deviation of L- Kurtosis values from simulation (σ^4) is calculated as:

$$2113 \quad \sigma^4 = \sqrt{\left\{ \left(\frac{1}{N_{sim}} \right) \left[\sum_{i=1}^{N_{sim}} (\tau_4^i - \tau_4^R)^2 - (N_{sim} B_4)^2 \right] \right\}} \quad (13)$$

2114 where N_{sim} is a large simulation of data sets for a region with N sites, each having the
2115 potential distribution as its frequency distribution, and τ_4^m is the m th simulated region
2116 average L-kurtosis value.

2117 Hosking and Wallis (2005) declare the fit to be adequate if Z_{dist} is sufficiently close to
2118 zero, while a reasonable criterion is having $| Z_{dist} | \leq 1.64$, at an approximate
2119 confidence level of 90%.

2120 4.4. Results

2121 4.4.1. Principal Components Analysis

2122 The variables presented in Table 3 were selected to capture the hydro-climatological
2123 characteristics of the UK hourly extremes, specifically spatial and temporal differences

2124 in frequency and intensity as reported in the literature (Blenkinsop *et al.*, 2017; Darwish
2125 *et al.*, 2018). PCA was carried out for different combinations of the rescaled variables
2126 to confirm their efficacy in describing and explaining the data patterns, and to identify
2127 repetitive variables that could be dropped. For instance, the PCA results (i.e. PC
2128 loadings and total explained variance) showed that including seasonal quantiles (SQ99
2129 and WQ99) might repeat information from the annual quantiles and did not increase
2130 the explained variance. Therefore, only the explanatory variables shaded in grey in
2131 Table 3 were retained for use.

2132 PCA results for the selected variables (Table 4) show the variation explained by each
2133 principal component and the loading of each variable. PC1 explains 49% of the total
2134 variance and is related to temperature, emphasising temperature's strong association
2135 with hourly extreme precipitation. PC2 explains 19% of the variance and is related to
2136 hourly extreme precipitation intensity, with the highest loadings associated with RMed
2137 and Q99. The absolute loadings of extreme precipitation intensity variables in PC2 are
2138 noticeably higher than for other variables. PC3 explains 11% of the variance and is
2139 related to the spatial seasonality and frequency of extreme hourly precipitation, in
2140 addition to orography. Finally, PC4 (not shown) explains less than 5% of the variance,
2141 with the highest loading variables similar to those of PC3 (elevation, N-SQ99, and $\bar{\theta}$).

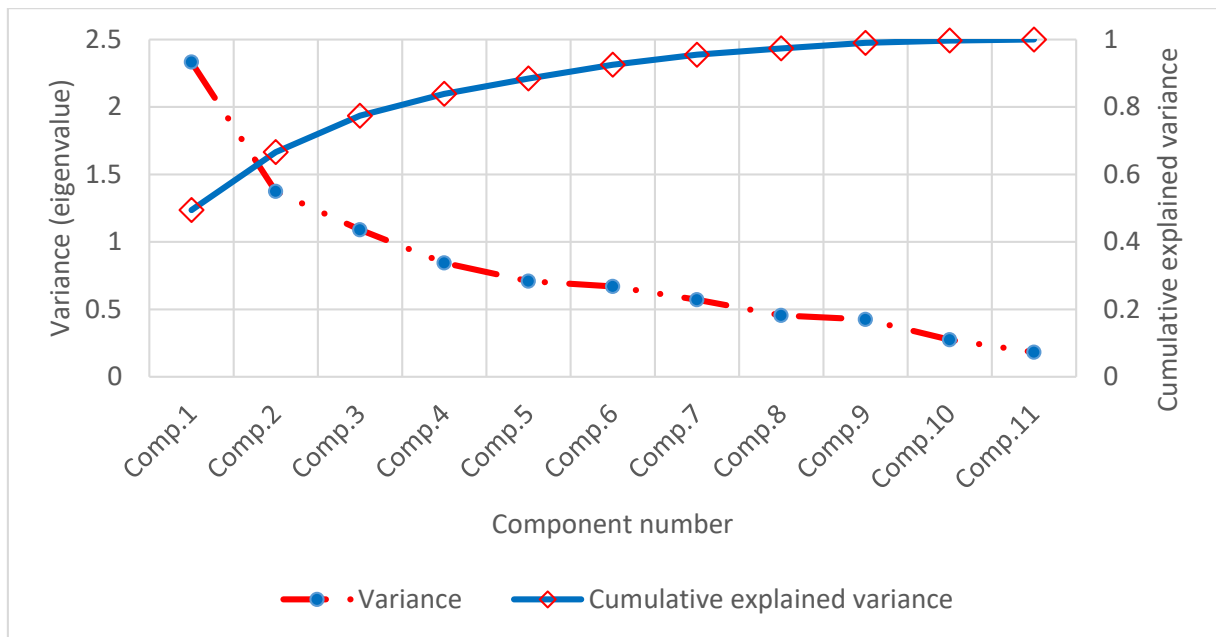
2142

Variable	PC1	PC2	PC3
LAT	0.318	0.329	0.133
LON	-0.317		-0.276
Elevation	0.229	-0.248	-0.459
Q99		-0.636	0.256
RMed		-0.619	
\bar{r}	0.366	-0.151	
$\bar{\theta}$	-0.255		0.541
N-SQ99	0.259		0.544
N-WQ99	0.383		0.138
Tmax	-0.406		
Tmin	-0.404		
<i>Proportional contribution (explained variance)</i>	<i>49%</i>	<i>19%</i>	<i>11%</i>

2144 Table 4: Loadings of each variable in the first three principal components and
 2145 proportional contribution to the explained variance. Values in bold are the 2 most
 2146 significant contributing variables for each principal component. Loadings smaller than
 2147 ± 0.1 are not reported for clarity.

2148 Selecting the adequate number of components to reflect the data characteristics is
 2149 subjective, and may be based on various factors such as the scree plot, which
 2150 measures the variance (i.e. eigenvalues) associated with each component, the total
 2151 explained variance, and the component eigenvalue. Jolliffe (2002) suggested using the
 2152 number of components on the scree plot where the slope of the curve shows a levelling
 2153 off (elbow). Other researchers have suggested using standard approaches such as
 2154 selecting components with eigenvalues > 1 (Eder, 1989), or using components that
 2155 explain most of the variability (i.e. greater than 70%) (Jolliffe, 1990).

2156 The scree plot (Figure 10) indicates that the variance curve (red line) decreases slightly
 2157 after the 3rd principal component, while the total explained variance (blue line) indicates
 2158 that the first three components capture 79% of the data variance. Moreover, the 4th
 2159 principal component (Comp.4) explains less than 5%. Additionally, only the
 2160 eigenvalues of the first three components are greater than 1 and therefore only these
 2161 (1-3) were retained for subsequent use in the clustering analysis.



2162

2163 *Figure 10:* Scree plot of the principle component analysis (PCA) for the various
 2164 climatological variables in Table 4. Eigenvalue of each component (left Y-axis) (Blue
 2165 line), cumulative explained variance (right Y-axis) (Red line), and component number
 2166 (X-axis).

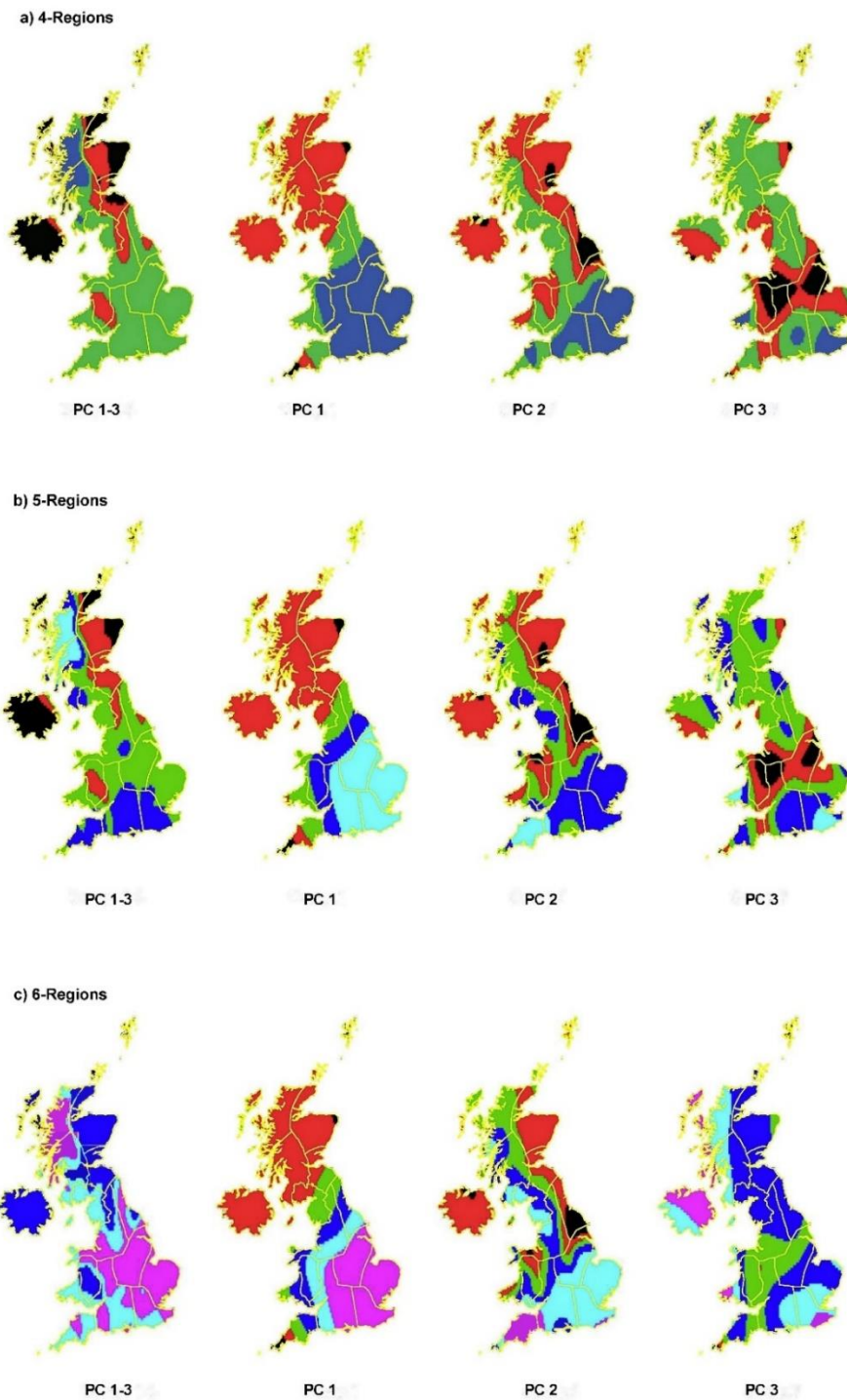
2167

4.4.2. Regional Clustering Analysis

2168 As outlined in Section 4.3.2, three different clustering approaches were assessed
 2169 (Wards, K-means, and average and complete linkage), with Wards method achieving
 2170 the highest “Cophenetic correlation” value (0.78) and most successfully delineating
 2171 spatially-contiguous homogeneous regions. Wards method has been used in other
 2172 hydro-climatic research (Jackson and Weinand, 1995; Ramos, 2001), and is
 2173 recommended as a robust method for variable classification (Modarres and Sarhadi,
 2174 2011).

2175 PC scores for the three components were calculated for each gauge. These scores
 2176 were then spatially clustered individually (i.e. PC1, PC2, and PC3) and jointly (i.e. PC
 2177 1-3) using Wards method for a range of 3 to 9 target clusters. Comparison of the
 2178 clusters from the individual component scores were assessed for their conformity to
 2179 the physical interpretations described above; while the cumulative scores helped to
 2180 visualise the best regional configuration. Figure 11 illustrates that clustering the gauges
 2181 into 4, 5, or 6 regions best captures the seasonal and locational differences in hourly
 2182 precipitation extremes. Using only three regions did not delineate orographic behaviour
 2183 sufficiently, while using greater than six regions subdivided the southernmost regions
 2184 with little physical justification. The results indicated that four regions (Figure 11a, PC1-
 2185 3 and PC2) were able to capture the east-west precipitation difference caused by

2186 orographic effects in the north and central UK, though it was not able to capture the
2187 variation in the south and south-eastern regions. On the other hand, 6 regions (Figure
2188 11c, PC1-3, PC1, and PC3) begin to subdivide parts of the south and south west UK,
2189 and clustered climatologically different regions together such as Northern Ireland and
2190 north-east England (Figure 11c, PC1-3, PC1, and PC2). Using 5 clusters (Figure 11b),
2191 best captured the east-west and north-south patterns, and reflected the orographic
2192 effects and seasonal drivers.

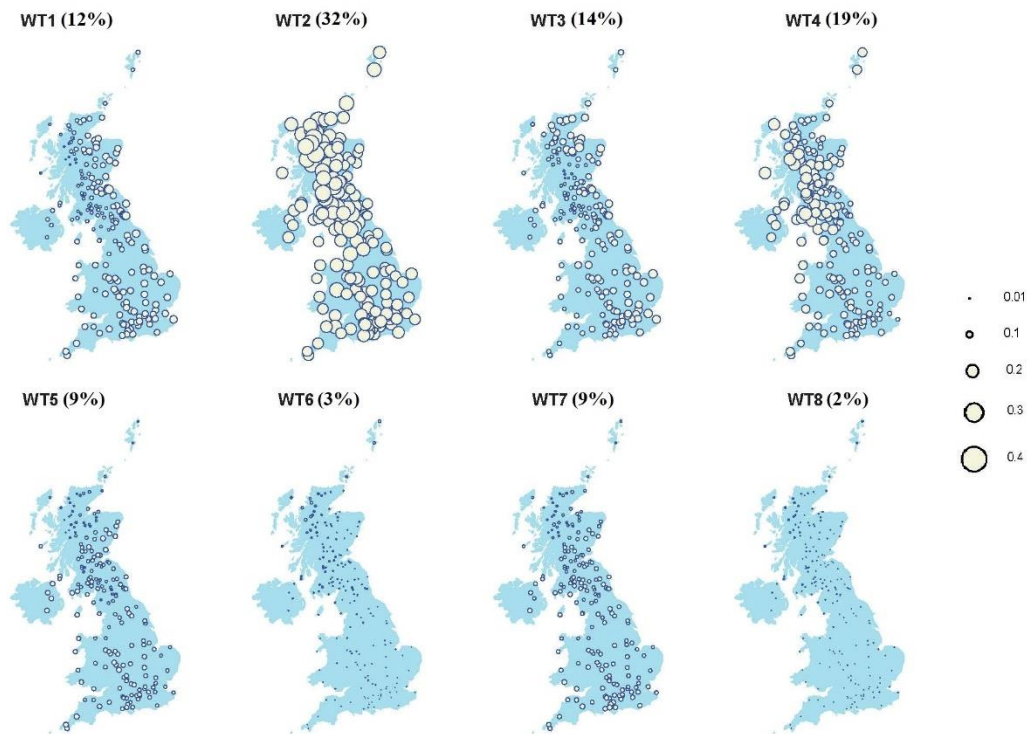


2193

2194 Figure 11: PCA clustering results for UK hourly precipitation using Wards clustering
 2195 approach for (a) 4 regions; (b) 5 regions; and (c) 6 regions. Kernel-smoothed PCA
 2196 scores for all components PC1 to 3 (left column) and individually (i.e. PC1, PC2, and
 2197 PC3) (right three columns) are illustrated. Yellow line are the existing daily extreme
 2198 regions by Jones et al, (2014), and presented here for reference only.

2199 As the choice of five regions rather than four or six is relatively subjective, a physical
2200 reasoning approach was also adopted to assess whether the statistically derived
2201 regions adequately encompass known weather patterns. Physical reasoning for the
2202 clusters was assessed by comparing the proportion of events exceeding Q99 at each
2203 gauge corresponding with each of the 8 daily WTs (Neal *et al.*, 2016) for the period
2204 1992-2014 (Figure 12). This was repeated for the winter half-year (N-WQ99) and
2205 summer half-year (N-SQ99) (Figures A9 and A10 respectively). The main WTs
2206 associated with extreme precipitation are WT2 (i.e. NAO+ pattern) and WT4 (i.e.
2207 Southwesterly pattern), which are associated with 51% (WT2: 32%, WT4: 19%) of
2208 precipitation exceeding Q99 (Figure 12). Both weather types are characterised by
2209 southwesterly flow, bringing warm, moist air, and more frequent stormy weather,
2210 especially in winter (Figure A9). WT2 contributes a similar proportion of events
2211 exceeding Q99 precipitation to most gauges, and affects the whole country, noticeably
2212 in winter where the UK is affected by westerly storms (Figure A9). However, in summer
2213 (Figure A10), the total contribution of WT2 (22%), is reduced compared to annual
2214 (32%) or winter (40%), and occurs mostly in the north-western UK. In contrast, WT4
2215 shows a high occurrence only in the north-western UK annually (Figure 12), and
2216 seasonally (Figures A9 and A10), which agrees with the direction and track of the
2217 dominant south-westerly flow characterising this WT.

2218 Conversely, WTs 6 and 8 (i.e. high pressure centred over UK and Azores high,
2219 respectively in Neal *et al.* (2016) are associated with only 5% of events exceeding Q99
2220 annually across the UK. Both WTs 6 and 8 are characterised by anticyclonic high
2221 pressure areas over the UK, leading to dry conditions and warm weather in summer,
2222 and clear skies and cold nights in winter, consistent with low precipitation frequency.

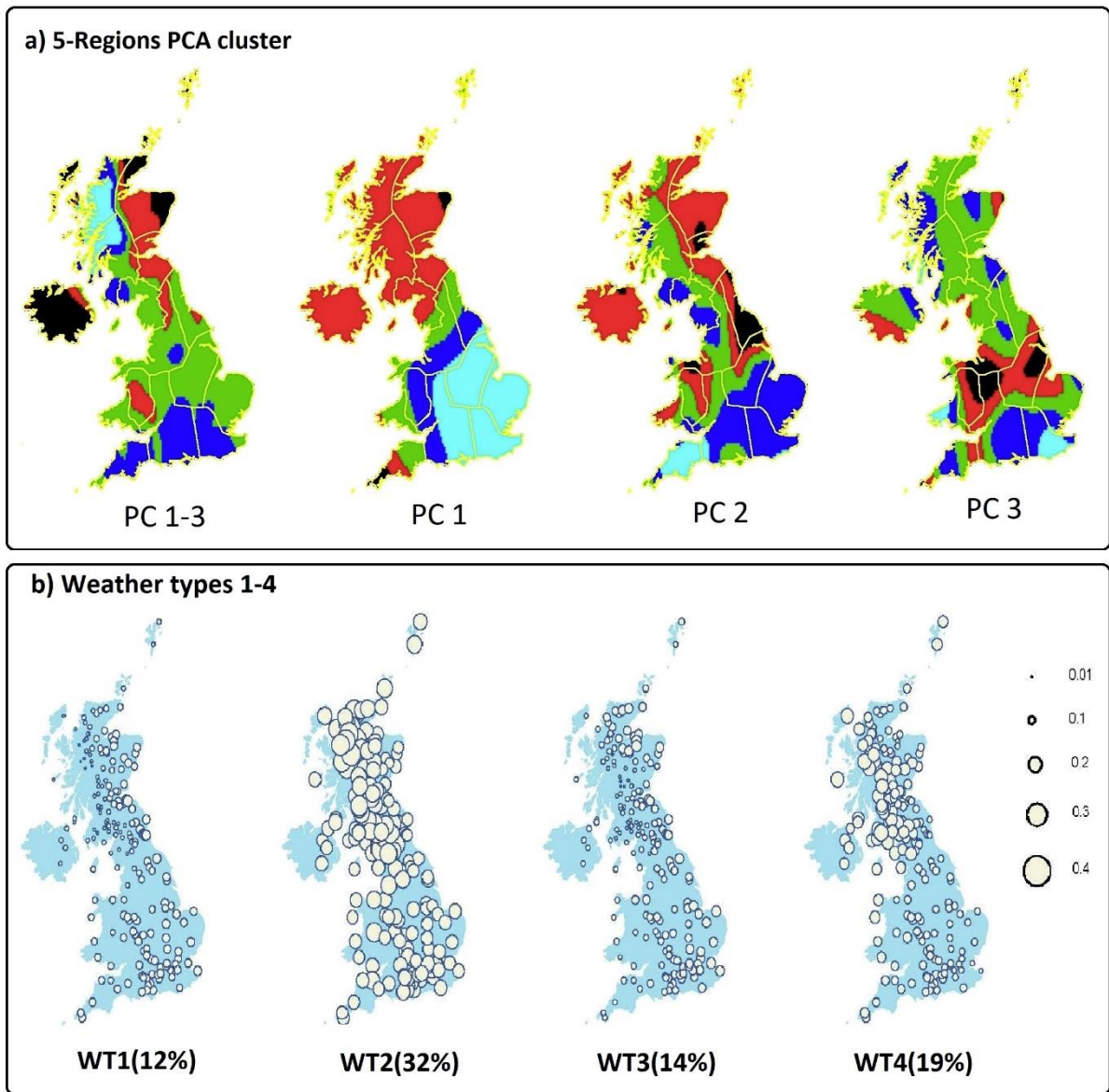


2223

2224 Figure 12: Proportion of days exceeding Q99 hourly precipitation for each gauge
 2225 across the 8 weather types identified by Neal et al. (2016) over the period 1992-2014.
 2226 Numbers in brackets represent the percentage of all days on which each weather type
 2227 occurs. Circle diameter indicates the proportion of Q99 events within each weather
 2228 type for each gauge.

2229

2230 Figures 12, A9 and A10 all show a clear east-west pattern in WTs 1, 3, and 4 caused
 2231 by the northeasterly, northwesterly, and southwesterly flow respectively, with a weaker
 2232 north-south precipitation pattern (e.g. WTs 3, and 4). While a formal cluster analysis of
 2233 the WT occurrence patterns was not carried out, visual comparison of Figures 13a and
 2234 13b indicates that the main regions of influence for each WT are broadly similar to
 2235 those derived from a statistical analysis. The WT results (Figure 12 and 13b) also
 2236 confirm that either 4 or 5 regions best accommodate the spatial characteristics of
 2237 extreme hourly precipitation. Based on the occurrence patterns and events exceeding
 2238 the annual and seasonal Q99 extremes in each gauge associated with WTs 1-4
 2239 (Figures 12, A9, and A10), the clustered PCA (Figure 11b), and the comparison
 2240 between WTs and PCA clusters in Figure 13, five regions were finally selected to
 2241 represent hourly precipitation extremes in the UK.



2242

2243 Figure 13: Comparison between (a) the PCA clustering results for UK hourly
 2244 precipitation using Wards clustering approach for 5 regions; and (b) the proportion of
 2245 days exceeding Q99 hourly precipitation for each gauge across weather types 1 to 4
 2246 identified by Neal et al. (2016) over the period 1992-2014. Yellow line (Figure 13a) are
 2247 the existing daily extreme regions by Jones et al, (2014), and presented here for
 2248 reference only. Numbers in brackets represent the percentage of all days on which
 2249 each weather type occurs. Circle diameter indicates the proportion of Q99 events
 2250 within each weather type for each gauge.

2251

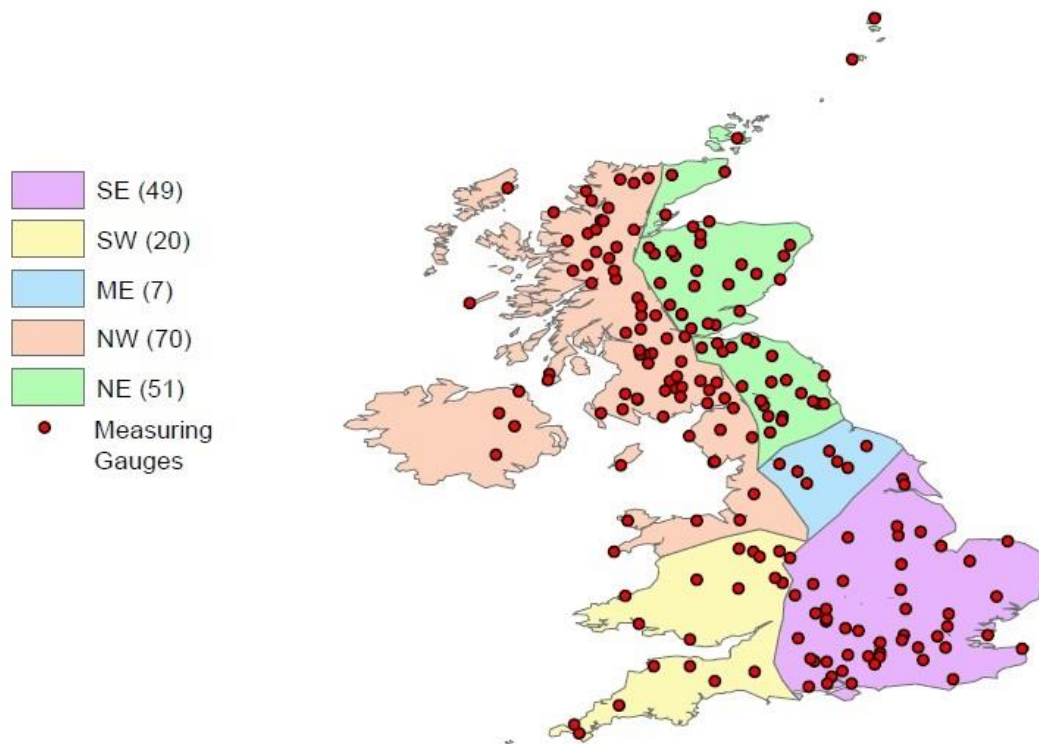
2252 The final selection of 5-regions and the defined boundaries are set to reflect the hourly
 2253 extremes spatial variation across the UK based on the PCs and WTs (Figures 13a and
 2254 13b). For instance, Figure 13a indicates that PC1 reflects the southeast and southwest
 2255 boundaries, while PC2 indicates northern regions east-west divide, which highlights
 2256 the orography and the role of the highlands. Furthermore, the east-west divide in PC2

2257 (Figure 13a) is in line with the existing daily regions (e.g. Alexander and Jones, 2000;
2258 Jones *et al.*, 2014), and the WT 4 (Figure 13b) occurrence patterns. In addition, both:
2259 PC 1 and PC 3 (Figure 13a) indicates the existence of a transitional region and
2260 separation between northern and southern regions, which is apparent in WT2 (Figure
2261 13b) frequency pattern, as it decreases from north to south. The final boundaries were
2262 selected based on visual inspection, the PCs results, and basic clustering of the WTs
2263 occurrence frequency pattern.

2264 **4.4.3. Regional homogeneity**

2265 Following the approximate delineation of five regions from the clustering analysis and
2266 subsequent visual confirmation that these are physically representative (Figure 13),
2267 formal regional boundaries draw on the extreme daily precipitation regions (Jones *et al.*,
2268 2014) with refinements from statistical analyses, below, and geographical
2269 knowledge. Each region was tested for homogeneity, using regional discordancy and
2270 homogeneity tests (Hosking and Wallis, 2005). Where gauges appeared to be
2271 inconsistent with the remaining region, we tested whether to place the gauge in an
2272 alternative region, remove it, or whether there was a justification for the discordancy.
2273 This resulted in no modifications or changes as described in further details below, since
2274 the investigations showed no physical reason or relocation possibility. The final five
2275 new regions are shown in Figure 14: North West (NW), North East (NE), South East
2276 (SE), Mid East (ME), and South West (SW). These contain 70, 51, 49, 7, and 20 hourly
2277 gauges respectively and satisfy the minimum station density and homogeneity criteria
2278 for RFA (Hosking and Wallis, 2005).

2279 The results illustrate that the new regions reflect the impact of UK orography, proximity
2280 to the sea, and large-scale atmospheric drivers, capturing the west-east precipitation
2281 gradient (demonstrated by NE-NW and SW-SE regions), as well as the north-south
2282 precipitation extremes variation along the eastern side of the country (regions SE-ME-
2283 NE).



2284

2285 Figure 14: Final delineation of UK extreme hourly precipitation regions. Regions are:
 2286 South East (SE), South West, Mid-East (ME), North West (NW), and North West (NW).
 2287 The value in parentheses denotes the number of hourly gauges in each region.

2288 Table 5 contains homogeneity measures (H_1 , H_2 , and H_3) and maximum gauge
 2289 discordancy measures (D) (Hosking and Wallis, 2005) for each region. The results
 2290 confirm that gauges in the regions SE, SW, NE and ME are not discordant ($D_{max} < D_{crit}$),
 2291 and that the SE, SW, and NW regions are “homogeneous” with (H_1) values of 0.83,
 2292 0.94, and 0.56 respectively. The results for ME show that the region is possibly
 2293 heterogeneous, with a H_1 value of 1.13, but no alterations were made as the gauges
 2294 are not discordant and the limited number of gauges (7) increases uncertainty
 2295 associated with this analysis (Jones *et al.*, 2010).

2296

2297

2298

2299

2300

Region	Homogeneity measures (H)			Goodness of fit measure (Z_{dist}) GEV/GP	No. of gauges	Max discordant gauge (D_{max})	D_{crit}
	H_1	H_2	H_3				
SE	0.83	0.32	0.04	-0.22/0.31	49	2.63	3.00
SW	0.94	0.96	0.89	-0.17/-0.43	20	1.84	3.00
ME	1.13	0.75	0.72	0.18/0.36	7	1.45	1.92
NW	0.56	-0.57	-0.06	-1.57/0.62	70	3.7	3.00
NE	2.71	0.87	0.23	1.18/-0.23	51	4.49	3.00

2301 Table 5: Gauge discordancy (D), region homogeneity (H) and goodness of fit (Z)
2302 assessment for the UK hourly extreme precipitation regions (SE, SW, ME, NW, and
2303 NE) shown in Figure 14. The table shows the number of gauges in each region and
2304 the maximum recommended gauge discordant value (D_{crit}) for each region.

2305 For NW, only one gauge is discordant ($D= 3.7 > D_{crit}= 3$), though the region is
2306 homogeneous, and removing it from the region only improves the homogeneity value
2307 slightly. Relocating the gauge to another region is not possible due to its location, but
2308 as the gauge observations match neighbouring gauges on the same day, we decided
2309 to retain the gauge within this region. For the NE region, one discordant gauge ($D=$
2310 $4.49 > D_{crit}= 3$) also makes the region heterogeneous ($H= 2.71$). The gauge has a very
2311 high 1h AMAX value in August 2007 (51.2mm, the highest of any gauge in that year),
2312 but there is no evidence that this is erroneous or the result of a malfunctioning gauge
2313 and it is in keeping with the observed weather during that period (Met Office, 2007).
2314 Relocating the gauge to other regions affected the homogeneity of the neighbouring
2315 regions, while subdividing the NE region also did not improve the results. While
2316 removing the gauge improved the homogeneity of the region noticeably ($H=1.2$),
2317 Hosking and Wallis (2005) recommend retaining discordant sites unless a physical
2318 reason justifies removing it. Thus, we decided to retain the gauge in the NE region.
2319 The other homogeneity measures (i.e. H_2 and H_3), though having less power to
2320 discriminate between homogeneous and heterogeneous regions, indicate that all
2321 regions are definitely homogeneous ($H_{2,3} \leq 1$), including NW, which confirms the
2322 suitability of 5 regions for further analysis.

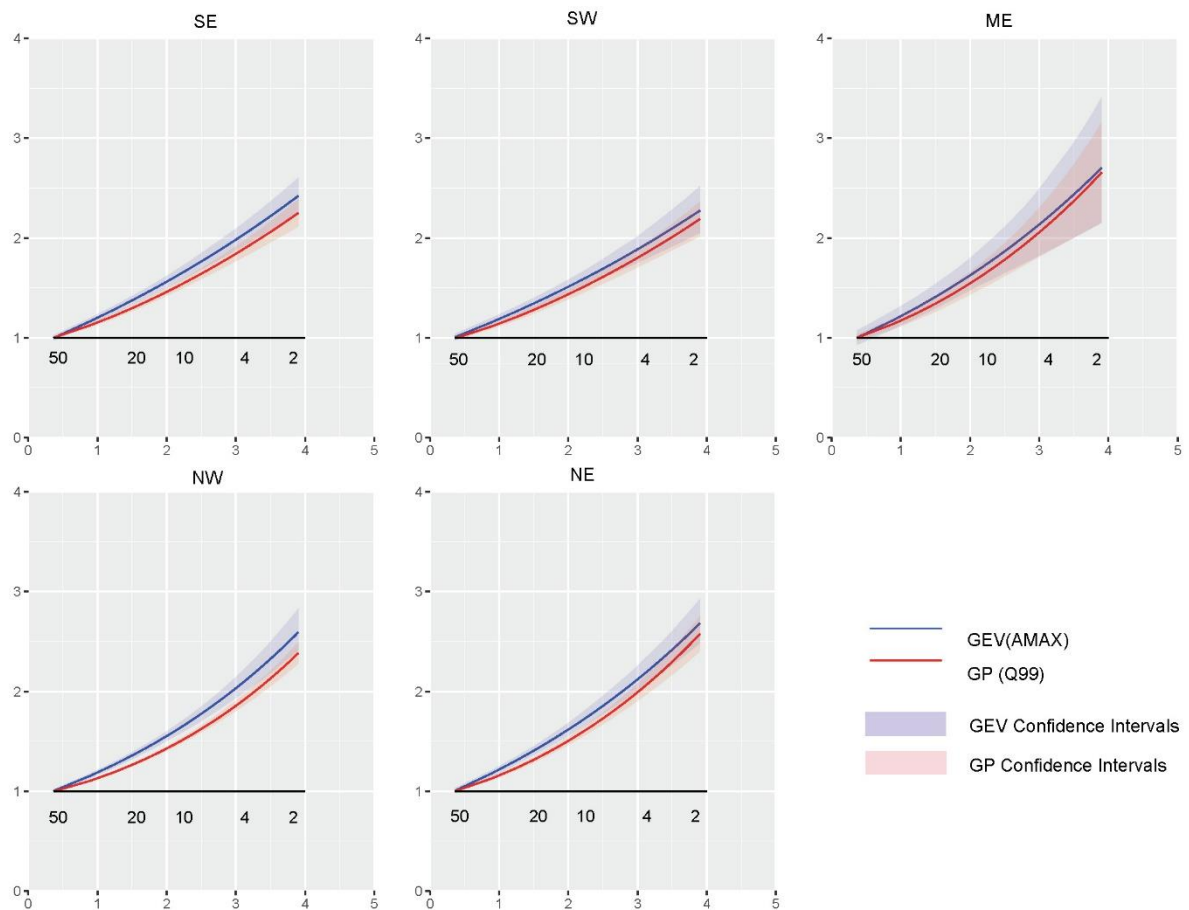
2323 Due to the nature of extremes and the limited availability of 1h precipitation
2324 observations, having definitively homogeneous regions for the RFA is challenging in
2325 practice, even after performing subjective modification, relocation, and elimination of
2326 discordant gauges to improve clustering results (Hosking and Wallis, 2005; Yang et

2327 *al.*, 2010; Sarhadi and Heydarizadeh, 2014). Thus, we believe that our results reflect
2328 the highest practical extent, considering the limited data availability and the spatially
2329 varying nature of hourly extremes in the UK.

2330 **4.4.4. Regional Frequency Analysis and AEP Estimates**

2331 The goodness of fit measure (Z_{dist}) for the GEV and GP distributions were assessed
2332 for AMAX and Q99 hourly precipitation, respectively, for each region. The results in
2333 Table 5 show that both distributions' Z_{dist} values are within the recommended guideline
2334 ($|Z_{dist}| < 1.64$) (Hosking and Wallis, 2005) and therefore should be able to reflect the
2335 spatial patterns in the AMAX and Q99 hourly precipitation in the UK.

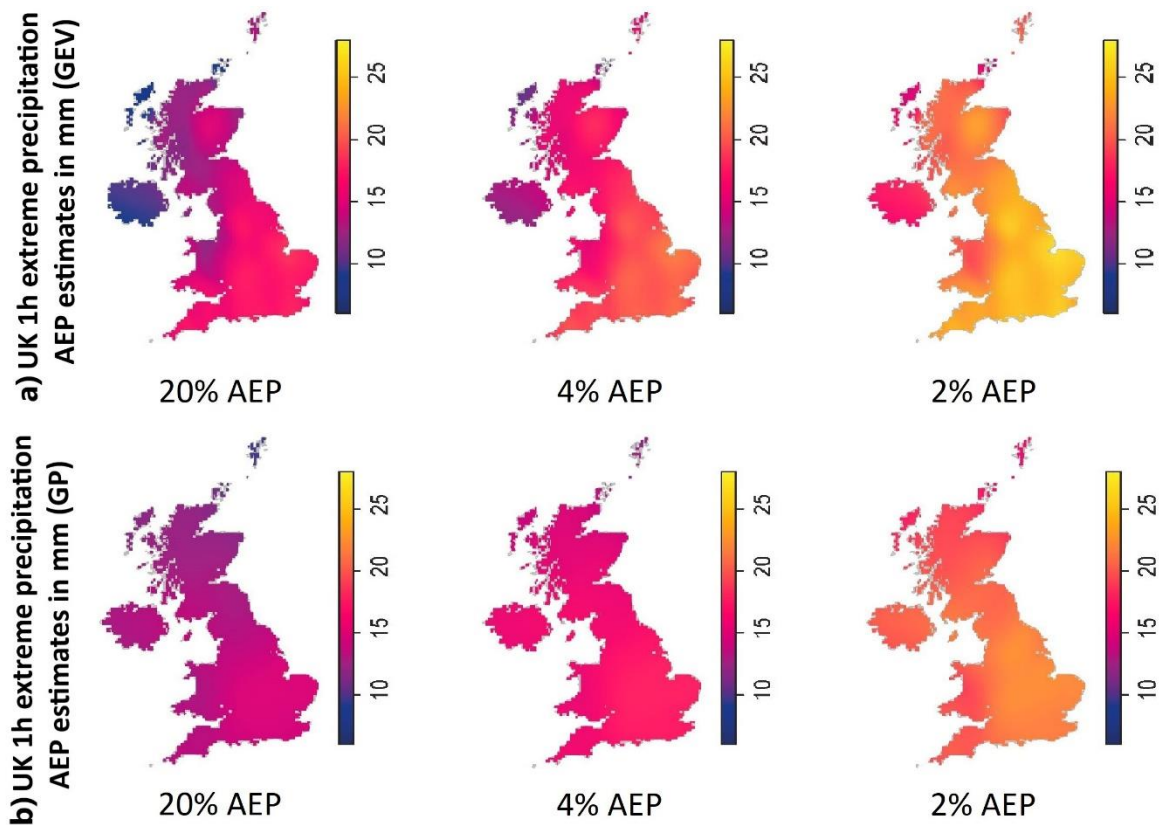
2336 The fitted growth curves for each region in Figure 15 show that both distributions have
2337 similar shapes and growth factors with overlapping confidence intervals, although the
2338 GEV growth curves are marginally steeper, in all regions. GEV confidence intervals
2339 are wider than those for the GP distribution due to the hourly Q99 having 2 to 3 times
2340 as many observations as those for hourly AMAX for the same period (1992- 2014), and
2341 less variance in the series. Growth curves are steeper for both distributions in northern
2342 regions (i.e. NE and NW), where the highest hourly extremes were recorded and
2343 precipitation generated by large-scale circulation dominates, than for southern regions
2344 (i.e. SE and SW), where convective precipitation mostly dominates extremes, reflecting
2345 the role of large synoptic circulation in producing high hourly extremes. Confidence
2346 intervals for the fitted distributions in ME are wide due to limited gauges (only 7) in the
2347 region, which increases the sensitivity to extreme values (Hosking and Wallis, 2005;
2348 Jones *et al.*, 2010).



2349

2350 Figure 15: Fitted regional GEV and GP growth curves for 1h standardized AMAX (blue)
 2351 and Q99 (red) respectively, and confidence intervals for the fitted GEV distribution
 2352 (blue shading) and GP distribution (red shading). Growth factor (y-axis), Annual
 2353 Exceedance Probability (AEP) in % (upper x-axis), and Gumbel reduced variate (lower
 2354 x-axis). The growth curve represents the multiple increase of a given AEP over an
 2355 index value, here the 50% AEP.

2356 Probability estimates were calculated for both regional distributions for 20%, 4%, and
 2357 2% AEPs across the UK by multiplying the regional GEV or GP growth factor by the
 2358 gauge specific RMed or median Q99, respectively. We produce a spatial estimate of
 2359 the AEPs through a kernel estimation smoothing on the gauge estimates. Figures 16a
 2360 and 16b highlight the increasing gradient of intensity from the northwest to southeast
 2361 UK for both the GEV and GP distributions for all AEP estimates. However, it should be
 2362 noted that differences between the RMed and median Q99 estimates can lead to
 2363 marginal differences in the AEP estimates even though the growth curves appear
 2364 similar in Figure 15. The GP estimates suggest smoother and more continuous
 2365 patterns, with a slightly lower precipitation intensity, compared to the GEV estimates.



2366

2367 Figure 16: Estimates for the UK 1h extreme precipitation in mm for 20%, 4%, 2%
 2368 annual exceedance probabilities (AEPs)) using the GEV distribution (a) and GP
 2369 distribution (b). Estimates for each gauge are calculated from the fitted regional growth
 2370 curve multiplied by the site scaling factor (gauge RMed).

2371 Assessing the frequencies of each WT (Table 6) shows that for WTs 1 to 4, which are
 2372 associated with more than 75% of hourly extremes exceeding Q99, WT2 (i.e. NAO+
 2373 pattern) and WT4 (i.e. south-westerly flow pattern) are associated with most of the
 2374 annual extremes (i.e. 51%) in the UK. Moreover, WT2 alone is associated with 40% of
 2375 extremes in winter, which is approximately double its summer frequency (22%). In
 2376 contrast, WT1 (i.e. NAO- pattern) and WT3 (i.e. north-westerly pattern) frequency in
 2377 summer increase noticeably compared to winter. Furthermore, the results indicate that
 2378 summer extreme precipitation is associated with a wider range of WTs (i.e. WTs 1 to
 2379 4), with comparable frequencies, while winter extremes are dominated by WT2.

2380 The WTs frequencies in Figures 13, A9, A10, and Table 6 indicate that WTs 1 and 3
 2381 are mostly associated with heavy showers over eastern England especially during
 2382 summer (Figure A10), suggesting the role of convective conditions in generating
 2383 precipitation. In contrast, WTs 2 and 4 are associated with more frequent stormy
 2384 weather, especially in winter (Figure A9), indicating the role of large-scale precipitation.

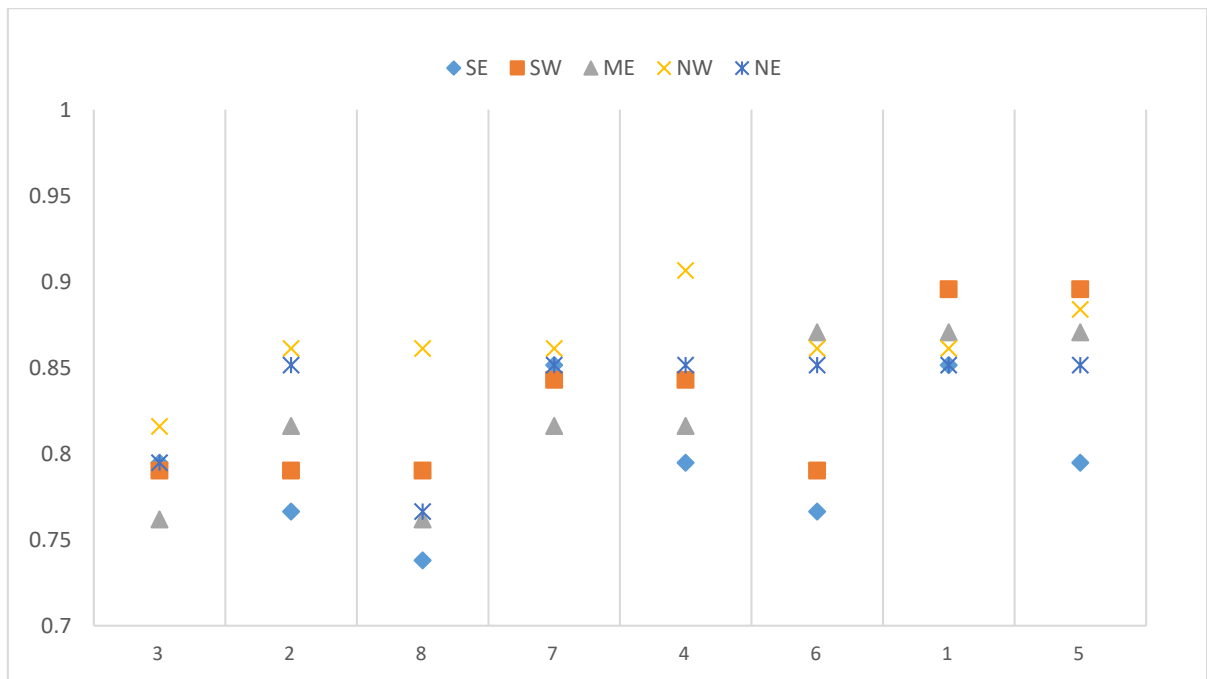
2385

		Weather Type							
		WT1	WT2	WT 3	WT 4	WT 5	WT 6	WT 7	WT 8
Proportion of each WT in all regions	Annual (Figure 12)	<u>12%</u>	<u>32%</u>	<u>14%</u>	<u>19%</u>	<u>9%</u>	<u>3%</u>	<u>9%</u>	<u>2%</u>
	Winter (Figure A9)	<u>9%</u>	<u>40%</u>	<u>11%</u>	<u>21%</u>	<u>7%</u>	<u>2%</u>	<u>8%</u>	<u>2%</u>
	Summer (Figure A10)	<u>17%</u>	<u>22%</u>	<u>16%</u>	<u>18%</u>	<u>11%</u>	<u>4%</u>	<u>10%</u>	<u>2%</u>

2387 Table 6: Proportion of Weather types (WT) 1 to 8 (Neal et al, 2016) across all the
2388 proposed UK 5 regions annually, in winter, and in summer (underlined).

2389 We also assessed the median of Q99 hourly precipitation for each weather pattern in
2390 each region, where the median of each region and weather type relative to the region
2391 mean was calculated, to evaluate the regional relation between the hourly extremes'
2392 magnitudes and the weather types. The results in Figure 17 show that the Q99 hourly
2393 precipitation median of WTs 3 and 2 are lower than for most of the other weather types,
2394 whilst the highest median values occur for WTs 5 and 1. This contrasts with the results
2395 for hourly extreme event frequencies presented in Figure 12 where those for WTs 3
2396 and 2 were noticeably higher than for WT5. This indicates that the highest hourly
2397 precipitation extremes might not be associated with the weather types that produce the
2398 most frequent Q99 hourly extremes.

2399



2400

2401 Figure 17: Median of hourly Q99 precipitation 1992–2014 for each region (SE, SE, ME,
 2402 NW, and NE) and for each of the 8 weather patterns (Neal et al., 2016) (X-Axis),
 2403 expressed as the median of each region and weather type relative to the region mean
 2404 (Y-axis). The weather types are ordered left to right from the lowest UK relative median
 2405 precipitation to the highest. Y-axis (after Richardson et al., 2018 Figure 5).

2406

4.5. Discussion and conclusions

2407

This study aimed to provide a reliable regional characterisation of hourly extremes
 2408 which could lead to improved estimates for various applications in different engineering
 2409 and climatological areas. Using the regional approach would reduce the impact of
 2410 hourly precipitation data scarcity and erroneous recorded data, while the existing daily
 2411 precipitation regions were not able to capture the spatial variation of hourly extremes
 2412 across the UK

2413

A principal component analysis and clustering approach was adopted to identify five
 2414 new, homogeneous extreme precipitation regions to reflect hourly extreme
 2415 precipitation variations across the UK. These were then adopted in a regional
 2416 frequency analysis to estimate precipitation annual exceedance probabilities for each
 2417 region. The study used a new, quality controlled hourly precipitation dataset
 2418 (Blenkinsop *et al.*, 2017; Lewis *et al.*, 2018) together with associated site
 2419 characteristics (e.g. elevation) and different at-site hydro-climatological characteristics
 2420 (i.e. temperature, precipitation seasonality) to identify the regions. Further, using
 2421 weather types as an auxiliary variable ensured characterising large-scale atmospheric
 2422 circulation systems, and representing important precipitation-generating processes,
 2423 which provided physical plausibility for the regional definition. Previous work in the UK

2424 identified precipitation regions using either daily mean (Wigley *et al.*, 1984; Gregory *et*
2425 *al.*, 1991), or extreme daily precipitation (Jones *et al.*, 2014). This research presents
2426 physically plausible regions to improve the characterisation and estimation of short-
2427 duration precipitation extremes.

2428 Orographic characteristics and large-scale atmospheric circulation patterns showed a
2429 noticeable role in delineating the extreme precipitation regions, which is consistent with
2430 daily extreme precipitation studies in the UK and elsewhere (e.g. Jones *et al.*, 2014;
2431 Johnson *et al.*, 2016). The impact of the Pennines and Southern Uplands and the
2432 Cambrian mountains is reflected in the east-west delineation, coupled with the most
2433 frequent weather types (i.e. WTs 2, 3, and 4) characterised by NAO+, south westerly,
2434 and north westerly circulation flows. This corroborates the northwest-southeast
2435 precipitation patterns reported in previous studies of daily (Jones *et al.*, 2014) and
2436 hourly precipitation extremes (Blenkinsop *et al.*, 2017).

2437 The new regions were assessed for homogeneity (Hosking and Wallis, 2005). The
2438 results showed that the most robust homogeneity measure, is either homogeneous or
2439 marginally exceeds the limit in all regions except NW. The heterogeneity in NW is
2440 caused by a single gauge which recorded a verified hourly observation of 51.2 mm in
2441 August 2007, and so was retained. The validity of subjective relocation or removal of
2442 gauges was confirmed with additional homogeneity measures and no further changes
2443 made.

2444 Growth curve estimates for regional GEV and GP distributions show similar results,
2445 with steeper curves for the GEV and overlapping confidence intervals. Wider
2446 confidence intervals in ME compared to other regions, arising from data scarcity,
2447 highlights the importance of having dense gauging networks. The growth curves
2448 estimates show a noticeable difference between northern and southern regions, with
2449 a steeper GEV curves in northern regions, contrasting with estimates made by Darwish
2450 *et al.* (2018) using the existing daily UK extreme regions (Jones *et al.*, 2014), where
2451 the growth curves indicated similar results across northern and southern regions. This
2452 indicates that the new proposed regions could capture the spatial variation and the
2453 hourly extremes patterns across the UK more precisely.

2454 The annual exceedance probability (AEP) maps for probabilities of 20%, 4%, and 2%
2455 concur with previous findings of an increasing pattern of hourly and daily extremes
2456 from the northwest to the southeast (Jones *et al.*, 2014; Blenkinsop *et al.*, 2017). While

2457 GP distribution probability estimates are marginally smoother and less sensitive to
2458 outliers compared with the GEV, estimates for both distributions are comparable
2459 across the UK.

2460 Finally, the relationship between hourly extremes and weather types showed that WTs
2461 5 and 1 have the highest relative median Q99 precipitation intensity, while WT2 has
2462 the highest frequency of Q99 precipitation events but a lower corresponding relative
2463 median intensity. These WTs are characterised by southeasterly and northeasterly
2464 flows that travel across southeast England. Although WT5 is not associated with a high
2465 frequency of hourly extremes, its dominance as a summer weather type influences the
2466 higher intensity of those precipitation events which do occur. Recent analysis of daily
2467 mean precipitation by Richardson *et al.* (2018) found a stronger relationship for the
2468 lower intensity results with WTs 2 and 7. While this may seem counterintuitive, it is
2469 corroborated by recent research indicating that changes in mean precipitation are not
2470 necessarily matched by those in the extremes (Swain *et al.*, 2018), and that the most
2471 intense precipitation occurs in fewer events (Westra *et al.*, 2014; Prein *et al.*, 2017;
2472 Pendergrass, 2018). The results also indicate a difference between weather types
2473 associated with mean daily and hourly extreme precipitation within the UK, and their
2474 different generating mechanisms. This confirms the inadequacy of the existing daily
2475 mean precipitation regions (Alexander and Jones, 2000) and daily extreme
2476 precipitation regions (Jones *et al.*, 2014) to assess hourly extreme precipitation in the
2477 UK, which was reported in Darwish *et al.* (2018).

2478 In conclusion, this chapter has analysed hourly extreme precipitation and associated
2479 climatological variables to identify new, homogeneous regions which facilitate the
2480 analysis and estimation of hourly extreme precipitation in the UK. The developed
2481 regions capture the hourly extremes spatial variation across the UK, and could be used
2482 to perform further regional investigation and statistical modelling of extreme
2483 precipitation.

2484

2485

2486 **Chapter 5. Statistical modelling of UK extreme hourly precipitation**
2487 **and future climate change responses**

2488 Quantifying extreme precipitation has always been a major challenge for both
2489 scientists and decision makers. Extreme precipitation is among the most destructive
2490 climatological events, is highly associated with flash floods, and poses a
2491 multidimensional threat to urbanised areas. Moreover, simulating extreme precipitation
2492 using climate models is highly associated with uncertainties, due to scarce data, high
2493 variability, coarse resolution, and interaction with different climatological variables.
2494 Typically, statistical analysis assuming stationary processes is used to assess extreme
2495 precipitation and implement urban drainage design guidelines, however, it is
2496 increasingly being observed that extreme precipitation is a non-stationary process due
2497 to both natural and anthropogenically induced climate variability.

2498 In this chapter the hourly precipitation dataset from 1992-2014, and other
2499 climatological variables (e.g. temperature, atmospheric pressure) acting as covariates,
2500 are employed to develop a statistical model that can simulate extreme precipitation
2501 frequency and intensity, and account for the non-stationary behaviour of extremes.
2502 This would provide an alternative to the computationally expensive climate models,
2503 and facilitate the assessment of hourly extremes across the UK.

2504 Among the objectives of this research is the quantification of the intensity and
2505 frequency of extreme hourly precipitation under potential climate change using the
2506 developed statistical model. Therefore, in this chapter extreme value theory and the
2507 newly developed regions for hourly extremes (Chapter 4) are used to simulate the
2508 response of future extreme precipitation to potential climate change.

2509 The chapter concludes with a skilful statistical model that simulates hourly extremes
2510 intensity and frequency in the UK. Furthermore, the statistical model indicated
2511 noticeable increase in the UK hourly extreme precipitation intensity and frequency
2512 during summer, as a response to potential climate change.

2513 **5.1. Introduction**

2514 Providing reliable precipitation simulations is of importance for many different
2515 applications, as they are used as basic input into precipitation-runoff, groundwater,
2516 agricultural and water-usage models (Yunus *et al.*, 2017). This is of particular
2517 importance as many studies have reported global increases in the frequency and

2518 intensity of extreme precipitation (Trenberth *et al.*, 2003; Alexander *et al.*, 2006; Fowler
2519 and Ekström, 2009; Maraun *et al.*, 2010b; Jones *et al.*, 2013; Simpson and Jones,
2520 2014) while the second UK Climate Change Risk Assessment (Defra, 2017) suggests
2521 that climate change will increase fluvial and surface flooding in the UK and related risks
2522 (e.g. coastal erosion, marine and fresh water ecosystems pollution). However, sub-
2523 daily extremes have so far received limited attention, mainly due to the limited
2524 availability of high-resolution precipitation observations, the statistical challenges of
2525 accurately determining sub-daily precipitation probabilities and the challenge of
2526 simulating the intensity and frequency of precipitation events in physically-based
2527 models (Westra *et al.*, 2014; Blenkinsop *et al.*, 2017).

2528 Convection-permitting models (CPMs) are now commonly used as powerful tools to
2529 simulate hourly extreme precipitation (Westra *et al.*, 2014; Chan *et al.*, 2016). However,
2530 achieving accurate and reliable simulations from CPMs is computationally-expensive
2531 and time-demanding (Chan *et al.*, 2014a). Therefore, statistical downscaling of climate
2532 model output is commonly used to provide a reliable, computationally inexpensive, and
2533 flexible approach to simulate and estimate extreme precipitation from coarse-
2534 resolution climate model outputs (Fowler *et al.*, 2007). Statistical downscaling has been
2535 employed to project changes in future precipitation (Dobler *et al.*, 2013; Shashikanth
2536 *et al.*, 2016), to derive extreme projections under climate change (Hertig *et al.*, 2014;
2537 Ning *et al.*, 2015), and to improve the statistical distribution of daily precipitation
2538 amounts (Benestad, 2010). Maraun *et al.* (2010b), who reviewed the use of
2539 precipitation downscaling methods for climate change projections, reported that the
2540 statistical downscaling of precipitation enhances the outputs from coarse-resolution
2541 climate models, adds considerable value to their projections, and facilitates end users'
2542 assessment of climate change and its hydrological impacts. Furthermore, Vrac and
2543 Naveau (2007) suggest that statistical downscaling approaches can incorporate
2544 different flexible statistical modelling such as generalized linear modelling (GLM) and
2545 extreme value theory (EVT), which are computationally efficient and practical, to
2546 improve estimation of extremes.

2547 The GLM has been used widely to simulate and characterise the frequency of intense
2548 precipitation in different locations (Chandler and Wheeler, 2002; Benestad, 2010;
2549 Hertig *et al.*, 2014). Yang *et al.* (2005) and Benestad (2007) used the GLM to model
2550 station-based daily precipitation data in southern England and extreme precipitation
2551 over northern Europe respectively. Recently, Hertig *et al.* (2014) adopted a GLM

2552 approach to perform statistical modelling of extreme precipitation indices for the
2553 Mediterranean area under future climate conditions.

2554 Extreme value theory (EVT) has also been used widely to characterise extreme
2555 precipitation in different locations and for different durations. Vrac and Naveau (2007)
2556 used EVT to improve the representation of local daily extreme precipitation in Illinois,
2557 USA, while Wi *et al.* (2016) adopted EVT to perform frequency analysis of extreme
2558 precipitation in South Korea for sub-daily durations (1-, 6-, 12-, and 24-hours). In the
2559 UK, Jones *et al.* (2013) employed EVT to assess changes in seasonal and annual daily
2560 extreme precipitation. Jones *et al.* (2014) further extended this approach to
2561 characterise daily extremes and identify extreme precipitation regions for the UK,
2562 before developing a Generalised Additive Model for UK daily precipitation extreme
2563 frequency (Tye *et al.*, 2016).

2564 UK extreme precipitation is influenced by both large scale atmospheric circulation
2565 patterns such as synoptic weather systems and atmospheric rivers, besides local
2566 weather such as convective instability (Cyril *et al.*, 2007; Champion *et al.*, 2015).
2567 Therefore, it is important to consider both as potential drivers of changes in sub-daily
2568 extreme precipitation. Recently, various studies investigated subdaily precipitation in
2569 the UK (e.g. Blenkinsop *et al.*, 2017; Darwish *et al.*, 2018; Lewis *et al.*, 2018; Xiao *et al.*,
2570 2018) Blenkinsop *et al.* (2017) developed a new quality controlled dataset for UK
2571 hourly precipitation, and examined its seasonal and diurnal climatology; Lewis *et al.*
2572 (2018) used this to produce a new 1 km resolution gridded hourly precipitation dataset
2573 for the UK. Additional analysis of average hourly precipitation over the UK by Xiao *et al.*
2574 (2018) reported noticeable peaks in early morning and afternoon, with apparent
2575 regional variation in spring and summer. Subsequently, as detailed in Chapter 3 of this
2576 thesis, Darwish *et al.* (2018) assessed sub-daily extreme precipitation patterns, their
2577 diurnal cycle, and produced annual probability estimates using regional frequency
2578 analysis (RFA) for the daily extreme precipitation regions developed by (Jones *et al.*,
2579 2014). This showed the need for new regions to capture spatial and temporal
2580 characteristics of hourly extremes, performed in Chapter 4. As detailed in Chapter 4 of
2581 this thesis, EVT, climatological clustering, and regional frequency analysis (RFA)
2582 approach are used to identify hourly extreme precipitation regions in the UK.

2583 Here, our goal is to develop a simple and reliable statistical model that can simulate
2584 hourly extreme precipitation patterns in the UK, using relevant climatological predictors
2585 reflecting large-scale and local conditions. This should provide a practical alternative

2586 to high-resolution climate modelling to simulate realistic frequencies and intensities of
2587 hourly precipitation extremes, as well as to assess the potential impact of climate
2588 change scenarios. We use a GLM embedded in EVT distributions to model hourly
2589 precipitation extremes across the UK, at 197 UK gauges using the hourly extreme
2590 precipitations regions established in Chapter 4. Although existing regulations and
2591 design guidelines for flood infrastructure assume stationary conditions (Madsen *et al.*,
2592 2013), this assumption in EVT is questionable, due to non-stationary caused by
2593 anthropogenic warming as well as natural climatic variability (Salas and Obeysekera,
2594 2013). Therefore, several studies recommend the adoption of non-stationary analyses
2595 (Renard *et al.*, 2006; Katz, 2010; Rootzén and Katz, 2013).

2596 In recent decades, various studies have adopted non-stationarity in the analysis of
2597 trends in observed hydrological events (e.g. Franks, 2002; Vogel *et al.*, 2011),
2598 estimation of frequency distribution (e.g. Katz *et al.*, 2002; Raff *et al.*, 2009), and
2599 determination of risk and design guidelines for hydrological structures within a non-
2600 stationary framework (e.g. Mailhot and Duchesne, 2009; Rootzén and Katz, 2013;
2601 Salas and Obeysekera, 2013).

2602 In this chapter, GLM and EVT non-stationary distributions coupled with downscaled
2603 climate variables and observed NAO datasets are adopted to quantify the UK hourly
2604 extreme precipitation (i.e. frequency and intensity). This is the first study to investigate
2605 hourly extreme precipitation in the UK, build a statistical model that employ various
2606 climatic variables to quantify hourly extreme precipitation characteristics (i.e. frequency
2607 and intensity) while considering for the non-stationary nature of the hydrological
2608 events, and evaluate potential changes under climate change scenario.

2609 The Chapter is structured as follows. Following a description of hourly precipitation
2610 data, and the potential climatological predictors in Section 2, the methodology,
2611 probability distributions, statistical model selection and validation process outlined in
2612 Section 3. The results of correlations between hourly extremes and related
2613 climatological variables (e.g. Temperature, Sea level pressure), selection of
2614 covariates, statistical model performance, and a pseudo-global warming approach to
2615 analyse future behaviour are presented in Section 4. Finally, Section 5 discusses the
2616 results, the potential implications from the statistical modelling, and future research.

2617 **5.2. Data**

2618 **5.2.1. Precipitation data**

2619 This research uses an hourly precipitation dataset for the UK derived from precipitation
2620 gauges covering the years from 1992 - 2014 (Blenkinsop *et al.*, 2017; Lewis *et al.*,
2621 2018). The dataset (up to 2011) was collected by Blenkinsop *et al.* (2017) from three
2622 sources: the UK Met Office Integrated Data Archive System (MIDAS), the Scottish
2623 Environmental Protection Agency (SEPA), and the UK Environment Agency (EA).
2624 Blenkinsop *et al.* (2017) performed a series of site-specific quality control (QC)
2625 procedures on the data to detect accumulated totals, malfunctioning gauges and
2626 unfeasible extreme precipitation totals. This was subsequently extended to 2014 and
2627 subjected to additional QC checks against neighbouring gauges (Lewis *et al.*, 2018).
2628 Here we apply the additional criteria of having at least 85% of the gauge record
2629 complete (i.e., non-missing and data not flagged by the QC process) for each year in
2630 the period 1992–2014. In total, 197 gauges distributed across the UK (shown in Figure
2631 1) fulfilled the criteria. These criteria were selected as a trade-off between having long
2632 records and data completeness. Further details on the adoption of these criteria can
2633 be found in Section 3.2.

2634 Moreover, the UK hourly extreme precipitation regions (Figure 14) developed in
2635 Chapter 4, which were identified from a principal components analysis of extreme
2636 precipitation statistics, climatological variables (e.g. temperature), location
2637 characteristics, and the spatial analysis of predominant weather types (Neal *et al.*,
2638 2016), are used to analyse the hourly extremes, as well as to build and validate the
2639 statistical model.

2640 **5.2.2. Predictors**

2641 In the UK, hourly extreme precipitation is related to both large-scale circulation patterns
2642 (Cyril *et al.*, 2007; Champion *et al.*, 2015) as well as to local, convective-scale
2643 processes (Blenkinsop *et al.*, 2015; Chan *et al.*, 2018b). There is a lack of
2644 understanding of conditions driving extreme hourly precipitation in the UK (Holley *et al.*,
2645 2014; Blenkinsop *et al.*, 2015). Therefore, a range of traditional and novel climatic
2646 variables associated with hourly precipitation extremes in the UK were investigated as
2647 potential predictors to build the statistical model (see Table 7 and further detailed
2648 below). These variables were selected to reflect both local conditions and large-scale

2649 circulation associated with extremes. They represent the convective potential,
2650 temperature, atmospheric pressure, and moisture content conditions.

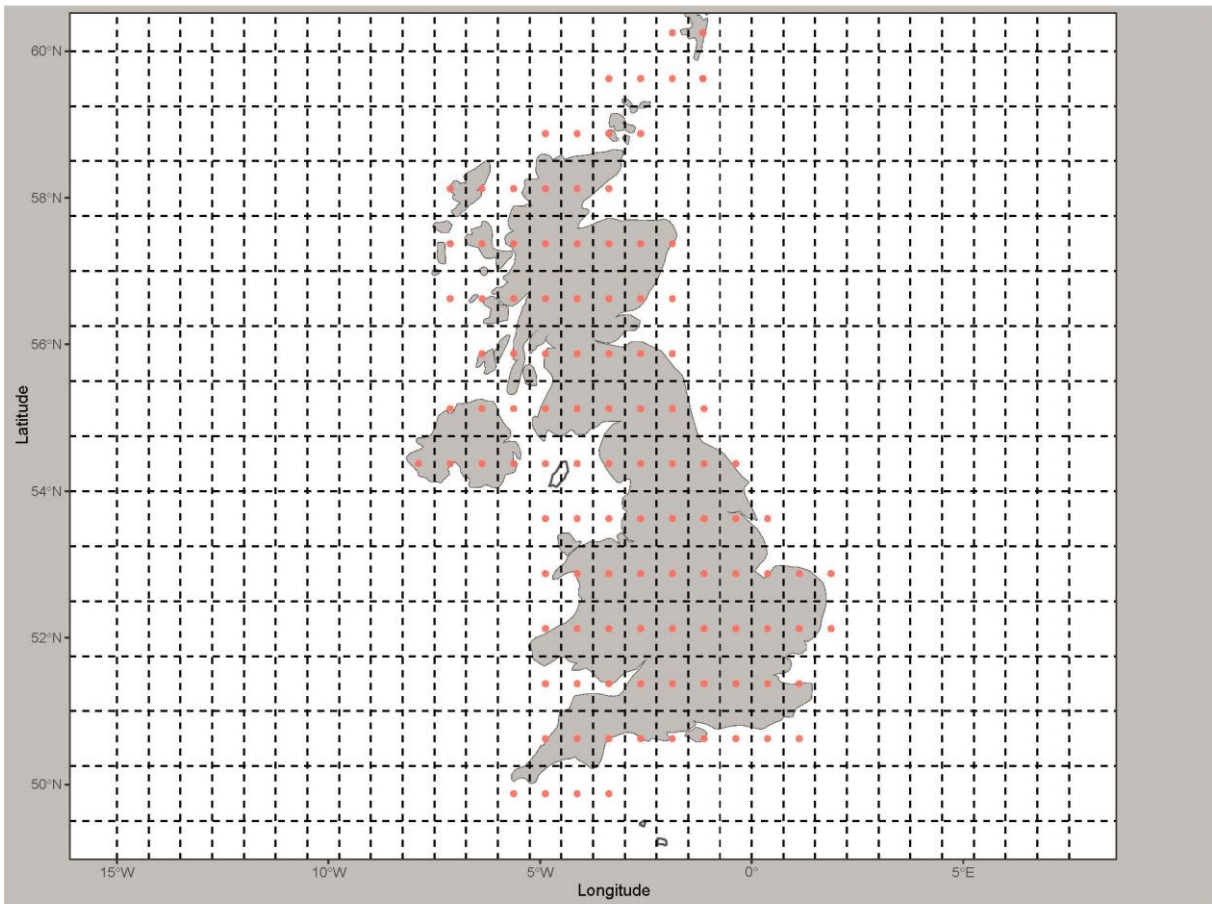
2651 A simple sinusoidal formula premised on the Julian day (number of elapsed days since
2652 the beginning of a particular year) of occurrence, and often adopted to simulate regular
2653 annual fluctuations (Rust *et al.*, 2009), was also used as a predictor to reflect the
2654 seasonality of the hourly extremes with all potential predictors. However, using the
2655 sinusoidal formula alone does not represent hydrological extreme (i.e. precipitation and
2656 floods) seasonality in the UK adequately, due to the fluctuations caused by
2657 atmospheric oscillations (Huntingford *et al.*, 2014; Tye *et al.*, 2016)

2658 All potential predictors and climatic variables except the NAO are based on $0.75^\circ \times$
2659 0.75° gridded daily averaged output (Figure 18) for the period 1992–2015 from the
2660 European Center for Medium-Range Weather Forecasts (ECMWF) Interim reanalysis
2661 dataset (Dee *et al.*, 2011). For each variable, a daily area average of each grid cell
2662 was calculated, thereafter, the value was assigned to the gauges within the grid cell.
2663 The NAO index, which is defined as the normalized pressure difference between
2664 Azores and Iceland, was derived from a monthly pressure observational dataset
2665 between 1992-2015 (Jones *et al.*, 1997).

2666

Variable	Measured phenomenon	Acronym
<i>Seasonality</i>		
$Sine\left(\frac{2\pi * Julian\ day}{365.25}\right)$	Seasonality	$Sin(\Theta)$
$Cosine\left(\frac{2\pi * Julian\ day}{365.25}\right)$	Seasonality	$Cos(\Theta)$
<i>Convective variables</i>		
Convective available potential energy	Availability of convective conditions	CAPE
Convective inhibition	Energy needed to initiate convective precipitation	CIN
<i>Temperature variables</i>		
Temperature at 2m level	Temperature near the surface ~2m above the ground	T-2m
Dew point temperature	Temperature to which air must be cooled to become saturated with water vapour	DPT
Sea surface temperature	Water temperature close to the ocean surface	SST
<i>Atmospheric variables</i>		
North Atlantic Oscillation	Normalized sea-level pressure difference between predefined locations	NAO
Sea level pressure	Atmospheric pressure at sea level	SLP
Atmospheric pressure 850-, 700-, 500hPa height	Actual height of a pressure surface above mean sea-level	Z850,Z700,and Z500
<i>Moisture variables</i>		
Total column water vapour	Total gaseous water contained in a vertical column of atmosphere	TCWV

2668 Table 7: Potential predictors used to develop a statistical model of the frequency and
2669 intensity of hourly precipitation extremes.



2671

2672 *Figure 18: The 0.75° × 0.75° grid, where the daily average of all potential climatic*
 2673 *variables (except the NAO) over the UK are extracted from European Center for*
 2674 *Medium-Range Weather Forecasts (ECMWF) Interim reanalysis dataset between*
 2675 *1990-2015 (Dee et al., 2011). For each variable, a daily area average of each grid cell*
 2676 *was calculated (red dots), thereafter, the value was assigned to the gauges within the*
 2677 *grid cell*

2678 • **North Atlantic Oscillation (NAO)**

2679 The NAO is defined as the normalized sea-level pressure (SLP) difference between
 2680 the subtropical high (i.e. Azores) and polar low (i.e. Iceland), and is the dominant mode
 2681 of climate variability around the North Atlantic (Hurrell, 1995; Hall and Hanna, 2018).
 2682 The NAO has positive and negative phases. In winter, a positive NAO phase is
 2683 associated with increasing storm activity over the UK and northern Europe, while in
 2684 summer, a negative NAO phase is associated with higher precipitation intensity (Hall
 2685 and Hanna, 2018). Recent improvements in seasonal NAO predictability have the
 2686 potential to improve precipitation predictability in the UK (Hanna and Cropper, 2017;
 2687 Hall and Hanna, 2018).

2688 Several studies have reported on the importance of the NAO in modulating
 2689 precipitation over Europe (e.g. Hurrell, 1995; Jones *et al.*, 1997; Cropper *et al.*, 2015).

2690 Hanna and Cropper (2017) reported a significant relation between the NAO and
2691 climate variability over the North Atlantic. In addition, Sutton and Dong (2012),
2692 analysing European climate using mean temperature, pressure, and precipitation,
2693 showed that during the 1990s, a substantial shift in the European climate coincided
2694 with a significant warming of the North Atlantic Ocean. This climate shift was
2695 characterised by anomalously wet summers in northern Europe, and hot, dry, summers
2696 in southern Europe, emphasising the important role of the North Atlantic Ocean for
2697 European weather. In the UK, the NAO index can be used as a proxy for north Atlantic
2698 jet streams and storm track variability and, hence, UK precipitation (Vallis and Gerber,
2699 2008; Hanna and Cropper, 2017). Therefore, the NAO index (Jones et al., 1997) is
2700 examined for use as a covariate in the statistical modelling to characterise the
2701 frequency and intensity of extremes.

2702 • **Convection parameters (CAPE and CIN)**

2703 In the UK, different studies have reported that extreme precipitation events in the UK,
2704 especially in summer, mostly occur due to convective conditions (Bennett *et al.*, 2006;
2705 Kendon *et al.*, 2014; Blenkinsop *et al.*, 2017; Darwish *et al.*, 2018). A significant
2706 proportion of UK precipitation is produced by convective clouds associated with both
2707 frontal activity and air-mass cumulonimbus clouds (Bennett *et al.*, 2006). The coastline,
2708 the topography, and the wind direction across the UK all have a significant influence
2709 on the initiation of convection (Hand, 2005; Bennett *et al.*, 2006); The UK is also often
2710 subject to convection that has initiated on the European continent (Flack et al., 2016).
2711 Moreover, convective conditions are highly variable in the UK, both spatially and
2712 temporally, with maximum activity during summer (Holley *et al.*, 2014).

2713 The initiation of convective precipitation conditions requires three components:
2714 atmospheric instability, moisture availability, and lifting forces (Johns and Doswell,
2715 1992). Two related parameters are used here that represent these components -
2716 convective available potential energy (CAPE) and convective inhibition (CIN).

2717 CAPE denotes the potential available energy to form cumulus convection which leads
2718 to convective precipitation. It is characterised by a positive virtual temperature
2719 difference between an idealised rising air parcel and its environment, vertically
2720 integrated with respect to the natural logarithm of pressure (p) between the level of
2721 free convection (LFC) and equilibrium level (EL) (Riemann-Campe et al., 2011). Parcel
2722 theory defines CAPE as a thermodynamic parameter reflecting atmospheric instability

2723 and moisture, which measures the potential buoyancy of a theoretical rising air parcel
2724 and its environment. CIN denotes the energy needed by the parcel to overcome the
2725 boundary layer to reach the CAPE (Moncrieff and Miller, 1976). For convection to
2726 occur, a rising air parcel must overcome any available convective inhibition (CIN).

2727 CAPE can be calculated as:

$$CAPE = \int_{LFC}^{EL} R_d (T_{vp} - T_{ve}) d\ln(p) \quad (14)$$

2728 while CIN is calculated as:

$$CIN = \int_{SFC}^{LFC} R_d (T_{ve} - T_{vp}) d\ln(p) \quad (15)$$

2729 Where *LFC* is the pressure of the level of free convection, *SFC* is level of the surface
2730 or beginning of parcel path, *EL* is pressure of the equilibrium level, R_d is the gas
2731 constant, p is the atmospheric pressure, T_{vp} and T_{ve} are parcel and environmental
2732 virtual temperatures respectively.

2733 Accordingly, the higher the value of CAPE, the greater the potential for severe
2734 convection. However, the ascent of air should also overcome any stable boundary
2735 layer (i.e. where the boundary layer has a high CIN value) to generate severe
2736 convection (Holley et al., 2014). Thus CAPE and CIN are explored for inclusion as
2737 covariates.

2738 • **Temperature (T-2m and DPT)**

2739 Temperature has a significant physical and climatological relation with precipitation,
2740 and is considered as one of the defining controls on precipitation intensity. It should be
2741 noted that the relationship with precipitation occurrence is far more complicated and
2742 can vary both by season and location (e.g. Cong and Brady, 2012; Tencer *et al.*, 2014).
2743 The relation between temperature and extreme precipitation are governed by the
2744 Clausius–Clapeyron (C-C) relation, which explains the increased capacity of warmer
2745 air to hold moisture under constant relative humidity. Trenberth *et al.* (2003)
2746 hypothesised that under the C-C relation a 6–7% increase in the intensity of extreme
2747 precipitation is expected per 1°C increase in temperature if relative humidity remains
2748 constant. This rate has been confirmed for daily precipitation intensities by a number
2749 of studies including Fischer and Knutti (2016) and Westra *et al.* (2013). However, the
2750 intensity relation with temperature is also complicated by other factors such as
2751 changes in large-scale circulation (Trenberth and Shea, 2005; Trenberth, 2011), event

2752 type (Wasko and Sharma, 2014), and moisture content (Lenderink and Van Meijgaard,
2753 2008).

2754 Climate models suggest that increasing temperature would increase the capacity of
2755 warm air to hold more moisture, leading to an increase in daily and hourly extreme
2756 precipitation (Allan and Soden, 2008; Arnbjerg-Nielsen *et al.*, 2013; Kendon *et al.*,
2757 2014). Observational studies support this result, and report increasingly intense
2758 precipitation extremes due to increasing temperature (Alexander *et al.*, 2006;
2759 Trenberth, 2011; Alexander, 2016).

2760 Recent studies of sub-daily extreme precipitation have confirmed the C-C relation and
2761 indicated an increase in intense precipitation on short observational timescales with
2762 temperature increase (Lenderink and Van Meijgaard, 2008; Hardwick Jones *et al.*,
2763 2010; Lenderink *et al.*, 2011; Barbero *et al.*, 2017; Blenkinsop *et al.*, 2018; Kendon *et*
2764 *al.*, 2018). In the UK, Blenkinsop *et al.* (2015) confirmed that hourly extremes follow
2765 approximately the C-C relation, and the increase is centred around 6.9% °C⁻¹, although
2766 the relation varies seasonally. Other studies have shown super C-C scaling for hourly
2767 precipitation intensities (e.g. Lenderink and Van Meijgaard, 2008).

2768 Lenderink and Van Meijgaard (2008) reported that highest sub-daily precipitation
2769 intensities are associated with convective showers, which are highly related to surface
2770 temperature and moisture availability. Therefore, 2m surface air temperature and dew
2771 point temperature (DPT) are investigated as potential covariates for the statistical
2772 modelling. Dew point temperature (DPT) reflects the temperature to which air must be
2773 cooled to become saturated with water vapour, which will be condensed into the liquid
2774 state, forming precipitation once air temperature cools further (Wallace and Hobbs,
2775 2006).

2776 Both of these variables have been used in previous research, and can be used to scale
2777 the relation between extreme precipitation and temperature, though using the dew
2778 point temperature is preferable as it has less spatial and temporal variation, and it
2779 quantifies explicit information on both temperature and near-surface humidity (Kürbis
2780 *et al.*, 2009; Lochbihler *et al.*, 2017; Ali *et al.*, 2018).

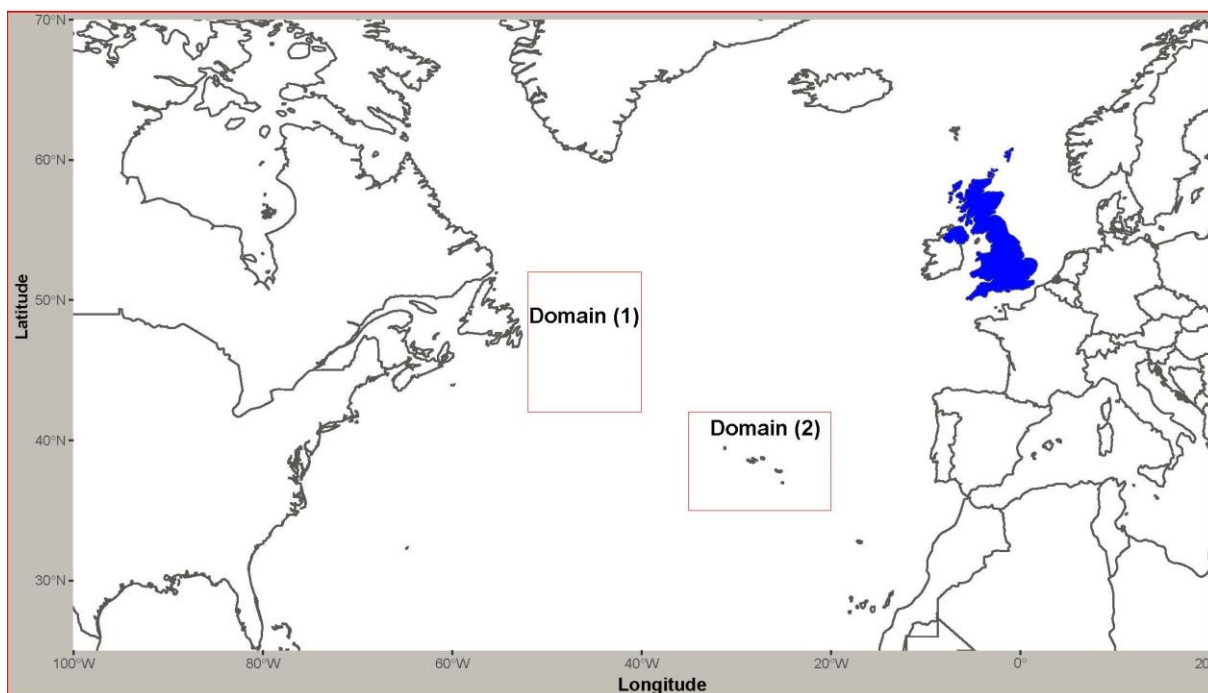
2781 • **Sea surface temperature (SST)**

2782 The North Atlantic plays a major role in determining the climatology of Europe and the
2783 UK. Gastineau and Frankignoul (2015) reported that summer atmospheric circulation
2784 and sea level pressure over the Atlantic are highly affected by the preceding spring

2785 Atlantic sea surface temperature (SST), and this affects European summer weather.
2786 The hydrological cycle, moisture content, and atmospheric circulation over the UK are
2787 largely affected by North Atlantic climatology (Colman, 1997; Sutton and Hodson,
2788 2005). Wang and Dong (2010) indicated that increased North Atlantic SSTs would
2789 increase oceanic evaporation, generating positive moisture anomalies moving over the
2790 UK. Moreover, Sutton and Dong (2012), analysing European climate change patterns
2791 in the 1990s, reported that North Atlantic Ocean warming is a key driver in determining
2792 European summer climate and precipitation patterns.

2793 Recently, Ossó et al. (2018) confirmed the SST relation with south east Atlantic
2794 summer precipitation, especially in the UK, and reported that summer precipitation
2795 patterns can be predicted using the preceding spring Atlantic SST index. In addition,
2796 SST patterns control the position of the jet stream over the North Atlantic, which affects
2797 UK precipitation in all seasons (Ossó et al., 2018). Similarly, Wilby et al. (2004) and
2798 Neal and Phillips (2009) reported robust relationships between summer precipitation
2799 in the UK south and southeast regions and preceding North Atlantic SSTs.
2800 Furthermore, Lavers et al. (2013), reported that transferred moisture from the North
2801 Atlantic, which has a directly proportional relationship with SSTs, contributes
2802 noticeably to winter extreme precipitation in the UK.

2803 Here, coincident and lagged SST values are considered as potential predictors. We
2804 examine the relation between hourly extremes in the UK and both SSTs and an SST
2805 index (Ossó et al., 2018). The SST mean over the domains located in the north west
2806 (42°N – 52°N , 52°W – 40°W) (Domain 1) and south east (35°N – 42°N , 35°W – 20°W)
2807 (Domain 2) of the North Atlantic on the day of the extreme (SST-Avg), and 4 months
2808 earlier (SST-Avg-lag) are investigated (Figure 19). The SST index, which is the
2809 difference in average SST between the two domains, is investigated over the same
2810 time frames (SST-Index and SST-Index-4lag).



2811

2812 *Figure 19: The domains located in the north west (42°N–52°N, 52°W–40°W) (Domain*
 2813 *1) and south east (35°N–42°N, 35°W–20°W) (Domain 2) of the North Atlantic, where*
 2814 *the sea surface temperature (SST) between 1990-2015 was extracted, to investigate*
 2815 *its relation with hourly extremes in the UK. Longitude (x-axis) and latitude (y-axis)*

2816 • **Atmospheric pressure**

2817 Atmospheric pressure, and its derived indices, play a significant role in the climatology
 2818 of the UK. High and low pressure systems have a significant role in determining airflow
 2819 directions and consequently influence heavy precipitation (Barry and Chorley, 2009).

2820 Hofstätter et al. (2018), who analysed large-scale, heavy precipitation over Europe and
 2821 the role of atmospheric cyclones, reported significant relations with the geopotential
 2822 height at different levels such as: 850-hPa (Z-850), 700-hPa (Z-700), and 500-hPa (Z-
 2823 500). Esteban et al. (2006) analysed the daily atmospheric circulation over western
 2824 Europe using reanalysis data and found that using Z-500 characterizes well enough
 2825 the complex circulation variability. Moreover, Kilsby et al. (1998) confirmed the benefit
 2826 of using mean sea level pressure (MSLP) to predict precipitation statistics in the UK,
 2827 suggesting that using other circulation data, such as upper air circulation (e.g. Z-750
 2828 or Z-500) would improve the physical basis of regression models.

2829 Tye et al. (2016) reported a strong significant seasonal relationship between daily
2830 precipitation extremes and MSLP, especially in the north and west of the UK. This
2831 supported prior research by Lavers et al. (2013) on the role of atmospheric rivers over
2832 the UK in transferring moisture from the Atlantic, and their dependence on MSLP.
2833 Recently, Chan *et al.* (2018b) used MSLP and Z-850 relative vorticity as predictors,
2834 among other large-scale variables, to assess convection-permitting climate simulations
2835 in the southern UK, demonstrating that their inclusion in a statistical model well
2836 enhance the simulation of hourly extreme precipitation.

2837 Therefore, the correlation of MSLP and geopotential height at different levels (i.e. Z-
2838 850, Z-700, and Z-500) with hourly extreme precipitation is also investigated for use
2839 as predictors in the statistical model.

2840 • **Total column of water vapour (TCWV)**

2841 Total column water vapour (TCWV) is a measure of the total gaseous water contained
2842 in a vertical column of the atmosphere. It represents over 99% of the atmospheric
2843 moisture, and comprises the major source of atmospheric energy governing the
2844 process of cloud formation, energy exchange within a system, and the development of
2845 weather systems on short time scales (Wypych et al., 2018).

2846 Trenberth (2011) indicated that the strong correlation between TCWV and SSTs, could
2847 lead to more extremes in the future under different climate change scenarios. Wypych
2848 et al. (2018) confirmed the importance of TCWV over Europe and the North Atlantic,
2849 besides the significance of atmospheric circulation in forming the moisture content,
2850 especially in winter. Furthermore, Beckmann and Adri Buishand (2002) used TCWV to
2851 statistically downscale and simulate precipitation occurrence and frequency in Europe
2852 (i.e. Germany and the Netherlands) from a GLM, and reported that TCWV is among
2853 the most powerful predictors of wet-day precipitation amounts. Blackburn et al. (2008)
2854 reported that during the UK 2007 floods, a similar weather system could not have
2855 produced the same floods without the available TCWV over the UK, which was much
2856 higher than the average. Therefore, the TCWV over the UK is also considered as a
2857 predictor for hourly extreme precipitation.

2858 **5.3. Methodology**

2859 Hourly precipitation across the UK is investigated and modelled using GLM and EVT
2860 to simulate both the occurrence and intensity at extreme levels. Extreme events are
2861 rare and infrequent by definition, which incorporates a noticeable uncertainty in

2862 estimating the underlying distribution parameters (Naveau et al., 2005). Here we use
2863 peak over threshold (POT) data to identify the parameters of a Poisson process.

2864 **5.3.1. Generalized linear model (GLM)**

2865 Adopting a stochastic weather generator approach (e.g. Furrer and Katz, 2008) we
2866 assume that the processes governing extreme precipitation occurrence and the
2867 extremity of the intensity are similar but not necessarily the same. Thus, we adopted
2868 the Poisson distribution to simulate the arrival rate, or occurrence, of an extreme event.
2869 Given that an event has occurred, its intensity is then described by the GPD.

2870 GLMs are a flexible generalization of ordinary linear regression that allow for response
2871 variables that have error distribution models other than a normal distribution (Olsson,
2872 2002). The GLM uses a link function to relate the linear model to the response variable
2873 and generalizes the linear regression, which allows the magnitude of the variance of
2874 each measurement to be a function of its predicted value.

2875 The Y outcome of the dependent variables is assumed to be generated from a
2876 particular distribution in the exponential family, such as normal, binomial, Poisson or
2877 gamma distributions (Madsen and Thyregod, 2010). The mean, μ , of the distribution
2878 depends on the independent variables, \mathbf{X} , through:

$$2879 \quad E(\mathbf{Y}) = \mu = g^{-1}(\mathbf{X}\boldsymbol{\beta}) \quad (16)$$

2880 where $E(\mathbf{Y})$ is the expected value of Y ; $\mathbf{X}\boldsymbol{\beta}$ is the linear predictor, a linear combination
2881 of unknown parameters $\boldsymbol{\beta}$; and g is the link function.

2882 **• Poisson distribution**

2883 The Poisson distribution is a discrete probability distribution that expresses the
2884 probability of a given number of events occurring in a fixed interval of time or space at
2885 a known constant rate (λ); each event is assumed independent of the previous
2886 (Madsen and Thyregod, 2010). For an average number of events in time interval (t),
2887 the Poisson probability density function (pdf) is:

$$2888 \quad \mathbb{P}(Y = y) = \frac{e^{-\lambda}\lambda^y}{y!}, y = 0,1,2,3, \dots \quad (17)$$

2889 Where λ is the average number of events occurring in time t , and y any positive number
2890 of events.

2891 Rearranging the proper functional form to solve for λ provides a construct for the log
2892 likelihood function and the parameter estimation. The resultant statistical model,

2893 referred to as the Poisson regression model, can then be used to predict the probability
2894 occurrence of extreme precipitation.

2895 The Poisson distribution assumes equality in the variance (V_i) and mean (E_i) of the
2896 data, both of which equal the event rate (λ_i), also referred to as equidispersion.
2897 Variance greater than mean of the data implies overdispersion, and a negative
2898 binomial distribution would be more appropriate. Contrary, estimated variance smaller
2899 than the mean of the data, underdispersion, indicates that events arrive at a rate which
2900 is more regular or uniform than expected from a Poisson process.

2901 • **Link function $g(\mu)$**

2902 The link function $g(\mu)$ is used to establish a relationship between the count response
2903 Y and the linear predictors X_1, \dots, X_n in a GLM. It is chosen based upon the type of data
2904 in the model. The general form of the link function is

$$2905 \quad g(\mu) = \mathbf{X}\beta \quad (18)$$

2906 In this research, the precipitation occurrence data is discrete count data; therefore, for
2907 Poisson distributed data, the link function is

$$2908 \quad g(\mu) = \log(\lambda) \quad (19)$$

2909 **5.3.2. Extreme Value Theory (EVT)**

2910 Extreme value theory describes a family of distributions which characterise the tail of
2911 the distribution of a series of maximum values without a priori knowledge of the
2912 underlying behaviour (Coles et al., 2001). When considering the maxima within a
2913 certain period, the two main approaches used are either block maxima (BM) where
2914 data are grouped into blocks of the same duration, or peaks over threshold (POT),
2915 where the values exceeding a specified threshold are selected for the analysis.

2916 Hourly precipitation data are limited and scarce, therefore, the POT approach is
2917 adopted here to maximise the available data. The POT approach utilizes additional
2918 information about the extreme upper tail, which provides more accurate parameter and
2919 quantile estimates (e.g. Katz et al., 2002). It has been widely used to estimate climatic
2920 extreme variables such as extreme precipitation (e.g. Francisco Javier et al., 2011;
2921 Thiombiano et al., 2017), temperature (e.g. Cheng et al., 2014), and wind velocity (e.g.
2922 Pandey et al., 2003).

2923 An adequate asymptotic distribution to describe the behaviour of events over a
2924 threshold is the Generalized Pareto Distribution (GPD) defined by Coles et al. (2001)
2925 with the following cumulative distribution function (CDF):

$$2926 \quad H(y) = 1 - \left(1 + \frac{\xi y}{\tilde{\sigma}}\right)^{-1/\xi} \quad (20)$$

2927 where ξ and $\tilde{\sigma}$ are the shape and scale parameters respectively, while y are the
2928 excesses over a selected threshold u . At a sufficiently high threshold, the Generalized
2929 Extreme Value (GEV) distribution (describing BM) and the GPD become
2930 mathematically equivalent, sharing a common shape parameter and with easily
2931 interpretable definitions of the GEV's location, and GP's threshold and scale
2932 parameters (Coles et al., 2001).

2933 Specifying the threshold in the POT approach is essential to achieve the balance
2934 between bias and the variance of the distributions (Coles et al., 2001; May, 2004).
2935 Generally speaking, defining the threshold will control the sample size and distribution
2936 behaviour. Having a low threshold would violate the GPD asymptotic and data
2937 independence assumptions. While having too high a threshold would eliminate some
2938 of the extreme values, and retain few values for the analysis (Coles et al., 2001).
2939 Previous examination of daily precipitation over Europe examined different thresholds
2940 such as the 0.95 and 0.99 quantiles, reporting better results for the 0.99 quantile
2941 (Anagnostopoulou and Tolika, 2012; Jones et al., 2014). Moreover, Anagnostopoulou
2942 and Tolika (2012) reported that this threshold is the most appropriate for extreme
2943 precipitation over Europe, and provides more coherent results compared to other
2944 thresholds and facilitates better comparison with a GEV analysis. In this research, the
2945 0.99 threshold was used since it achieves a balance between having a high threshold
2946 and sufficient sample size.

2947 *The GPD density functions assume stationarity, therefore, it can capture the temporal*
2948 *behaviour of extremes within the analysis period given that the extreme mechanisms*
2949 *are stationary. However, assuming a stationary climate might not be valid due to both*
2950 *naturally occurring climate oscillations or anthropogenic activities. Therefore, a non-*
2951 *stationary approach is adopted in this chapter to account for climate variation, where*
2952 *time-dependent variables are incorporated in parameter (i.e. shape and scale*
2953 *parameters) estimation.*

2954 *Accordingly, different climatological predictors (Table 7) were employed to estimate*
 2955 *the GPD parameters (i.e. shape and scale) in this chapter, with the most suitable*
 2956 *predictors retained to account for the parameter estimation. This would allow the*
 2957 *parameters to vary with time based on the combination of climatological variables such*
 2958 *as temperature and atmospheric pressure. However, the shape parameter (ξ), which*
 2959 *is the most complex to be estimated, was considered constant due to its noisy pattern,*
 2960 *and to keep in line with previous similar studies (e.g. Haagensohn et al., 2013; Jones et*
 2961 *al., 2014; Condon et al., 2015; Wi et al., 2016). Therefore, the GPD parameters are*
 2962 *introduced to the GPD distribution as following:*

2963

$$\log[\sigma(x)] = \beta_{0,\sigma} + \beta_{1,\sigma}x_1 + \dots + \beta_{n,\sigma}x_n \quad (21)$$

2964

$$\xi(tx) = \xi \quad (22)$$

2965 where (σ) is the scale parameter, (ξ) is the shape parameter, variables x_1, x_2, \dots, x_n are
 2966 the covariates (which can include time as a covariate to consider a temporal trend),
 2967 and $\beta_0, \beta_1, \dots, \beta_n$ are the coefficients, at time t .

2968 Meanwhile, most of the existing metrics and design guidelines in Europe are based on
 2969 stationary data analysis (Madsen et al., 2013). The existing design guidelines account
 2970 for hydrological risks (e.g. pluvial and fluvial floods, extreme precipitation) using the
 2971 “return period” variable, where the designed structures (e.g. dams, sewers) are able to
 2972 cope with hydrological events of a specified return period (e.g., the 100-year flood),
 2973 and the event frequency distribution remains stationary through time (e.g. from 20 up
 2974 to 100 years).

2975 However, while using the non-stationary approach it should be noted that the
 2976 distribution frequency reflects the probability of a given event (e.g. flood, extreme
 2977 precipitation) magnitude occurring over a specified time period (e.g. 20 year). A similar
 2978 concept was introduced for hydrological analysis purposes by various researchers,
 2979 using “design life level” instead of “return period” to reflect the risk associated with a
 2980 specific magnitude event (e.g. Rootzén and Katz, 2013; Salas and Obeysekera, 2013;
 2981 Condon et al., 2015).

2982 In this research, the non-stationary GPD distribution along with the NAO observational
 2983 dataset (Jones et al., 1997) and downscaled climatic variables from the European

2984 Center for Medium-Range Weather Forecasts (ECMWF) Interim reanalysis dataset
2985 (Dee *et al.*, 2011) were adopted to characterise hourly extreme precipitation intensity
2986 in the UK.

2987 **5.3.3. Poisson-GPD Distribution relation**

2988 The GPD is used to assess the magnitude of hourly precipitation events exceeding the
2989 predefined threshold, while the Poisson distribution is used to model the occurrence of
2990 extreme precipitation exceeding the threshold u in any given year. Therefore, the
2991 combined Poisson-GPD relationship can be defined using the following probability
2992 distribution function (PDF) (Wi *et al.*, 2016):

$$H(y) = \exp \left\{ -\lambda \left(1 + \frac{\xi y}{\bar{\sigma}} \right)^{-1/\xi} \right\} \quad (23)$$

2993

2994 where λ is the arrival rate of excesses over the threshold.

2995 **5.3.4. Data independence**

2996 The Poisson distribution and EVT assume observations above the defined threshold
2997 to be statistically independent (Coles *et al.*, 2001), which is hard to achieve in real
2998 climatological applications. Furthermore, since the data has a short time-scale (i.e.
2999 hourly), dependence may occur frequently, even if only values above a very high
3000 threshold are selected. Hourly extreme precipitation in UK northern regions are often
3001 generated by large-scale mechanisms (Blenkinsop *et al.*, 2017; Darwish *et al.*, 2018),
3002 which can lead to a temporal dependence.

3003 Therefore, the 0.99 quantile (Q99) for each gauge was calculated, and observations
3004 above Q99 were declustered and retained for further analysis. Subsequently, the Q99
3005 observations from all the gauges within each region was grouped, and only the highest
3006 hourly precipitation value per day in each region was selected. The “run decluster”
3007 approach detailed in section 4.3.4 was adopted to perform the declustering, with the
3008 independence of each gauge data assessed using the extremal index ($E\Theta$). This
3009 measures the degree of local dependence in the extremes of a stationary process
3010 (Northrop, 2015). For independent data, $E\Theta = 1$, while $E\Theta = 0$ indicates full data
3011 dependence (clustering). The results showed that most of the gauges have values
3012 higher than 0.7, indicating generally independent values.

3013 **5.3.5. Regional Data Pooling**

3014 Here, we aim to characterise hourly extreme precipitation regionally, using the new
3015 homogeneous extreme precipitation regions developed from the Q99 precipitation
3016 extremes in Chapter 4. Therefore, a predefined location for each region, at which the
3017 model will be built and validated, is required, and for which the geometric centres of
3018 the hourly extreme regions shown in Figure 14 are used.

3019 Finally, to overcome any residual regional dependence, as extremes will likely be
3020 observed at more than one station in a region (Khaliq *et al.*, 2006; Sugahara *et al.*,
3021 2009; AghaKouchak and Nasrollahi, 2010), the retained data in the previous step
3022 (Section 5.3.4) (i.e. the highest Q99 hourly precipitation value per day in each region)
3023 will be used to develop the model.

3024 **5.3.6. Parameter Estimation**

3025 To facilitate the inclusion of time-dependent parameters that account for seasonality,
3026 the maximum likelihood estimation (MLE) method (Coles *et al.*, 2001), is used in this
3027 research to estimate the GPD parameters. MLE is asymptotically normally distributed
3028 and the variance is asymptotically minimal, which facilitates the derivation of
3029 confidence intervals for the distribution quantiles. Millar (2011) described the MLE as
3030 following:

3031 Let $x_1, x_2, x_3, \dots, x_n$ be n observations of a random sequence with probability density
3032 function $f(x|\theta)$, where θ is the vector of parameters of this function. If one considers
3033 that the observations x_i is statistically independent, the joint probability density function
3034 for this sample is the product of the individual densities, called the likelihood function:

$$L(\theta|x) = \prod_i^n f(x_i|\theta) \quad (24)$$

3035

3036 In general, this function is written as:

$$\text{Log } L(x|\theta) = \sum_{i=1}^n \text{Log } f(x_i|\theta) \quad (25)$$

3037

3038 In the process of the inference of θ , the MLE aims that all the relevant information in
3039 the observed data is contained in the likelihood function, to determine the best
3040 probability density functions that produce the given sample.

3041 Katz et al. (2002) indicated that MLE outperform other approaches in having
3042 consistency parameters estimates, and flexibility of incorporating non-stationary
3043 features into the distribution parameters as covariates. Moreover, MLE performance
3044 has been reported to be better than other approaches (e.g. L-Moments) in the
3045 presence of time-varying climatic variables and for adequate sample sizes (Zhang et
3046 al., 2005; White et al., 2008; Jones et al., 2014; Wi et al., 2016)

3047 **5.3.7. Model selection**

3048 Model assessment is essential to validate the proposed statistical model, thus the
3049 predictive ability, model consistency, and model structure are evaluated using
3050 statistical and graphical approaches. The literature on extreme precipitation modelling
3051 using either GLM or EVT suggests different methods to assess model efficacy such as
3052 parameter significance, quantile plots, the Akaike Information Criterion (AIC),
3053 distribution plotting, or likelihood ratio tests (Coles et al., 2001; Chatterton et al., 2010;
3054 Davison and Huser, 2015).

3055 The AIC, which estimates the relative quality and predictive power of statistical models
3056 for a given set of data (Akaike, 1981), is used to select the best model and predictive
3057 variables. The AIC estimates the likelihood of a model to predict the future values, and
3058 the number of used variables in each model, where a trade-off between the model
3059 goodness of fit and complexity is evaluated (Burnham and Anderson, 2003). The AIC
3060 model selection criteria recommends choosing the model with the lowest AIC value;
3061 however, further investigation should be performed before choosing the model with the
3062 lowest AIC value, especially when the difference between models is small (Akaike,
3063 1992) as the method penalises more complex models. AIC is a relative measure of
3064 goodness of fit, and does not assess the absolute model quality or the null model,
3065 hence, it should be used in combination with other statistical tests (Akaike, 1992).

3066 An alternative statistical measure, the likelihood-ratio test (LRT) is also used to
3067 compare the goodness of fit between models. LRT compares a relatively more
3068 complex model to a simpler model, and reports the significance of adding more
3069 parameters to the model (Nogaj et al., 2006). Therefore, the method is valid when

3070 analysing nested models, where the complex model has one or more additional
3071 variables.

3072 Visual comparison of the fitted models' performance is achieved with quantile-quantile
3073 (Q-Q) plots, which assess the similarity between observed and predicted quantiles. If
3074 the model fits the data perfectly, the plotted points will approximately lie on the line
3075 $y=x$, while a large deviation is evidence of the opposite. Confidence estimates of the
3076 model fit are developed from 500 bootstrapped samples.

3077 **5.3.8. Model predictions**

3078 Finally, the statistical model is used to assess the potential impact of climate change
3079 and temperature increase in the UK. Significant increases in temperature and
3080 precipitation in recent decades have been reported and confirmed globally (Rahmstorf
3081 and Coumou, 2011; Donat et al., 2013), while climate models project a further increase
3082 either in temperature or in precipitation frequency and intensity across northern Europe
3083 (Fischer and Knutti, 2015). Using the statistical model to identify the nature of future
3084 changes is a robust alternative to support future adaptation plans and design
3085 guidelines where complex dynamical models are not affordable or achievable.

3086 In this research, the pseudo global warming (PGW) method (Kimura and Kitoh, 2007)
3087 for a scenario that restricts global warming to 2 degrees Celsius or lower, as suggested
3088 by the Paris climate agreement (Paris agreement, 2015), is adopted to assess future
3089 extreme precipitation patterns. The gridded daily averaged data between 1990-2015
3090 from the European Center for Medium-Range Weather Forecast Interim reanalysis
3091 (ECMWF) dataset (Dee et al., 2011), will be used to establish a control climate (CTL),
3092 and the 2°C degrees increase will be relative to this period. Dynamical models
3093 premised on PGW use the sum of observations (reanalysis data) as the initial and
3094 boundary conditions for regional model integrations, with the global warming increment
3095 is estimated from simulations with global coupled climate models (Kimura and Kitoh,
3096 2007). The statistical equivalent adopts predictive parameters that are broadly dictated
3097 by their physical response to an increase in global mean temperature of 2° C.

3098 **5.4. Results**

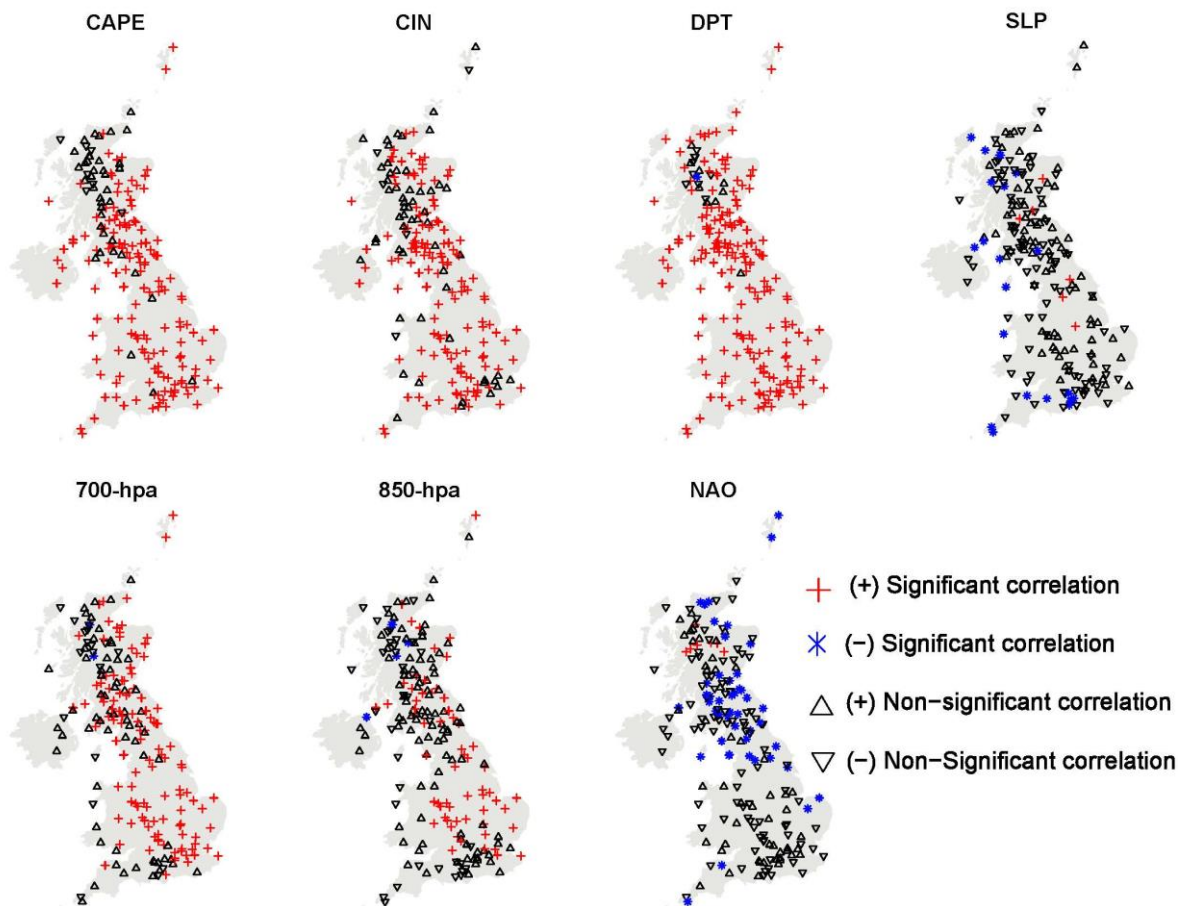
3099 As discussed in previous sections, pooled hourly Q99 were declustered to ensure
3100 higher probability of independence. Extremal index $E\Theta$ values of 0.79, 0.74, 0.77, 0.73,
3101 and 0.71 for the regions SE, SW, ME, NE, and NW, respectively, indicate that the

3102 remaining data in each region can be considered to be independent. All subsequent
3103 analyses presented below use the declustered data.

3104 ***5.4.1. Climatic predictor initial selection***

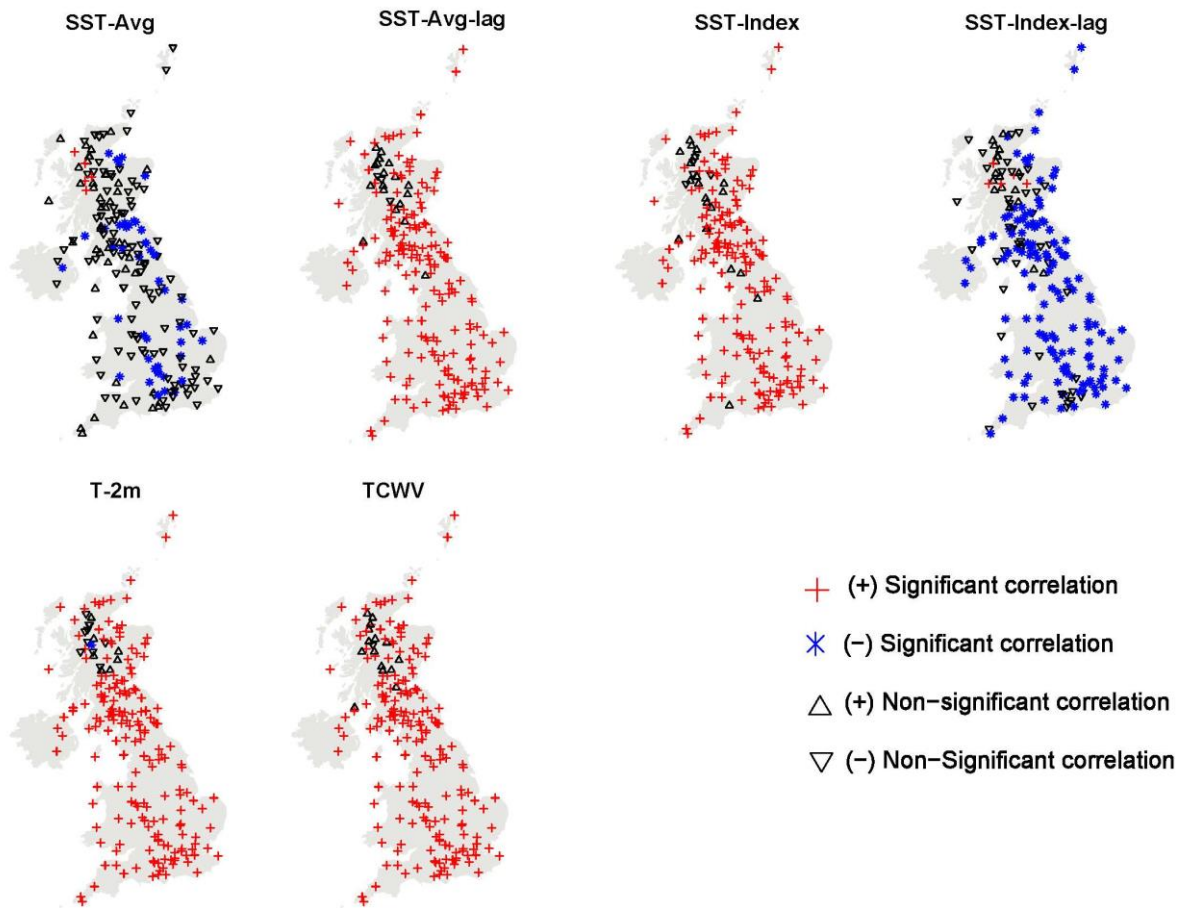
3105 Before developing the statistical model to simulate UK hourly extreme precipitation, an
3106 exploratory analysis of the correlation between hourly extreme intensity and the
3107 proposed variables (Table 7) was performed. Some of these variables are physically
3108 related (e.g. temperature, CAPE), therefore, collinearity should be considered when
3109 choosing the best statistical predictors. The correlation analyses shown in Figures 20
3110 and 21 are derived from simple linear models of precipitation intensity against the
3111 relevant time-dependent variable. Regressions for precipitation occurrence are not
3112 shown as the results are broadly similar.

3113 The results in Figures 20 and 21 show that a majority of the potential variables are
3114 significantly correlated with hourly extreme precipitation intensity across the UK, while
3115 most of the non-significantly correlated gauges are in the north west region (NW). For
3116 instance, CAPE and CIN are known to drive short duration convective events, which
3117 are more common in the warmer southern regions. In contrast, air flow (represented
3118 by geopotential height), NAO and SLP are more frequently associated with large-scale
3119 frontal systems over the north and west of the UK; such events may have embedded
3120 convective cells, making these variables more significant in NW rather than the south.
3121 Thus, all variables in Table 7 are explored further in deriving the statistical models for
3122 hourly extreme precipitation occurrence and intensity.



3123

3124 Figure 20: The Spearman correlation between hourly extreme intensities above the
 3125 Q99 and potential climatological predictors. The assessed predictors are: convective
 3126 available potential energy (CAPE), convective inhibition (CIN), dew point temperature
 3127 (DPT), sea level pressure (SLP), pressure level height 700-, 850hPa (Z700-, Z850),
 3128 and North Atlantic oscillation (NAO). The positive and negative significantly correlated
 3129 gauges are indicated by red and blue colour respectively. Moreover, positive and
 3130 negative non-significantly correlated gauges are indicated by black upward and
 3131 downward arrows respectively.



3132

3133 Figure 21: As for Figure 20 but assessed predictors are: sea surface temperature
 3134 average over NW (42°N–52°N, 52°W–40°W), and SE (35°N–42°N, 35° W–20°W)
 3135 domains of the North Atlantic on Q99 days (SST-Avg), 4-month lagged sea surface
 3136 temperature average (SST-Avg-lag), sea surface temperature difference between NW
 3137 and SE domains on Q99 days (SST index), 4-month lagged sea surface temperature
 3138 difference between NW and SE domains (SST-index-lag), near-surface air
 3139 temperature (T-2m), and total column water vapour (TCWV). The positive and negative
 3140 significantly correlated gauges are indicated by red and blue colour respectively.
 3141 Moreover, positive and negative non-significantly correlated gauges are indicated by
 3142 black upward and downward arrows respectively.

3143

5.4.2. Poisson model

3144

The statistical models use climatic variable measurements between 1992 and 2014 in
 3145 each regions' geometric centroid. The period 1992-2011 was used for parameter
 3146 estimation and model fitting, while the period 2012-2014 was used for model validation.

3147

Potential climatic variables were used as predictors in the GLM, and a backward model
 3148 selection approach was adopted to determine the most significant predictors. The initial
 3149 GLM (for each of the estimated parameter sets of the Poisson and the GPD) included
 3150 all the candidate variables. Then the variables' significance was assessed, to remove
 3151 the least significant variable. The process was then repeated until only significant

3152 variables remained and deleting further variables would reduce the models' adequacy.
3153 Furthermore, model fit criterion (AIC), histograms, Q-Q plots, and Likelihood-ratio test
3154 (LRT) of the model before and after removing each variable was checked after each
3155 iteration, to ensure statistical improvement at each stage. Additionally, variables with
3156 potential interaction such as: convective variables (i.e. CAPE and CIN), atmospheric
3157 pressure (i.e. Z-850 and Z-700), and temperature (i.e. T-2m and DPT) were assessed
3158 separately and simultaneously.

3159 • **Poisson**

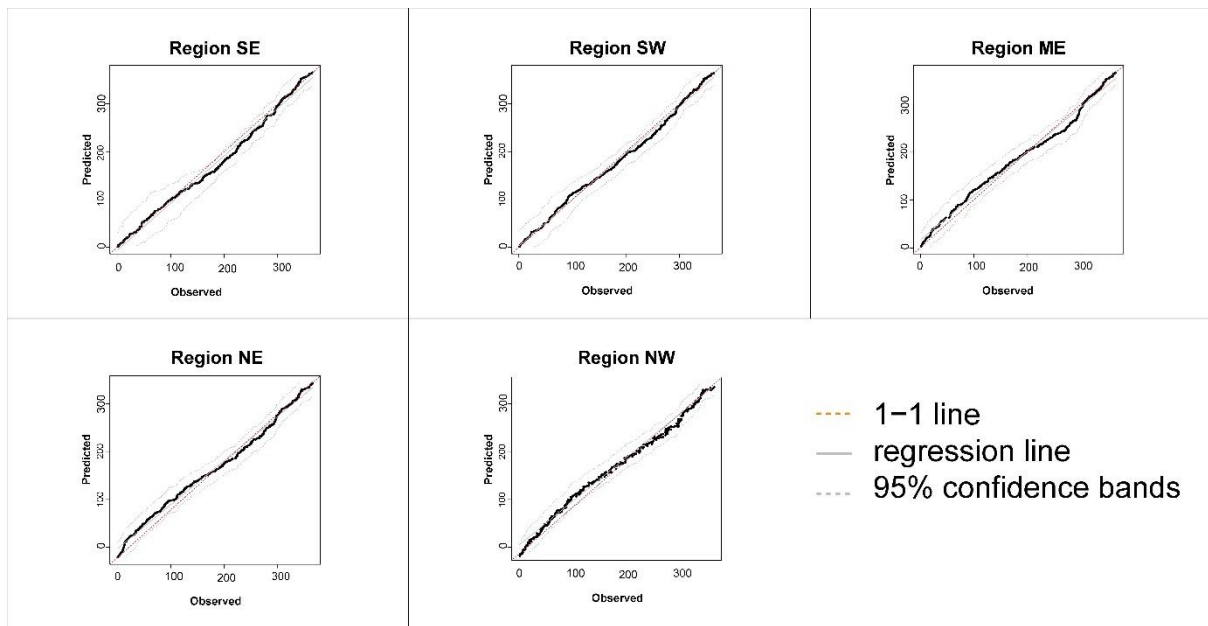
3160 The Poisson model utilises the GLM to predict a time-varying arrival rate (λ) for hourly
3161 extreme precipitation occurrences. The final selection of covariates includes the North
3162 Atlantic Oscillation (NAO), dew point temperature (DPT), atmospheric pressure at 700-
3163 hPa (Z-700), and the sinusoidal values of the Julian day of occurrence (Sin (Θ), Cos
3164 (Θ)) in the form:

$$3165 \quad \text{Log}\lambda(x) = \beta_0 + \beta_1(\text{Sin}(\Theta_t)) + \beta_2(\text{Cos}(\Theta_t)) + \beta_3(\text{NAO}_t) + \beta_4(\text{DPT}_t) + \beta_5(\text{Z-700}_t) \quad (26)$$

3166 Figure 22 shows the Q-Q plots for each region, and indicate a similar agreement
3167 between the observed and statistically simulated data for hourly extremes between
3168 1992-2011.

3169

3170

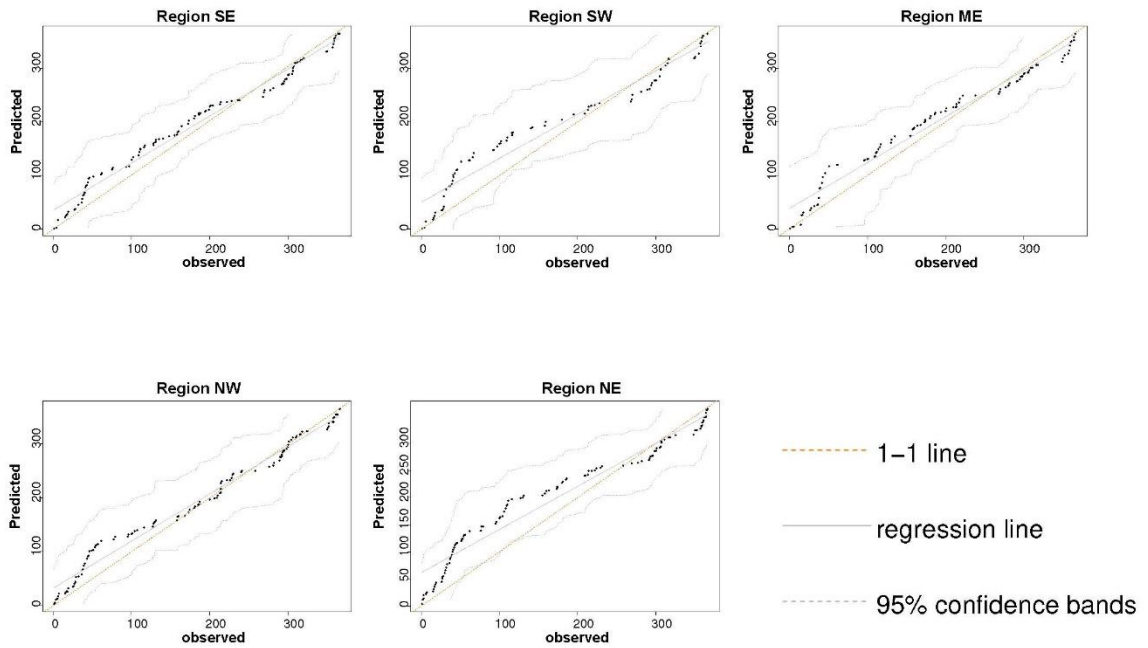


3171

3172 Figure 22: Q-Q plots for Q99 hourly extreme frequency predicted by the Poisson GLM
 3173 for the years 1992-2011 in each region. Q99 hourly extreme occurrence by
 3174 Julian day for observed quantiles (x-axis), and Poisson predicted quantiles
 3175 using NAO, Z-700, DPT, and sine/cosine Julian day as predictors (y-axis).
 3176 Confidence bands are developed from 500 bootstrapped samples. The
 3177 continuous solid line is the prediction regression line, while the dotted line is
 3178 the 1-1 reference line.

3179

3180 Figure 23 shows the model validation results for each region, using the observed and
 3181 statistically simulated Q-Q plots for years 2012-2014. The results again show
 3182 concordance between the regression line and 1-1 line, indicating reliable simulation.



3183

3184 Figure 23: Validation Q-Q plots for the Q99 hourly extremes frequency predicted by
 3185 the Poisson model for years 2012-2014 in each region. Q99 hourly extremes
 3186 occurrence by Julian day for observed quantiles (x-axis), and Poisson
 3187 predicted quantiles (y-axis). Details as for Figure 22.

3188 • **Generalized Pareto distribution (GPD)**

3189 The statistical model development utilises the observed precipitation intensity and the
 3190 corresponding time-dependent covariates – as for the Poisson model. Initial GPD
 3191 parameter estimates are obtained from a stationary model fit to the observed pooled
 3192 precipitation data. Climatic variables are then only incorporated in the GPD scale
 3193 parameter to account for non-stationarity; the shape parameter and threshold are both
 3194 assumed to remain constant (e.g. Katz *et al.*, 2002; Cheng *et al.*, 2014).

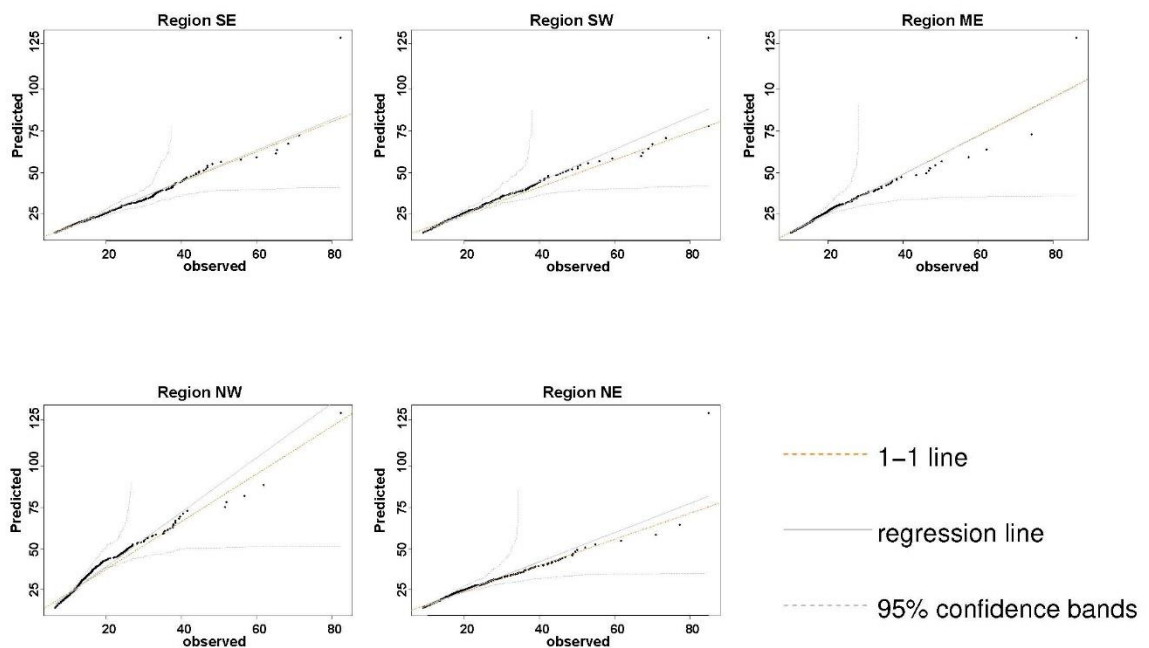
3195 The final model includes the sine and cosine terms for Julian day ($\text{Sin}(\Theta)$, $\text{Cos}(\Theta)$),
 3196 combined with CAPE. The statistical model takes the relationship:

3197
$$\log \tilde{\sigma} = \beta_0 + \beta_1(\text{Sin}(\Theta_t)) + \beta_2(\text{Cos}(\Theta_t)) + \beta_3(\text{CAPE}_t) \quad (27)$$

3198
$$\log(\xi + 1/2) = \beta_0 \quad (28)$$

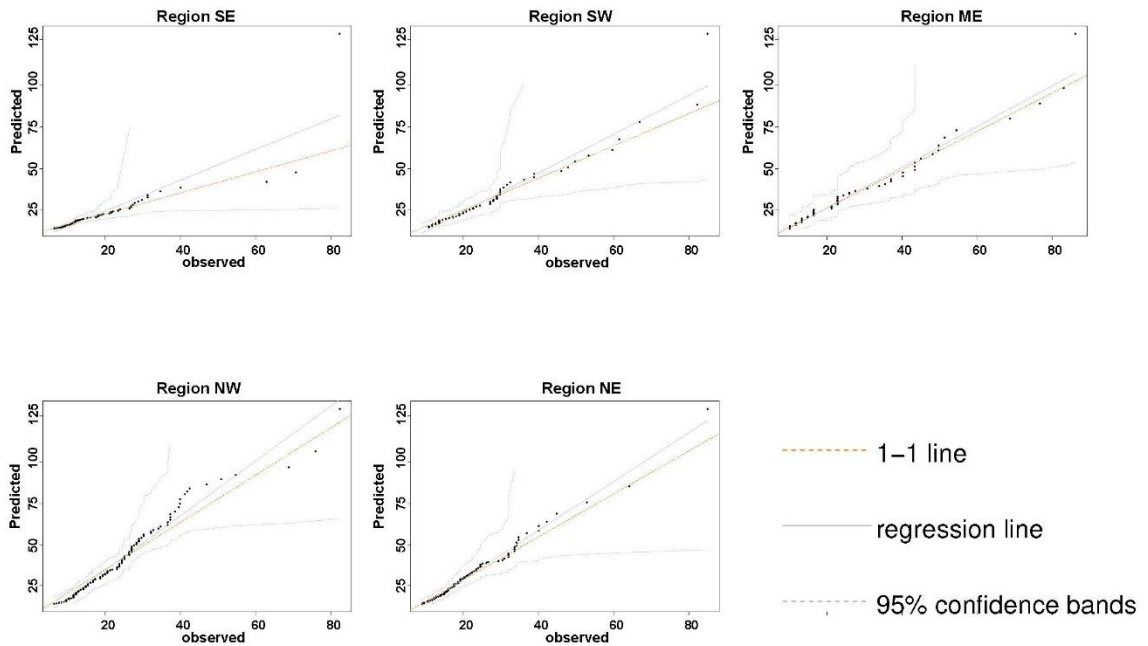
3199 This produced the most predictive model, with the lowest AIC value. Assessing the
 3200 likelihood ratio test between the base model and the final model shows a very
 3201 significant improvement in the time-dependent model at a 5% level.

3202 The Q-Q plots in Figure 24 show the statistically predicted vs observed hourly extreme
 3203 quantiles for each region between 1992-2011. Subsequently, the proposed GPD
 3204 model was validated using data between 2012-2014 (Figure 25). For a meaningful
 3205 comparison and interpretation of the two statistical models, precipitation intensities are
 3206 estimated utilising covariates for the days of occurrence predicted by the Poisson
 3207 model. As with the Poisson model, the results show concordance between the $y=x$ and
 3208 regression lines, indicating reliable performance for the statistical model.



3209

3210 Figure 24: Q-Q plots for Q99 hourly extremes predicted intensity by the GPD for the
 3211 years 1992-2011 in each region. Q99 hourly extreme intensity for observed
 3212 quantiles in mm/hr (x-axis), and GPD predicted extreme intensity quantiles in
 3213 mm/hr (y-axis). The continuous solid line is the prediction regression line, while
 3214 the dotted line is the 1-1 reference line.



3215

3216 Figure 25: Validation Q-Q plots for the Q99 hourly predicted intensities by the GPD for the years 2011-2014 in each region. Q99 hourly extreme intensity for observed
 3217 quantiles in mm/hr (x-axis), and GPD predicted extreme intensity quantiles in
 3218 mm/hr (y-axis). The continuous solid line is the prediction regression line, while
 3219 the dotted line is the 1-1 reference line.
 3220

3221 **5.4.3. Pseudo Global Warming Method**

3222 Finally, the statistical model is used to assess the potential impact of a simple scenario
 3223 of 2°C warming in the UK using a PGW approach. DPT (in the Poisson model) was
 3224 increased by a corresponding 2°C. The relation between the T-2m and DPT is
 3225 controlled by the relative humidity equation, which reflects the ratio between available
 3226 moisture in the air (i.e. vapour pressure, E) and the air moisture capacity (i.e. saturation
 3227 humidity, Es). The RH equation formula is:

3228
$$RH = 100\% \times (E/E_s) \tag{29}$$

3229 as stated in Stull (2018) for which, according to an approximation of the Clausius-
 3230 Clapeyron equation:

3231
$$E = E_0 \times \exp[(L/R_v) \times ((1/T_0) - (1/DPT))] \tag{30}$$

3232 and

3233
$$E_s = E_0 \times \exp\left[\left(\frac{L}{R_v}\right) \times \left(\frac{1}{T_0} - \frac{1}{T}\right)\right] \quad (31)$$

3234 where $E_0 = 0.611$ kPa, L is a latent-heat parameter and R_v is water-vapor gas constant
3235 where $(L/R_v) = 5423$ K (in Kelvin, over a flat surface of water), $T_0 = 273$ K (Kelvin), T
3236 is temperature (in Kelvin), and DPT is dew point temperature (also in Kelvin).

3237 Accordingly, for T -2m (T in Equation 31) between 5 - 25°C , and under constant relative
3238 humidity, the DPT ranges between 1.8°C and 21.4°C respectively. The difference
3239 between T -2m and DPT is relatively constant and varies slightly between 3.2°C - 3.6°C .
3240 Thus, in this research the difference between T -2m and DPT is assumed constant, and
3241 DPT was increased by 2°C , to match the adopted climate warming scenario (i.e. 2°C
3242 increase according to Paris agreement).

3243 On the other hand, large-scale atmospheric variables (i.e. Z-700 and NAO), were
3244 retained without modification. Gastineau and Frankignoul (2015) reported that Z-700
3245 and NAO are related to large-scale atmospheric circulation rather than atmospheric
3246 temperature. Moreover, though SST has a noticeable relation with the NAO and might
3247 increase due to global warming, no significant causal effect of SST anomalies on the
3248 NAO has been identified (Weile *et al.*, 2004). Furthermore, Rind, D. *et al.* (2005)
3249 suggested that no sufficient information and research are available to evaluate impact
3250 of potential climate change on the NAO, while available research and model
3251 simulations reported an inconsistent prediction. Finally, SST is not used as a predictor
3252 neither in the statistical model nor in the PGW. Thus Z-700 and NAO were used without
3253 adjustment.

3254 Thereafter, CAPE (in the GPD model) was increased using the relationship between
3255 temperature and precipitation quantiles identified by North and Erukhimova (2009):

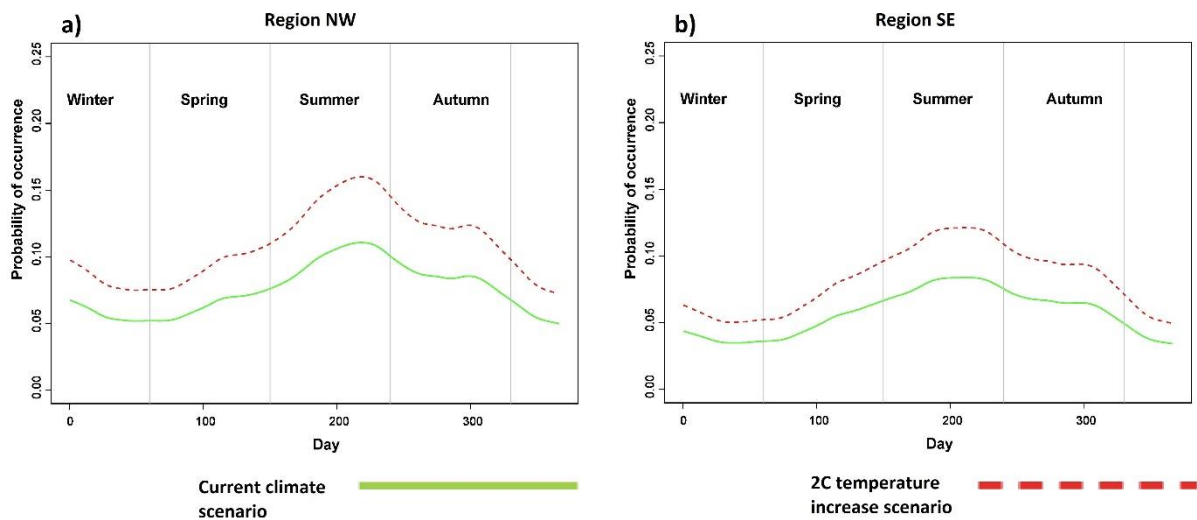
3256
$$\ln I_p = C + 0.068 \text{ DPT} + 0.5 \ln \text{CAPE} \quad (32)$$

3257 where C is a constant value of 0.2 , equals to slope coefficients of simple $\ln I_p$ and \ln
3258 CAPE regression as suggested by Lepore *et al.* (2015).

3259 The probability of extreme precipitation, and associated intensity, on each calendar
3260 day for the base climatology (derived from control years 1990-2015) and with the
3261 effects of 2°C PGW were assessed for each region. As with the model development
3262 and validation, the Poisson model simulates the most likely days of extreme
3263 precipitation occurrence, and the GPD simulates the range of probable precipitation
3264 intensities on those days. As the Poisson model can only simulate the probability of an

3265 event, given that climatological rather than observed variables are used, we consider
 3266 the extreme precipitation days to be days with the highest 1% probability of occurrence,
 3267 defined by region. The Poisson model uses unchanged climatologically averaged
 3268 values for NAO, and climatologically averaged DPT uplifted by 2°C. While the GPD
 3269 uses climatologically averaged CAPE as modified by the relationship in Equation 32.

3270 The results in Figure 26 (a and b) show the probability of extreme precipitation for each
 3271 calendar day in the NW and SE regions. A similar pattern is apparent across all UK
 3272 regions, where the highest probability of Q99 occurring is in summer. The PGW results
 3273 show that the probability of occurrence of hourly extreme precipitation would increase
 3274 up to 60% due to the temperature increase in all seasons, while the highest increase
 3275 would occur in summer. Results for the regions NE, ME, and SW are very similar and
 3276 not presented.

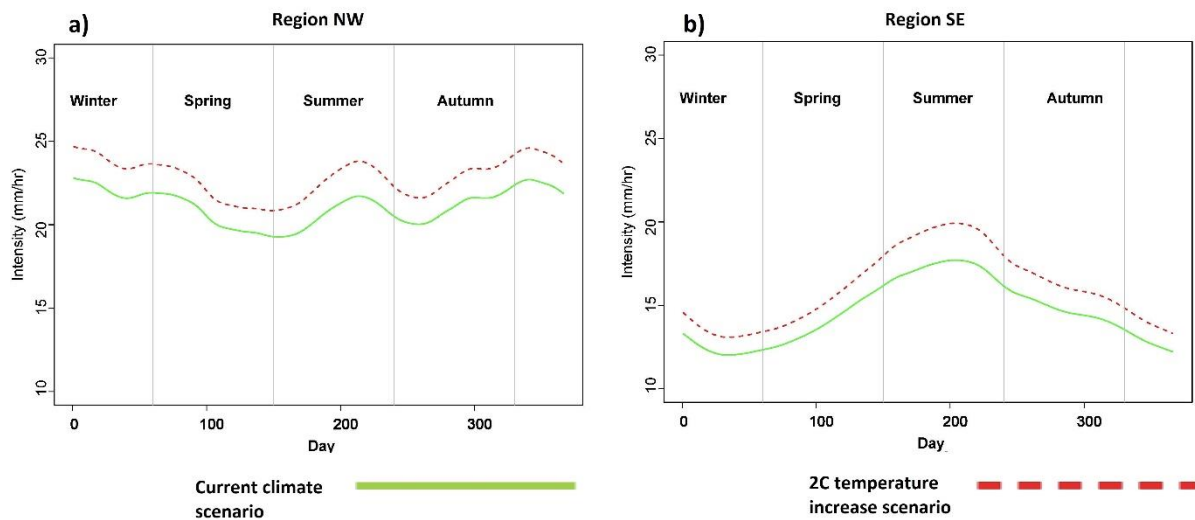


3277

3278 Figure 26: Comparison of daily probability of Q99 occurrence under current climate
 3279 (solid line) and predicted global temperature increase of 2C (dotted line) in a) NW and
 3280 b) SE. Julian days of occurrence (X-axis), and the probability of occurrence (Y-axis).

3281 The GPD model results in Figure 27 show estimated precipitation intensity with an
 3282 annual exceedance probability (AEP) of 5% (20-year return level equivalent) for each
 3283 calendar day under current and PGW climate conditions. However, it should be noted
 3284 that these results should be interpreted in conjunction with the Poisson model where
 3285 approximately 30 days would actually occur. The result is similar for all seasons, with
 3286 slight variations in northern regions (e.g. NW), while the annual probability estimates
 3287 in southern regions (e.g. SE) noticeably peak in summer. Furthermore, the response
 3288 to the 2°C warming shows a predicted intensity increase of between 13% and 17%, at
 3289 or just above C-C scaling. The highest increase occurs in SE during summer. The

3290 results indicate clearly that the intensity of hourly precipitation extremes in southern
 3291 regions (e.g. SE) are more sensitive to convective conditions, which are reflected by
 3292 the CAPE variable.



3293

3294 Figure 27: Comparison of extreme precipitation intensity under current climate (solid
 3295 line) and predicted global temperature increase of 2C (dotted line) according to Paris
 3296 agreement in a) NW and b) SE. Julian days of occurrence (X-axis), and the intensity
 3297 in mm/hr (Y-axis).

3298

3299 5.5. Discussion and Conclusion

3300 This research presents non-stationary Poisson-GPD models to simulate the frequency
 3301 and intensity of hourly precipitation extremes in the UK. Large-scale atmospheric
 3302 variables, local conditions, and seasonality including NAO, CAPE, Dew point
 3303 temperature and sine/cosine Julian day, were incorporated in GLMs to estimate the
 3304 statistical model parameters. Each climatic variable was selected on the basis of its
 3305 physical plausibility and knowledge of atmospheric processes, then examined for
 3306 statistical significance before being confirmed as a predictor. However, the statistical
 3307 model results also highlighted that a longer hourly precipitation record is necessary to
 3308 generate more robust results and reduce uncertainty.

3309 Resultant Poisson and GPD statistical models generally performed well across the UK.
 3310 However, greater uncertainty surrounds the predictions for northern regions (e.g. NW),
 3311 where there was less significance in the correlations between hourly precipitation
 3312 extremes and the selected covariates. As expected, the Poisson model across
 3313 southern regions (i.e. SW and SE) identifies a noticeable peak in summer precipitation
 3314 probability and intensity compared to other seasons. Seasonal extreme precipitation

3315 occurrence is similar in other regions, but there is less seasonal variability in extreme
3316 precipitation intensity. The differences between northern and southern regions are
3317 likely attributable to the different precipitation generating mechanisms in across the
3318 UK, as summarised by previous research (Blenkinsop *et al.*, 2017; Darwish *et al.*,
3319 2018). Northern regions are mostly dominated by large-scale forcing, while central and
3320 southern regions are dominated by convective precipitation. Initial examination of other
3321 large-scale predictors (i.e. NAO, SLP, SST) indicated that there is a more important
3322 role for local conditions compared to large-scale climatic variables in the prediction of
3323 hourly extreme precipitation across the UK.

3324 The Poisson model, which simulates the occurrence of hourly precipitation extremes,
3325 highlights that extreme hourly events have a strong dependence on both large-scale
3326 circulation (i.e. NAO and Z-700), and local-scale thermodynamic conditions reflected
3327 by the dew point temperature (DPT). This agrees with Chan *et al.* (2018b) who reported
3328 that large-scale predictors from regional climate models demonstrate skill in predicting
3329 the occurrence of extreme hourly events in convective permitting models (CPMs) for
3330 the southern UK. Furthermore, Ali *et al.* (2018) indicated a strong linkage between
3331 hourly precipitation extremes intensity and DPT, and the suitability of using DPT as an
3332 indicator of thermodynamically-driven future changes.

3333 Simulating the intensity of hourly extremes using the GPD distribution indicates that
3334 local conditions play a major role in determining the intensity of extremes, more so than
3335 large-scale atmospheric processes. The statistical model shows that convective
3336 available potential energy (CAPE), is the best potential predictor in combination with
3337 seasonality for the intensity of UK precipitation extremes. This is consistent with the
3338 identified important role of CAPE in generating extreme precipitation over the UK
3339 (Holley *et al.*, 2014; Blenkinsop *et al.*, 2015). While convective inhibition (CIN) could
3340 also be used, CAPE and CIN are related, which would lead to collinearity within a
3341 statistical model. Using a non-stationary GPD with CAPE as a covariate to characterise
3342 extreme precipitation intensity, is a flexible and appropriate method to incorporate the
3343 complex relationship between precipitation and temperature (Lenderink and Van
3344 Meijgaard, 2008; Blenkinsop *et al.*, 2015).

3345 The utility of the statistical model is demonstrated by examining changes in the
3346 probability and intensity of hourly extreme precipitation, at the geometric centre of each
3347 region, under a pseudo-global warming scenario of 2°C utilising ECMWF reanalysis
3348 data (Dee *et al.*, 2011) from 1990-2015, to simulate hourly extreme precipitation. The

3349 PGW approach indicates increasing probability of hourly extreme occurrence in
3350 summer up to 60%, especially in southern regions (e.g. SE). Associated annual
3351 probability estimates of hourly extreme intensity also increase; the increases are
3352 noticeably higher in the summer across southern regions. The transition from the
3353 dominance of large-scale frontal systems to localized convective rain with higher
3354 temperatures across the UK in summer and spring (Blenkinsop *et al.*, 2015), means
3355 that the seasonal peak in intensity is not as important in other regions. However, all
3356 regions indicated an increase in intensity of between 13% and 17% in response to a
3357 potential 2°C climate change scenario in the UK. This increase is consistent with the
3358 C-C scaling of observed hourly extremes across the UK, with a slight super C-C scaling
3359 during summer, especially in the south of the UK (Champion *et al.*, 2015)

3360 Running the statistical models presented here is considerably less computer intensive
3361 than developing and running convection permitting models (CPMs). Thus, for
3362 applications where knowledge of the full dynamical processes is not essential, or
3363 where time and resources do not permit, these models could be used to downscale
3364 and simulate hourly extremes in the UK. Changes to sub-daily extremes have
3365 previously been assessed either by disaggregating daily precipitation from coarse
3366 resolution regional climate models (RCMs) or directly from regional climate models
3367 (RCMs). However, both methods are computationally expensive, and the former can
3368 introduce additional high uncertainty in disaggregating the data. A further benefit of the
3369 statistical models developed in this research is that they confirm hypotheses that were
3370 previously only tested dynamically, providing decision-makers with a general direction
3371 of future changes.

3372 Madsen *et al.* (2013) reported that most of the existing guidelines in Europe on design
3373 floods and design precipitation are based on frequency analyses assuming stationary
3374 conditions in a certain time window. Using GLMs within the Poisson and GP
3375 distributions allows for flexible incorporation of temporally and spatially varying external
3376 predictors to account for non-stationarity in hourly extreme precipitation.

3377 The statistical model can be used for different hydrological applications, such as
3378 estimating the future intensity or frequency of hourly extremes at a regional or site
3379 specific scale. For instance, other reanalysis datasets or PGW scenarios, or indeed
3380 model predicted values of CAPE, NAO, and DPT from coarse resolution model results,
3381 could be used to estimate future precipitation in specific regions. Alternatively, these
3382 same data and statistical relationships could be used in conjunction with regional and

3383 site specific growth curve relationships to estimate future at-site precipitation
3384 conditions, and hence likely flood impacts.

3385 This chapter demonstrates that large-scale dynamics as well as local thermodynamic
3386 processes exert an influence over UK hourly extremes, but further understanding of
3387 these and their spatial variability is required. The results confirm the importance of
3388 seasonality, where the models suggested including the Julian day sine and cosine to
3389 simulate extremes, while the model predictions showed peaks in summer intensity and
3390 frequency compared to other seasons. Design assumptions are often made based on
3391 pre-determined seasons; decision-makers would welcome planning information where
3392 there is strong evidence for changes that might affect water resource operations (e.g.
3393 Morss *et al.*, 2018). The main challenges in this research would be having a longer
3394 quality controlled hourly data record, better characterising hourly extremes in terms of
3395 their spatial and temporal variance across the UK, and determining the best approach
3396 to modify the statistical model to account for each site specific characteristics. In
3397 particular, the spatial coverage within some regions, e.g. MW, is weak and would
3398 benefit from additional observational records. Ongoing research in Newcastle
3399 University is investigating these issues with the INTENSE project (Blenkinsop *et al.*,
3400 2018), and will be addressed in future research.

3401 Design guidance and adaptation plans in the UK adopt the estimates and approaches
3402 provided by Defra (Defra, 2017) and the Environment Agency (Environment Agency,
3403 2014), where an increase in precipitation intensity (referred to in practice as an uplift)
3404 of around 10% for the period 2025-2055 is estimated relative to the 1961-90 baseline.
3405 However, these estimates are based on daily precipitation data. The results in our
3406 research show that for a 20 year return period (5% AEP), an increase of up to ~17%
3407 could occur due to 2°C global warming, suggesting that the existing guidance may not
3408 be valid for sub-daily extremes. Using output from a convection permitting climate
3409 model, Kendon *et al.* (2018) also reported that changes in hourly precipitation extremes
3410 in the UK would occur before changes in daily precipitation.

3411 Similarly, Dale *et al.* (2017) suggest the importance of having updated and dedicated
3412 allowance estimates to account for sub-daily extreme precipitation changes, especially
3413 to reduce the risk for vulnerable locations to flash flooding and short intense
3414 precipitation such as urbanised areas. Moreover, Madsen *et al.* (2013) reported that
3415 the existing regulations and design guidelines for flood infrastructure assume
3416 stationary conditions, which is questionable in the EVT. Therefore, developing a

3417 statistical model while adopting non-stationary analyses would enhance the simulation
3418 of precipitation events and designing guidelines.

3419

3420

3421

3422

3423

3424

3425

3426

3427

3428

3429

3430

3431

3432

3433

3434

3435

3436

3437

3438

3439

3440

3441

3442

3443

Chapter 6. Conclusion

3444

3445 6.1 Summary of results

3446 This thesis has investigated sub-daily extreme precipitation in the UK to develop a
3447 statistical model which simulates the frequency and intensity patterns of hourly
3448 extreme precipitation. The thesis used a recently collated and quality controlled hourly
3449 precipitation dataset collected from 1900 gauges covering the period 1949 - 2014,
3450 distributed across the UK (Blenkinsop *et al.*, 2017; Lewis *et al.*, 2018). This is the first
3451 observed hourly precipitation dataset in the UK to have gone through an extensive
3452 series of site-specific, quality control procedures and a comparison with a gridded daily
3453 precipitation dataset to identify malfunctioning gauges and erroneously recorded
3454 readings, in particular to exclude suspect extreme precipitation totals. Furthermore, an
3455 additional criterion of having less than 15% missing or excluded data per year was
3456 implemented, as detailed in section 3.2, to ensure use of reliable and representative
3457 data. In total, the data from 197 gauges, which fulfilled the quality control procedure
3458 (Blenkinsop *et al.*, 2017; Lewis *et al.*, 2018) and the additional record completion
3459 criteria (i.e. having less than 15% missing or excluded data per year) between 1992 –
3460 2014, have been employed in this research.

3461 The thesis motivations, aims, and objectives were discussed in Chapter 1, and
3462 indicated a substantial need to quantify the frequency and intensity of sub-daily
3463 extreme precipitation in the UK. This was justified by the recent short, intense
3464 precipitation generated floods and the contrasting characteristics of sub-daily and daily
3465 precipitation extremes (e.g. in terms of frequency, seasonality, processes).
3466 Furthermore, the existing urban drainage design guidelines are based on daily and
3467 multi-day precipitation extremes, and using these guidelines to assess the short
3468 intense events might provide imprecise results. Moreover, climate models expect sub-
3469 daily precipitation extremes to increase at a rate exceeding that for daily extremes.
3470 This could lead to increased flooding, especially in urbanised areas.

3471 However, and despite the importance of investigating sub-daily extreme events,
3472 relatively few studies have investigated observed sub-daily extremes compared to
3473 daily extremes due to data scarcity, while using climate models to derive projections of
3474 sub-daily extremes is computationally expensive. Thus, statistical downscaling and
3475 modelling of hourly precipitation extremes in the UK are suggested as alternatives to

3476 characterise sub-daily extremes and estimate return levels, providing the information
3477 necessary to update infrastructure design guidelines, and implement adaptation plans.

3478 In Chapter 2, a comprehensive review of the existing literature and the latest studies
3479 related to daily and sub-daily extreme precipitation were reported. The chapter
3480 reviewed a wide range of studies which employed various approaches to investigate
3481 mean and extreme precipitation characteristics on daily timescales, and related
3482 climatic drivers in the UK. Daily mean precipitation has shown seasonally varying
3483 trends, with an increasing trend in winter, decreasing in summer, and mixed non-
3484 significant trends in autumn and spring (Gregory *et al.*, 1991; Alexander and Jones,
3485 2000; Osborn *et al.*, 2000; Jones *et al.*, 2013). Furthermore, studies on daily timescales
3486 have indicated increases in the intensity of winter precipitation extremes, while
3487 increasing frequencies of summer extreme precipitation have been observed (Fowler
3488 and Kilsby, 2003b; Jones *et al.*, 2013; Simpson and Jones, 2014). In addition,
3489 analysing daily precipitation in the UK indicated a noticeable seasonality, especially for
3490 extremes.

3491 Daily extremes have been investigated using point of interest and regional approaches.
3492 In the UK, the Flood Studies Report (FSR) (NERC, 1975) followed by the Flood
3493 Estimation Handbook (FEH) (Faulkner, 1999) have been used to estimate precipitation
3494 and flood frequency on-site, while the HadUKP regions (Alexander and Jones, 2000)
3495 have been used for regional analysis. On-site approaches provide a reliable estimate
3496 for mean precipitation, whereas, the regional frequency approach provides a more
3497 accurate estimate for extremes, with the benefit of using regionally pooled data,
3498 reducing the impact of missing and erroneous values, and facilitating the evaluation of
3499 ungauged locations (Alexander and Jones, 2000). Nevertheless, a recent investigation
3500 of the efficacy of the HadUKP regions by Jones *et al.* (2014), indicated that these
3501 regions are not appropriate for use with extremes even, on daily timescales. Thus, new
3502 regions were developed to assess daily extreme precipitation in the UK (Jones *et al.*,
3503 2014). In contrast, relatively few studies have investigated sub-daily precipitation
3504 extremes in the UK, due to short and poor quality data records (Westra *et al.*, 2013;
3505 Blenkinsop *et al.*, 2018), although there is a strong association with flash floods (Dale
3506 *et al.*, 2017).

3507 Thus, an exploratory analysis of annual maxima (AMAX) of hourly and multi-hourly (i.e.
3508 3-, 6-, 12-, and 24-hr) extreme precipitation accumulations in the UK was carried out
3509 in Chapter 3. Using the regional frequency analysis approach, the seasonality and

3510 diurnal cycle were investigated. The findings indicated a noticeable peak in the
3511 frequency of short-duration extremes (i.e. 1- and 3-hr) between 1400 and 1700,
3512 especially in the southern UK, which is in line with results from (Xiao et al., 2018). This
3513 peak indicates a strong relation with convection-generating mechanisms, especially in
3514 southern UK regions. Furthermore, the results showed a difference in the seasonality
3515 of short-duration (i.e. 1- and 3-hr) and long-duration precipitation extremes (i.e. 12- and
3516 24-hr). Short-duration extremes occur mostly in summer, while long-duration extremes
3517 occur throughout late autumn and winter. This study is the first to quantify and compare
3518 the seasonality of hourly, multi-hourly, and daily (i.e. 3-, 6-, 12-, and 24-hr) extreme
3519 precipitation accumulations in the UK, and to extend the limited analysis of subdaily
3520 extremes by Blenkinsop *et al.* (2017) (Objective 1). Further, regional hourly return level
3521 estimates across the UK were calculated by fitting both the Generalized Extreme Value
3522 (GEV) and Generalized Pareto (GP) distributions, using the existing daily extreme
3523 regions of Jones *et al.* (2014). The results showed higher return level estimates for
3524 southern regions compared with other parts of the UK. In addition, the return estimates
3525 for the 24-hr extremes and daily extremes from (Jones *et al.*, 2013) showed similar
3526 results, which indicates the accuracy and reliability of the hourly used data. However,
3527 the hourly return level estimates indicated some similarity across regions with no
3528 significant differences. Moreover, hourly and daily precipitation extremes in the UK
3529 demonstrate a noticeable spatial variation in occurrence patterns and frequency.
3530 Combined, these suggest that new and potentially fewer representative regions would
3531 adequately reflect the spatial variation of UK short-duration precipitation extremes.
3532 This study is the first to introduce a formal assessment of hourly UK extreme
3533 precipitation using extreme value theory (EVT) and the existing daily extreme regions
3534 (Objectives 2 and 4).

3535 Accordingly, new hourly UK extreme precipitation regions were defined in Chapter 4.
3536 The new regions were developed using the quality controlled hourly dataset and
3537 various extreme precipitation indices (e.g. annual 0.99 quantile, median of AMAX
3538 precipitation), geographical and topographical characteristics (i.e. latitude, longitude,
3539 elevation), rotated seasonal statistics, temperature, and weather types reflecting
3540 atmospheric and large circulations.

3541 The five new hourly extreme precipitation regions fulfil the regional homogeneity
3542 requirements (Hosking and Wallis, 2005), while the regional delineation indicates a
3543 strong relation with the large-scale atmospheric circulation and local conditions. In

3544 addition to that, the developed regions show a clear east-west delineation in the UK,
3545 which is in line with the daily extreme precipitation regions reported by Jones *et al.*
3546 (2014) and indicate the important role of orography and the prevailing westerly winds
3547 in also characterising hourly precipitation extremes. The new regions are the first to be
3548 developed based on hourly extreme precipitation in the UK, and to reflect their spatial
3549 variation. In addition, they can serve hydrologists, climatologists, and policy makers
3550 either for formal or indicative assessment of extreme precipitation return estimates and
3551 design guidelines (Objective 3). Thereafter, the new extreme regions were employed
3552 to quantify regional hourly precipitation extremes by estimating return levels across the
3553 UK regions using the GEV and GP distributions (i.e. EVT distributions). The return level
3554 maps indicated an increasing pattern from northwest towards southeast, which
3555 supports the reported UK hourly extreme precipitation climatology published in
3556 Blenkinsop *et al.* (2017).

3557 Moreover, the new hourly extreme precipitation regions were better able to capture
3558 variations in hourly extreme precipitation across the UK compared to the existing
3559 regions. For example, the fitted GEV and GP growth curves for the new regions
3560 indicated steeper curves in northern regions compared to southern regions. This is in
3561 contrast to growth curves for hourly precipitation extremes developed using the daily
3562 UK extreme regions (Jones *et al.*, 2014), which showed similar estimates of return level
3563 for all regions. Moreover, the results indicate the efficacy and potential capabilities of
3564 using the new regions for investigating extremes in the UK.

3565 Accordingly, the new hourly extreme precipitation regions were used in Chapter 5 to
3566 develop a statistical model simulating the frequency and intensity of UK hourly
3567 precipitation extremes. To start with, the statistical correlation between different
3568 climatological variables and hourly extremes were explored, where the results showed
3569 that local condition variables (e.g. Convective Available Potential Energy (CAPE), dew
3570 point temperature (DPT)) have a higher correlation compared to large-scale variables
3571 (e.g. North Atlantic oscillation (NAO), sea surface temperature (SST)) across the UK.
3572 Moreover, the results confirmed the role of local climatic variables, especially the
3573 hypothesised strong relation between hourly precipitation extremes and convection-
3574 generating mechanisms (Blenkinsop *et al.*, 2017; Darwish *et al.*, 2018). Furthermore,
3575 the correlation between hourly extremes and climatic variables in southern regions is
3576 higher than in northern regions, especially for temperature, convection (e.g. CAPE),
3577 and water vapour content (e.g. total column water vapour (TCWV)) variables, which

3578 indicates the strong relation between hourly extremes and local scale processes in
3579 southern parts of the UK.

3580 Thereafter, a statistical model was developed using the Poisson-GPD distribution
3581 approach, employing different potential driving climatological variables representing
3582 both the large-scale climatic circulation and local conditions. Investigating the
3583 correlation of hourly rainfall extremes with various climatological variables and
3584 employing them in the development of the model was an essential part of quantifying
3585 the behaviour of UK hourly extremes (Objectives 5 and 6).

3586 Using various model selection and evaluation techniques (e.g. Q-Q plots, AIC) to
3587 determine the best predictors, the results showed that employing the Julian day sine
3588 and cosine, the NAO, atmospheric pressure at 700hPa height (Z-700), and DPT in the
3589 Poisson model would best simulate hourly extreme precipitation frequency. In contrast,
3590 the GPD approach employing the Julian day sine and cosine, and the convective
3591 available potential energy (CAPE) best simulates hourly extreme precipitation
3592 intensity. This indicates that the occurrence of extremes has a strong relation to both
3593 large-scale circulation (i.e. NAO and Z-700) and local conditions (i.e. DPT), while
3594 intensity is controlled by local conditions of instability (i.e. CAPE). However, including
3595 the seasonality as a predictor is essential to simulate both the frequency and intensity,
3596 which is in line with the observed seasonality in UK hourly precipitation extremes. The
3597 resultant model is the first to simulate hourly extreme frequency and intensity reliably,
3598 and could serve as an indicative alternative to dynamical climate models, with
3599 noticeably lower computational demand (Objectives 4 and 6).

3600 Thereafter, the Poisson-GP statistical model was used to simulate hourly precipitation
3601 extremes in the UK under a simple scenario of potential climate change. The pseudo
3602 global warming (PGW) method (Kimura and Kitoh, 2007), and a scenario of 2°C
3603 increase in mean temperature as agreed in the Paris Agreement (Paris agreement,
3604 2015) was adopted to evaluate change to the 20-yr return level estimate. The results
3605 indicated that this scenario would lead to an increase in both the frequency and the
3606 intensity of hourly precipitation extremes across the UK (e.g. NW and SE regions).
3607 Moreover, the change in the frequency of hourly extremes showed that the increase in
3608 summer is higher than other seasons across the UK.

3609 However, intensity changes showed that the highest increase would occur in summer
3610 across the southern regions only, while the increase in northern regions would be

3611 comparable in all seasons. The future scenario indicated an increase between 13%-
3612 17% in the 20-yr return level estimates under a 2°C warming across the UK regions
3613 (e.g. NW and SE regions), which is slightly higher than the C-C scaling rate. On the
3614 other hand, existing urban drainage guidelines in the UK (e.g. DEFRA, 2012), which
3615 are based on daily precipitation data, suggest a climate uplift of 10% for 2025-2055.
3616 Thus, the results in this research suggest that existing guidelines for hourly
3617 precipitation extremes should be reviewed. This is in line with recent research by
3618 Kendon et al. (2018), where CPMs were used to project changes to future hourly
3619 precipitation extremes. The results suggested that hourly precipitation extremes will
3620 intensify at a rate higher than both the rate of increase of daily precipitation extremes
3621 and the suggested rates for existing guidelines in the UK.

3622 The results indicate that the developed model can capture the seasonality and spatial
3623 variation across the UK, and indicates comparable results to CPM projections, without
3624 the need for high computational requirements, through the demonstration of a very
3625 simple scenario approach. This model can be used to provide drainage authorities with
3626 a scenario or probabilistic decision making approach to address the potential changes
3627 in future precipitation.

3628 This research 3stationary EVT methods coupled with regional frequency analysis
3629 (RFA) and downscaled climatic variables to simulate hourly extreme precipitation
3630 frequency and intensity in the UK. In addition, a demonstration of its potential
3631 application to project potential changes under a climate warming scenario is presented
3632 (Objective 4 and 7).

3633 **6.2 Results in the context of the existing literature**

3634 Statistical modelling and downscaling have been adopted widely to simulate extreme
3635 precipitation characteristics. In this research, we aimed to quantify hourly extreme
3636 precipitation intensity and frequency in the UK to enhance the existing literature, and
3637 develop a model that is predictive but simple.

3638 The results in Chapter 3 presented the noticeable difference between hourly and daily
3639 precipitation extremes in terms of frequency and intensity patterns. These results
3640 indicate that existing approaches of using the scaling relation or simple disaggregation
3641 to simulate sub-daily extremes from daily extremes (e.g. UKCP09) might be
3642 misleading, while updated hourly extreme precipitation return estimates and urban
3643 drainage design guidelines should be developed for sub-daily precipitation. Similarly,

3644 Kendon et al. (2018) indicated that changes in sub-daily precipitation extremes would
3645 emerge sooner than daily extremes, while sub-daily precipitation rates (i.e. intensity)
3646 rather than daily accumulations should be evaluated to determine the impacts of
3647 extremes. Moreover, Dale et al. (2017) reported similar results, and indicated that
3648 existing guidelines are not designed to be applied to sub-daily precipitation. The results
3649 presented in Chapter 3 support the fact that quantifying the nature of hourly and multi-
3650 hourly extremes in the UK enhances our understanding of current extreme patterns,
3651 diurnal cycle, and seasonality in the UK. All these are within the scope of the INTENSE
3652 project (Blenkinsop et al., 2018) that is currently investigating sub-daily extremes to
3653 quantify observed historical changes and characterise sub-daily extremes on a
3654 broader, global scale.

3655 Importantly, the newly defined hourly extreme regions in Chapter 4 are the first to
3656 employ the weather patterns of (Neal *et al.*, 2016), besides extreme precipitation
3657 indices, to delineate precipitation regions in the UK. The new regions outperform the
3658 existing daily mean (Alexander and Jones, 2000) and extreme (Jones *et al.*, 2014)
3659 regions in evaluating the return estimates and growth curves for hourly extremes.
3660 Additionally, they can be employed to estimate growth curves either using the single
3661 largest event per year (AMAX) or using precipitation over a selected threshold (POT).
3662 Moreover, existing urban drainage design guidelines focus on the single largest event
3663 per year, which might not be adequate for planning in regions under multiple
3664 consecutive intense events, particularly with climate change. Thus using the new
3665 regions provides the capability of using and comparing both approaches: AMAX and
3666 POT. It is paramount that policy makers should consider embedding both approaches
3667 in practice. Additionally, employing weather patterns in the prediction of hydrological
3668 events is well established in the literature (Vuillaume and Herath, 2017), and in this
3669 research we showed the potential of using these to reflect the relationship between
3670 large-scale atmospheric variables and hourly extreme precipitation in the UK.

3671 Thereafter, the statistical model developed in Chapter 5, which simulates the
3672 frequency and intensity of hourly extreme precipitation in the UK could enhance
3673 ongoing research by helping to evaluate the performance of convection-permitting
3674 models (CPMs). The statistical model indicated the potential of simulating the
3675 frequency of extremes using large-scale variables (e.g. NAO, Z-700), which would
3676 allow effective targeting of CPM downscaling simulations. Recently, Chan *et al.*
3677 (2018b) employed large-scale and other variables to quantify the regression

3678 relationship between the occurrence of extreme hourly precipitation events and vertical
3679 stability and circulation predictors in the southern UK 1.5km resolution CPM, finding
3680 similar predictors were of importance in model simulations.

3681 However, the results presented in this thesis are based on a limited precipitation record
3682 (i.e. 23 years). Providing robust quantitative estimates of the future frequency of such
3683 extremes are essential to implement adaptation planning. Thus, the statistical model
3684 developed in this study can be employed alongside the improvements in CPM
3685 simulations to, for example, create an ensemble of observational and modelling based
3686 predictions. Additionally, it could be employed to improve existing UK climate
3687 projections (e.g. as part of UKCP18), as part of improving sub-daily modelling
3688 capabilities (e.g. in projects such as INTENSE), or more widely as part of coordinated
3689 regional climate multi-model downscaling projects (e.g. CORDEX-FPS).

3690 Moreover, the statistical model showed a strong relation between convective
3691 conditions and hourly precipitation extremes with CAPE employed to simulate extreme
3692 precipitation intensities. These results can be incorporated into ongoing research into
3693 the roles of local thermodynamics and large-scale atmospheric circulation as drivers
3694 of changes in intense precipitation through linking observational analyses with those
3695 based on CPMs. The statistical model, using CAPE among other predictors, estimated
3696 an intensity increase of between 13%-17% under a simple 2°C warming scenario,
3697 which slightly exceeds the C-C relationship and agrees with the approximate C-C
3698 scaling found by Blenkinsop *et al.* (2015) for UK hourly observations and the scaling
3699 rate obtained from a CPM by Chan *et al.* (2016) for the southern UK.

3700 In meeting each of the objectives outlined in Chapter 1 of this thesis, the results
3701 presented here add to our knowledge of extreme precipitation in the UK. The observed
3702 hourly extreme precipitation climatology, regional growth curves, and statistical model
3703 indicate a noticeable seasonality and an increase in summer extremes with
3704 thermodynamic warming, which are consistent with future projections from dynamical
3705 climate models. Importantly, the statistical model did not assume stationarity when
3706 estimating the model parameters which is a common assumption with methods used
3707 to create the current hydrological and drainage guidelines in Europe. Thus, the
3708 statistical model could be used together with estimates of change in the model
3709 predictors from climate models to help provide robust quantitative estimates and
3710 enhance the existing literature to implement and develop the required adaptation and
3711 design guidelines under a warming climate.

3712 **6.3 Future work**

3713 Considering the nature of extreme precipitation, and the wide range of uncertainties
3714 associated with their patterns and behaviour, this research could be enhanced in
3715 several ways, to achieve a better understanding of sub-daily precipitation extremes
3716 and to employ the results further to improve the existing literature and hydrological
3717 application in practice.

3718 **6.3.1 Data collection**

3719 In this research, hourly extreme precipitation was investigated using 197 gauges
3720 across the UK representing extremes between 1992 and 2014 (i.e. only 23 years). The
3721 limited data range was necessary to ensure having a complete and representative
3722 record of hourly extremes. However, this short record was reflected in the relatively
3723 wide confidence intervals in the estimated regional growth curves, especially in regions
3724 with limited rain gauges. Furthermore, most of the hourly precipitation data in the UK
3725 is accumulated from tipping bucket data, thus, future work could include improvements
3726 in data collection and exploring the use of different datasets (e.g. gauges, radar, and
3727 satellite data). The analysis should then be expanded to include the newly collected
3728 data, which would add further value to the hourly extreme precipitation analysis.
3729 Recent research has achieved a notable advance in sub-daily precipitation data
3730 collection and quality control across the UK (e.g. Blenkinsop et al., 2017; Lewis et al.,
3731 2018), and future plans would suggest the use of the gridded dataset (Lewis *et al.*,
3732 2018) and historical UK precipitation archive (Rodda et al., 2009) , which would
3733 facilitate the assessment of ungauged locations.

3734 **6.3.2 Seasonal assessment**

3735 This study found noticeable seasonality in hourly extreme precipitation, which is in line
3736 with the existing literature that has studied extremes, either using observations or
3737 climate models. The results illustrated a visible peak in occurrence for hourly extremes
3738 in summer, in particular for the southern UK. Investigating extreme precipitation in each
3739 season using the same dataset used in this research would limit the data availability
3740 per season. Thus, future research should take the advantage of the advancement in
3741 data collection to investigate hourly precipitation extremes seasonally using both
3742 AMAX and POT approaches, which may reflect the characteristics of extremes more
3743 closely.

3744 **6.3.3 Statistical model transferability**

3745 The statistical model in this research (Chapter 5) was developed at the centroid of the
3746 defined homogeneous regions (Chapter 4), to facilitate the consideration of different
3747 climatological variables (e.g. NAO, DPT, CAPE), which were used as predictors. The
3748 regions homogeneity was tested and indicated similar hourly extreme precipitation
3749 patterns across each region, with marginal spatial variation. The model used regionally
3750 pooled hourly precipitation data, which increases the reliability of the model and
3751 reduces the impact of spatial variation but does not necessarily allow robust local
3752 estimates. Therefore, further investigation could include determining the scaling
3753 relation between hourly precipitation extremes and the predictor variables at individual
3754 locations, to implement and transfer the model in various locations across each region.

3755 **6.3.4 Comparison with existing approaches**

3756 In this research, developing new hourly extreme precipitation regions was motivated
3757 by the inadequacy of the existing daily extreme precipitation regions to capture the
3758 spatial and temporal variation in hourly extremes across the UK. The new regions
3759 employed different extremes and indices in their construction than their daily
3760 counterparts, with the novel use of European weather patterns to delineate the new
3761 regions and provided more reliable estimates compared to existing regional
3762 assessment approaches in the UK (e.g. Alexander and Jones, 2000; Jones *et al.*,
3763 2014). However, future work could include a comparison with existing on-site, station-
3764 centred return level estimate approaches (e.g. FEH) to augment our understanding
3765 about the impact of data scarcity in the regionalisation approach, and to provide a tool
3766 to improve and validate the current hourly extreme precipitation regions.

3767 **6.3.5 Urbanised area adaptation plans**

3768 The defined extreme regions reflect hourly extreme precipitation on a regional scale
3769 and can be used to estimate growth curves at different locations by using the scaling
3770 relation between the hourly extreme precipitation regional median (RMed) and the
3771 gauge median as described in Chapter 4. However, in urbanised areas, where short,
3772 intense precipitation is associated with flash flooding which poses a significant threat
3773 to lives and infrastructure, further investigation should be conducted to feed this
3774 information into effective adaptation plans. Future research could build on this study to
3775 assess the impact of climate change on return level estimates for different durations
3776 and return periods using the outputs of current state-of-the-art climate models to

3777 provide the predictors. Moreover, this research might be used in conjunction with the
3778 UK future projections (e.g. UKCP18) to provide decision makers an insight of potential
3779 impact across the urbanised areas.

3780

3781

3782

3783

3784

3785

3786

3787

3788

3789

3790

3791

3792

3793

3794

3795

3796

3797

3798

3799

3800

3801

3802

3803

3804

References

- 3806 Acero, F.J., García, J.A. and Gallego, M.C. (2011) 'Peaks-over-threshold study of trends in extreme
3807 rainfall over the Iberian Peninsula', *Journal of Climate*, 24(4), pp. 1089-1105.
- 3808 AghaKouchak, A. and Nasrollahi, N. (2010) 'Semi-parametric and parametric inference of extreme
3809 value models for rainfall data', *Water resources management*, 24(6), pp. 1229-1249.
- 3810 Akaike, H. (1981) 'Likelihood of a model and information criteria', *Journal of econometrics*, 16(1), pp.
3811 3-14.
- 3812 Akaike, H. (1992) 'Information theory and an extension of the maximum likelihood principle', in
3813 *Breakthroughs in statistics*. Springer, pp. 610-624.
- 3814 Alexander, L.V. (2016) 'Global observed long-term changes in temperature and precipitation
3815 extremes: A review of progress and limitations in IPCC assessments and beyond', *Weather and
3816 Climate Extremes*, 11(Supplement C), pp. 4-16.
- 3817 Alexander, L.V. and Arblaster, J.M. (2009) 'Assessing trends in observed and modelled climate
3818 extremes over Australia in relation to future projections', *International Journal of Climatology: A
3819 Journal of the Royal Meteorological Society*, 29(3), pp. 417-435.
- 3820 Alexander, L.V. and Jones, P.D. (2000) 'Updated precipitation series for the UK and discussion of
3821 recent extremes', *Atmospheric science letters*, 1(2), pp. 142-150.
- 3822 Alexander, L.V., Zhang, X., Peterson, T.C., Caesar, J., Gleason, B., Klein Tank, A.M.G., Haylock, M.,
3823 Collins, D., Trewin, B., Rahimzadeh, F., Tagipour, A., Rupa Kumar, K., Revadekar, J., Griffiths, G.,
3824 Vincent, L., Stephenson, D.B., Burn, J., Aguilar, E., Brunet, M., Taylor, M., New, M., Zhai, P., Rusticucci,
3825 M. and Vazquez-Aguirre, J.L. (2006) 'Global observed changes in daily climate extremes of
3826 temperature and precipitation', *Journal of Geophysical Research: Atmospheres*, 111(D05109).
- 3827 Ali, H., Fowler, H.J. and Mishra, V. (2018) 'Global Observational Evidence of Strong Linkage Between
3828 Dew Point Temperature and Precipitation Extremes', *Geophysical Research Letters*, 45(22), pp.
3829 12,320-12,330.
- 3830 Ali, H. and Mishra, V. (2017) 'Contrasting response of rainfall extremes to increase in surface air and
3831 dewpoint temperatures at urban locations in India', *Scientific reports*, 7(1), p. 1228.
- 3832 Allan, R., Tett, S. and Alexander, L. (2009) 'Fluctuations in autumn–winter severe storms over the
3833 British Isles: 1920 to present', *International Journal of Climatology*, 29(3), pp. 357-371.
- 3834 Allan, R.P. and Soden, B.J. (2008) 'Atmospheric Warming and the Amplification of Precipitation
3835 Extremes', *Science*, 321(5895), pp. 1481-1484.
- 3836 Allen, M.R. and Ingram, W.J. (2002) 'Constraints on future changes in climate and the hydrologic
3837 cycle', *Nature*, 419(6903), pp. 224-232.
- 3838 Anagnostopoulou, C. and Tolika, K. (2012) 'Extreme precipitation in Europe: statistical threshold
3839 selection based on climatological criteria', *Theoretical and applied climatology*, 107(3-4), pp. 479-
3840 489.
- 3841 Archer, D.R. and Fowler, H.J. (2018) 'Characterising flash flood response to intense rainfall and
3842 impacts using historical information and gauged data in Britain', *Journal of Flood Risk Management*,
3843 11, pp. S121-S133.
- 3844 Archer, D.R., Parkin, G. and Fowler, H.J. (2017) 'Assessing long term flash flooding frequency using
3845 historical information', *Hydrology Research*, 48(1), pp. 1-16.
- 3846 Arnbjerg-Nielsen, K., Willems, P., Olsson, J., Beecham, S., Pathirana, A., Gregersen, I.B., Madsen, H.
3847 and Nguyen, V.T.V. (2013) 'Impacts of climate change on rainfall extremes and urban drainage
3848 systems: a review', *Water Science and Technology*, 68(1), pp. 16-28.
- 3849 Arnell, N.W. and Gosling, S.N. (2016) 'The impacts of climate change on river flood risk at the global
3850 scale', *Climatic Change*, 134(3), pp. 387-401.
- 3851 Arnone, E., Pumo, D., Viola, F., Noto, L.V. and La Loggia, G. (2013) 'Rainfall statistics changes in Sicily',
3852 *Hydrology and Earth System Sciences*, 17(7), pp. 2449-2458.
- 3853 Barbero, R., Fowler, H.J., Lenderink, G. and Blenkinsop, S. (2017) 'Is the intensification of
3854 precipitation extremes with global warming better detected at hourly than daily resolutions?',
3855 *Geophysical Research Letters*, 44(2), pp. 974-983.
- 3856 Barry, R.G. and Chorley, R.J. (2009) *Atmosphere, weather and climate*. Routledge.

3857 Beckmann, B.R. and Adri Buishand, T. (2002) 'Statistical downscaling relationships for precipitation in
3858 the Netherlands and North Germany', *International Journal of Climatology*, 22(1), pp. 15-32.

3859 Benestad, R.E. (2007) 'Novel methods for inferring future changes in extreme rainfall over Northern
3860 Europe', *Climate Research*, 34(3), pp. 195-210.

3861 Benestad, R.E. (2010) 'Downscaling precipitation extremes', *Theoretical and Applied Climatology*,
3862 100(1-2), pp. 1-21.

3863 Bennett, L.J., Browning, K.A., Blyth, A.M., Parker, D.J. and Clark, P.A. (2006) 'A review of the initiation
3864 of precipitating convection in the United Kingdom', *Quarterly Journal of the Royal Meteorological
3865 Society: A journal of the atmospheric sciences, applied meteorology and physical oceanography*,
3866 132(617), pp. 1001-1020.

3867 Berg, P. and Haerter, J.O. (2013) 'Unexpected increase in precipitation intensity with temperature—A
3868 result of mixing of precipitation types?', *Atmospheric Research*, 119, pp. 56-61.

3869 Bissolli, P. and Dittmann, E. (2001) *The objective weather type classification of the German Weather
3870 Service and its possibilities of application to environmental and meteorological investigations*.

3871 Blackburn, M., Methven, J. and Roberts, N. (2008) 'Large-scale context for the UK floods in summer
3872 2007', *Weather*, 63(9), pp. 280-288.

3873 Blenkinsop, S., Chan, S.C., Kendon, E.J., Roberts, N.M. and Fowler, H.J. (2015) 'Temperature
3874 influences on intense UK hourly precipitation and dependency on large-scale circulation',
3875 *Environmental Research Letters*, 10(5), p. 054021.

3876 Blenkinsop, S. and Fowler, H. (2013) *Vulnerability, Uncertainty, and Risk@ sQuantification,
3877 Mitigation, and Management*. ASCE.

3878 Blenkinsop, S., Fowler, H.J., Barbero, R., Chan, S.C., Guerreiro, S.B., Kendon, E., Lenderink, G., Lewis,
3879 E., Li, X.-F. and Westra, S. (2018) 'The INTENSE project: using observations and models to understand
3880 the past, present and future of sub-daily rainfall extremes', *Advances in Science and Research*, 15, pp.
3881 117-126.

3882 Blenkinsop, S., Lewis, E., Chan, S.C. and Fowler, H.J. (2017) 'Quality-control of an hourly rainfall
3883 dataset and climatology of extremes for the UK', *International Journal of Climatology*, 37(2), pp. 722-
3884 740.

3885 Brown, S., Boorman, P., Buonomo, E., Burke, E., Caesa, J., Clark, R., McDonald, R. and Perry, M.
3886 (2008) *Extremes atlas: A climatology of extremes for the UK. A baseline for UKCP09*. The Met Office,
3887 H.C. [Online]. Available at:
3888 <http://ukclimateprojections.metoffice.gov.uk/media.jsp?mediaid=87920&filetype=pdf>.

3889 Brown, S.J. (2018) 'The drivers of variability in UK extreme rainfall', *International Journal of
3890 Climatology*, 38(S1), pp. e119-e130.

3891 Brunson, C., McClatchey, J. and Unwin, D.J. (2001) 'Spatial variations in the average rainfall–altitude
3892 relationship in Great Britain: an approach using geographically weighted regression', *International
3893 Journal of Climatology: A Journal of the Royal Meteorological Society*, 21(4), pp. 455-466.

3894 Burn, D.H., Mansour, R., Zhang, K. and Whitfield, P.H. (2011) 'Trends and variability in extreme
3895 rainfall events in British Columbia', *Canadian Water Resources Journal*, 36(1), pp. 67-82.

3896 Burnham, K.P. and Anderson, D.R. (2003) *Model selection and multimodel inference: a practical
3897 information-theoretic approach*. Springer Science & Business Media.

3898 Burt, S. (2005) 'Cloudburst upon Hendraburnick down: the Boscastle storm of 16 August 2004',
3899 *Weather*, 60(8), pp. 219-227.

3900 Burt, T.P. and Ferranti, E.J.S. (2012) 'Changing patterns of heavy rainfall in upland areas: a case study
3901 from northern England', *International Journal of Climatology*, 32(4), pp. 518-532.

3902 Burt, T.P., Jones, P.D. and Howden, N.J.K. (2014) 'An analysis of rainfall across the British Isles in the
3903 1870s', *International Journal of Climatology*.

3904 CCRA (2017) *UK Climate Change Risk Assessment 2017*. London, UK. [Online]. Available at:
3905 [https://assets.publishing.service.gov.uk/government/uploads/system/uploads/attachment_data/file/
3906 /584281/uk-climate-change-risk-assess-2017.pdf](https://assets.publishing.service.gov.uk/government/uploads/system/uploads/attachment_data/file/584281/uk-climate-change-risk-assess-2017.pdf) (Accessed: 02/02/2019).

3907 Champion, A.J., Allan, R.P. and Lavers, D.A. (2015) 'Atmospheric rivers do not explain UK summer
3908 extreme rainfall', *Journal of Geophysical Research: Atmospheres*, 120(14), pp. 6731-6741.

3909 Chan, S.C., Kahana, R., Kendon, E.J. and Fowler, H.J. (2018a) 'Projected changes in extreme
3910 precipitation over Scotland and Northern England using a high-resolution regional climate model',
3911 *Climate Dynamics*, pp. 1-19.

3912 Chan, S.C., Kendon, E.J., Fowler, H.J., Blenkinsop, S., Ferro, C.A.T. and Stephenson, D.B. (2013) 'Does
3913 increasing the spatial resolution of a regional climate model improve the simulated daily
3914 precipitation?', *Climate dynamics*, 41(5-6), pp. 1475-1495.

3915 Chan, S.C., Kendon, E.J., Fowler, H.J., Blenkinsop, S. and Roberts, N.M. (2014a) 'Projected increases in
3916 summer and winter UK sub-daily precipitation extremes from high-resolution regional climate
3917 models', *Environmental Research Letters*, 9(8), p. 084019.

3918 Chan, S.C., Kendon, E.J., Fowler, H.J., Blenkinsop, S., Roberts, N.M. and Ferro, C.A. (2014b) 'The value
3919 of high-resolution Met Office regional climate models in the simulation of multihourly precipitation
3920 extremes', *Journal of Climate*, 27(16), pp. 6155-6174.

3921 Chan, S.C., Kendon, E.J., Roberts, N., Blenkinsop, S. and Fowler, H.J. (2018b) 'Large-scale predictors
3922 for extreme hourly precipitation events in convection-permitting climate simulations', *Journal of
3923 Climate*, 31(6), pp. 2115-2131.

3924 Chan, S.C., Kendon, E.J., Roberts, N.M., Blenkinsop, S. and H.J., F. (2017) 'Synoptic predictors for
3925 extreme hourly precipitation events in convection-permitting climate simulations', *Journal of
3926 Climate*.

3927 Chan, S.C., Kendon, E.J., Roberts, N.M., Fowler, H.J. and Blenkinsop, S. (2016) 'The characteristics of
3928 summer sub-hourly rainfall over the southern UK in a high-resolution convective permitting model',
3929 *Environmental Research Letters*, 11(9), p. 094024.

3930 Chandler, R.E. and Wheeler, H.S. (2002) 'Analysis of rainfall variability using generalized linear
3931 models: a case study from the west of Ireland', *Water Resources Research*, 38(10), pp. 10-1-10-11.

3932 Chang, C.-P., Lei, Y., Sui, C.-H., Lin, X. and Ren, F. (2012) 'Tropical cyclone and extreme rainfall trends
3933 in East Asian summer monsoon since mid-20th century', *Geophysical Research Letters*, 39(18), pp.
3934 n/a-n/a.

3935 Chatterton, J., Viavattene, C., Morris, J., Penning-Rowsell, E.C. and Tapsell, S.M. (2010) 'The costs of
3936 the summer 2007 floods in England'.

3937 Cheng, L., AghaKouchak, A., Gilleland, E. and Katz, R.W. (2014) 'Non-stationary extreme value
3938 analysis in a changing climate', *Climatic change*, 127(2), pp. 353-369.

3939 Chung, E.-S., Soden, B., Sohn, B.J. and Shi, L. (2014) 'Upper-tropospheric moistening in response to
3940 anthropogenic warming', *Proceedings of the National Academy of Sciences*, 111(32), pp. 11636-
3941 11641.

3942 CIWEM (2016) *Rainfall Modelling Guide*. London: Urban Drainage Group- Chartered Institute of
3943 Water and Environmental Management, Urban Drainage Group-Chartered Institute of Water and
3944 Environmental Management. [Online]. Available at: [http://www.ciwem.org/wp-
3945 content/uploads/2016/03/CIWEM-UDG-Rainfall-Guide-2016.pdf](http://www.ciwem.org/wp-content/uploads/2016/03/CIWEM-UDG-Rainfall-Guide-2016.pdf) (Accessed: 22 July 2017).

3946 Clark, P.U., Weaver, A.J., Brook, E., Cook, E.R., Delworth, T.L. and Steffen, K. (2008) 'Abrupt Climate
3947 Change. A report by the US Climate Change Science Program and the Subcommittee on Global
3948 Change Research', *US Geological Survey, Reston, VA*.

3949 Coles, S., Bawa, J., Trenner, L. and Dorazio, P. (2001) *An introduction to statistical modeling of
3950 extreme values*. Springer.

3951 Collins, M., Knutti, R., Arblaster, J., Dufresne, J.L., Fichet, T., Friedlingstein, P., Gao, X., Gutowski,
3952 W.J., Johns, T. and Krinner, G. (2013) 'Long-term climate change: projections, commitments and
3953 irreversibility'.

3954 Colman, A. (1997) 'Prediction of summer central England temperature from preceding North Atlantic
3955 winter sea surface temperature', *International Journal of Climatology: A Journal of the Royal
3956 Meteorological Society*, 17(12), pp. 1285-1300.

3957 Condon, L.E., Gangopadhyay, S. and Pruitt, T. (2015) 'Climate change and non-stationary flood risk for
3958 the upper Truckee River basin', *Hydrology and Earth System Sciences*, 19(1), pp. 159-175.

3959 Cong, R.-G. and Brady, M. (2012) 'The interdependence between rainfall and temperature: copula
3960 analyses', *The Scientific World Journal*, 2012.

- 3961 Conway, D., Wilby, R.L. and Jones, P.D. (1996) 'Precipitation and air flow indices over the British Isle',
3962 *Climate Research*, 7(2), pp. 169-183.
- 3963 Cropper, T., Hanna, E., Valente, M.A. and Jónsson, T. (2015) 'A daily Azores–Iceland North Atlantic
3964 Oscillation index back to 1850', *Geoscience Data Journal*, 2(1), pp. 12-24.
- 3965 Cyril, M., Humphrey, L., Keith, B., John, N., Nigel, R., Peter, C., Andrew, R. and Alan, B. (2007)
3966 'Combination of Mesoscale and Synoptic Mechanisms for Triggering an Isolated Thunderstorm:
3967 Observational Case Study of CSIP IOP 1', *Monthly Weather Review*, 135(11), pp. 3728-3749.
- 3968 Dale, M. (2005) 'Impact of climate change on UK flooding and future predictions', *Proceedings of the
3969 ICE-Water Management*, 158(4), pp. 135-140.
- 3970 Dale, M., Luck, B., Fowler, H.J., Blenkinsop, S., Gill, E., Bennett, J., Kendon, E. and Chan, S. (2017)
3971 'New climate change rainfall estimates for sustainable drainage', *Proceedings of the Institution of Civil
3972 Engineers - Engineering Sustainability*, 170(4), pp. 214-224.
- 3973 Dales, M.Y. and Reed, D.W. (1989) *Regional flood and storm hazard assessment*. Institute of
3974 Hydrology.
- 3975 Darwish, M., Fowler, H.J., Blenkinsop, S. and Tye, M.R. (2018) 'A regional frequency analysis of UK
3976 sub-daily extreme precipitation and assessment of their seasonality', *International Journal of
3977 Climatology*, 38(13), pp. 4758–4776.
- 3978 Davison, A.C. and Huser, R. (2015) 'Statistics of extremes', *Annual Review of Statistics and its
3979 Application*, 2, pp. 203-235.
- 3980 de Leeuw, J., Methven, J. and Blackburn, M. (2016) 'Variability and trends in England and Wales
3981 precipitation', *International Journal of Climatology*, 36(8), pp. 2823-2836.
- 3982 Dee, D.P., Uppala, S.M., Simmons, A.J., Berrisford, P., Poli, P., Kobayashi, S., Andrae, U., Balmaseda,
3983 M.A., Balsamo, G. and Bauer, d.P. (2011) 'The ERA-Interim reanalysis: Configuration and performance
3984 of the data assimilation system', *Quarterly Journal of the royal meteorological society*, 137(656), pp.
3985 553-597.
- 3986 DEFRA (2012) *The UK climate change risk assessment 2012 evidence report*.
- 3987 Defra, U.K. (2017) *UK Climate Change Risk Assessment 2017*. London, UK: Department for
3988 Environment, Food & Rural Affairs,
- 3989 . [Online]. Available at: www.gov.uk/government/publications.
- 3990 Demirdjian, L., Zhou, Y. and Huffman, G.J. (2018) 'Statistical Modeling of Extreme Precipitation with
3991 TRMM Data', *Journal of Applied Meteorology and Climatology*, 57(1), pp. 15-30.
- 3992 Dittrich, R., Wreford, A. and Moran, D. (2016) 'A survey of decision-making approaches for climate
3993 change adaptation: Are robust methods the way forward?', *Ecological Economics*, 122, pp. 79-89.
- 3994 Dobler, C., Bürger, G. and Stötter, J. (2013) 'Simulating future precipitation extremes in a complex
3995 Alpine catchment', *Natural Hazards and Earth System Sciences*, 13(2), pp. 263-277.
- 3996 Donat, M.G., Alexander, L.V., Yang, H., Durre, I., Vose, R., Dunn, R.J.H., Willett, K.M., Aguilar, E.,
3997 Brunet, M. and Caesar, J. (2013) 'Updated analyses of temperature and precipitation extreme indices
3998 since the beginning of the twentieth century: The HadEX2 dataset', *Journal of Geophysical Research:
3999 Atmospheres*, 118(5), pp. 2098-2118.
- 4000 Donat, M.G., Lowry, A.L., Alexander, L.V., O'Gorman, P.A. and Maher, N. (2017) 'Addendum: More
4001 extreme precipitation in the world's dry and wet regions', *Nature Climate Change*, 7(2), pp. 154-158.
- 4002 Durrans, S.R. and Kirby, J.T. (2004) 'Regionalization of extreme precipitation estimates for the
4003 Alabama rainfall atlas', *Journal of Hydrology*, 295(1-4), pp. 101-107.
- 4004 Durre, I., Williams, C.N., Yin, X. and Vose, R.S. (2009) 'Radiosonde-based trends in precipitable water
4005 over the Northern Hemisphere: An update', *Journal of Geophysical Research: Atmospheres (1984–
4006 2012)*, 114(D5).
- 4007 Eder, B.K. (1989) 'A principal component analysis of SO₂– 4 precipitation concentrations over the
4008 eastern United States', *Atmospheric Environment (1967)*, 23(12), pp. 2739-2750.
- 4009 Environment Agency (2014) *Flood and coastal erosion risk management. Long-term investment
4010 scenarios (LTIS) 2014*. Environment Agency, Bristol, UK.
- 4011 Esteban, P., Martin-Vide, J. and Mases, M. (2006) 'Daily atmospheric circulation catalogue for
4012 Western Europe using multivariate techniques', *International Journal of Climatology: A Journal of the
4013 Royal Meteorological Society*, 26(11), pp. 1501-1515.

4014 Faulkner, D. (1999) *Flood estimation handbook, volume 2: Rainfall frequency estimation*. United
4015 Kingdom: Institute of Hydrology Wallingford.

4016 Fereday, D., Chadwick, R., Knight, J. and Scaife, A.A. (2018) 'Atmospheric Dynamics is the Largest
4017 Source of Uncertainty in Future Winter European Rainfall', *Journal of Climate*, 31(3), pp. 963-977.

4018 Ferro, C.A.T. and Segers, J. (2003) 'Inference for clusters of extreme values', *Journal of the Royal
4019 Statistical Society: Series B (Statistical Methodology)*, 65(2), pp. 545-556.

4020 Fischer, E.M. and Knutti, R. (2015) 'Anthropogenic contribution to global occurrence of heavy-
4021 precipitation and high-temperature extremes', *Nature Climate Change*, 5, p. 560.

4022 Fischer, E.M. and Knutti, R. (2016) 'Observed heavy precipitation increase confirms theory and early
4023 models', *Nature Climate Change*, 6, p. 986.

4024 Flack, D.L.A., Plant, R.S., Gray, S.L., Lean, H.W., Keil, C. and Craig, G.C. (2016) 'Characterisation of
4025 convective regimes over the British Isles', *Quarterly Journal of the Royal Meteorological Society*,
4026 142(696), pp. 1541-1553.

4027 Forestieri, A., Lo Conti, F., Blenkinsop, S., Cannarozzo, M., Fowler, H.J. and Noto, L.V. (2018) 'Regional
4028 frequency analysis of extreme rainfall in Sicily (Italy)', *International Journal of Climatology*.

4029 Fowler, H.J., Blenkinsop, S. and Tebaldi, C. (2007) 'Linking climate change modelling to impacts
4030 studies: recent advances in downscaling techniques for hydrological modelling', *International Journal
4031 of Climatology*, 27(12), pp. 1547-1578.

4032 Fowler, H.J. and Ekström, M. (2009) 'Multi-model ensemble estimates of climate change impacts on
4033 UK seasonal precipitation extremes', *International Journal of Climatology*, 29(3), pp. 385-416.

4034 Fowler, H.J. and Kilsby, C.G. (2003a) 'Implications of changes in seasonal and annual extreme rainfall',
4035 *Geophysical Research Letters*, 30(13).

4036 Fowler, H.J. and Kilsby, C.G. (2003b) 'A regional frequency analysis of United Kingdom extreme
4037 rainfall from 1961 to 2000', *International Journal of Climatology*, 23(11), pp. 1313-1334.

4038 Fowler, H.J. and Kilsby, C.G. (2007) 'Using regional climate model data to simulate historical and
4039 future river flows in northwest England', *Climatic Change*, 80(3-4), pp. 337-367.

4040 Fowler, H.J. and Wilby, R.L. (2010) 'Detecting changes in seasonal precipitation extremes using
4041 regional climate model projections: Implications for managing fluvial flood risk', *Water Resources
4042 Research*, 46(3).

4043 Francisco Javier, A., José Agustín, G. and María Cruz, G. (2011) 'Peaks-over-Threshold Study of Trends
4044 in Extreme Rainfall over the Iberian Peninsula', *Journal of Climate*, 24(4), pp. 1089-1105.

4045 Franks, S.W. (2002) 'Identification of a change in climate state using regional flood data', *Hydrology
4046 and Earth System Sciences*, 6(1), pp. 11-16.

4047 Frei, C., Schöll, R., Fukutome, S., Schmidli, J. and Vidale, P.L. (2006) 'Future change of precipitation
4048 extremes in Europe: Intercomparison of scenarios from regional climate models', *Journal of
4049 Geophysical Research: Atmospheres*, 111(D6), pp. n/a-n/a.

4050 Furrer, E.M. and Katz, R.W. (2008) 'Improving the simulation of extreme precipitation events by
4051 stochastic weather generators', *Water Resources Research*, 44(12).

4052 Gabriele, C.H., Emily, B., Richard, P.A., William, J.I., Debbie, P., Kevin, E.T., Robin, S.C., Phillip, A.A.,
4053 Beena Balan, S., Andreas, B., Aiguo, D., Paul, J.D., David, E., Hayley, J.F., Elizabeth, J.K., George, J.H.,
4054 Chunlei, L., Robert, M., Mark, N., Timothy, J.O., Nikolaos, S., Peter, A.S., Pier-Luigi, V., Susan, E.W.,
4055 Laura, J.W., Kate, M.W. and Xuebin, Z. (2015) 'Challenges in Quantifying Changes in the Global Water
4056 Cycle', *Bulletin of the American Meteorological Society*, 96(7), pp. 1097-1115.

4057 Galarneau, T.J., Bosart, L.F. and Schumacher, R.S. (2010) 'Predecessor Rain Events ahead of Tropical
4058 Cyclones', *Monthly Weather Review*, 138(8), pp. 3272-3297.

4059 Gastineau, G. and Frankignoul, C. (2015) 'Influence of the North Atlantic SST variability on the
4060 atmospheric circulation during the twentieth century', *Journal of Climate*, 28(4), pp. 1396-1416.

4061 Gillett, N.P. (2005) 'Climate modelling: northern hemisphere circulation', *Nature*, 437(7058), pp. 496-
4062 496.

4063 Gimeno, L., Stohl, A., Trigo, R.M., Dominguez, F., Yoshimura, K., Yu, L., Drumond, A., Durán-Quesada,
4064 A.M. and Nieto, R. (2012) 'Oceanic and terrestrial sources of continental precipitation', *Reviews of
4065 Geophysics*, 50(4).

4066 Golding, B., Clark, P. and May, B. (2005) 'The Boscastle flood: Meteorological analysis of the
4067 conditions leading to flooding on 16 August 2004', *Weather*, 60(8), pp. 230-235.

4068 Gosling, S.N., Dunn, R., Carrol, F., Christidis, N., Fullwood, J., Gusmao, D.d., Golding, N., Good, L., Hall,
4069 T. and Kendon, L. (2011) 'Climate: Observations, projections and impacts', *Climate: Observations,
4070 projections and impacts*.

4071 Gottschalk, L. (1985) 'Hydrological regionalization of Sweden', *Hydrological Sciences Journal*, 30(1),
4072 pp. 65-83.

4073 Gregory, J.M., Jones, P.D. and Wigley, T.M.L. (1991) 'Precipitation in Britain: An analysis of area-
4074 average data updated to 1989', *International Journal of Climatology*, 11(3), pp. 331-345.

4075 Grounds, M.A., LeClerc, J.E. and Joslyn, S. (2018) 'Expressing flood likelihood: return period versus
4076 probability', *Weather, climate, and society*, 10(1), pp. 5-17.

4077 Guerreiro, S.B., Fowler, H.J., Barbero, R., Westra, S., Lenderink, G., Blenkinsop, S., Lewis, E. and Li, X.-
4078 F. (2018) 'Detection of continental-scale intensification of hourly rainfall extremes', *Nature Climate
4079 Change*, 8(9), pp. 803-807.

4080 Guerreiro, S.B., Kilsby, C.G. and Serinaldi, F. (2014) 'Analysis of time variation of rainfall in
4081 transnational basins in Iberia: abrupt changes or trends?', *International Journal of Climatology*, 34(1),
4082 pp. 114-133.

4083 Haagenson, E., Rajagopalan, B., Summers, R.S. and Roberson, J.A. (2013) 'Projecting demand
4084 extremes under climate change using extreme value analysis', *Journal-American Water Works
4085 Association*, 105(2), pp. E40-E50.

4086 Haerter, J.O., Berg, P. and Hagemann, S. (2010) 'Heavy rain intensity distributions on varying time
4087 scales and at different temperatures', *Journal of Geophysical Research: Atmospheres (1984–2012)*,
4088 115(D17).

4089 Hailegeorgis, T.T., Thorolfsson, S.T. and Alfredsen, K. (2013) 'Regional frequency analysis of extreme
4090 precipitation with consideration of uncertainties to update IDF curves for the city of Trondheim',
4091 *Journal of Hydrology*, 498(0), pp. 305-318.

4092 Hajani, E., Rahman, A. and Ishak, E. (2017) 'Trends in extreme rainfall in the state of New South
4093 Wales, Australia', *Hydrological Sciences Journal*, 62(13), pp. 2160-2174.

4094 Hall, R.J. and Hanna, E. (2018) 'North Atlantic circulation indices: links with summer and winter UK
4095 temperature and precipitation and implications for seasonal forecasting', *International Journal of
4096 Climatology*, 38, pp. e660-e677.

4097 Hallegatte, S., Green, C., Nicholls, R.J. and Corfee-Morlot, J. (2013) 'Future flood losses in major
4098 coastal cities', *Nature climate change*, 3(9), pp. 802-806.

4099 Hand, W.H. (2005) 'Climatology of shower frequency in the British Isles at 5 km resolution', *Weather*,
4100 60(6), pp. 153-158.

4101 Hand, W.H., Fox, N.I. and Collier, C.G. (2004) 'A study of twentieth-century extreme rainfall events in
4102 the United Kingdom with implications for forecasting', *Meteorological Applications*, 11(1), pp. 15-31.

4103 Hanel, M., Buishand, T.A. and Ferro, C.A.T. (2009) 'A nonstationary index flood model for
4104 precipitation extremes in transient regional climate model simulations', *Journal of Geophysical
4105 Research: Atmospheres*, 114(D15).

4106 Hanel, M., Pavlásková, A. and Kyselý, J. (2016) 'Trends in characteristics of sub-daily heavy
4107 precipitation and rainfall erosivity in the Czech Republic', *International Journal of Climatology*, 36(4),
4108 pp. 1833-1845.

4109 Hanna, E. and Cropper, T.E. (2017) 'North Atlantic oscillation', *Oxford Research Encyclopedia of
4110 Climate Science*.

4111 Hardwick Jones, R., Westra, S. and Sharma, A. (2010) 'Observed relationships between extreme sub-
4112 daily precipitation, surface temperature, and relative humidity', *Geophysical Research Letters*, 37(22).

4113 Hartmann, D.L., Klein Tank, A.M.G., Ruscicucci, M., Alexander, L.V., Broenniman, B., Charabi, Y.,
4114 Dentener, F.J., Dlugokencky, E.J., Easterling, D.R. and Kaplan, A. (2013) 'Observations: atmosphere
4115 and surface'.

4116 Herring, S.C., Hoerling, M.P., Peterson, T.C. and Stott, P.A. (2014) 'Explaining extreme events of 2013
4117 from a climate perspective', *Bulletin of the American Meteorological Society*, 95(9), pp. S1-S104.

4118 Hertig, E., Seubert, S., Paxian, A., Vogt, G., Paeth, H. and Jacobeit, J. (2014) 'Statistical modelling of
4119 extreme precipitation indices for the Mediterranean area under future climate change', *International*
4120 *Journal of Climatology*, 34(4), pp. 1132-1156.

4121 Hofstätter, M., Lexer, A., Homann, M. and Blöschl, G. (2018) 'Large-scale heavy precipitation over
4122 central Europe and the role of atmospheric cyclone track types', *International journal of climatology :*
4123 *a journal of the Royal Meteorological Society*, 38(Suppl Suppl 1), pp. e497-e517.

4124 Holley, D.M., Dorling, S.R., Steele, C.J. and Earl, N. (2014) 'A climatology of convective available
4125 potential energy in Great Britain', *International Journal of Climatology*, 34(14), pp. 3811-3824.

4126 Hollis, D. and McCarthy, M. (2017) 'UKCP09: Met Office gridded and regional land surface climate
4127 observation datasets' Met Office; Centre for Environmental Data Analysis. UK. Available at:
4128 <http://catalogue.ceda.ac.uk/uuid/87f43af9d02e42f483351d79b3d6162a> (Accessed: 29-11-2018).

4129 Holt, M.A., Hardaker, P.J. and McLelland, G.P. (2001) 'A lightning climatology for Europe and the UK,
4130 1990–99', *Weather*, 56(9), pp. 290-296.

4131 Hosking, J.R.M. and Wallis, J.R. (2005) *Regional frequency analysis: an approach based on L-*
4132 *moments*. New York: Cambridge University Press.

4133 Hulme, M. (2014) 'Attributing weather extremes to 'climate change' A review', *Progress in Physical*
4134 *Geography*, 38(4), pp. 499-511.

4135 Huntingford, C., Marsh, T., Scaife, A.A., Kendon, E.J., Hannaford, J., Kay, A.L., Lockwood, M.,
4136 Prudhomme, C., Reynard, N.S., Parry, S., Lowe, J.A., Screen, J.A., Ward, H.C., Roberts, M., Stott, P.A.,
4137 Bell, V.A., Bailey, M., Jenkins, A., Legg, T., Otto, F.E.L., Massey, N., Schaller, N., Slingo, J. and Allen,
4138 M.R. (2014) 'Potential influences on the United Kingdom's floods of winter 2013/14', *Nature*
4139 *Climate Change*, 4, p. 769.

4140 Huntington, T.G. (2006) 'Evidence for intensification of the global water cycle: review and synthesis',
4141 *Journal of Hydrology*, 319(1), pp. 83-95.

4142 Hurrell, J.W. (1995) 'Decadal trends in the North Atlantic Oscillation: regional temperatures and
4143 precipitation', *Science*, 269(5224), pp. 676-679.

4144 Hurrell, J.W. and Deser, C. (2010) 'North Atlantic climate variability: the role of the North Atlantic
4145 Oscillation', *Journal of Marine Systems*, 79(3), pp. 231-244.

4146 IPCC (2007) 'Impacts, Adaptation and Vulnerability. Contribution of Working Group II to the Fourth
4147 Assessment Report of the Intergovernmental Panel on Climate Change', *UK and NEW YORK, USA:*
4148 *Cambridge University Press*.

4149 IPCC (2012) *Managing the risks of extreme events and disasters to advance climate change*
4150 *adaptation : Special report of the Intergovernmental Panel on Climate Change*. Cambridge, England &
4151 New York, NY, USA: Cambridge University Press.

4152 IPCC (2013) 'Climate change 2013 the physical science basis, working group I contribution to the fifth
4153 assessment report of the intergovernmental panel on climate change'. Cambridge University Press
4154 Cambridge, UK.

4155 Isik, S. and Singh, V.P. (2008) 'Hydrologic regionalization of watersheds in Turkey', *Journal of*
4156 *Hydrologic Engineering*, 13(9), pp. 824-834.

4157 Jackson, I.J. and Weinand, H. (1995) 'Classification of tropical rainfall stations: a comparison of
4158 clustering techniques', *International Journal of Climatology*, 15(9), pp. 985-994.

4159 Jarvis, A., Reuter, H., Nelson, A. and Guevara, E. (2008) *Hole-filled seamless SRTM data V4. Tech. rep.,*
4160 *International Centre for Tropical Agriculture (CIAT)*.

4161 Jenkinson, A.F. and Collison, F.P. (1977) 'An initial climatology of gales over the North Sea', *Synoptic*
4162 *climatology branch memorandum*, 62, p. 18.

4163 Johns, R.H. and Doswell, A.D. (1992) 'Severe Local Storms Forecasting', *Weather and Forecasting*,
4164 7(4), pp. 588-612.

4165 Johnson, F., Hutchinson, M.F., Beesley, C. and Green, J. (2016) 'Topographic relationships for design
4166 rainfalls over Australia', *Journal of Hydrology*, 533, pp. 439-451.

4167 Jolliffe, I.T. (1990) 'Principal component analysis: a beginner's guide—I. Introduction and application',
4168 *Weather*, 45(10), pp. 375-382.

4169 Jolliffe, I.T. (2002) 'Choosing a subset of principal components or variables', *Principal component*
4170 *analysis*, pp. 111-149.

4171 Jones, M., Fowler, H.J., Kilsby, C.G. and Blenkinsop, S. (2010) 'An updated regional frequency analysis
4172 of United Kingdom extreme rainfall 1961–2009', *Proceedings of BHS 2010: Role of Hydrology in
4173 Managing Consequences of a Changing Global Environment*, pp. 110-118.

4174 Jones, M.R., Blenkinsop, S., Fowler, H.J. and Kilsby, C.G. (2014) 'Objective classification of extreme
4175 rainfall regions for the UK and updated estimates of trends in regional extreme rainfall', *International
4176 Journal of Climatology*, 34(3), pp. 751-765.

4177 Jones, M.R., Fowler, H.J., Kilsby, C.G. and Blenkinsop, S. (2013) 'An assessment of changes in seasonal
4178 and annual extreme rainfall in the UK between 1961 and 2009', *International Journal of Climatology*,
4179 33(5), pp. 1178-1194.

4180 Jones, P.D. and Conway, D. (1997) 'PRECIPITATION IN THE BRITISH ISLES: AN ANALYSIS OF AREA-
4181 AVERAGE DATA UPDATED TO 1995', *International Journal of Climatology*, 17(4), pp. 427-438.

4182 Jones, P.D., Hulme, M. and Briffa, K.R. (1993) 'A comparison of Lamb circulation types with an
4183 objective classification scheme', *International Journal of Climatology*, 13(6), pp. 655-663.

4184 Jones, P.D., Jonsson, T. and Wheeler, D. (1997) 'Extension to the North Atlantic oscillation using early
4185 instrumental pressure observations from Gibraltar and south-west Iceland', *International Journal of
4186 Climatology*, 17(13), pp. 1433-1450.

4187 Jones, P.D., Kilsby, C.G., Harpham, C., Glenis, V. and Burton, A. (2009) 'UK Climate Projections science
4188 report: Projections of future daily climate for the UK from the Weather Generator'.

4189 Katz, R.W. (2010) 'Statistics of extremes in climate change', *Climatic Change*, 100(1), pp. 71-76.

4190 Katz, R.W., Parlange, M.B. and Naveau, P. (2002) 'Statistics of extremes in hydrology', *Advances in
4191 Water Resources*, 25(8), pp. 1287-1304.

4192 Kellagher, R.B.B., Cesses, Y., Di Mauro, M. and Gouldby, B.P. (2009) 'An urban drainage flood risk
4193 procedure-a comprehensive approach', *The WaPUG Annual Conference*. HR Wallingford, Blackpool.

4194 Kendon, E.J., Ban, N., Roberts, N.M., Fowler, H.J., Roberts, M.J., Chan, S.C., Evans, J.P., Fosser, G. and
4195 Wilkinson, J.M. (2017) 'Do convection-permitting regional climate models improve projections of
4196 future precipitation change?', *Bulletin of the American Meteorological Society*, 98(1), pp. 79-93.

4197 Kendon, E.J., Blenkinsop, S. and Fowler, H.J. (2018) 'When will we detect changes in short-duration
4198 precipitation extremes?', *Journal of Climate*, 31(7), pp. 2945-2964.

4199 Kendon, E.J., Roberts, N.M., Fowler, H.J., Roberts, M.J., Chan, S.C. and Senior, C.A. (2014) 'Heavier
4200 summer downpours with climate change revealed by weather forecast resolution model', *Nature
4201 Climate Change*, 4(7), pp. 570-576.

4202 Khaliq, M.N., Ouarda, T., Ondo, J.C., Gachon, P. and Bobée, B. (2006) 'Frequency analysis of a
4203 sequence of dependent and/or non-stationary hydro-meteorological observations: A review', *Journal
4204 of hydrology*, 329(3-4), pp. 534-552.

4205 Kharin, V.V., Zwiers, F.W., Zhang, X. and Hegerl, G.C. (2007) 'Changes in temperature and
4206 precipitation extremes in the IPCC ensemble of global coupled model simulations', *Journal of Climate*,
4207 20(8), pp. 1419-1444.

4208 Kilsby, C.G., Cowpertwait, P.S.P., O'Connell, P.E. and Jones, P.D. (1998) 'Predicting rainfall statistics in
4209 England and Wales using atmospheric circulation variables', *International Journal of Climatology: A
4210 Journal of the Royal Meteorological Society*, 18(5), pp. 523-539.

4211 Kimura, F. and Kitoh, A. (2007) 'Downscaling by pseudo global warming method', *The Final Report of
4212 ICCAP*, 4346.

4213 Kjeldsen, T.R., Jones, D.A. and Bayliss, A.C. (2008) *Improving the FEH statistical procedures for flood
4214 frequency estimation* (SC050050). Bristol, UK: Environment Agency Agency, E. [Online]. Available at:
4215 https://assets.publishing.service.gov.uk/government/uploads/system/uploads/attachment_data/file/291096/scho0608boff-e-e.pdf (Accessed: 20/02/2019).

4216 Knight, J.R., Maidens, A., Watson, P.A.G., Andrews, M., Belcher, S., Brunet, G., Fereday, D., Folland,
4217 C.K., Scaife, A.A. and Slingo, J. (2017) 'Global meteorological influences on the record UK rainfall of
4218 winter 2013–14', *Environmental Research Letters*, 12(7), p. 074001.

4219 Knippertz, P. and Wernli, H. (2010) 'A Lagrangian Climatology of Tropical Moisture Exports to the
4220 Northern Hemispheric Extratropics', *Journal of Climate*, 23(4), pp. 987-1003.

4222 Kuhlbrodt, T., Griesel, A., Montoya, M., Levermann, A., Hofmann, M. and Rahmstorf, S. (2007) 'On
4223 the driving processes of the Atlantic meridional overturning circulation', *Reviews of Geophysics*,
4224 45(2).

4225 Kunkel, K.E., Karl, T.R., Brooks, H., Kossin, J., Lawrimore, J.H., Arndt, D., Bosart, L., Changnon, D.,
4226 Cutter, S.L., Doesken, N., Emanuel, K., Groisman, P.Y., Katz, R.W., Knutson, T., apos, Brien, J.,
4227 Paciorek, C.J., Peterson, T.C., Redmond, K., Robinson, D., Trapp, J., Vose, R., Weaver, S., Wehner, M.,
4228 Wolter, K. and Wuebbles, D. (2013) 'Monitoring and understanding trends in extreme storms: state
4229 of knowledge', *Bulletin of the American Meteorological Society*, 94(4), 2013/04//, p. 461+.

4230 Kürbis, K., Mudelsee, M., Tetzlaff, G. and Brázdil, R. (2009) 'Trends in extremes of temperature, dew
4231 point, and precipitation from long instrumental series from central Europe', *Theoretical and Applied
4232 Climatology*, 98(1-2), pp. 187-195.

4233 Labat, D., Godd ris, Y., Probst, J.L. and Guyot, J.L. (2004) 'Evidence for global runoff increase related
4234 to climate warming', *Advances in Water Resources*, 27(6), pp. 631-642.

4235 Lamb, H.H. (1991) 'British Isles daily wind and weather patterns 1588, 1781–86, 1972–91, and
4236 shorter earlier sequences', *Climate Monitor*, 20, pp. 47-70.

4237 Lapworth, A. and McGregor, J. (2008) 'Seasonal variation of the prevailing wind direction in Britain',
4238 *Weather*, 63(12), pp. 365-368.

4239 Lavers, D.A., Allan, R.P., Villarini, G., Lloyd-Hughes, B., Brayshaw, D.J. and Wade, A.J. (2013) 'Future
4240 changes in atmospheric rivers and their implications for winter flooding in Britain', *Environmental
4241 Research Letters*, 8(3), p. 034010.

4242 Lavers, D.A., Allan, R.P., Wood, E.F., Villarini, G., Brayshaw, D.J. and Wade, A.J. (2011) 'Winter floods
4243 in Britain are connected to atmospheric rivers', *Geophysical Research Letters*, 38(23).

4244 Leadbetter, M.R., Weissman, I., De Haan, L. and Rootz n, H. (1989) 'On clustering of high values in
4245 statistically stationary series', *Proc. 4th Int. Meet. Statistical Climatology*, 16, pp. 217-222.

4246 Leahy, P. and Kiely, G. (2011) 'Short Duration Rainfall Extremes in Ireland: Influence of Climatic
4247 Variability', *Water Resources Management*, 25(3), pp. 987-1003.

4248 Lean, H.W., Clark, P.A., Dixon, M., Roberts, N.M., Fitch, A., Forbes, R. and Halliwell, C. (2008)
4249 'Characteristics of high-resolution versions of the Met Office Unified Model for forecasting
4250 convection over the United Kingdom', *Monthly Weather Review*, 136(9), pp. 3408-3424.

4251 Lee, S.H. and Maeng, S.J. (2003) 'Frequency analysis of extreme rainfall using L-moment. Irrigation
4252 Drain', *Irrigation Drain*, 52(3), pp. 219-230.

4253 Leeuw, J., Methven, J. and Blackburn, M. (2015) 'Variability and trends in England and Wales
4254 precipitation', *International Journal of Climatology*.

4255 Lenderink, G., Mok, H.Y., Lee, T.C. and Van Oldenborgh, G.J. (2011) 'Scaling and trends of hourly
4256 precipitation extremes in two different climate zones–Hong Kong and the Netherlands', *Hydrology
4257 and Earth System Sciences*, 15(9), pp. 3033-3041.

4258 Lenderink, G. and Van Meijgaard, E. (2008) 'Increase in hourly precipitation extremes beyond
4259 expectations from temperature changes', *Nature Geoscience*, 1(8), pp. 511-514.

4260 Lenderink, G. and Van Meijgaard, E. (2010) 'Linking increases in hourly precipitation extremes to
4261 atmospheric temperature and moisture changes', *Environmental Research Letters*, 5(2), p. 025208.

4262 Lepore, C., Veneziano, D. and Molini, A. (2015) 'Temperature and CAPE dependence of rainfall
4263 extremes in the eastern United States', *Geophysical Research Letters*, 42(1), pp. 74-83.

4264 Levermann, A., Griesel, A., Hofmann, M., Montoya, M. and Rahmstorf, S. (2005) 'Dynamic sea level
4265 changes following changes in the thermohaline circulation', *Climate Dynamics*, 24(4), pp. 347-354.

4266 Lewis, E., Quinn, N., Blenkinsop, S., Fowler, H.J., Freer, J., Tanguy, M., Hitt, O., Coxon, G., Bates, P.
4267 and Woods, R. (2018) 'A rule based quality control method for hourly rainfall data and a 1 km
4268 resolution gridded hourly rainfall dataset for Great Britain: CEH-GEAR1hr', *Journal of hydrology*, 564,
4269 pp. 930-943.

4270 Liu, C. and Allan, R.P. (2012) 'Multisatellite observed responses of precipitation and its extremes to
4271 interannual climate variability', *Journal of Geophysical Research: Atmospheres (1984–2012)*, 117(D3).

4272 Lochbihler, K., Lenderink, G. and Siebesma, A.P. (2017) 'The spatial extent of rainfall events and its
4273 relation to precipitation scaling', *Geophysical Research Letters*, 44(16), pp. 8629-8636.

4274 Lowe, J.A., Bernie, D., Bett, P., Bricheno, L., Brown, S., Calvert, D., Clark, R., Eagle, K., Edwards, T.,
4275 Fosser, G., Fung, F., Gohar, L., Good, P., Gregory, J., Harris, G., Howard, T., Kaye, N., Kendon, E.,
4276 Krijnen, J., Maisey, P., McDonald, R., McInnes, R., McSweeney, C., Mitchell, J.F.B., Murphy, J., Palmer,
4277 M., Roberts, C., Rostron, J., Sexton, D., Thornton, H., Tinker, J., Tucker, S., Yamazaki, K. and Belcher, S.
4278 (2018) *UKCP18 Science Overview report*. Exeter, UK: Met Office, H.C. [Online]. Available at:
4279 [https://www.metoffice.gov.uk/pub/data/weather/uk/ukcp18/science-reports/UKCP18-Overview-](https://www.metoffice.gov.uk/pub/data/weather/uk/ukcp18/science-reports/UKCP18-Overview-report.pdf)
4280 [report.pdf](https://www.metoffice.gov.uk/pub/data/weather/uk/ukcp18/science-reports/UKCP18-Overview-report.pdf) (Accessed: 03/02/2019).

4281 Madsen, H., Arnbjerg-Nielsen, K. and Mikkelsen, P.S. (2009) 'Update of regional intensity–duration–
4282 frequency curves in Denmark: tendency towards increased storm intensities', *Atmospheric Research*,
4283 92(3), pp. 343-349.

4284 Madsen, H., Lawrence, D., Lang, M., Martinkova, M. and Kjeldsen, T.R. (2013) *A review of applied*
4285 *methods in Europe for flood-frequency analysis in a changing environment: Floodfreq COST action*
4286 *ES0901 European procedures for flood frequency estimation (1906698368)*. Wallingford, U. K.: Centre
4287 for Ecology & Hydrology on behalf of COST

4288

4289 Madsen, H. and Thyregod, P. (2010) *Introduction to general and generalized linear models*. CRC Press.

4290 Mailhot, A. and Duchesne, S. (2009) 'Design criteria of urban drainage infrastructures under climate
4291 change', *Journal of Water Resources Planning and Management*, 136(2), pp. 201-208.

4292 Maraun, D., Osborn, T.J. and Gillett, N.P. (2008) 'United Kingdom daily precipitation intensity:
4293 improved early data, error estimates and an update from 2000 to 2006', *International Journal of*
4294 *Climatology*, 28(6), pp. 833-842.

4295 Maraun, D., Rust, H.W. and Osborn, T.J. (2010a) 'Synoptic airflow and UK daily precipitation
4296 extremes', *Extremes*, 13(2), pp. 133-153.

4297 Maraun, D., Wetterhall, F., Ireson, A.M., Chandler, R.E., Kendon, E.J., Widmann, M., Brienen, S., Rust,
4298 H.W., Sauter, T., Themeßl, M., Venema, V.K.C., Chun, K.P., Goodess, C.M., Jones, R.G., Onof, C., Vrac,
4299 M. and Thiele-Eich, I. (2010b) 'Precipitation downscaling under climate change: Recent developments
4300 to bridge the gap between dynamical models and the end user', *Reviews of Geophysics*, 48(3), pp.
4301 n/a-n/a.

4302 Marshall, J., Kushnir, Y., Battisti, D., Chang, P., Czaja, A., Dickson, R., Hurrell, J., McCartney, M.,
4303 Saravanan, R. and Visbeck, M. (2001) 'North Atlantic climate variability: phenomena, impacts and
4304 mechanisms', *International Journal of Climatology*, 21(15), pp. 1863-1898.

4305 May, W. (2004) 'Variability and extremes of daily rainfall during the Indian summer monsoon in the
4306 period 1901–1989', *Global and Planetary Change*, 44(1-4), pp. 83-105.

4307 Mayes, J. (2000) 'Changing regional climatic gradients in the United Kingdom', *Geographical Journal*,
4308 166(2), pp. 125-138.

4309 Mayes, J. (2013) 'Regional weather and climates of the British Isles – Part 2: South East England and
4310 East Anglia', *Weather*, 68(3), pp. 59-65.

4311 Mayes, J. and Wheeler, D. (2013) 'Regional weather and climates of the British Isles - Part 1:
4312 Introduction', *Weather*, 68(1), pp. 3-8.

4313 Meehl, G.A., Stocker, T.F., Collins, W.D., Friedlingstein, P., Gaye, A.T., Gregory, J.M., Kitoh, A., Knutti,
4314 R., Murphy, J.M. and Noda, A. (2007) 'Global climate projections', *Climate change*, 283.

4315 Met-Office (2016) *UK climate*. Available at: <http://www.metoffice.gov.uk/public/weather/climate>
4316 (Accessed: 26/01/2016).

4317 Met Office (2007) *August 2007 UK overview*. Available at:
4318 <https://www.metoffice.gov.uk/climate/uk/summaries/2007/august> (Accessed: 08/02/2019).

4319 Millar, R.B. (2011) *Maximum likelihood estimation and inference: with examples in R, SAS and ADMB*.
4320 John Wiley & Sons.

4321 Mills, T.C. (2005) 'Modelling precipitation trends in England and Wales', *Meteorological applications*,
4322 12(02), pp. 169-176.

4323 Min, S.-K., Zhang, X., Zwiers, F.W. and Hegerl, G.C. (2011) 'Human contribution to more-intense
4324 precipitation extremes', *Nature*, 470(7334), pp. 378-381.

4325 Mishra, V., Wallace, J.M. and Lettenmaier, D.P. (2012) 'Relationship between hourly extreme
4326 precipitation and local air temperature in the United States', *Geophysical Research Letters*, 39(16).

- 4327 Modarres, R. and Sarhadi, A. (2011) 'Statistically-based regionalization of rainfall climates of Iran',
4328 *Global and Planetary Change*, 75(1-2), pp. 67-75.
- 4329 Moncrieff, M.W. and Miller, M.J. (1976) 'The dynamics and simulation of tropical cumulonimbus and
4330 squall lines', *Quarterly Journal of the Royal Meteorological Society*, 102(432), pp. 373-394.
- 4331 Morbidelli, R., Saltalippi, C., Flammini, A., Cifrodelli, M., Picciafuoco, T., Corradini, C., Casas-Castillo,
4332 M.C., Fowler, H.J. and Wilkinson, S.M. (2017) 'Effect of temporal aggregation on the estimate of
4333 annual maximum rainfall depths for the design of hydraulic infrastructure systems', *Journal of*
4334 *Hydrology*, 554, pp. 710-720.
- 4335 Morss, R.E., Cuite, C.L., Demuth, J.L., Hallman, W.K. and Shwom, R.L. (2018) 'Is storm surge scary?
4336 The influence of hazard, impact, and fear-based messages and individual differences on responses to
4337 hurricane risks in the USA', *International journal of disaster risk reduction*, 30, pp. 44-58.
- 4338 Murphy, J.M., Sexton, D.M., Jenkins, G.J., Booth, B.B., Brown, C.C., Clark, R.T., Collins, M., Harris, G.R.,
4339 Kendon, E.J. and Betts, R.A. (2009) 'UK climate projections science report: climate change
4340 projections'.
- 4341 Murphy, S.J. and Washington, R. (2001) 'United Kingdom and Ireland precipitation variability and the
4342 North Atlantic sea-level pressure field', *International Journal of Climatology*, 21(8), pp. 939-959.
- 4343 Murray, V. and Ebi, K.L. (2012) 'IPCC special report on managing the risks of extreme events and
4344 disasters to advance climate change adaptation (SREX)', *Journal of epidemiology and community*
4345 *health*, 66(9), pp. 759-760.
- 4346 Muschinski, T. and Katz, J.I. (2013) 'Trends in hourly rainfall statistics in the United States under a
4347 warming climate', *Nature Climate Change*, 3(6), pp. 577-580.
- 4348 National Suds Working Group (2004) 'Interim code of practice for sustainable drainage systems',
4349 *Londres: National SUDS Working Group*.
- 4350 Naveau, P., Nogaj, M., Ammann, C., Yiou, P., Cooley, D. and Jomelli, V. (2005) 'Statistical methods for
4351 the analysis of climate extremes', *Comptes Rendus Geoscience*, 337(10-11), pp. 1013-1022.
- 4352 Neal, R., Dankers, R., Saulter, A., Lane, A., Millard, J., Robbins, G. and Price, D. (2018) 'Use of
4353 probabilistic medium-to long-range weather-pattern forecasts for identifying periods with an
4354 increased likelihood of coastal flooding around the UK', *Meteorological Applications*, 25(4), pp. 534-
4355 547.
- 4356 Neal, R., Fereday, D., Crocker, R. and Comer Ruth, E. (2016) 'A flexible approach to defining weather
4357 patterns and their application in weather forecasting over Europe', *Meteorological Applications*,
4358 23(3), pp. 389-400.
- 4359 Neal, R.A. and Phillips, I.D. (2009) 'Summer daily precipitation variability over the East Anglian region
4360 of Great Britain', *International Journal of Climatology: A Journal of the Royal Meteorological Society*,
4361 29(11), pp. 1661-1679.
- 4362 NERC (1975) *Flood Studies Report, Natural Environment Research Council*,. London, UK.
- 4363 Ning, L., Riddle, E.E. and Bradley, R.S. (2015) 'Projected changes in climate extremes over the
4364 northeastern United States', *Journal of Climate*, 28(8), pp. 3289-3310.
- 4365 Nogaj, M., Yiou, P., Parey, S., Malek, F. and Naveau, P. (2006) 'Amplitude and frequency of
4366 temperature extremes over the North Atlantic region', *Geophysical Research Letters*, 33(10).
- 4367 Norbiato, D., Borga, M., Sangati, M. and Zanon, F. (2007) 'Regional frequency analysis of extreme
4368 precipitation in the eastern Italian Alps and the August 29, 2003 flash flood', *Journal of Hydrology*,
4369 345(3-4), pp. 149-166.
- 4370 North, G.R. and Erukhimova, T.L. (2009) *Atmospheric thermodynamics: elementary physics and*
4371 *chemistry*. Cambridge University Press.
- 4372 Northrop, P.J. (2015) 'An efficient semiparametric maxima estimator of the extremal index',
4373 *Extremes*, 18(4), pp. 585-603.
- 4374 O'Gorman, P.A. and Schneider, T. (2009) 'The physical basis for increases in precipitation extremes in
4375 simulations of 21st-century climate change', *Proceedings of the National Academy of Sciences*,
4376 106(35), pp. 14773-14777.
- 4377 O'Gorman, P.A. (2015) 'Precipitation Extremes Under Climate Change', *Current Climate Change*
4378 *Reports*, 1(2), pp. 49-59.
- 4379 Olsson, U. (2002) 'Generalized linear models', *An applied approach. Studentlitteratur, Lund*, 18.

4380 Osborn, T.J. (2004) 'Simulating the winter North Atlantic Oscillation: the roles of internal variability
4381 and greenhouse gas forcing', *Climate Dynamics*, 22(6-7), pp. 605-623.

4382 Osborn, T.J., Conway, D., Hulme, M., Gregory, J.M. and Jones, P.D. (1999) 'Air flow influences on local
4383 climate: observed and simulated mean relationships for the United Kingdom', *Climate Research*,
4384 13(3), pp. 173-191.

4385 Osborn, T.J., Hulme, M., Jones, P.D. and Basnett, T.A. (2000) 'Observed trends in the daily intensity of
4386 United Kingdom precipitation', *International Journal of Climatology*, 20(4), pp. 347-364.

4387 Ossó, A., Sutton, R., Shaffrey, L. and Dong, B. (2018) 'Observational evidence of European summer
4388 weather patterns predictable from spring', *Proceedings of the National Academy of Sciences*, 115(1),
4389 pp. 59-63.

4390 Paixao, E., Auld, H., Mirza, M.M.Q., Klaassen, J. and Shephard, M.W. (2011) 'Regionalization of heavy
4391 rainfall to improve climatic design values for infrastructure: case study in Southern Ontario, Canada',
4392 *Hydrological Sciences Journal*, 56(7), pp. 1067-1089.

4393 Pall, P., Allen, M.R. and Stone, D.A. (2007) 'Testing the Clausius–Clapeyron constraint on changes in
4394 extreme precipitation under CO2 warming', *Climate Dynamics*, 28(4), pp. 351-363.

4395 Pandey, M.D., Van Gelder, P.H.A.J.M. and Vrijling, J.K. (2003) 'Bootstrap simulations for evaluating
4396 the uncertainty associated with peaks-over-threshold estimates of extreme wind velocity',
4397 *Environmetrics*, 14(1), pp. 27-43.

4398 Paris agreement (2015) *PARIS AGREEMENT* Paris, France. [Online]. Available at:
4399 https://unfccc.int/sites/default/files/english_paris_agreement.pdf.

4400 Pattison, I. and Lane, S.N. (2012) 'The relationship between Lamb weather types and long-term
4401 changes in flood frequency, River Eden, UK', *International Journal of Climatology*, 32(13), pp. 1971-
4402 1989.

4403 Paulin, C., Yonas, B.D. and François, A. (2005) 'Downscaling Precipitation and Temperature with
4404 Temporal Neural Networks', *Journal of Hydrometeorology*, 6(4), pp. 483-496.

4405 Pendergrass, A.G. (2018) 'What precipitation is extreme?', *Science*, 360(6393), pp. 1072-1073.

4406 Perry, M. (2006) 'A spatial analysis of trends in the UK climate since 1914 using gridded datasets',
4407 *Climate memorandum*.

4408 Pfahl, S., O’Gorman, P.A. and Fischer, E.M. (2017) 'Understanding the regional pattern of projected
4409 future changes in extreme precipitation', *Nature Climate Change*, 7(6), p. 423.

4410 Pitt, M. (2008) 'The Pitt review: learning lessons from the 2007 floods', *London: Cabinet Office*.

4411 Prein, A.F., Langhans, W., Fosser, G., Ferrone, A., Ban, N., Goergen, K., Keller, M., Tölle, M., Gutjahr,
4412 O. and Feser, F. (2015) 'A review on regional convection-permitting climate modeling:
4413 Demonstrations, prospects, and challenges', *Reviews of geophysics*, 53(2), pp. 323-361.

4414 Prein, A.F., Rasmussen, R.M., Ikeda, K., Liu, C., Clark, M.P. and Holland, G.J. (2017) 'The future
4415 intensification of hourly precipitation extremes', *Nature Climate Change*, 7(1), p. 48.

4416 Prudhomme, C., Reynard, N. and Crooks, S. (2002) 'Downscaling of global climate models for flood
4417 frequency analysis: where are we now?', *Hydrological processes*, 16(6), pp. 1137-1150.

4418 Raff, D.A., Pruitt, T. and Brekke, L.D. (2009) 'A framework for assessing flood frequency based on
4419 climate projection information', *Hydrology and Earth System Sciences*, 13(11), pp. 2119-2136.

4420 Rahmstorf, S. and Coumou, D. (2011) 'Increase of extreme events in a warming world', *Proceedings
4421 of the National Academy of Sciences*, 108(44), pp. 17905-17909.

4422 Ramos, M.C. (2001) 'Divisive and hierarchical clustering techniques to analyse variability of rainfall
4423 distribution patterns in a Mediterranean region', *Atmospheric Research*, 57(2), pp. 123-138.

4424 Ramsbottom, D., Sayers, P. and Panzeri, M. 2012. Climate change risk assessment for the floods and
4425 coastal erosion sector. UK Climate Change Risk Assessment. Defra, London. , D, Sayers, P. and
4426 Panzeri, M. (2012) 'Climate change risk assessment for the floods and coastal erosion sector', *Defra
4427 Project Code GA0204. Report to Defra, London, UK*.

4428 Rao, A.R. and Srinivas, V.V. (2006) 'Regionalization of watersheds by hybrid-cluster analysis', *Journal
4429 of Hydrology*, 318(1-4), pp. 37-56.

4430 Reed, D. and Robson, A. (1999) *Procedures for flood freequency estimation, Volume 3: Statistical
4431 procedures for flood freequency estimation*. Wallingford: Institute of Hydrology.

- 4432 Renard, B., Lang, M. and Bois, P. (2006) 'Statistical analysis of extreme events in a non-stationary
4433 context via a Bayesian framework: case study with peak-over-threshold data', *Stochastic
4434 environmental research and risk assessment*, 21(2), pp. 97-112.
- 4435 Richardson, D., Fowler, H.J., Kilsby, C.G. and Neal, R. (2018) 'A new precipitation and drought
4436 climatology based on weather patterns', *International Journal of Climatology*, 38(2), pp. 630-648.
- 4437 Riemann-Campe, K., Blender, R. and Fraedrich, K. (2011) 'Global memory analysis in observed and
4438 simulated CAPE and CIN', *International Journal of Climatology*, 31(8), pp. 1099-1107.
- 4439 Rodda, H.J.E., Little, M.A., Wood, R.G., MacDougall, N. and McSharry, P.E. (2009) 'A digital archive of
4440 extreme rainfalls in the British Isles from 1866 to 1968 based on British Rainfall', *weather*, 64(3), pp.
4441 71-75.
- 4442 Rohrbeck, C., Eastoe, E.F., Frigessi, A. and Tawn, J.A. (2018) 'Extreme value modelling of water-
4443 related insurance claims', *The Annals of Applied Statistics*, 12(1), pp. 246-282.
- 4444 Rootzén, H. and Katz, R.W. (2013) 'Design life level: quantifying risk in a changing climate', *Water
4445 Resources Research*, 49(9), pp. 5964-5972.
- 4446 Roy, S.S. and Rouault, M. (2013) 'Spatial patterns of seasonal scale trends in extreme hourly
4447 precipitation in South Africa', *Applied Geography*, 39, pp. 151-157.
- 4448 Rust, H.W., Maraun, D. and Osborn, T.J. (2009) 'Modelling seasonality in extreme precipitation', *The
4449 European Physical Journal Special Topics*, 174(1), pp. 99-111.
- 4450 Salas, J.D. and Obeysekera, J. (2013) 'Revisiting the concepts of return period and risk for
4451 nonstationary hydrologic extreme events', *Journal of Hydrologic Engineering*, 19(3), pp. 554-568.
- 4452 Santer, B.D., Mears, C., Wentz, F.J., Taylor, K.E., Gleckler, P.J., Wigley, T.M.L., Barnett, T.P., Boyle, J.S.,
4453 Brüggemann, W. and Gillett, N.P. (2007) 'Identification of human-induced changes in atmospheric
4454 moisture content', *Proceedings of the National Academy of Sciences*, 104(39), pp. 15248-15253.
- 4455 Sarhadi, A. and Heydarizadeh, M. (2014) 'Regional frequency analysis and spatial pattern
4456 characterization of Dry Spells in Iran', *International Journal of Climatology*, 34(3), pp. 835-848.
- 4457 Scaife, A.A., Folland, C.K., Alexander, L.V., Moberg, A. and Knight, J.R. (2008) 'European climate
4458 extremes and the North Atlantic Oscillation', *Journal of Climate*, 21(1), pp. 72-83.
- 4459 Schindler, A., Maraun, D. and Luterbacher, J. (2012) 'Validation of the present day annual cycle in
4460 heavy precipitation over the British Islands simulated by 14 RCMs', *Journal of Geophysical Research:
4461 Atmospheres*, 117(D18).
- 4462 Schmittner, A. (2005) 'Decline of the marine ecosystem caused by a reduction in the Atlantic
4463 overturning circulation', *Nature*, 434(7033), pp. 628-633.
- 4464 Schumacher, R.S. and Johnson, R.H. (2005) 'Organization and environmental properties of extreme-
4465 rain-producing mesoscale convective systems', *Monthly weather review*, 133(4), pp. 961-976.
- 4466 Serinaldi, F. and Kilsby, C.G. (2015) 'Stationarity is undead: Uncertainty dominates the distribution of
4467 extremes', *Advances in Water Resources*, 77, pp. 17-36.
- 4468 Shashikanth, K., Ghosh, S., Vittal, H. and Karmakar, S. (2016) 'Future projections of Indian summer
4469 monsoon rainfall extremes over India with statistical downscaling and its consistency with observed
4470 characteristics', *Climate Dynamics*, pp. 1-15.
- 4471 Simpson, I.R. and Jones, P.D. (2012) 'Updated precipitation series for the UK derived from Met Office
4472 gridded data', *International Journal of Climatology*, 32(15), pp. 2271-2282.
- 4473 Simpson, I.R. and Jones, P.D. (2014) 'Analysis of UK precipitation extremes derived from Met Office
4474 gridded data', *International Journal of Climatology*, 34(7), pp. 2438-2449.
- 4475 Smithers, J.C. and Schulze, R.E. (2001) 'A methodology for the estimation of short duration design
4476 storms in South Africa using a regional approach based on L-moments', *Journal of Hydrology*, 241(1-
4477 2), pp. 42-52.
- 4478 Stern (2006) *The economics of climate change, the Stern review*. . Cambridge, UK: Cambridge
4479 University Press.
- 4480 Stocker, T.F., Qin, D., Plattner, G.K., Tignor, M., Allen, S.K. and Boschung, J. (2013) *IPCC, 2013:
4481 summary for policymakers in climate change 2013: the physical science basis, contribution of working
4482 group I to the fifth assessment report of the intergovernmental panel on climate change*. Cambridge
4483 University Press, Cambridge, New York, USA.
- 4484 Stull, R.B. (2018) 'Practical meteorology: an algebra-based survey of atmospheric science'.

4485 Sugahara, S., Da Rocha, R.P. and Silveira, R. (2009) 'Non-stationary frequency analysis of extreme
4486 daily rainfall in Sao Paulo, Brazil', *International Journal of Climatology: A Journal of the Royal*
4487 *Meteorological Society*, 29(9), pp. 1339-1349.

4488 Sutton, R.T. and Dong, B. (2012) 'Atlantic Ocean influence on a shift in European climate in the
4489 1990s', *Nature Geoscience*, 5, p. 788.

4490 Sutton, R.T. and Hodson, D.L.R. (2005) 'Atlantic Ocean forcing of North American and European
4491 summer climate', *science*, 309(5731), pp. 115-118.

4492 Svensson, C. and Jakob, D. (2002) 'Diurnal and seasonal characteristics of precipitation at an upland
4493 site in Scotland', *International journal of climatology*, 22(5), pp. 587-598.

4494 Swain, D., Langenbrunner, B., David Neelin, J. and Hall, A. (2018) *Increasing precipitation volatility in*
4495 *twenty-first-century California*.

4496 Tan, P.-N. (2018) *Introduction to data mining*. Pearson Education India.

4497 Tencer, B., Weaver, A. and Zwiers, F. (2014) 'Joint occurrence of daily temperature and precipitation
4498 extreme events over Canada', *Journal of Applied Meteorology and Climatology*, 53(9), pp. 2148-2162.

4499 Thiombiano, A.N., El Adlouni, S., St-Hilaire, A., Ouarda, T.B.M.J. and El-Jabi, N. (2017) 'Nonstationary
4500 frequency analysis of extreme daily precipitation amounts in Southeastern Canada using a peaks-
4501 over-threshold approach', *Theoretical and Applied Climatology*, 129(1), pp. 413-426.

4502 Timmermann, A., An, S.I., Krebs, U. and Goosse, H. (2005) 'ENSO Suppression due to Weakening of
4503 the North Atlantic Thermohaline Circulation*', *Journal of Climate*, 18(16), pp. 3122-3139.

4504 Trefry, C.M., Watkins Jr, D.W. and Johnson, D. (2005) 'Regional rainfall frequency analysis for the
4505 state of Michigan', *Journal of Hydrologic Engineering*, 10(6), pp. 437-449.

4506 Trenberth, K.E. (2011) 'Changes in precipitation with climate change', *Climate Research*, 47(1), p. 123.

4507 Trenberth, K.E. and Caron, J.M. (2001) 'Estimates of meridional atmosphere and ocean heat
4508 transports', *Journal of Climate*, 14(16), pp. 3433-3443.

4509 Trenberth, K.E., Dai, A., Rasmussen, R.M. and Parsons, D.B. (2003) 'The Changing Character of
4510 Precipitation', *Bulletin of the American Meteorological Society*, 84(9), pp. 1205-1217.

4511 Trenberth, K.E. and Shea, D.J. (2005) 'Relationships between precipitation and surface temperature',
4512 *Geophysical Research Letters*, 32(14).

4513 Trenberth, K.E., Smith, L., Qian, T., Dai, A. and Fasullo, J. (2007) 'Estimates of the Global Water
4514 Budget and Its Annual Cycle Using Observational and Model Data', *Journal of Hydrometeorology*,
4515 8(4), pp. 758-769.

4516 Tye, M.R. (2015) 'Understanding the risks from extreme rainfall', *Proceedings of the Institution of Civil*
4517 *Engineers - Forensic Engineering*, 168(2), pp. 71-80.

4518 Tye, M.R., Blenkinsop, S., Fowler, H.J., Stephenson, D.B. and Kilsby, C.G. (2016) 'Simulating
4519 multimodal seasonality in extreme daily precipitation occurrence', *Journal of hydrology*, 537, pp. 117-
4520 129.

4521 U.S. Geological Survey (2012) *Atlantic meridional overturning circulation*. Available at:
4522 www.eoearth.org/view/article/150290/ (Accessed: January 19).

4523 Utsumi, N., Seto, S., Kanae, S., Maeda, E.E. and Oki, T. (2011) 'Does higher surface temperature
4524 intensify extreme precipitation?', *Geophysical Research Letters*, 38(16).

4525 Uvo, C.B. (2003) 'Analysis and regionalization of northern European winter precipitation based on its
4526 relationship with the North Atlantic oscillation', *International Journal of Climatology*, 23(10), pp.
4527 1185-1194.

4528 Vallebona, C., Pellegrino, E., Frumento, P. and Bonari, E. (2015) 'Temporal trends in extreme rainfall
4529 intensity and erosivity in the Mediterranean region: a case study in southern Tuscany, Italy', *Climatic*
4530 *Change*, 128(1-2), pp. 139-151.

4531 Vallis, G.K. and Gerber, E.P. (2008) 'Local and hemispheric dynamics of the North Atlantic Oscillation,
4532 annular patterns and the zonal index', *Dynamics of atmospheres and oceans*, 44(3-4), pp. 184-212.

4533 van Delden, A. (2001) 'The synoptic setting of thunderstorms in western Europe', *Atmospheric*
4534 *research*, 56(1-4), pp. 89-110.

4535 Vellinga, M. and Wood, R.A. (2002) 'Global Climatic Impacts of a Collapse of the Atlantic
4536 Thermohaline Circulation', *Climatic Change*, 54(3), pp. 251-267.

4537 Vogel, R.M., Yaindl, C. and Walter, M. (2011) 'Nonstationarity: flood magnification and recurrence
4538 reduction factors in the United States 1', *JAWRA Journal of the American Water Resources*
4539 *Association*, 47(3), pp. 464-474.

4540 Vrac, M. and Naveau, P. (2007) 'Stochastic downscaling of precipitation: From dry events to heavy
4541 rainfalls', *Water resources research*, 43(7).

4542 Vuillaume, J.-F. and Herath, S. (2017) 'Improving global rainfall forecasting with a weather type
4543 approach in Japan', *Hydrological sciences journal*, 62(2), pp. 167-181.

4544 Wallace, J.M. and Hobbs, P.V. (2006) *Atmospheric science: an introductory survey*. Elsevier.

4545 Wallis, J.R., Schaefer, M.G., Barker, B.L., Taylor, G.H. and Hydrol. Earth Syst. Sci. (HESS) 11 (1) (2007)
4546 'Regional precipitation-frequency analysis and spatial mapping for 24-hour and 2-hour durations for
4547 Washington State', *Hydrology and Earth System Sciences*, 11(1), pp. 415-442.

4548 Wang, C. and Dong, S. (2010) 'Is the basin-wide warming in the North Atlantic Ocean related to
4549 atmospheric carbon dioxide and global warming?', *Geophysical Research Letters*, 37(8).

4550 Wasko, C. and Sharma, A. (2014) 'Quantile regression for investigating scaling of extreme
4551 precipitation with temperature', *Water Resources Research*, 50(4), pp. 3608-3614.

4552 Weile, W., Bruce, T.A., Robert, K.K. and Ranga, B.M. (2004) 'The Relation between the North Atlantic
4553 Oscillation and SSTs in the North Atlantic Basin', *Journal of Climate*, 17(24), pp. 4752-4759.

4554 Westra, S., Alexander, L.V. and Zwiers, F.W. (2013) 'Global increasing trends in annual maximum daily
4555 precipitation', *Journal of Climate*, 26(11), pp. 3904-3918.

4556 Westra, S., Fowler, H.J., Evans, J.P., Alexander, L.V., Berg, P., Johnson, F., Kendon, E.J., Lenderink, G.
4557 and Roberts, N.M. (2014) 'Future changes to the intensity and frequency of short-duration extreme
4558 rainfall', *Reviews of Geophysics*, 52(3), pp. 522-555.

4559 White, E.P., Enquist, B.J. and Green, J.L. (2008) 'On estimating the exponent of power-law frequency
4560 distributions', *Ecology*, 89(4), pp. 905-912.

4561 Wi, S., Valdés, J.B., Steinschneider, S. and Kim, T.-W. (2016) 'Non-stationary frequency analysis of
4562 extreme precipitation in South Korea using peaks-over-threshold and annual maxima', *Stochastic*
4563 *environmental research and risk assessment*, 30(2), pp. 583-606.

4564 Wigley, T.M.L. and Jones, P.D. (1987) 'England and Wales precipitation: a discussion of recent
4565 changes in variability and an update to 1985', *Journal of Climatology*, 7(2), pp. 1-246.

4566 Wigley, T.M.L., Lough, J.M. and Jones, P.D. (1984) 'Spatial patterns of precipitation in England and
4567 Wales and a revised, homogeneous England and Wales precipitation series', *Journal of Climatology*,
4568 4(1), pp. 1-25.

4569 Wilby, R.L., O'Hare, G. and Barnsley, N. (1997) 'The North Atlantic Oscillation and British Isles climate
4570 variability, 1865–1996', *Weather*, 52(9), pp. 266-276.

4571 Wilby, R.L., Wedgbrow, C.S. and Fox, H.R. (2004) 'Seasonal predictability of the summer
4572 hydrometeorology of the River Thames, UK', *Journal of Hydrology*, 295(1-4), pp. 1-16.

4573 Wilks, D.S. (2011) *Statistical methods in the atmospheric sciences*. Academic press.

4574 Willett, K.M., Jones, P.D., Thorne, P.W. and Gillett, N.P. (2010) 'A comparison of large scale changes
4575 in surface humidity over land in observations and CMIP3 general circulation models', *Environmental*
4576 *Research Letters*, 5(2), p. 025210.

4577 Woollings, T. (2010) 'Dynamical influences on European climate: an uncertain future', *Philosophical*
4578 *Transactions of the Royal Society of London A: Mathematical, Physical and Engineering Sciences*,
4579 368(1924), pp. 3733-3756.

4580 Wypych, A., Bochenek, B. and Różycki, M. (2018) 'Atmospheric Moisture Content over Europe and
4581 the Northern Atlantic', *Atmosphere*, 9(1), p. 18.

4582 Xiao, C., Yuan, W. and Yu, R. (2018) 'Diurnal cycle of rainfall in amount, frequency, intensity, duration,
4583 and the seasonality over the UK', *International Journal of Climatology*, 38(13), pp. 4967-4978.

4584 Xu, C.-y. (1999) 'Climate change and hydrologic models: A review of existing gaps and recent research
4585 developments', *Water Resources Management*, 13(5), pp. 369-382.

4586 Xu, G., Osborn, T., Matthews, A. and Joshi, M. (2015) 'Different atmospheric moisture divergence
4587 responses to extreme and moderate El Niños', *Climate Dynamics*, pp. 1-18.

4588 Yang, C., Chandler, R.E., Isham, V.S. and Wheeler, H.S. (2005) 'Spatial-temporal rainfall simulation
4589 using generalized linear models', *Water Resources Research*, 41(11).

4590 Yang, T., Shao, Q., Hao, Z.-C., Chen, X., Zhang, Z., Xu, C.-Y. and Sun, L. (2010) 'Regional frequency
4591 analysis and spatio-temporal pattern characterization of rainfall extremes in the Pearl River Basin,
4592 China', *Journal of Hydrology*, 380(3-4), pp. 386-405.

4593 You, Q., Kang, S., Aguilar, E., Pepin, N., Flügel, W.-A., Yan, Y., Xu, Y., Zhang, Y. and Huang, J. (2011)
4594 'Changes in daily climate extremes in China and their connection to the large scale atmospheric
4595 circulation during 1961–2003', *Climate Dynamics*, 36(11), pp. 2399-2417.

4596 Yunus, R.M., Hasan, M.M., Razak, N.A., Zubairi, Y.Z. and Dunn, P.K. (2017) 'Modelling daily rainfall
4597 with climatological predictors: Poisson-gamma generalized linear modelling approach', *International
4598 Journal of Climatology*, 37(3), pp. 1391-1399.

4599 Zhang, X., Hegerl, G., Zwiers, F.W. and Kenyon, J. (2005) 'Avoiding inhomogeneity in percentile-based
4600 indices of temperature extremes', *Journal of Climate*, 18(11), pp. 1641-1651.

4601 Zheng, F., Westra, S. and Leonard, M. (2015) 'Opposing local precipitation extremes', *Nature Climate
4602 Change*, 5(5), p. 389.

4603 Zhou, Y. and Lau, W.K.M. (2017) 'The relationships between the trends of mean and extreme
4604 precipitation', *International Journal of Climatology*, 37(10), pp. 3883-3894.

4605

4606

4607

4608

4609

4610

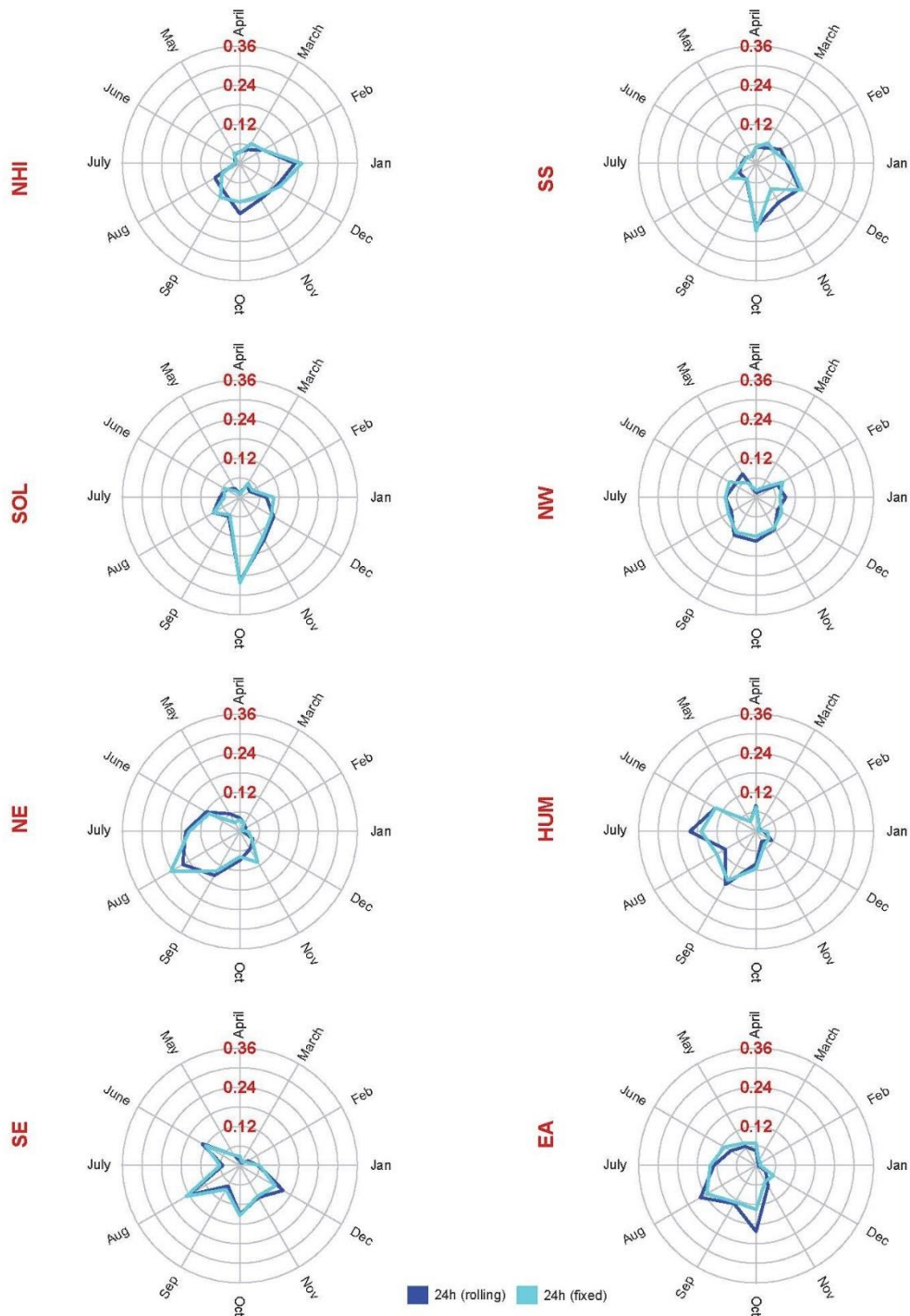
4611

4612

Appendices

4613

Appendix A: Supporting figures



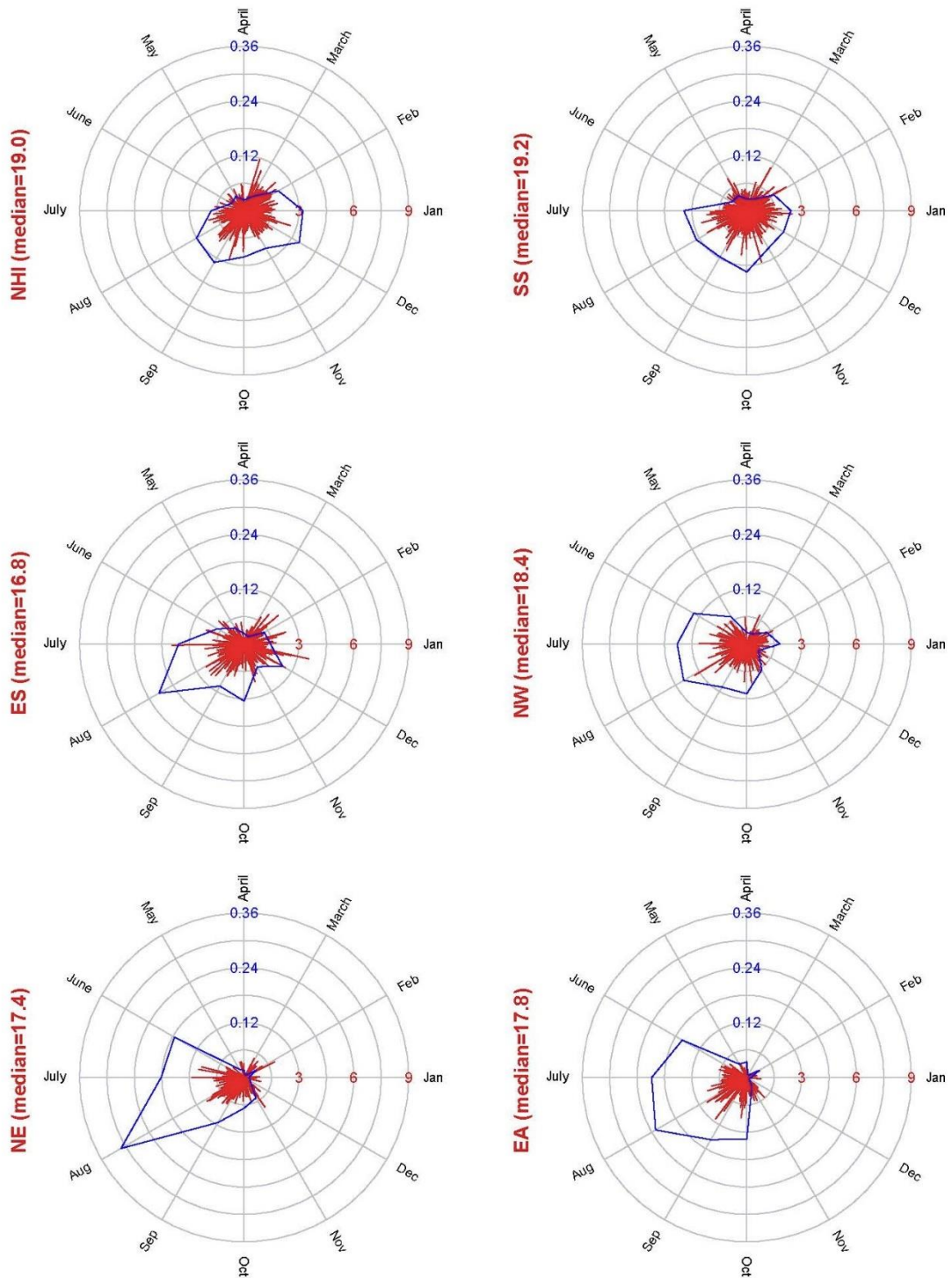
4614

4615

4616

4617

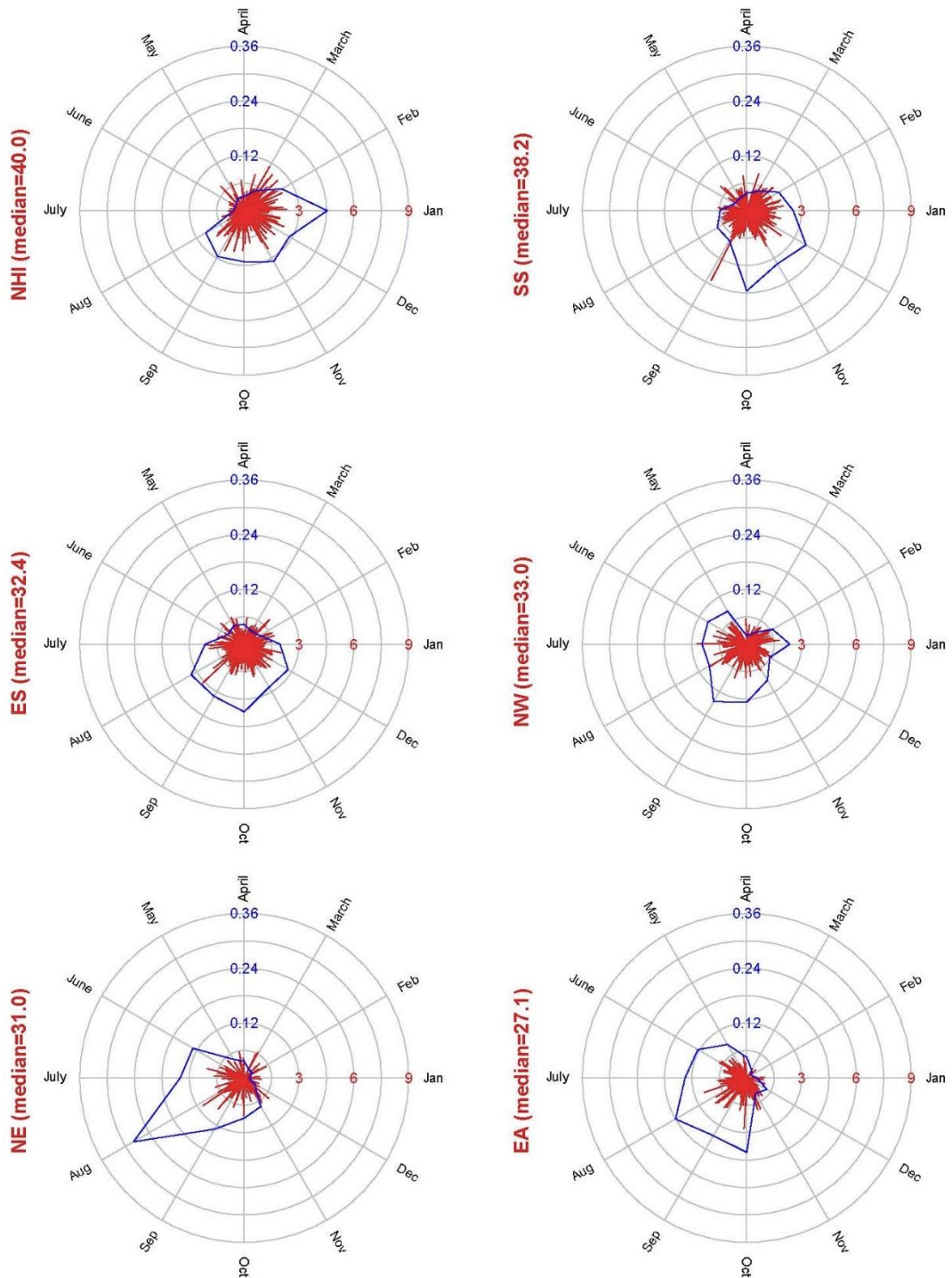
Figure A 1: Regional monthly frequency densities of 24h AMAX rolling window accumulation (dark blue) and 24h AMAX fixed window accumulation at 09:00 (cyan) in the UK. Values in red denote the frequency density scale.



4618

4619 Figure A 2: Monthly 3h AMAX frequency density (blue), and 3h AMAX standardised by
 4620 the regional median (red). The regional median (mm) is stated for each region, and
 4621 radial lines denote 1st day of each month. Selected regions shown as in main paper.

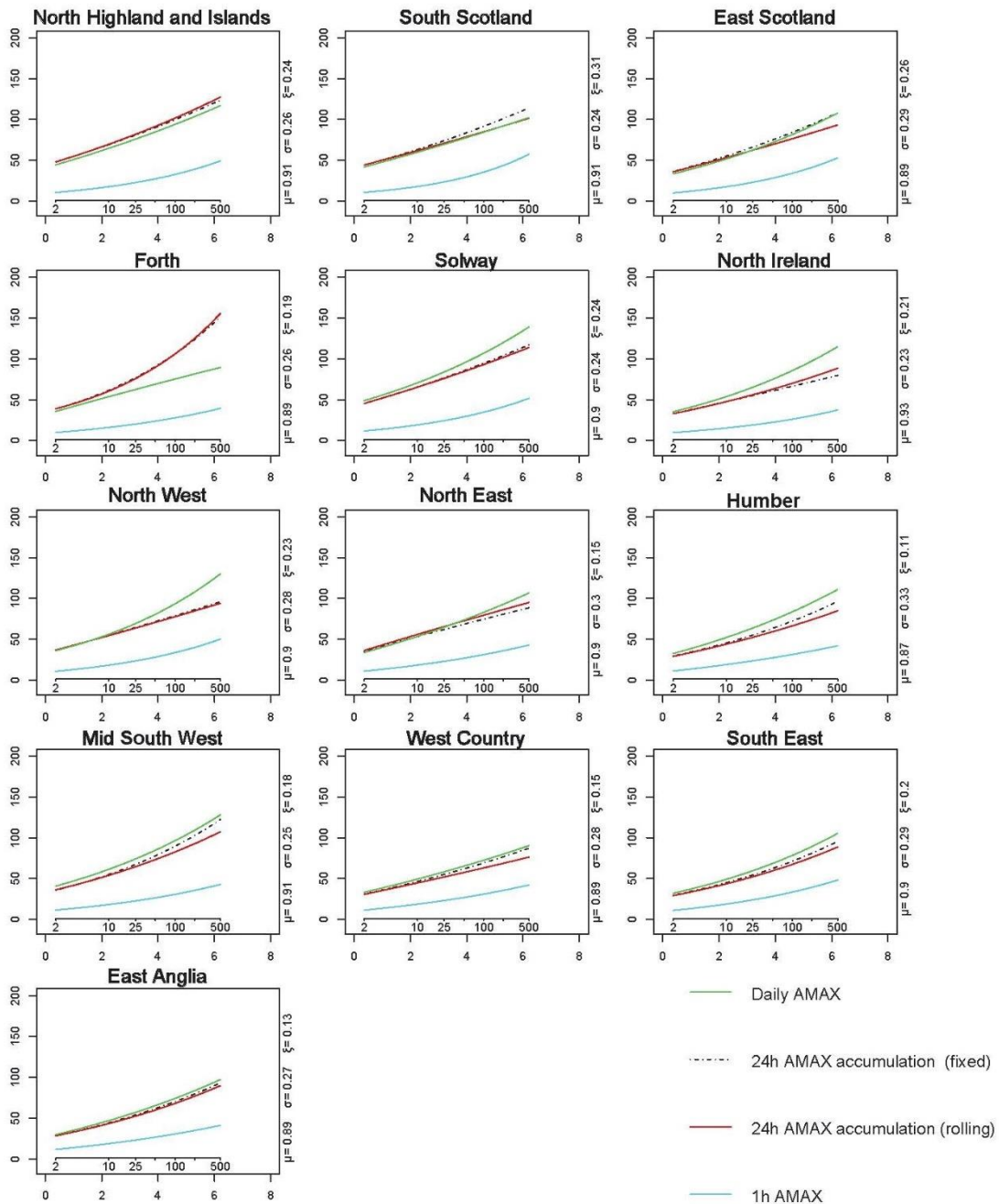
4622



4623

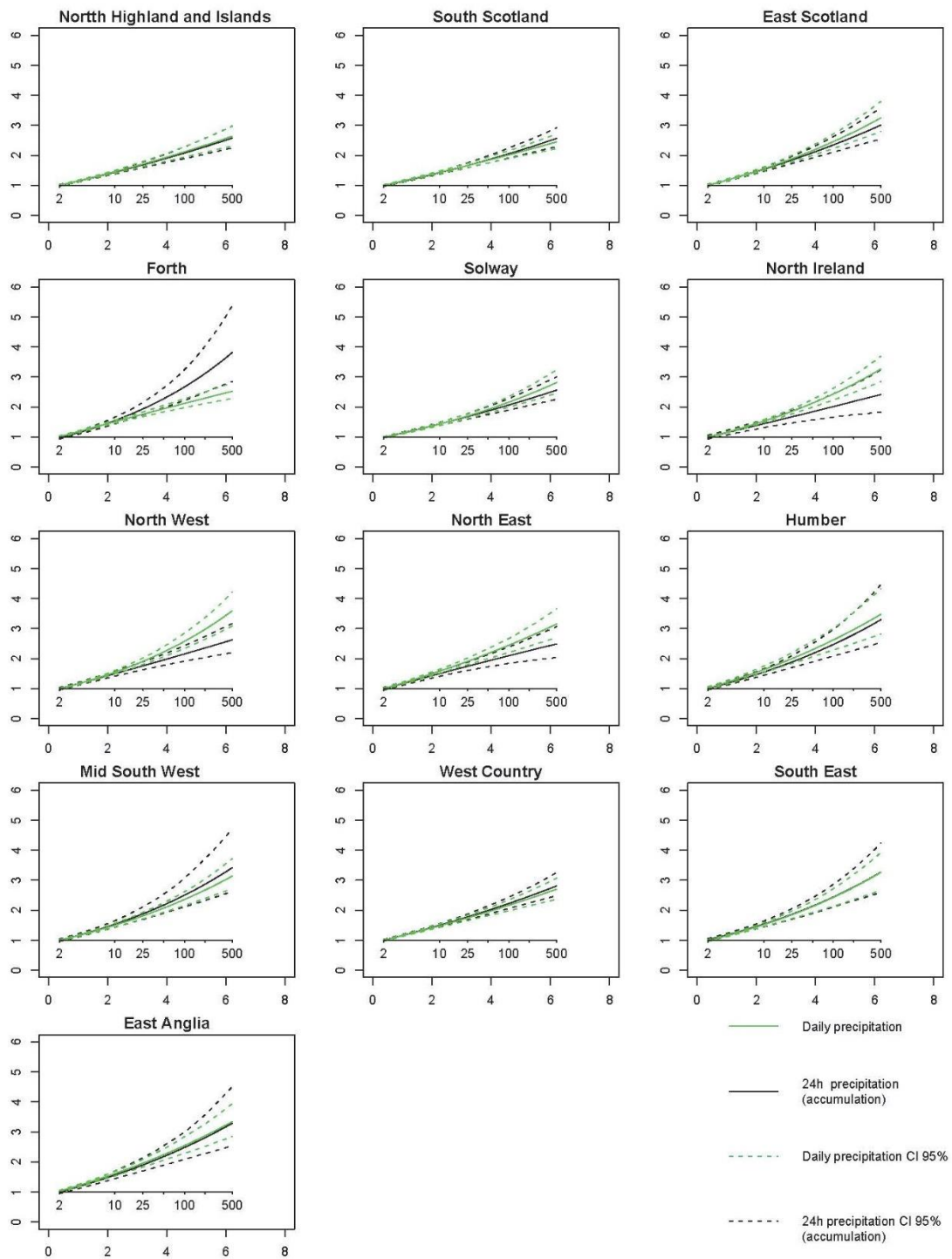
4624 Figure A 3: Monthly 12h AMAX frequency density (blue), and 12h AMAX standardised
 4625 by the regional median (red). The regional median (mm) is stated for each region, and
 4626 radial lines denote 1st day of each month. Selected regions shown as in main paper.

4627



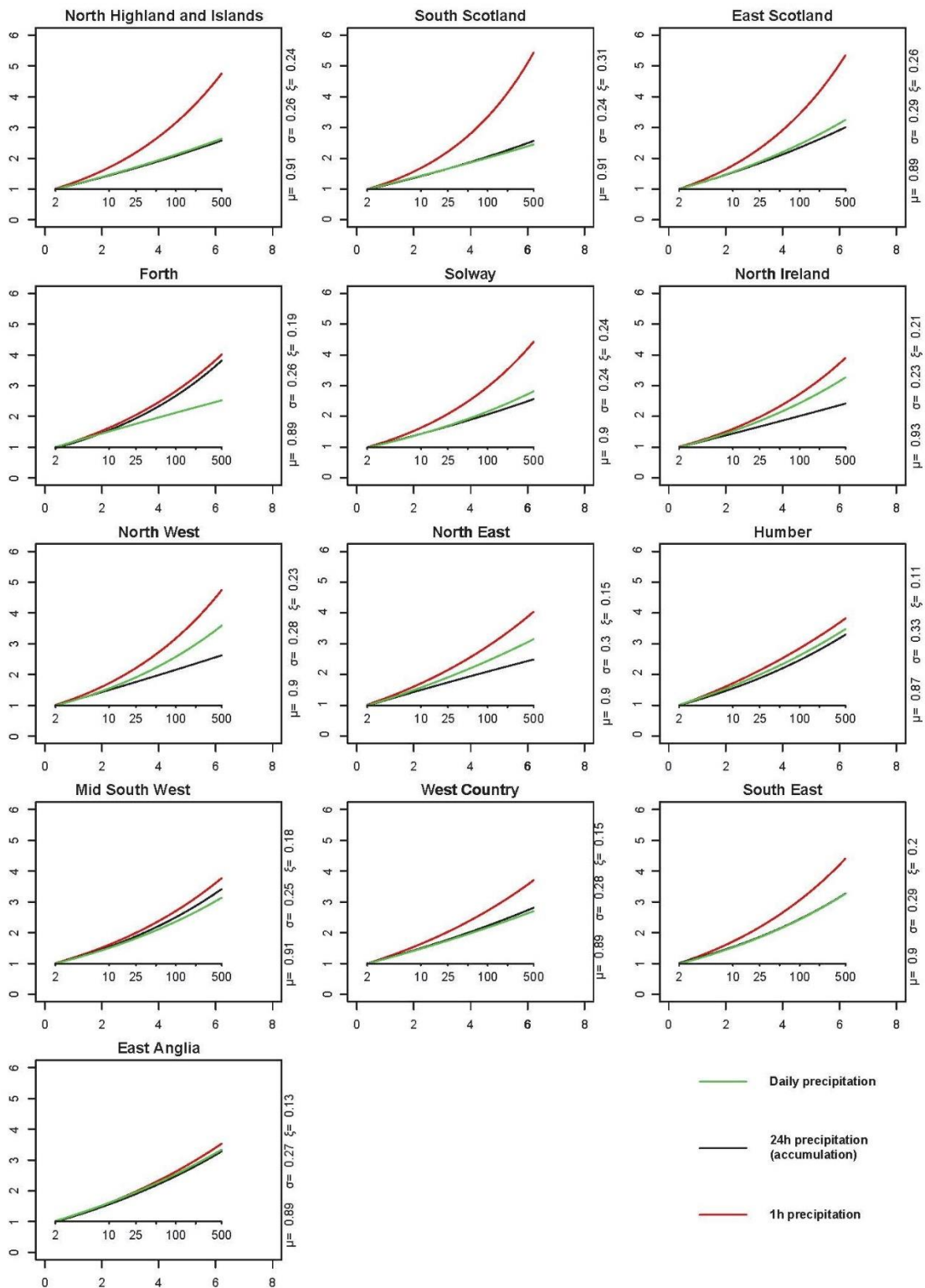
4628

4629 Figure A 4: Return level plots of fitted regional GEV distributions for daily AMAX (from
 4630 Jones et al. 2014) (green), 24h AMAX fixed window accumulation at 09:00 (dashed
 4631 black), 24h AMAX rolling window accumulation (red), and 1h AMAX (cyan). Return
 4632 level estimates in mm (left y-axis), return periods in years (upper x-axis) and Gumbel
 4633 reduced variate (lower x-axis). The 1h AMAX GEV distribution parameters μ , σ , and ξ
 4634 are also shown.



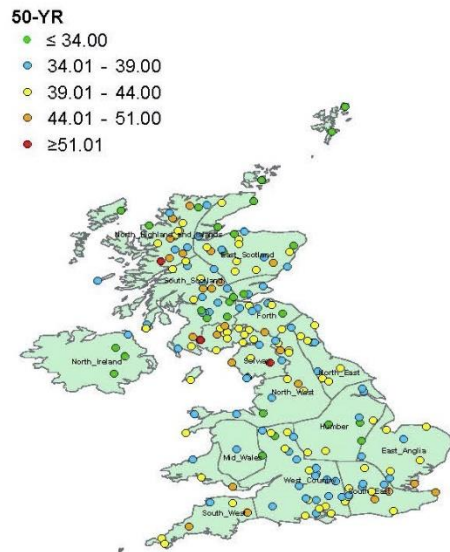
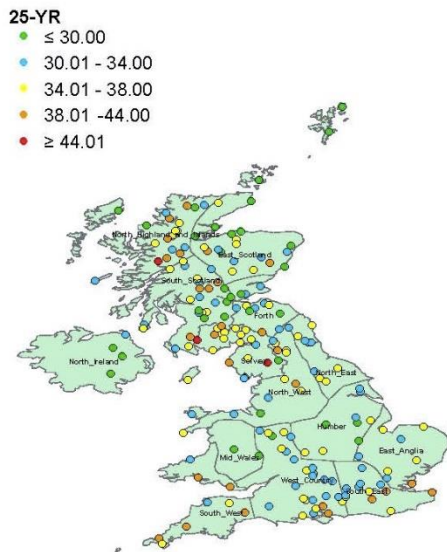
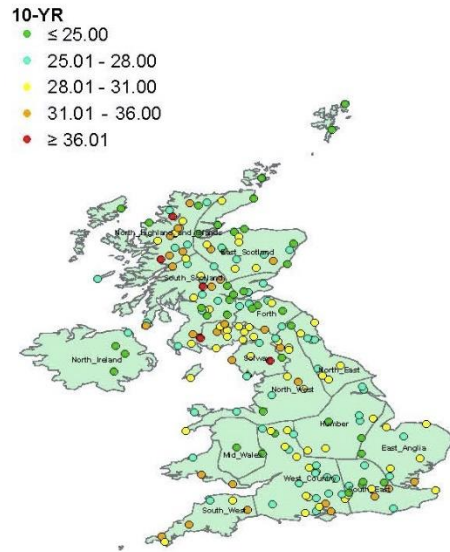
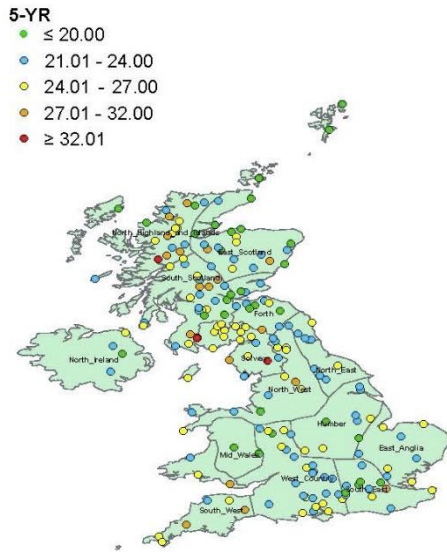
4635

4636 Figure A 5: Fitted growth curves for 24h standardized AMAX accumulation (black), and
 4637 daily AMAX (from Jones et al. 2014) (green), and confidence interval for each
 4638 distribution (dashed lines). Growth factor (y-axis), return periods in years (upper x-axis)
 4639 and Gumbel reduced variate (lower x-axis). The growth curve represents the multiple
 4640 increase of a given return level over an index value, here the 2-year return level.



4641

4642 Figure A 6: Fitted growth curves for standardized 1h AMAX (red), 24h AMAX (black),
 4643 and daily AMAX (from Jones et al. 2014) (green). Growth factor (left y-axis), return
 4644 periods in years (upper x-axis) and Gumbel reduced variate (lower x-axis). The 1h
 4645 AMAX GEV distribution parameters μ , σ , and ξ are also shown. The growth curve
 4646 represents the multiple increase of a given return level over an index value, here the
 4647 2-year return level.



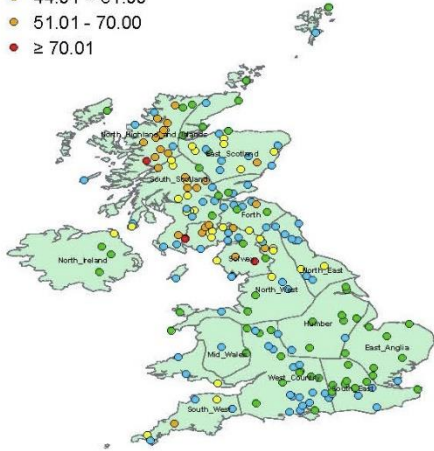
4648

4649 Figure A 7: Return level estimates (mm h⁻¹) for UK 3h AMAX precipitation at each
 4650 gauge for return periods of 5-, 10-, 25- and 50 years (20%, 10%, 4%, 2% annual
 4651 exceedance probabilities (AEPs)). Estimates for each gauge are calculated from the
 4652 fitted regional GEV growth curve multiplied by the site scaling factor (gauge RMed).

4653

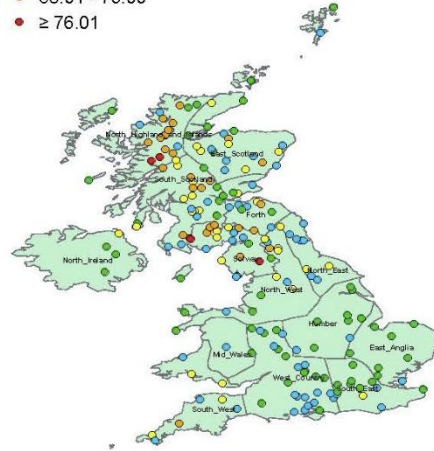
5-YR

- ≤ 37.00
- 37.01 - 44.00
- 44.01 - 51.00
- 51.01 - 70.00
- ≥ 70.01



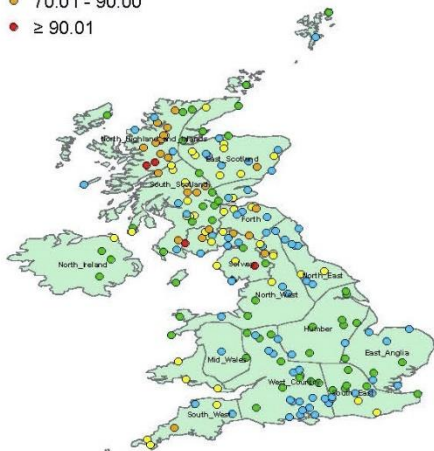
10-YR

- ≤ 43.00
- 43.01 - 50.00
- 50.01 - 58.00
- 58.01 - 76.00
- ≥ 76.01



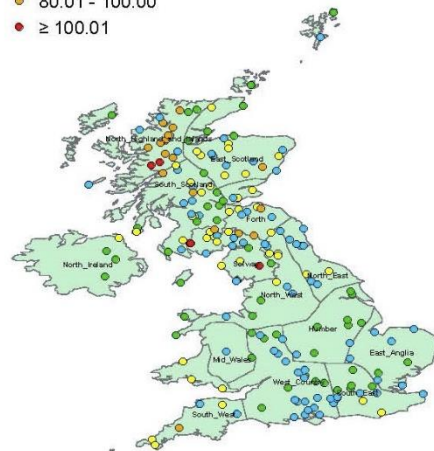
25-YR

- ≤ 50.00
- 50.01 - 58.00
- 58.01 - 70.00
- 70.01 - 90.00
- ≥ 90.01



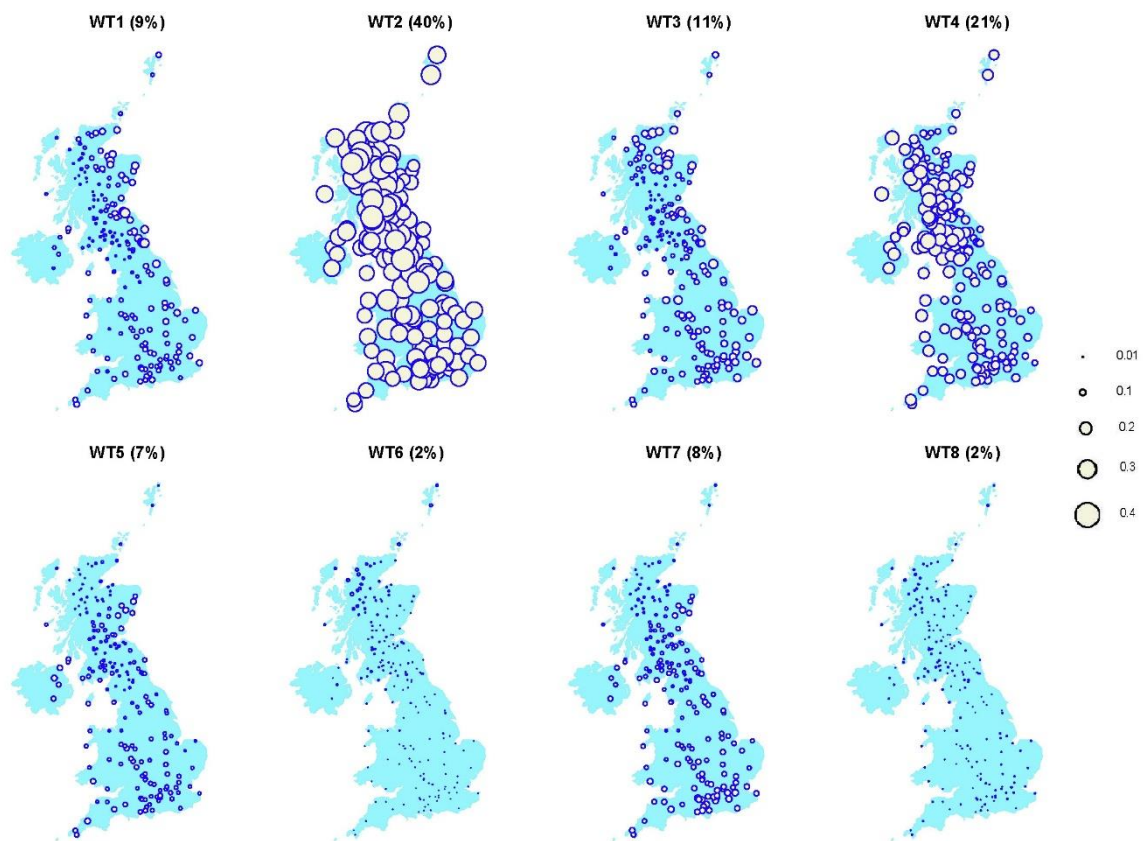
50-YR

- ≤ 55.00
- 55.01 - 65.00
- 65.01 - 80.00
- 80.01 - 100.00
- ≥ 100.01



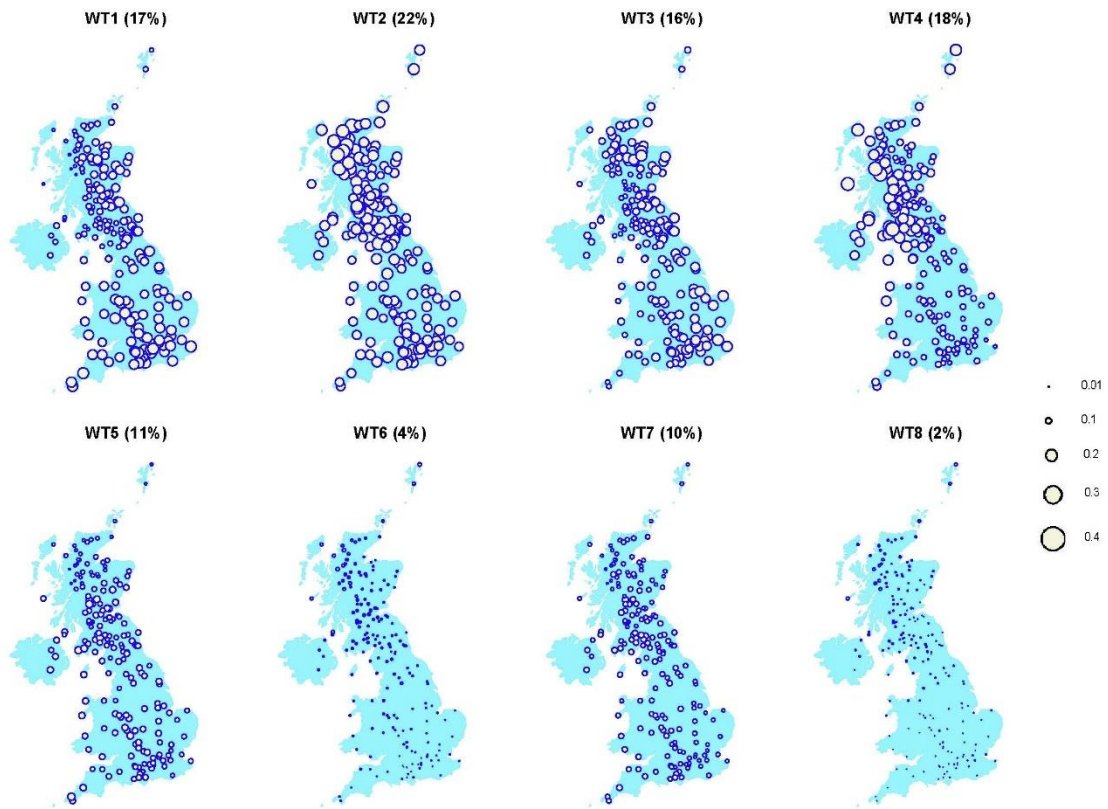
4654

4655 Figure A 8: Return level estimates (mm h⁻¹) for UK 12h AMAX precipitation at each
 4656 gauge for return periods of 5-, 10-, 25- and 50 years (20%, 10%, 4%, 2% annual
 4657 exceedance probabilities (AEPs)). Estimates for each gauge are calculated from the
 4658 fitted regional GEV growth curve multiplied by the site scaling factor (gauge RMed).



4659

4660 Figure A 9: Occurrence proportion of days exceeding the Q99 hourly precipitation for
 4661 each gauge across the 8 weather types identified by Neal et al. (2016) in the winter
 4662 half year (Oct-March, N-WQ99) over the period 1992-2014. Circle diameter indicates
 4663 the proportion of events within each weather type for each gauge.



4664

4665 Figure A 10: Occurrence proportion of days exceeding the Q99 hourly precipitation for
 4666 each gauge across the 8 weather types identified by Neal et al. (2016) in the summer
 4667 half year (Apr-Sept, N-SQ99) over the period 1992-2014. Circle diameter indicates the
 4668 proportion of events within each weather type for each gauge.

4669

4670

4671

4672

4673

4674

4675

4676

4677

4678

4679

4680

4681

4682

Appendix B: Supporting tables

4683

	(θ)					r				
Region	1h	3h	6h	12h	24h	1h	3h	6h	12h	24h
North Highland and Islands	277	310	327	333	342	0.24	0.31	0.4	0.39	0.42
South Scotland	236	278	306	324	326	0.4	0.28	0.32	0.37	0.34
East Scotland	229	248	266	278	284	0.42	0.37	0.33	0.32	0.35
Forth	224	243	247	263	276	0.56	0.46	0.36	0.35	0.36
Solway	229	259	287	300	304	0.5	0.41	0.41	0.42	0.43
North West	216	223	243	260	281	0.48	0.35	0.28	0.24	0.24
North East	215	219	217	221	230	0.72	0.64	0.56	0.54	0.5
Humber	205	213	219	221	225	0.68	0.64	0.53	0.48	0.44
West Country	220	234	251	255	257	0.55	0.49	0.41	0.36	0.36
Mid South West	236	238	250	251	269	0.51	0.39	0.34	0.32	0.27
South East	222	235	252	266	264	0.64	0.5	0.4	0.36	0.35
East Anglia	217	220	225	230	225	0.74	0.66	0.59	0.49	0.42
North Ireland	235	244	255	269	276	0.49	0.41	0.38	0.36	0.34

4684

4685

4686

4687

4688

4689

4690

4691

4692

4693

4694

4695

4696

4697

Table B 1: Regional circular statistics representing seasonality of occurrence of hourly and multi-hourly AMAX events. Statistic θ denotes mean occurrence day (Julian day); r indicates the degree to which events are seasonally concentrated, ranging from 0 to 1, with higher values indicating greater concentration around θ .